Fall 2011 | Winter 2012 | Spring 2012 | Summer 2012 | Volume XL, Number 4

JNMM Journal of Nuclear Materials Management

JNMM 40 FORTIETH ANNIVERSARY 1997–2011

Non-Profit Organization
U.S. POSTAGE
PAID
Permit No. 2066
Eau Claire, WI

INMM
INSTITUTE OF NUCLEAR MATERIALS MANAGEMENT

Published by the Institute of Nuclear Materials Management

SAVE THE DATE

INSTITUTE OF NUCLEAR MATERIALS MANAGEMENT

INMM

July 14–18, 2013

54th INMM Annual Meeting

Desert Springs
JW Marriott Resort
in Palm Desert, CA USA

www.inmm.org

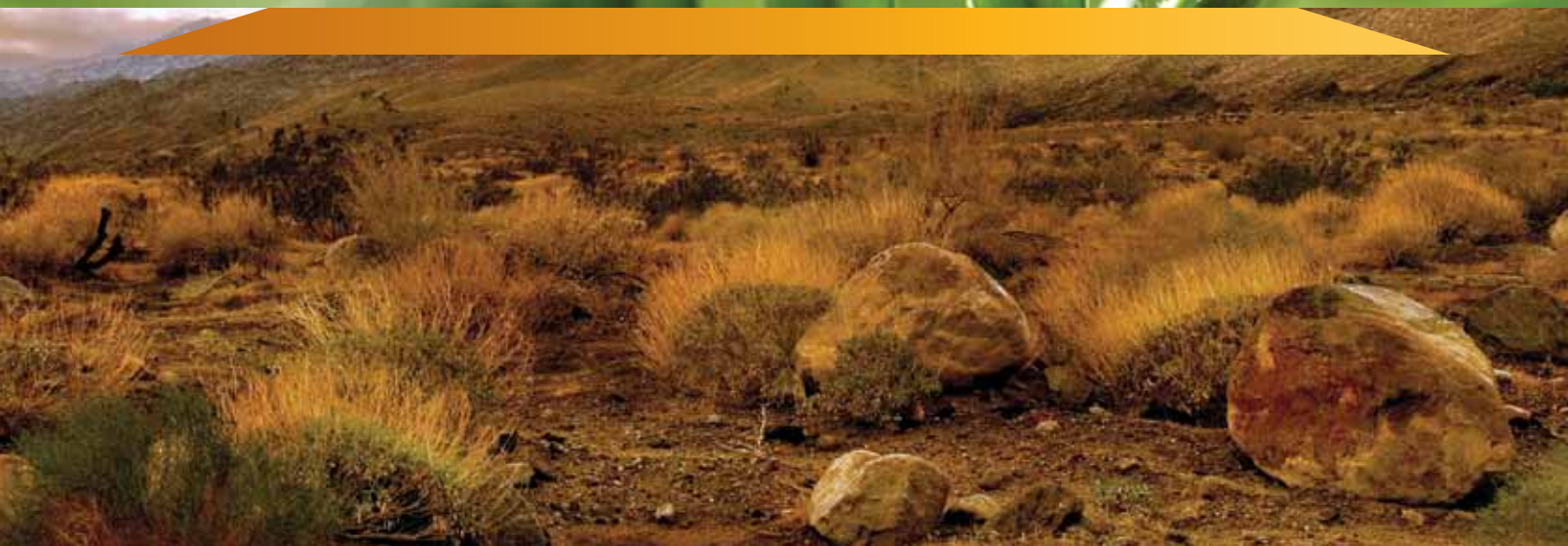

JNMM Journal of Nuclear Materials Management

JNMM (ISSN 0893-6188) is published four times a year by the Institute of Nuclear Materials Management Inc., a not-for-profit membership organization with the purpose of advancing and promoting responsible management of nuclear materials.

SUBSCRIPTION RATES: Annual (United States, Canada, and Mexico) $200; annual (other countries) $270 (shipped via air mail printed matter); single copy regular issues (United States and other countries) $55; single copy of the proceedings of the Annual Meeting (United States and other countries) $175. Mail subscription requests to *JNMM*, 111 Deer Lake Road, Suite 100, Deerfield, IL 60015 U.S.A. Make checks payable to INMM.

DISTRIBUTION and delivery inquiries should be directed to *JNMM*, 111 Deer Lake Road, Suite 100, Deerfield, IL 60015 U.S.A., or contact Anne Czeropski at +1-847-480-9573; fax, +1-847-480-9282; or E-mail, inmm@inmm.org. Allow eight weeks for a change of address to be implemented.

JNMM Journal of Nuclear Materials Management

JNMM 40 FORTIETH ANNIVERSARY 1971–2011

Special Issue: Science for Verification

Topical Papers

Departments

Wrapping Up Two Years

By Scott Vance
INMM President

In May, I performed my last international representation as INMM president at the 34th Annual Meeting of the European Safeguards Research and Development Association (ESARDA) in Luxembourg. ESARDA and INMM have a long history, and the fundamental goals of the two organizations are very similar. In recognition of these similarities, ESARDA and INMM have recently signed an agreement to officially commit to working together to further these mutual goals. One of the most rewarding aspects of serving as INMM president is personally witnessing the high level of professionalism displayed by individuals in this field. Regardless of where an individual is from or their particular specialty, their passion for the appropriate handling and control of nuclear material has been evident and gratifying. My experience has made me all the more confident that INMM and similar global organizations can have a significant impact on the future appropriate uses of nuclear materials.

Speaking of "final duties," this is also my final column as president. This has been an extremely rewarding experience, and I am grateful to all of you for the opportunity. My greatest hope is that I was able to maintain the stature and respect that the organization has developed over the previous fifty years. The weight of responsibility that accompanies this office is significant, due to the quality of the individuals who have previously served. I owe all of them a great debt of gratitude because the reputation that they established for INMM made my term all the more meaningful.

Of course, this is one of those cases where I get undeserved recognition. The fact is, INMM is a successful and respected organization because it represents the collected activities of an incredible group of nuclear professionals. The individuals who serve in the various roles in INMM provide countless hours of significant work on a volunteer basis. They deserve the credit for the impact that INMM has on the global management of nuclear materials. Because they serve without the expectation of any compensation other than their own personal satisfaction, it is possible that much of what they do goes completely unnoticed; however, the cumulative impact of their service is significant. I offer my deepest respect and sincere thanks to everyone who has supported the Executive Committee over the past two years.

In addition to this volunteer community, INMM is also served by an outstanding professional administrative staff. The Sherwood Group has provided administrative support to INMM for more than thirty years, and their expertise and experience is evident in everything they do. INMM's headquarters staff kept me on the right path too many times to count over the past two years, and it would not have been possible for me to perform my role as president if not for their incredible organization and insights. All of the INMM support staff are exceptional, but I am compelled to specifically recognize Jodi Metzgar for her assistance. Jodi assumed the role of executive director of INMM shortly after I became president, and she provided support as if she had held the position for many years. "Thank you" is not adequate to express my gratitude to Jodi and the rest of the headquarters' staff.

I am also compelled to recognize those who supported me even before I assumed the office of INMM president. I have encouraged all of you to mentor young nuclear professionals in previous columns, and the reason that I am passionate about mentoring is because of the impact it had on my own INMM experience. Fresh out of graduate school in 1988, I took my first job and was immediately told to support Billy Cole in his role as chair of the Packaging and Transportation Committee within INMM. I did not even know how to spell INMM, let alone understand what the organization was about. But with Billy's guidance, as well as personal interaction with Ed Johnson, I quickly came to appreciate the significance of the Institute and the impact it has on global nuclear materials management.

I was unable to accomplish everything that I set out to do two years ago, but I do not intend to discontinue pursuit of those goals even though my term as president is ending. My most significant "unfinished business" is pursuing greater involvement in INMM by the legal community. I recently assumed the role as vice chair of the Nuclear Regulatory Committee within the Energy Bar Association, and I hope to use this platform to inform this community of the resource available to them through INMM.

Finally, INMM has a very strong incoming president. I have worked with Ken over the past two years, and I am confident that he will provide INMM with the strong and insightful leadership that will successfully increase the recognition and respect of INMM across the globe.

On Science for Verification

By Dennis Mangan
INMM Technical Editor

This issue of our *Journal* on Science for Verification was requested and formulated by Jim Larrimore, the chair of the INMM International Safeguards Technical Division. Mark Schanfein of Idaho National Laboratory, USA, was instrumental in collecting the articles for this issue and was also instrumental in accomplishing the peer-review process. There are fifteen technical articles in this issue, representing a eight countries, which reflects our international support. Within the United States, eight different national laboratories contributed. These fifteen articles reflect a wide diversity of topics and technologies. Larrimore and Schanfien are to be complimented, along with all the authors who contributed.

Herman Nackaerts, the Deputy Director General for Safeguards at the International Atomic Energy Agency, provides an interesting and excellent foreword for this issue. He provides excellent insight into the proliferation future that the IAEA needs to address.

Associate Book Review Editor Mark Maiello provides interesting review of Richard Rhodes' new book, *The Twilight of the Bombs.* As many of you may recall, Rhodes was a well appreciated plenary speaker at our Annual Meeting several years ago. His new book appears to be one worth reading, just as his others have been. He apparently visits the past in the area of nuclear weapons.

Jack Jekowski, our Industry News Editor and chair of the INMM Strategic Planning Committee, continues to give us very good insights into "Taking the Long View" with regards to the future of the Institute, including the potential impact of the global economic and fiscal crisis on the attendance at our Annual Meeting.

This issue contains much to read and enjoy.

Should you have any questions or comments, please feel free to contact me.

JNMM *Technical Editor Dennis Mangan can be reached by e-mail at dennismangan@comcast.net.*

In our on-going celebration of forty years of JNMM, we present some of articles from the past on the INMM Web site. Visit www.inmm.org/JNMM40 to review the featured articles, and read about the history of the Journal.

Foreword

By Herman Nackaerts, Deputy Director General for Safeguards, International Atomic Energy Agency, Vienna, Austria

To deter effectively the proliferation of nuclear weapons, the International Atomic Energy Agency (IAEA) must look beyond the nuclear material and facilities declared by a state and provide assurance that there are no undeclared nuclear material and activities in the state. In other words, the IAEA needs to have a better understanding of a state's nuclear program as a whole. That is why the IAEA, when also faced with an increasing workload and a static budget, has decided that it must continue to evolve the way it implements safeguards.

The focus of this evolution is the advancement of the state-level concept: a holistic approach to safeguards implementation. In practice, this involves maintaining a continuous state evaluation process, re-assessing traditional approaches to risk and placing renewed emphasis on the objectives of safeguards rather than the criteria applied to their implementation. It means making use of all available safeguards-relevant information and of the collaborative analytical culture and procedures necessary to process it. These developments, which are being actively and systematically pursued within the IAEA, also have implications for the role of science and technology in safeguards implementation.

The need to provide assurance of the completeness of state declarations significantly complicates the analytical process that supports safeguards conclusions: it cannot solely rely on an analysis of discrepancies between state nuclear material accounting declarations and the IAEA's verification results. The IAEA must draw on a vast amount of available information emanating from a wide variety of sources—for example, satellite imagery, international trade data, open-source literature—all of which needs to be gathered, processed, certified, and analyzed in a consistent and structured way. It is the knowledge obtained through such analysis, rather than the quantity and type of nuclear material involved, that determines the verification approach to be implemented in each state. This is where scientific applications come into play. In recent years, impressive developments have occurred in the automated analysis of unstructured information, dedicated network search engines, game theory applications, image processing, geo-information systems and so on. These have already influenced significantly safeguards implementation.

Looking beyond declared nuclear material and facilities requires the agency to make better use of all the tools it has available, such as special inspections, and, where additional protocols are in force, complementary access. Facilitating the execution of such inspections and access is one of the most challenging tasks for scientific support. Alongside powerful laboratory analytical capabilities applied to samples obtained during such inspections and access, there is potential for the extended use of portable field instrumentation. In addition to already available portable radiation tools, specific new technological innovations with potential in-field safeguard applications include: the miniaturization of traditional "laboratory-based" techniques, such as laser and Raman spectroscopy; chip-based chemical analysis; and early versions of portable mass-spectrometers, some of which are now approaching sufficient maturity to meet in-field requirements.

Science also continues to play a crucial role in the verification of declared nuclear material. Here, measurement techniques relating to nuclear material accountancy have benefited from rapid progress in such areas as computer sciences, information and communication technologies, and statistical analysis. Maintaining the highest standard of operation and attaining further improvements and efficiencies in the traditional safeguards toolkit will remain essential for the foreseeable future.

Without doubt, science sits at the forefront of effective international safeguards implementation. The international community of scientists, engineers, and innovators who participate in safeguards-relevant work continues to contribute significantly to meeting the IAEA's requirements by finding specific technical solutions in relation to all aspects of the verification process. We greatly welcome scientific innovation and support in relation to new analytical capabilities at IAEA headquarters, just as we appreciate the improvements to the technological capabilities our inspectors take into the field. It is very encouraging to observe increasing efforts being devoted to cross-cutting areas of verification activities such as integrated information analysis, knowledge management concepts, and acquisition path analysis. It is equally encouraging to see new ideas and approaches being promoted in the traditional safeguards domain of nuclear materials accountancy,

I believe that the contributors to this special issue of *JNMM*, as well as their colleagues in the wider scientific community working on safeguards-relevant technologies, can play a vital role in helping the IAEA to implement safeguards more effectively and efficiently and thereby to deter the spread of nuclear weapons.

A Canadian Perspective in the Development of IAEA Equipment

R. Kosierb, P. Button, and R. Awad
Canadian Nuclear Safety Commission, Ottawa, Ontario, Canada

Abstract

In order to perform their verification duties, International Atomic Energy Agency (IAEA) inspectors require robust, lightweight, user-friendly, and proven instrumentation. The Canadian Safeguards Support Program (CSSP) recognizes the need for these characteristics along with the requirement for immediate results while in the field. When the CSSP researches technologies for development, it attempts to ensure the science will meet these and other beneficial traits and ensure it resolves an IAEA operational issue. Three successful technologies pursued by the CSSP have been in ultra-violet light analysis, data acquisition, and laser induced breakdown spectroscopy sciences with the development of the Digital Cerenkov Viewing Device (DCVD), the Next Generation Autonomous Data Acquisition Module2 (ADAM2) Module (NGAM), and the Hand-Held LIBS System (HHLS). In designing these devices, the CSSP attempts to include resources that exceed the requirements of a basic model. In the situation for NGAM, the device has the ability to expand beyond the present replacement need. The other two instruments have different traits which exceed the operational requirement. This paper reports on these characteristics for these three instruments that go beyond the basic functionality.

Introduction

A major shift in the safeguards paradigm took place with the adoption of INFCIRC/540, the Additional Protocol. These arrangements allow the International Atomic Energy Agency (IAEA) to seek assurance on the completeness of a state's nuclear declaration. Prior to this, the IAEA only needed to verify declared material. The agency faces a much broader set of challenges when trying to verify the absence of undeclared material/activities. The determination of the correctness of a state's declaration in this aspect is a much more open-ended objective.

Trying to meet these objectives with limited resources and the expected expansion of the nuclear fuel cycle worldwide, the IAEA needs to rely heavily on science and technology to assist in performing this mandate. Instruments employed to assist the IAEA in completing this mandate offer some unique challenges beyond those present in a nuclear environment. Operationally, the IAEA is an international organization and any employed equipment must meet global standards. This requirement is unlike devices used solely within a specific state. Having a single instrument meet the diverse worldwide power standards is just one of the demanding traits an IAEA instrument must possess. These challenging capabilities must be addressed in any instrumentation being introduced or developed in consideration for employment by the IAEA for them to achieve their global verification mandate.

Specifications

The key to successfully introducing/developing a device for the IAEA is to know the functional requirements the equipment is to perform. Is the equipment going to be employed throughout the world or in a specific location? Will the instrument be used in an internal or external environment? This latter need introduces other parameters such as extreme temperature fluctuations, ruggedness to weather conditions, etc., which the instrument must possess. Will the device be permanently installed at the nuclear facility (i.e., unattended) or constantly transported to perform the verification task? Size, weight, and ruggedness influence the characteristics of the equipment in response to this question. These traits are highly influential if the instrument is to be employed in a hand-held mode but somewhat less if permanently affixed at a nuclear site. Transportability is an issue if hazardous material (radioactive source, lithium-ion battery, etc.) are present within the device.

Functionality should also address the communication question. How is the instrument intended to interact with the user? The resulting information can be presented to the user in an easily interpreted format (the simplest being a "go/no go" style) or a complicated spectrum that needs to be deciphered prior to performing any further actions. Is the required information available instantaneously to the equipment user, or immediately processed to the IAEA headquarters in Vienna, or both? This question poses further inquiries on the needs for security and storage of the instrument's results. It is essential the IAEA maintains tight security on the information so transmission of the data across the world requires enhanced security. The situation where the device is left unattended, be it for a short time or constantly, needs to be addressed by means of a thorough Vulnerability Assessment.

These questions/challenges and many others including maintenance, training, and cost requirements can be dealt with

by employing either proven equipment or specially developed "state-of-the-art" instrumentation. These two equipment categories even have their own challenges. Proven instruments are devices that have been developed and have been in operation for at least, a few years. Usually, this type of equipment requires modifications to suit the IAEA's needs, possibly imposing cost and design challenges. State-of-the-art technology provides the IAEA with a more effective and efficient means to perform their duties. However it does have the drawback in that the equipment, in most cases, will not be physically adaptable and/or rugged enough to meet their needs initially. Although these past paragraphs only discussed a few of the challenges in developing or adopting equipment for the IAEA, the Canadian Safeguards Support Program (CSSP) considers these requirements and many others in providing instruments to the IAEA. It further considers some other unique needs which go beyond the functionality requirements of the IAEA.

Canadian Perspective

Since 1978, the CSSP has been providing instrumentation to the IAEA for the verification requirements within Canada and abroad. In doing so, the CSSP recognized that any instrumentation provided to the IAEA should have the capabilities of being *expandable*. An expandable capability avoids the equipment being obsolete within a few years of its deployment within the IAEA. This trait also allows other features to be added, upon the IAEA recognizing other uses the instrument could serve to assist in their verification task. This additional employment is not restricted solely for the IAEA environment.

It has been long recognized by the CSSP that it was difficult for commercial entities to support products developed specifically for the IAEA due to the specialized requirements and the low product volume. A wider application of the same equipment to different markets and various applications would strongly benefit the IAEA in the quality, performance, supportability, sustainability, and cost of the instrumentation. The increased use of a modular concept with electronics has made the adoption of this functionality capability much easier. However, there are situations where a dual use capability is not available initially. In this situation, the CSSP tries to ensure the equipment is expandable.

Three examples of CSSP sponsored equipment in exceeding the basic functionality are the Digital Cerenkov Viewing Device (DCVD); the Next Generation ADAM (Autonomous Data Acquisition Module) Module (NGAM) and the Hand-Held Laser-induced breakdown spectroscopy [LIBS] System (HHLS).

Digital Cerenkov Viewing Device (DCVD)

In 1993, the IAEA requested that the CSSP and the Swedish Safeguards Support Program jointly develop a more sensitive Cerenkov Viewing Device (CVD) to verify long-cooled light water reactor (LWR) spent fuel. The practical limit for the CVD to detect long-cooled spent fuel is about twenty-five years. A requirement to verify forty-year cooled spent fuel with a burnup of 10,000 MWd/t U was then set as the goal because forty years was the anticipated lifespan of a reactor and the first fuel discharge from these reactors is frequently low in burnup. A number

Figure 1. First workable DCVD version

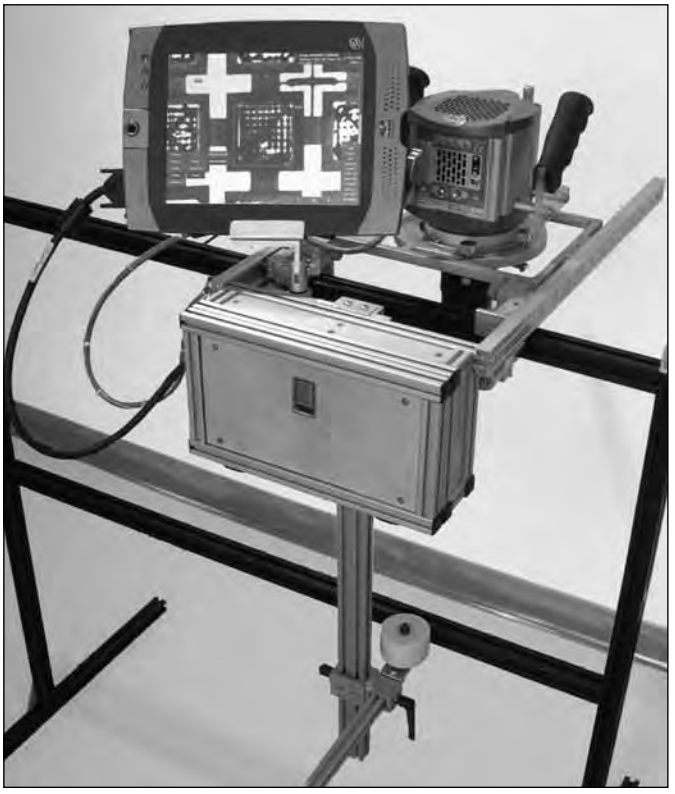

Figure 2. Agesta fuel, which was thirty-six years old (2004) with a burnup of 1180 MWd/t U

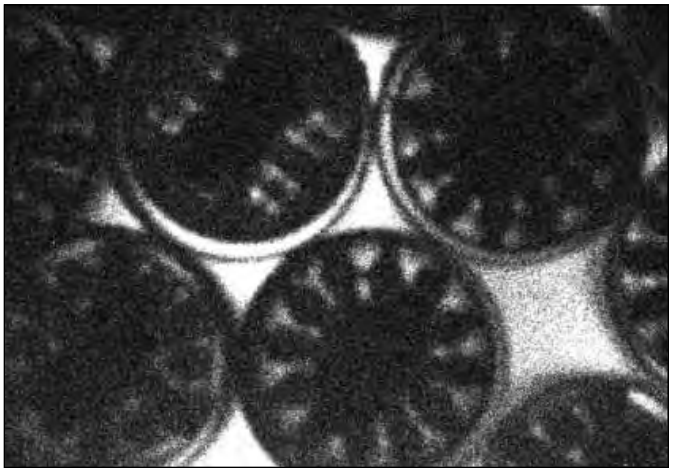

Figure 3. LWR spent fuel assemblies with missing (a) and substituted rods (b) Rods accessed Alphabet across/Numbers down
a) PWR 15x15 17 years cooled (2007) and burnup of 42,998 MWd/t U - Missing K, L, M, and N area of 2-3
b) BWR Exxon 9x9 10-years-cooled (2007) and burnup of 34,403 MWd/t U – at D3, EA, F5 and G6 and zircaloy rod at C8.

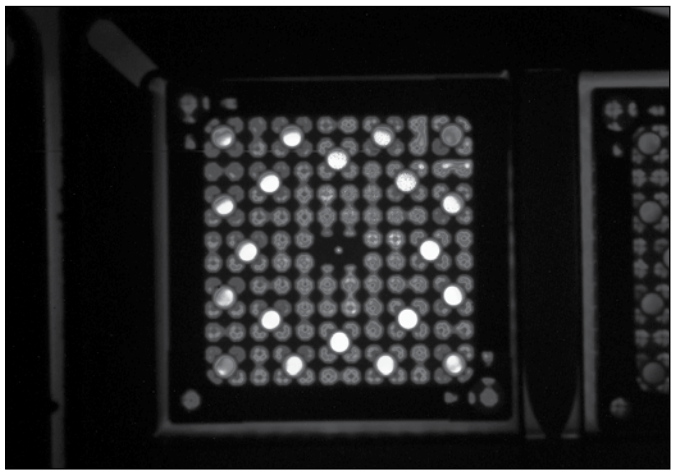

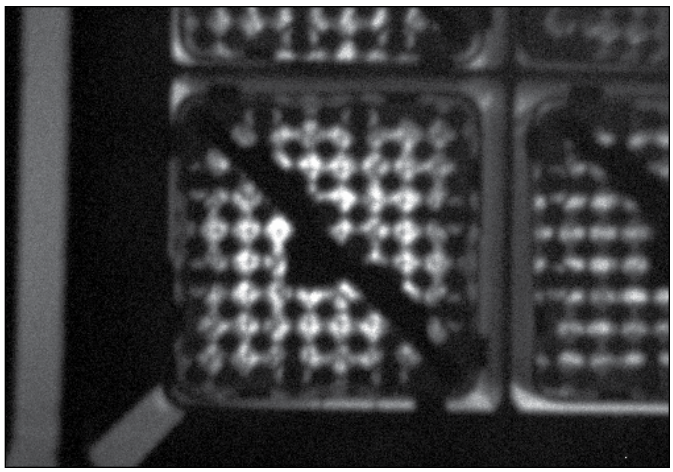

Figure 4. Enhanced DCVD

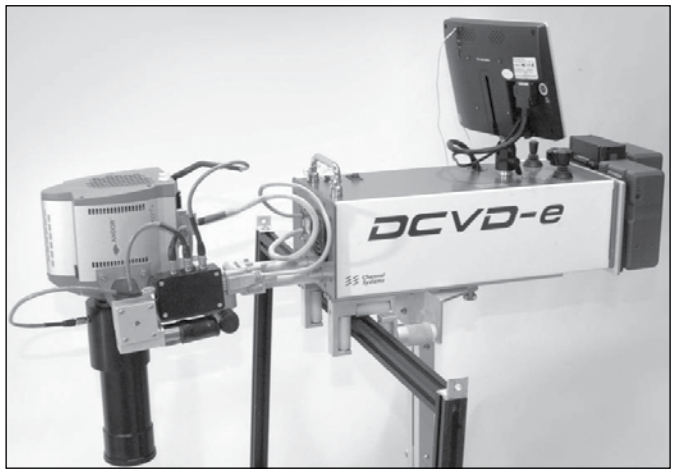

Figure 5. IAEA staff investigating the DCVD as a partial defect indentifier

of instruments with high sensitivity were developed to meet the measurement criteria.[1-5] However, it wasn't until 2002 when technology advanced sufficiently enough to meet the challenge: high sensitivity and high frame rate. Thus, the new advancements allowed the support programs to develop a device that exceeded the original requirement. A device was donated to the IAEA, Figure 1. This DCVD was able to verify thirty-six-year-cooled spent fuel with an extremely low burnup of 1180 MWd/t U which is about eight times lower in intensity than the target fuel,[6] Figure 2.

Like its predecessor, the CVD, the DCVD verifies spent fuel using a scanning technique where the DCVD is moved along a row of fuel. The detection of the Cerenkov light is due to the characteristic collimation effect of the spent fuel. Light intensity values and images are dynamically displayed on the LCD screen. The DCVD has the advantages that it is not intrusive (no immersion into the water pond) and the analysis is relatively fast. Due to its ability of measuring the light intensities, it was thought the DCVD had the potential to detect partial defects. A partial defect is presently defined by the IAEA as a LWR spent fuel assembly having 50 percent of its fuel rods missing and/or substituted, Figure 3. After the IAEA approved the DCVD as gross defect verifier, the IAEA requested the two support programs to investigate this partial defect potential.

Development of the equipment itself continued while studies were investigating this dual functionality. In 2008 a new version, Figure 4, was introduced. This version had the benefit of a 80-200mm zoom lens vice having to manually interchange between a 105mm and a 250mm lens. The measurement sensitivity was also improved to more than three times that of the previous version. Motorized controls were added for the focus, zoom, pan, and

Figure 6. The present DCVD version

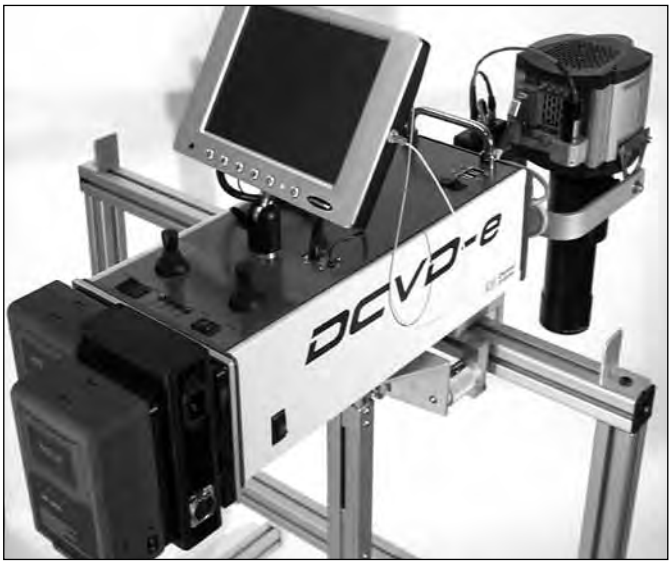

tilt operations. Battery technology also advanced so this version only required two batteries instead of three without sacrificing runtime. This DCVD-e version provided improved sensitivity to better detect partial defects.

It was in 2011, Figure 5, that the two support programs were able to demonstrate to the IAEA that the DCVD could detect partial defects.[7-10] The newest version assisted in achieving this goal with an enhanced graphic user interface, an alignment aid, and a region of interest follower.

With 194 LWRs worldwide (2009 Figure), the Canadian and Swedish Safeguards Support Programs were able to provide the IAEA with an instrument which could verify long-cooled fuel beyond forty years old as well as provide the dual functionality of detecting partial defects in fuel assemblies generated by these facilities. Presently, other possible employments are being investigated for this instrument. The two support programs have successfully provided the IAEA with much more user friendly and automated instrument in which the inspector can spend more time in reviewing the results rather acquiring the data, Figure 6, and fulfill two of their needs.

Next Generation ADAM Module (NGAM)

A further example of expandability is the Next Generation ADAM (Autonomous Data Acquisition Module) or NGAM, Figure 7: a successor to the ADAM module originally developed for the VXI [Vmebus eXtensions for Instrumentation] Irradiated Fuel Monitor (VIFM) system. The VIFM system was an initiative established in the early 1990s by the Canadian Nuclear Safety Commission (CNSC) and the International Atomic Energy Agency (IAEA) to create a standardized platform for monitoring equipment within CANadian Deuterium Uranium (CANDU)

Figure 7. The ADAM2

reactors. Originally configured for the VXI bus standard, it has evolved to operate over a standard network connection. The NGAM was designed to be backward compatible with both the VIFM family of systems and to anticipate future and expanded requirements.

The NGAM is a data acquisition module for up to eight radiation detectors with extensive data storage and connectivity capabilities. Like its predecessor, it can be configured in groups to form a facility specific system. Signals from the current VIFM type detectors (Core Discharge Monitor, Bundle Counters and Yes/No monitors) pass through an amplifier, discriminator, and then a counter. The signal then goes to a Digital Signal Processor (DSP). The digitized data then goes to an Advanced RISC [Reduced Instruction Set Computing] Machine (ARM) 7 processor, which stores the data in a Structured Query Language (SQL) database on a main and backup universal serial bus (USB) drive (i.e., redundant storage). Requests for data via the Ethernet connection are routed through an ARM 9 processor which then communicates with the ARM 7 processor to retrieve any requested data from the USB drives. The ARM 9 processor provides full support for Web browser screens. In total, these features amply support the requirements of the legacy VIFM systems.

Generic requirements for a non-destructive analysis instrument would also include multi-channel analysis (MCA) and specialized counting such as neutron coincidence counting. Due to advances in technology, the implementation of an MCA is a relatively simple exercise once the basic analog and digital infrastructure is in place. The NGAM hardware incorporates both a field programmable gate array (FPGA) and a DSP, both relatively underutilized in the current NGAM. It would also appear that a coincidence counter complete with list processing of events could also be implemented given the hardware capabilities. The various applications would require inputs from a variety of detector types. Fortunately, interfaces to those detectors are already available as commercial off-the-shelf (COTS) items. Whereas the current installed VIFM systems rely on a local "collect computer" to aggregate, evaluate and forward data to the IAEA, this function will likely be moved to a central location in

Figure 8. A basic schematic of LIBS technology

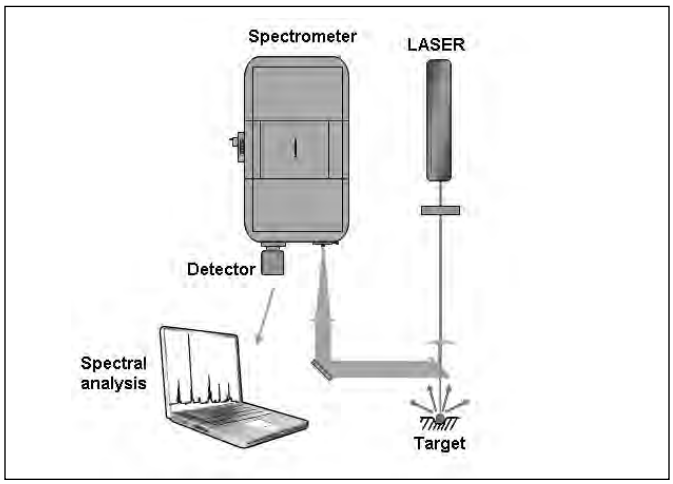

the near future. Since the NGAM has a separate processor dealing with external requests for data and browser compatible screens, this is easily achievable.

Dispensing with the traditional collect computer also opens up a number of environmental and security monitoring applications. These applications need equipment that is rapidly deployable. There is also likely to be a need for geo-location and a central command structure with real time data communications. To these ends, the NGAM basic design requirements were extended to include not only local display and control but also the integration of a global positioning system (GPS) capability and a communications capability (via general packet radio service [GPRS] and a local wireless network).

The Hand-Held LIBS System (HHLS)

As a third example of the expandable and dual functionality characteristics, the CSSP introduced the IAEA to the laser-induced breakdown spectroscopy (LIBS) technology shortly after their announcement seeking assistance from member states to acquire novel technologies. The IAEA considers the word *novel* to indicate technologies never used within its organization. It could be either well-established worldwide or be state-of-the-art technology. This novel methodology was thinking beyond the traditional sense of detecting radiation.

In simple terms, LIBS is where a high-power laser is focused on a material to be analyzed. A very small amount of the material (nanogram) is vaporized, producing plasma. The light emitted by the plasma is analyzed by an optical spectrometer. With the appropriate software, the elemental composition can be used to identify the material compound, Figure 8. The advantages of this technology are no sample preparation is required; only a small amount of the material is actually sampled (typically a fraction of a ng); with the appropriate equipment the sample can be any form; the sampling can be performed on the surface or concentrated

Figure 9. The CSSP donating a portable LIBS system to the IAEA

Figure 10. A conceptual image of the handheld LIBS System

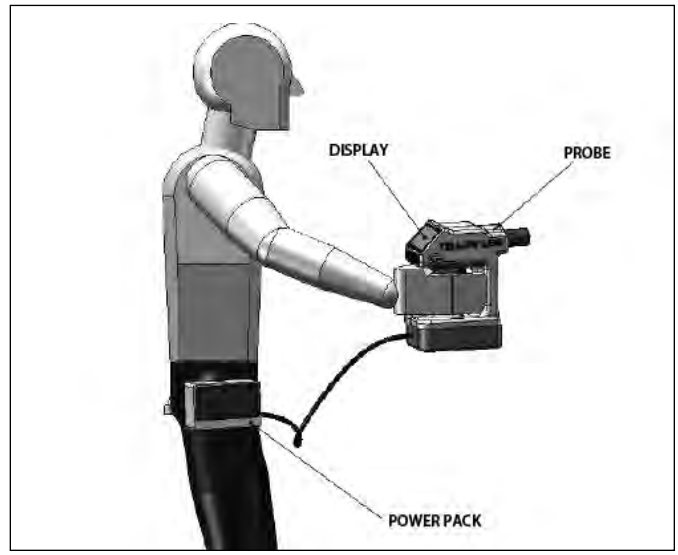

further within the material; samples do not need to be removed to another location for analysis unless for confirmation purposes; it requires little training to operate; and a single or a multiple shot analysis can be performed within seconds.

Because of these advantages, a handheld version can fulfill two roles for the IAEA, Figure 9. In a complementary access mode, it would provide instant identification of unknown material allowing appropriate and timely modification of the inspection process to resolve any anomalies. The device can also enhance the in-field measurements taken during an inspection by identifying material and screening that material to minimize the number of samples requiring further detailed laboratory analysis. This capability would be an asset to any first responder (police and fire fighters) or border security personnel.

A handheld version depicted in Figure 10 would assist this group of people by identifying or confirming suspicious material at an event. The internal database containing the data on the

material of interest would be the only item requiring change between the various user groups. The CSSP is the process of developing such an instrument, which could have a larger market than solely the IAEA.

Conclusion

Expandability and dual functionality characteristics, as well as other unique traits such as worldwide usage, must be considered when developing equipment for the IAEA. Fortunately, there are numerous technologies, both state-of-the-art or mature, that could have possible employment by the IAEA. Three such technologies have been described here. They have been designed to overcome many of these unique challenges in the areas of functionality, communication, security, etc., while adding expandability and dual-use features. The IAEA needs effective tools to achieve its objectives and understanding their needs is the first step in developing/introducing equipment for their employment.

References:

1. Attas, E. M., G. R. Burton, J. D. Chen, G. J. Young, L. Hildingsson, and O. Trepte. 1997. A Nuclear Fuel Verification System Using Digital Imaging of Cerenkov Light, *Nuclear Instruments and Methods in Physics Research A* 384, 522-530.
2. Hildingsson, L., J. D. Chen, A. F. Gerwing, B. Lindberg, E. Sundkvist, O. Trepte, and P. Ward-Whate. 1999. Digital Cerenkov Viewing Devices, *Proceedings of the 21st Annual ESARDA Meeting on Safeguards and Nuclear Materials Management.*
3. Chen, J. D., A. F. Gerwing, R. Keeffe, M. Larsson, K. Jansson, B. Lindberg, E.Sundkvist, U. Meijer, M. Thorsell, and M. Ohlsson. 2001. Long-cooled Spent Fuel Verification Using a Digital Cerenkov Viewing Device, *IAEA Symposium on International Safeguards: Verification and Nuclear Material Security.*
4. Axell, K., J. D. Chen, A. F. Gerwing, R. Keeffe, L. Hildingsson, M. Larsson, B. Lindberg, R. Maxwell, M. Thorsell, and F. Vinnå. 2003. The Digital Cherenkov Viewing Device – A Means to Verify 40 Years Cooled Spent Fuel, *Proceedings of the 25th Annual ESARDA Meeting on Safeguards and Nuclear Materials Management.*
5. Chen, J. D., A. F. Gerwing, R. Maxwell, M. Larsson, K. Axell, L. Hildingsson, B. Lindberg, and F. Vinnå. 2003. An Advanced High Sensitivity Digital Cerenkov Viewing Device, *Proceedings of the Institute of Nuclear Materials Management 44th Annual Meeting.*
6. Chen, J. D., R. Kosierb, A. F. Gerwing, D. A. Parcey, B. D. Wilcox, M. Larsson, K. Axell, J. Dahlberg, B. Lindberg, E. Sundkvist, and F. Vinna. 2008. DCVD Consolidated Summary Report, unpublished.
7. Chen, J. D., D. A. Parcey, A. F. Gerwing, R. Kosierb, M. Larsson, K. Axell, J. Dahlberg, B. Lindberg, and E. Sundkvist. 2009. Quantitative Studies for the Detection of Partial Defects in LWR spent fuel, CSI Report CN36D06.
8. Chen, J. D., and D. A. Parcey. 2011. Detection of Partial Defects Using a Digital Cerenkov Viewing Device, CSI Report CN47D08.
9. Chen, J. D., D. A. Parcey, R. Kosierb, M. Larsson, K. Axell, J. Dahlberg, B. Lindberg, S. Grape, and E. Sundkvist. 2011. Detectopm of Partial Defects in LWR Spent Fuel Using a DCVD.
10. Kosierb, R., D. A. Parcey, K. Axell, J. Dahlberg, A. S. Jung, B. Lindberg, S. Grape, and E. Sundkvist. 2011. The Digital Cerenkov Viewing Device Uncertainty Study, CSSP Report #2011-10, Ver 1.3.

Recent JRC Achievements and Future Challenges in Verification for Nuclear Safeguards and Nonproliferation

W. Janssens, K. Luetzenkirchen, H. Emons, S. Abousahl, Y. Aregbe, R. Berndt, G. Cojazzi, M. Hedberg, F. Littmann, K. Mayer, P. Peerani, and V. Sequeira
European Commission, Joint Research Centre, Ispra, Italy

Abstract

Research and development (R&D) in nuclear safeguards, nonproliferation, and nuclear security is a cornerstone of the Joint Research Centre (JRC) Nuclear Safety and Security Work Program. The main stakeholders are the Euratom safeguards authority and the International Atomic Energy Agency and close contact is maintained with the nuclear facility plant operators. More recent customers include, e.g., authorities dealing with trade of sensitive goods and those dealing with nuclear security measures. This paper illustrates a number of the latest JRC safeguards and nonproliferation related developments, describing the rationale for the R&D, the recent achievements, the continuing challenges, and the outlook for deployment in future nuclear fuel cycle facilities and activities. With respect to the nuclear materials verification, examples of recent developments focus on the front end of the nuclear fuel cycle, high-level quality systems, and quality control tools for the measurements in enrichment and reprocessing facilities and the fuel cycle back end. At the facility level, continued emphasis is put on enhanced process monitoring and modeling of material flows, advanced sealing and surveillance techniques, and unattended and remotely operated systems. Both inside and outside the facility, environmental sampling and other verification methods (e.g., laser-based methods and satellite imagery) continue to pose challenges. With respect to the overall evaluation and/or verification of state activities and capabilities, open-source analysis, mainly focusing on trade of sensitive technologies, proves to provide significant potential. Finally at the conceptual level, the activities of safeguards by design and assessment of proliferation resistance of future nuclear fuel cycles allow to both assess and integrate the developments previously referred to. The paradigm of nuclear safety, security and safeguards is also shortly touched upon in this paper.

Introduction

The R&D in nuclear safeguards and nonproliferation at Joint Research Centre (JRC) is oriented towards the needs of its main customers. These are within the European Commission (EC) in a first instance Directorate General (DG) for Energy (ENER) (best known as "Euratom") and globally the International Atomic Energy Agency (IAEA). Strong collaboration exists between the JRC and the U.S. Department of Energy (DOE), based on a long-standing agreement, whereas strategic partnerships have been signed more recently with the French CEA and the British AWE. In addition, JRC has memoranda of understanding in this field also with Japan, China, and others.

JRC is a major driving force behind ESARDA (the European Safeguards Research and Development Association) and a regular contributor to INMM (Institute for Nuclear Materials Management). As a further input for the establishment of its R&D program, JRC has regular contacts with the nuclear fuel cycle industry, both in Europe and abroad. JRC also is gaining significant field experience through its support program outside Europe (previously under TACIS and more recently under InSC (Instrument for Nuclear Safety Collaboration, including safeguards) and also under IfS (Instrument for Stability, including more of the nonproliferation work). Other more recent customers to its program are DG Trade and DG Taxud.

Nuclear safeguards and nonproliferation continues to pose significant challenges due to a variety of factors despite its existence for more than fifty years as a legal and scientific discipline, as confirmed in the strategy papers of the organizations listed above. First of all, the high expectations of the international community have to be satisfied regarding the avoidance of any clandestine activities using nuclear materials. This includes the prevention or detection of misuse of nuclear fuel cycle technology for non-civil purposes. Secondly, the legal obligations have to be fulfilled for assuring the verification of all declared nuclear materials in a set of, sometimes highly complex, nuclear fuel cycle facilities, with large (international) flows of nuclear materials and with the continuous request to increase efficiency and effectiveness of the inspections. Thirdly, the commercial sensitivity of many nuclear fuel cycle steps has to be respected, not allowing a priori the *inspectors* to have full details of all processes and parameters in the facilities. Fourth, the *competition* between the importance of safeguards and nonproliferation considerations has to be considered in relation to safety and security issues. There are both synergies and possible conflicts between the 3S and striking the right balance requires consistent analysis methodologies and approaches.

Figure 1. NUSIMEP-7 results for n(^{235}U)/n(^{238}U) sorted according to instrumental techniques

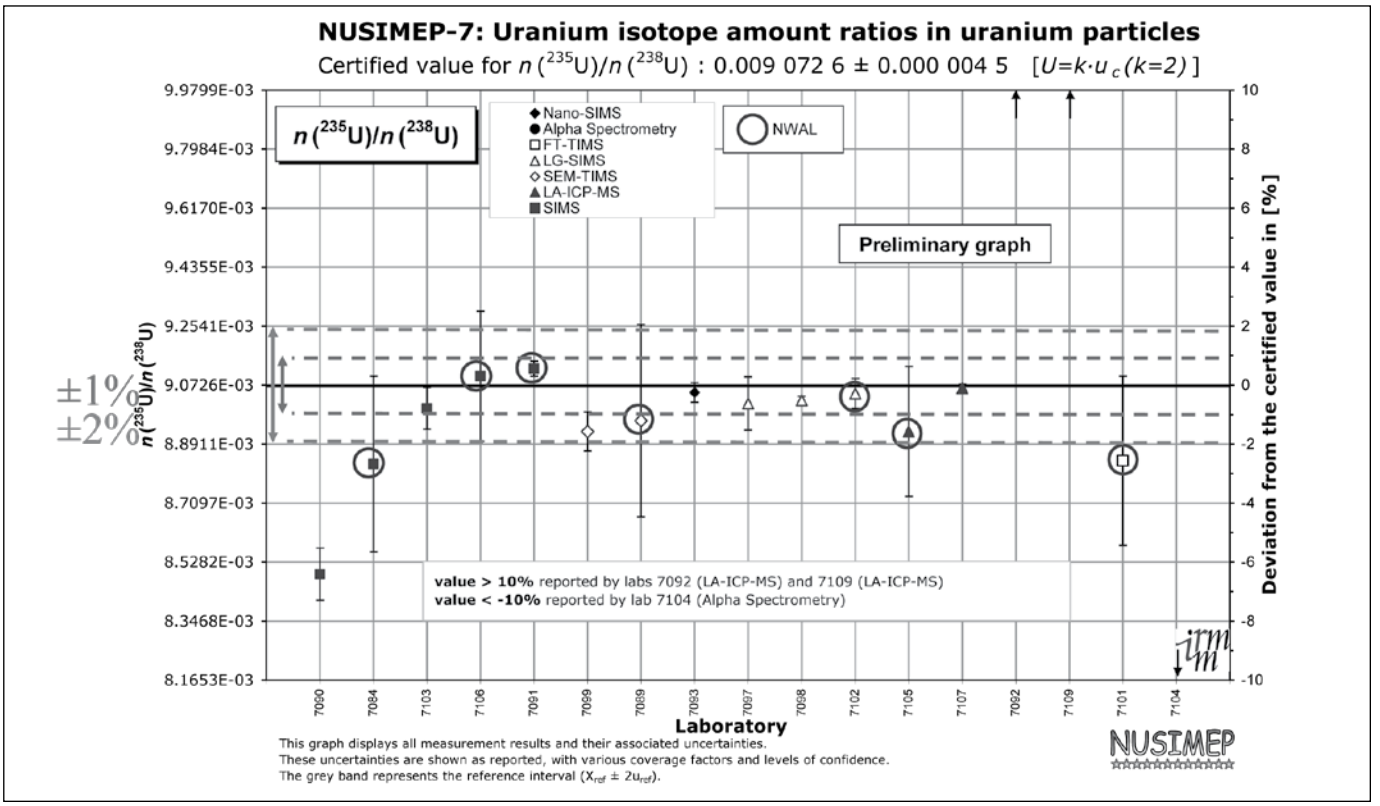

This paper highlights some key developments and future plans of the JRC R&D portfolio in nuclear safeguards and nonproliferation. The first part contains a few chapters with distinct novelties, based on the competencies of the different research groups on the three sites where JRC executes safeguards R&D at IRMM (Institute for Reference Materials and Measurements) at Geel, Belgium, and at ITU (Institute for Transuranium Elements) at Karlsruhe, Germany, and Ispra, Italy. The second and third parts include examples where different competences are integrated to develop new safeguards concepts/approaches, to contribute to proliferation resistance and to tackle the challenge of controlling the use and trading of sensitive technologies.

New Developments in Safeguards R&D to Support Verification of Declared Activities and Prevent/Detect Misuse of Declared Facilities (e.g., with Use of Non-Declared Materials)

Measurements of Nuclear Materials

Development of Reference Materials and Standards

In the context of the *ISO/IEC Guide 2:2004 'Standardization and related activities - General vocabulary'* a documentary standard ("norm") is a prescription of characteristics for products, processes (including services), systems, or persons, whereas 'material(ized) standards' are either prototype devices/products or measurement standards ('etalons') and benchmarks, e.g., certified reference materials. Verification and detection in safeguarding nuclear material, conformity of information on materials and processes in nuclear forensics, as well as decisions and actions in nuclear security must be based on reliable measurement results ensured with appropriate material standards and quality control/conformity assessment tools. The IRMM is one of the leading institutes for supplying nuclear reference materials and providing dedicated inter-laboratory comparison schemes in the frame of fulfilling the existing requirements for nuclear material and environmental sample analyses. Reference materials are indispensible for method validation/verification and instrument calibration, for establishing metrological traceability and thereby comparability of measurement results, for estimating the respective uncertainty of measurement results and for sound internal and external performance evaluations.

At IRMM, emphasis is given to the development and optimization of new isotopic reference materials to support nuclear laboratories in meeting the revised International Target Values for Measurement Uncertainties in Safeguarding Nuclear Materials (ITVs).[1] Recently IRMM has organized the inter-laboratory comparison NUSIMEP-7 focusing on measurements

Figure 2. The real-time simulation process instrumental techniques

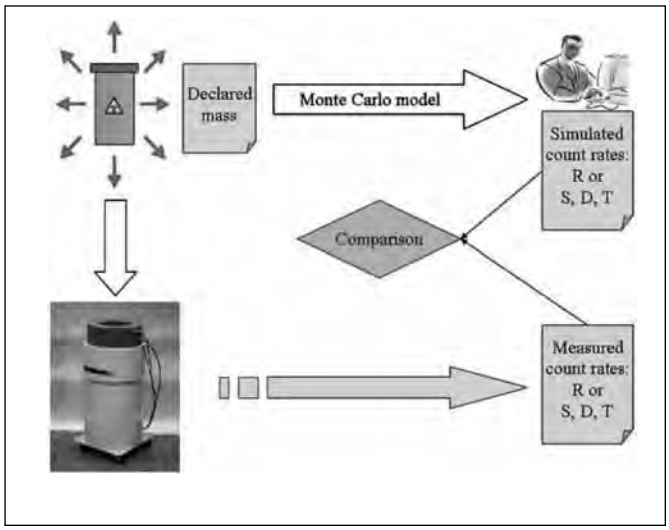

of uranium isotope amount ratios in uranium particles (diameter < 1 µm).)(see Figure 1.) This was highly appreciated by European Safeguards and the IAEA's Network of Analytical Laboratories (NWAL). NUSIMEP-7 has not only confirmed the capability of laboratories worldwide, but has also underpinned the recent advances in instrumental techniques in the field of particle analysis.[2] There is an urgent need for uranium reference particles standards, particularly with the installation of Large Geometry Secondary Ion Mass Spectrometry (LG-SIMS) instruments at the leading laboratories in this field.

Currently IRMM is engaged in cooperation with ITU, in a study on the development of plutonium reference materials for "age determination," i.e., to measure reliably the time elapsed since the last separation of plutonium from its daughter nuclides. The disintegration of a radioactive parent isotope and the build-up of a corresponding amount of daughter nuclide serve as built-in chronometer to calculate the age of the material needed in nuclear forensics and nuclear security. There are no such certified reference materials available yet.

Non-destructive Analysis Supported by Modeling

Non-destructive analysis is a cornerstone of nuclear material accountancy and accounts for the majority of measurements performed by nuclear inspectors for verification purposes. Notwithstanding the long experience developed in fifty years of inspections, non-destructive analysis techniques have followed a continuous evolution process aiming to reach better performances (higher accuracy, shorter measurement time) or reduce the inspection effort (unattended equipment, remote operation). The development of novel, more efficient, better deployable non-destructive analysis instruments has recently encountered some difficulties linked to two major problems:

- the availability of appropriate nuclear material standards for calibration of instruments
- the shortage of He-3, historically the technology on which neutron counting techniques rely for nuclear materials (NM) mass determination

JRC has oriented its R&D efforts on non-distructive analysis towards the solution of the above-mentioned issues.

Computational simulation of non-destructive analysis equipment, generally through Monte Carlo codes, has been developed and successfully applied to numerical calibration of instruments in cases where experimental calibration was not applicable due to lack of standards or complex geometries.[3] The recent achievements and future trends are directed towards the automation of modeling (allowing the use of Monte Carlo technique without needing the inspector to be an expert modeler) and the real-time computation (running the numerical simulation during the non-distructive analysis measurement in order to have immediately the confirmation of the measurement results).

Moreover JRC is analyzing suitable technologies for He-3 replacements by testing the performances of innovative neutron sensors and analyzing their possible application to nuclear safeguards instruments. Several concepts have been considered: plastic and liquid scintillators coupled with neutron absorbers (Gd, Cd, Li, B) in different configurations (homogeneous doping or heterogeneous coating); gas-filled proportional counters with boron; scintillating fibers with Li and high pressure scintillating gas. A prototype of neutron well coincidence counter as replacement of high-level neutron coincidence counter (HLNCC) based on liquid scintillators with pulse shape discrimination is under design in collaboration with the IAEA.

A very good example of a currently still open issue with regard to NDA on declared nuclear material is the supervision of the contents of the very large UF_6 containers, which remains a challenge for nuclear safeguards. Inside their large volume and protected by the self-attenuation of the large U mass is a place to hide other material than declared. This gap in a very large stream of nuclear material can for the time being only be closed by the right combination of different measures, esp. the observation of the mass flow with balances in combination with NDA methods which "see" the whole container volume. In a study for the IAEA[4] it was proposed to use the fast neutron emission mainly from ^{234}U as indicator for the ^{235}U mass in the drums. In a well chosen geometry it is possible to cope with the unknown and potentially very heterogeneous filling profile of these twelve-ton containers. The modeling work has to be verified by measurements. The results can be integrated with other methods developed at JRC for the application in enrichment plants, e.g., at GB2.

Destructive Analysis of Nuclear Materials, Impurities, and Fingerprints

In recent years the scope of destructive analysis (DA) of samples

Figure 3. Rare earth element pattern as identified in natural uranium samples from different mines (different types of ore deposits). The shape of the curve (relative concentration of the rare earth elements) is characteristic for the geological origin of the natural uranium.

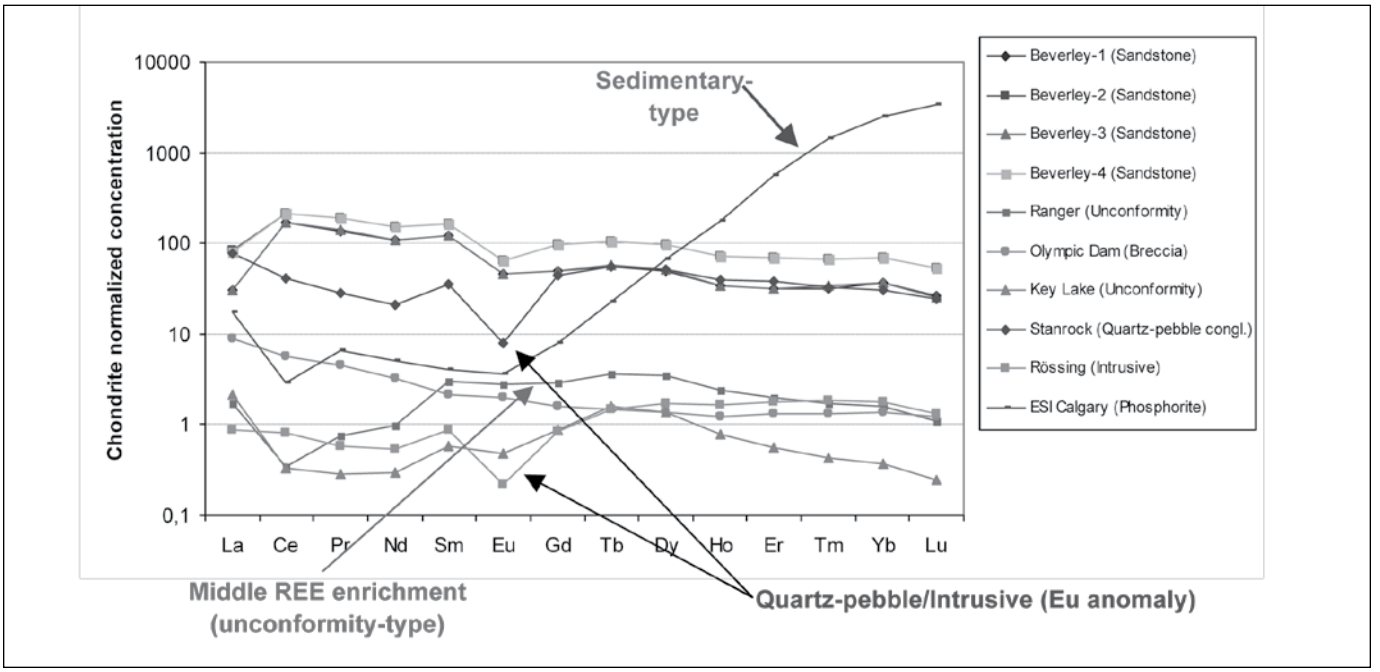

of nuclear material has changed. While DA remains a core element of safeguards measurements for bias defect detection, new applications in the context of strengthened safeguards have been developed. Investigative analytical and interpretational techniques are increasingly applied in information driven safeguards. The objective of the analysis is essentially to verify the consistency of declared processes with measurable material parameters. Obviously, these new safeguards applications benefit from developments in and from synergies with the nuclear forensics area. The concentration of metallic impurities in uranium materials is an example of such new parameters that are considered for evaluating the consistency of declared processes with material properties. Impurities may be source material inherited or they may be process inherited. Process inherited impurities may have been added intentionally (in order to achieve certain material properties) or they may have accidentally entered the material (e.g., originating from chemical reagents, from vessel corrosion, etc.). The interpretational challenge is thus to identify the correlations between trace element concentration (or the combination of several trace elements, i.e., a pattern) and the origin of these trace elements (e.g., source material or process). In uranium ore concentrate samples (colloquially referred to as yellow cake) the rare earth elements have proven to be a robust indicator of the geographic origin of the natural uranium. As can be seen from Figure 3, the pattern of rare earth elements is characteristic for the type of ore deposit, thus enabling to trace back a sample of natural uranium.[5,6]

In addition to the typology of the source material, uranium ore concentrate also contains trace impurities which are pointing at the process used for dissolution and extraction. Infrared spectroscopy is a well established analytical method providing information on the molecular structure of the compound under investigation and at the same time also offering information on anionic impurities. Such impurities are typically residuals of the chemicals used for dissolving and for purifying the uranium. As can be seen from the spectrum in Figure 4, peaks of sulfate ions point at a process using sulfuric for dissolving the uranium, while nitrate peaks indicate the use of nitric acid for back extraction of uranium during the purification process.[7]

Mass-volume Determinations in Complex Fuel Cycle Facilities

Solution monitoring plays an important role in the field of near real time accountancy (cross-correlation between interconnected tanks) and ensures that the plant is operated as declared (auto-correlation of process cycle). Most of the techniques to determine the *quantity* of solution being present in a tank necessitate the use of a calibration curve determined during the *cold* commissioning of the plant. This is the case for the popular dip tube technique for which the solution level and its density are determined by measuring the pressure of air on lines feeding tubes immerged at several levels in the tank, one close to its bottom.

During the lifetime of the tank it might be necessary to perform calibration verifications for several reasons, e.g., to check that no deliberate change was made to the vessel that would allow the diversion of nuclear material or to check that the repetition of the process cycles with liquors having densities higher that the

Figure 4. Infrared spectra of different types of "yellow cake" showing the characteristic vibrational peaks of the uranium compound and smaller peaks indicating anionic impurities arising from uranium processing

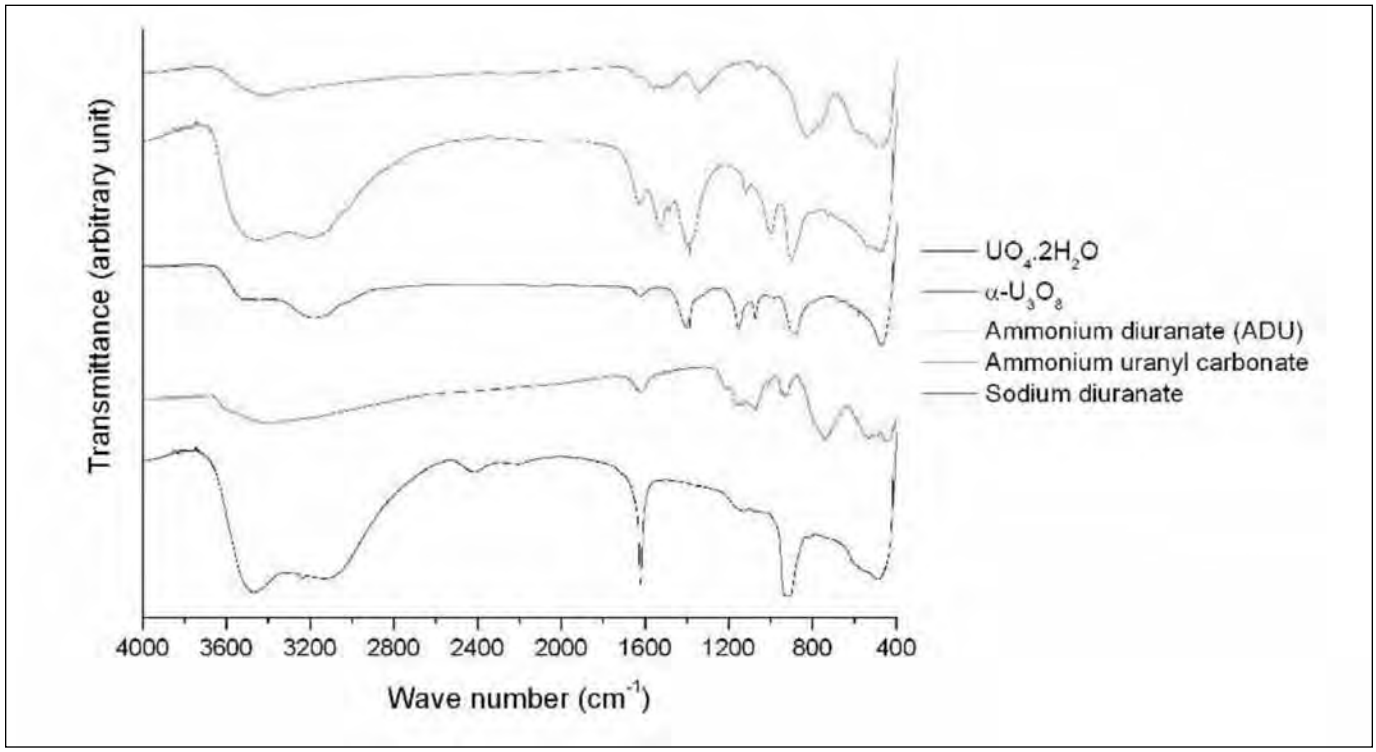

calibration solution (usually water) did not induce some changes due to mechanical stresses.

Tank calibration verification performed in step mode like the initial tank calibration is accurate but is a great consumer of manpower and time during which the plant cannot be operated. The Process Monitoring Laboratory (PML) at JRC Ispra is developing a technique that will allow to perform the tank calibration verification in a (quasi-unattended) continuous flow mode controlled by a computer. Figure 5 shows the installation developed by PML to obtain an accurate mass flow of calibration solution.

Calibration in continuous flow mode could also be useful before performing the accurate step-by-step mass calibration of a tank in case some information such as precise mechanical drawings of the installation were missing or incomplete to determine all "regions of interest" of the vessel.

Figure 5. Continuous flow mode calibration set-up for solution monitoring

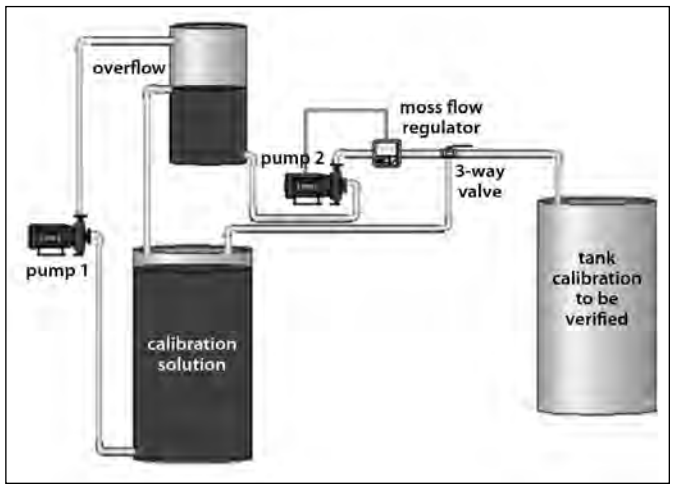

Enhanced Containment and Surveillance Measures

Innovative Sealing Technologies

The JRC Candu Sealing System (JCSS) is implemented in three different CANDU nuclear facilities, in Romania (Cernavoda I & II), Pakistan (Karachi, KANUPP), and Canada (Darlington). In parallel with the implementation and support of the JCSS, continuous improvements are made to the existing design. See Figure 6. Following feedback from field use, modification and enhancement to the installation tools, reading head, and acquisition system are implemented. The customers, DG ENER and IAEA, seek to automate as far as possible measurements currently being made by inspectors, freeing them to perform other investigations. The sealing of spent fuel is one measurement that is extremely time consuming and intrusive to the facility. The challenge for the next years will be to redesign all the sealing equipment currently in use to cope with the unattended monitoring of seals

Figure 6. Ultrasonic bolt as developed at JRC and in use in a variety of spent fuel ponds

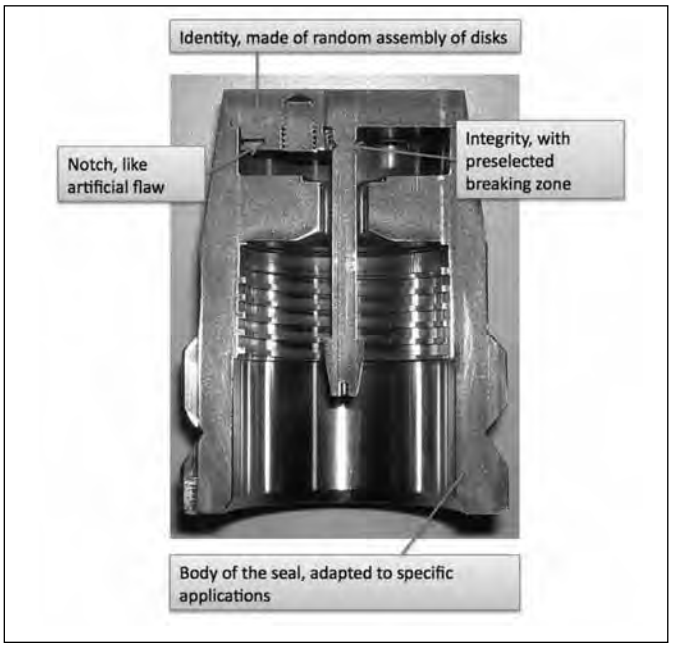

with automation of measurements currently being made by inspectors (development of remote techniques, secure transmission of data).

Ultrasonic bolt seals developed for underwater applications can be used also for dry storage applications. They are passive, and can stand for years in very harsh environmental conditions without any alterations. One application concerns the sealing of the biological concrete shield of Constor containers for Ignalina (Lithuania) Nuclear Power Plant long-term dry-storage repository. Another potential application of the ultrasonic bolt seals, is the replacement of the standard drilled bolts, looped with an optical fiber seal to protect opening of containers. Ultrasonic features will give those bolts a unique identity, and an integrity broken when opened.

JRC is also developing a low-cost electronic seal for long-term dry storage depositories, adapted to harsh conditions (-40°C to +85°C). The seal requirements are for long-life batteries, and active monitoring of the closing cable (up to 15m). The main difficulty in the design of the seal lies in the two conflicting requirements of having a low cost seal (target price < $200) with a long continuity (ten years) of the battery life. JRC already developed electronic radio frequency indentification (RFID) active seals for the security of the supply chain, and will adapt it to nuclear conditions and requirements.

Surveillance and Identification Through Laser Scanning

Design Information Verification (DIV) is becoming increasingly important in international safeguard activities. Given the complexity of nuclear sites and thereby the complexity of performing a correct and accurate DIV activity, efficient tools are needed to execute the activities in a time-efficient manner. The JRC has developed a 3D laser-based tool for DIV activities.[8] The system contains two essential components; (i) a commercial off-the-shelf laser scanner that acquires 3D data with millimetre precision and (ii) a hosting and processing application that is used to manage/model/analyze data sets. The scanner is used in the field which within a minute acquires a precise dataset from the specific viewpoint. By repeating this step, a complete representation of a plant or parts thereof can be constructed using the processing application. The technique to accurately model certain areas or entire plants using 3D laser scanners provides the means to perform a variety of tasks; such as: (i) verifying plant set-up during the initial plant commissioning phase, (ii) re-verifying the correctness of plants at any given time during a plant's life-time, or (iii) to verify declared or undeclared changes which have taken place. (see Figure 7.) The complete suite developed by JRC-ITU, denoted 3D-LVS, is currently in use by IAEA and the Euratom.

Another area of research is to provide a reliable and robust real-time monitoring of safeguards relevant objects in a plant. The Laser Item Identification System (L2IS) aims to perform monitoring of UF_6 cylinders in an enrichment plant. The system is capable of monitoring and uniquely identifying all the transferred UF_6 cylinders between process and storage area. The technique used is to scan the end-phase of the drum passing with laser scanners and thereby acquiring a micrometre accurate 3D fingerprint. A pilot L2IS system is now installed at an enrichment plant in Japan.

Improved Image Review Tools

Safeguards surveillance images are reviewed in batches of several thousands. In a batch, less than 0.01percent of the total number of images is expected to be safeguards-relevant. Because events are to be detected and annotated by nuclear inspectors in review reports, there is a need for tools to focus the inspector's attention directly to the relevant parts of the image stream.

To assist video reviews, JRC has developed VideoZoom[9] a tool that builds *summaries* out of large surveillance streams. The purpose of summaries is to guide the review of the image stream and reduce the number of images seen by inspectors to perform the review work correctly. It is assumed that inspectors use the review tool in an *active* way, for example, by browsing the summaries to search for 'logically expected events,' to spot anomalies, and to decide when to expand a summary to reveal the images as taken by the camera. VideoZoom is currently under evaluation by safeguards inspectorates.

Figure 7. Automatic detected changes

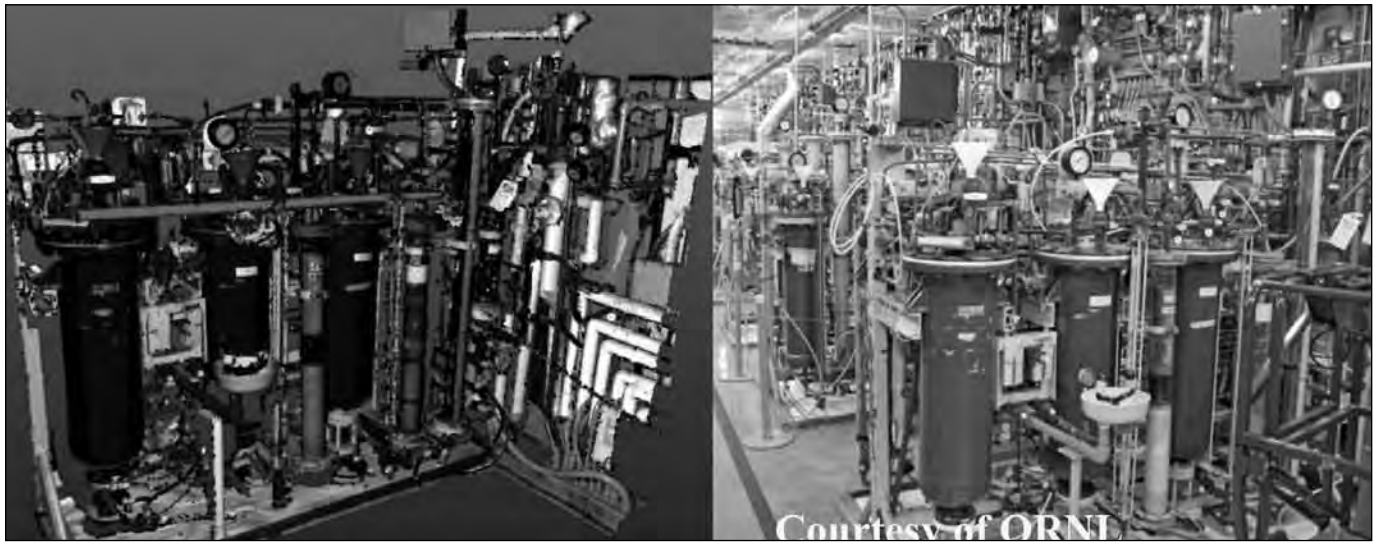

Facility Monitoring, Verification and Observations

Effective Use of Process Control and Data Integration in the Monitoring of Operations

The implementation of an effective and efficient safeguards approach at large scale reprocessing facilities with large throughput and continuous flow of nuclear material requires the introduction of enhanced safeguards measures to provide added assurance about the absence of diversion of nuclear material and confirmation that the facility is operated as declared. One of the enhanced safeguards measures in this type of facility is the solution monitoring and measurement, comprising data collection instruments, data transmission equipment and a solution monitoring software. Such a tool allows automatic calculations of volumes, densities, and flow rates in selected process vessels, including most of the vessels of the main nuclear material stream. The software also includes automatic features to support the inspectorate in verifying inventories and inventory changes and to analyze the flows of nuclear material within the process and of specified *cycles* of operation.

Similarly the follow-up of material flows in a gas centrifuge enrichment plant (GCEP) is very challenging and will have to rely also upon data from the process control.[10] The safeguards measures and analysis of results in these complex facilities need to be able to *digest* a large number of signals from a variety of instruments, maintain these data for a posteriori review, and allow to draw safeguards relevant conclusions. JRC has been developing in the past the "safeguards analysis tool" for this purpose that can accommodate also data from specific analytical measurements (e.g., from an on-site laboratory) and from the Operator "process declarations." An illustration of the challenge for future integration is provided in Figure 9 for GCEP.

Enhanced Design Information Verification and Control

For quite some time now, the safeguards approach has included the verification of the state of the completeness of state declarations. To this effect, the Additional Protocol introduced a family of legal instruments and modalities toward that objective. Unannounced inspections are one of such instruments, which led to changes in the way safeguards inspectors operate. Monitoring for undeclared activities includes checking predictable compliance criteria as well as coping with unexpected scenarios. For the latter, the provision of in-field information to support the inspection is of paramount importance—as not all scenarios can be studied at headquarters while preparing an unannounced inspection. To be useful, the information to be provided to the inspector must relate to the field context and must be comprehensive in content. The R&D activities are rooted mainly in the field of machine intelligence including: virtual reality, human-computer interactions involving augmented reality, and information integration for improved situation awareness.

The scope of this activity is to investigate tools, components, and system architectures to be used by a safeguards inspector to enhance her/his observation and *investigative* skills as well as securely retrieve local, just-in-time information while performing a complementary access inspection. The scientific disciplines supporting this project include augmented and mixed reality, ambient intelligence, and environment localisation as well as secure communications.

As an example of the current work, JRC implements and demonstrates a prototype system of a multifunctional handheld device equipped with positioning sensors and a combined real-time 2D/3D data capture to assist an inspector in performing a complementary access inspection. The inspector will be able to interact with the device and have additional information,

Figure 8. VideoZoom illustrated on a stream from an airport Web cam. Top: Image summaries are rendered at different level of detail—from abstract representations to the images as taken by the camera. Bottom: Image summaries are navigated by a zooming interface allowing the user to move from abstract summaries to the detailed ones as necessary.

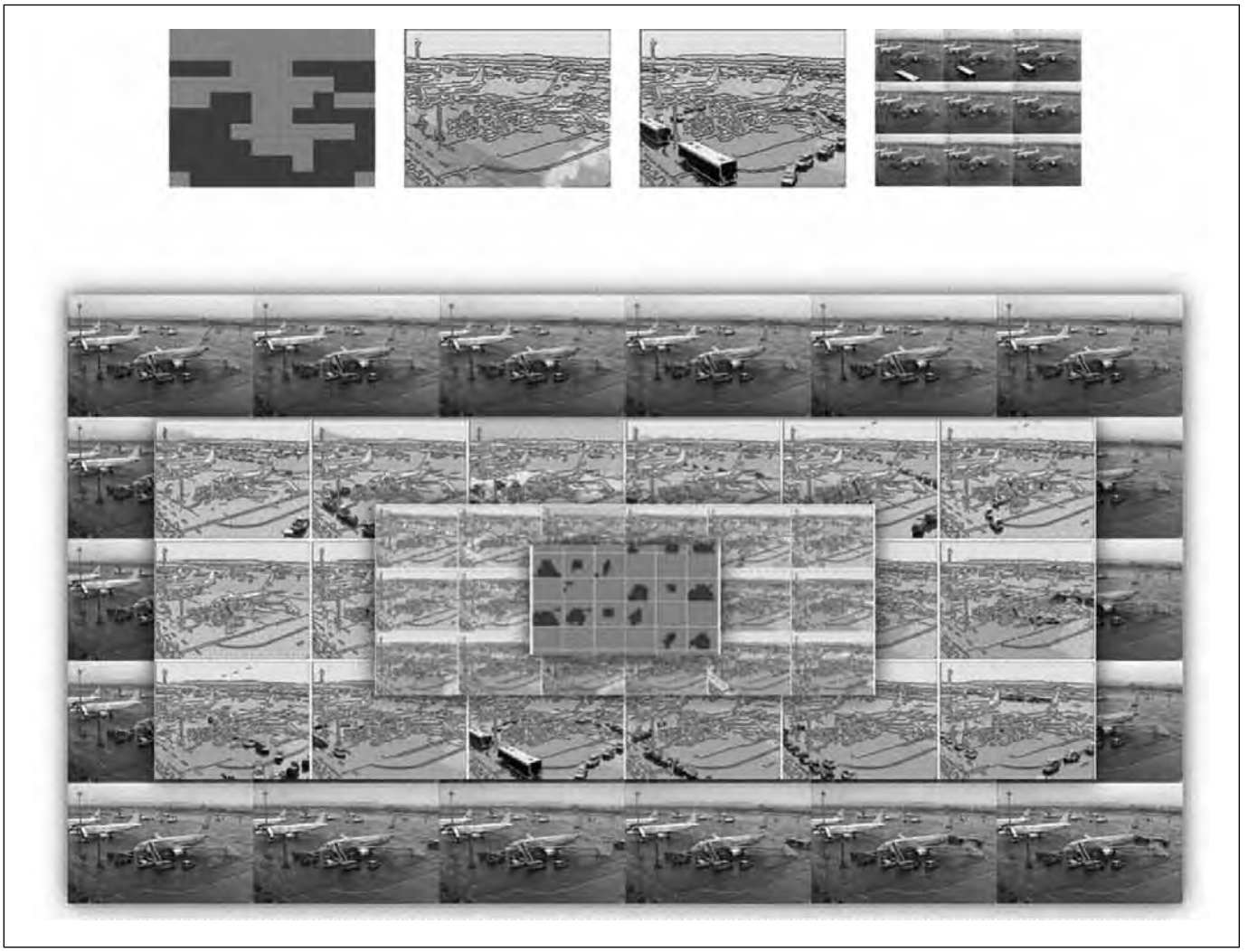

such as description of physical objects and instruction for performing physical tasks in form of annotation, off-the-shelf synthesizer-based speech instruction, image, and 3D model. Such a prototype will illustrate the potential of the new tools assisting an inspector. A possible goal includes the incorporation into one handheld piece of equipment diversified data gathering (e.g., radiation, thermal, spatial, chemical, environmental, distance measurements) and analysis capabilities. Figure 10 illustrates the concept. The purpose is to assist the inspector in the field when doing an inspection, i.e., allowing the making of decisions in the field (including further investigations) rather than waiting for the results to be available at headquarters.

New Developments Supporting the Prevention and Detection of Clandestine Facilities

Environmental Sampling

Environmental sampling in the form of dust samples collected on cotton swipes are routinely taken in search of particles containing sub-pg to pg levels of uranium, released from nuclear material handling. This sampling has been proven as an efficient tool for international safeguards purposes in the search for undeclared nuclear material handling. The isotopic composition provides information of the uranium materials handled at the facility. Precise and accurate measurement of both enrichment and the minor isotopes is, however, a challenging analytical task due to the low levels of material. One of the mainstay techniques for particle measurement is Secondary Ion Mass Spectrometry (SIMS). Re-

Figure 9. Data integration at plant level, illustrated for a gas centrifuge enrichment plant

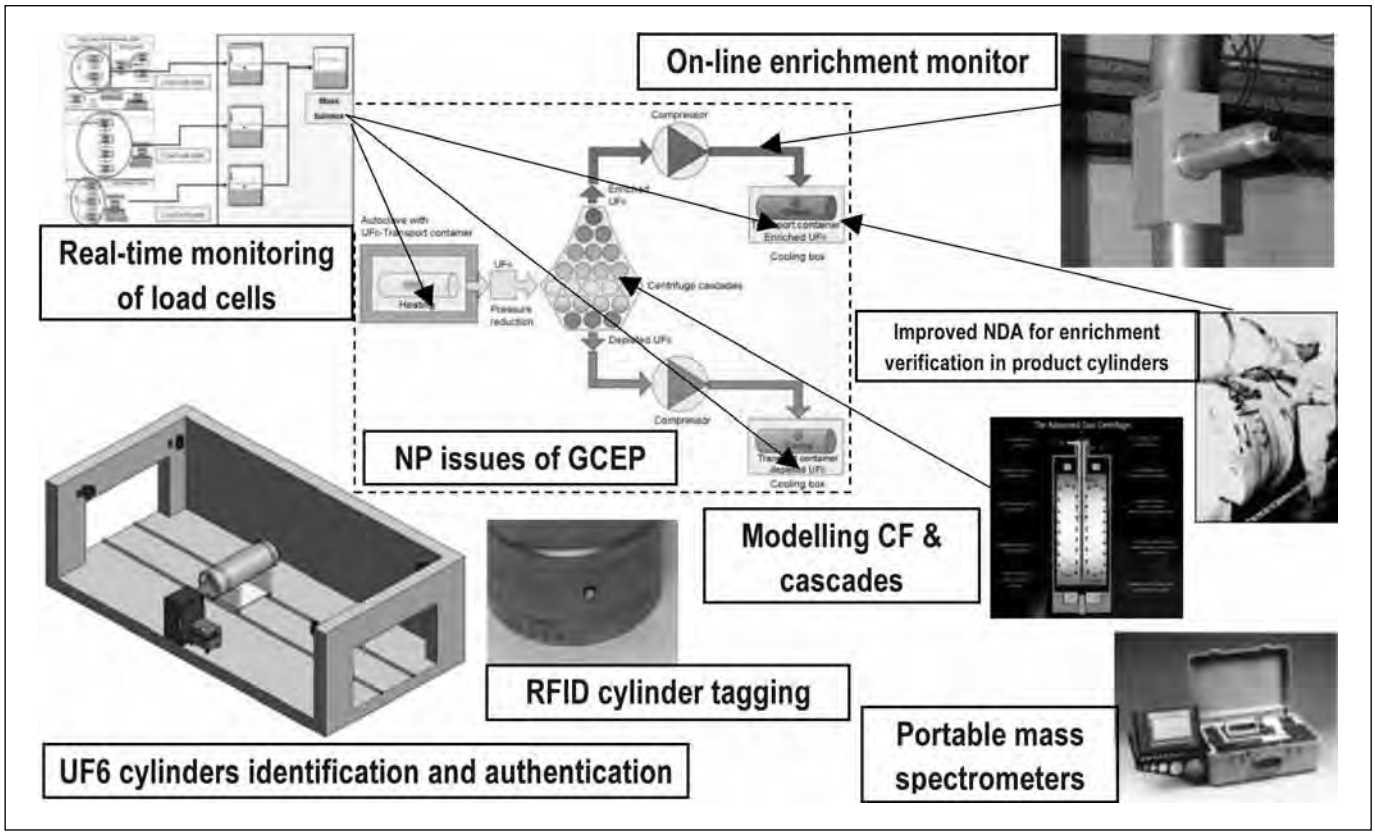

cent improvements in particle analysis for safeguards purposes will include at JRC Karlsruhe the use of Large Geometry—SIMS (LG-SIMS) rather than the previously used Small Geometry—SIMS (SG-SIMS) instruments. LG-SIMS instruments have a larger magnetic sector radius that provides improved performance for uranium particle analysis mainly due to their high transmission at high mass resolution. Common molecular interferences that can hamper the measurement in normal SIMS analysis are removed efficiently, thus greatly improving the precision and accuracy for the uranium isotope measurements on small particles.

Remote Sensing

Since the late 1990s, satellite imagery has become an important tool for nuclear safeguards and nonproliferation. It is routinely used to support the verification, the correctness, and completeness of the member states' declarations, and to provide preparatory information for on-site inspections. Furthermore, satellite imagery can provide invaluable information for analyzing and monitoring suspected nuclear activities and facilities that can not be visited on the ground.

Over the last years, JRC has been developing concepts and tools that aim at supporting the work of the nonproliferation imagery analyst who is faced with new and increased challenges, as for example the detection of clandestine nuclear activities and the assessment of an increasing amount of multi-type information. As current analysis tools usually provide an isolated view on satellite imagery with poor integration of collateral data (such as open source information, GIS data, internal databases, reports, etc.), JRC developed an integrated information platform that provides a single, map-based point-of-entry to the information required for a specific analysis task.[11] It is designed to facilitate information sharing between analysts as well as to ensure long-term knowledge preservation.

Export Control and Trade Analysis

Following the disclosure of undeclared nuclear programs in Iraq and DPRK, the IAEA sought those sources of information in addition to state-declared information to derive indicators of possible undeclared safeguards-relevant activities.[12] New sources taken into account include trade-related information. JRC has surveyed and catalogued open sources on import-export, customs trade data[13] and developed tools for their use in safeguards.[14] Tests on the use of these data by the IAEA suggest safeguards relevance along the following lines.[15]

* Technical reports for all fourteen NDA techniques are available through correspondence with the author.

Figure 10. Automatic detected changes and guidance

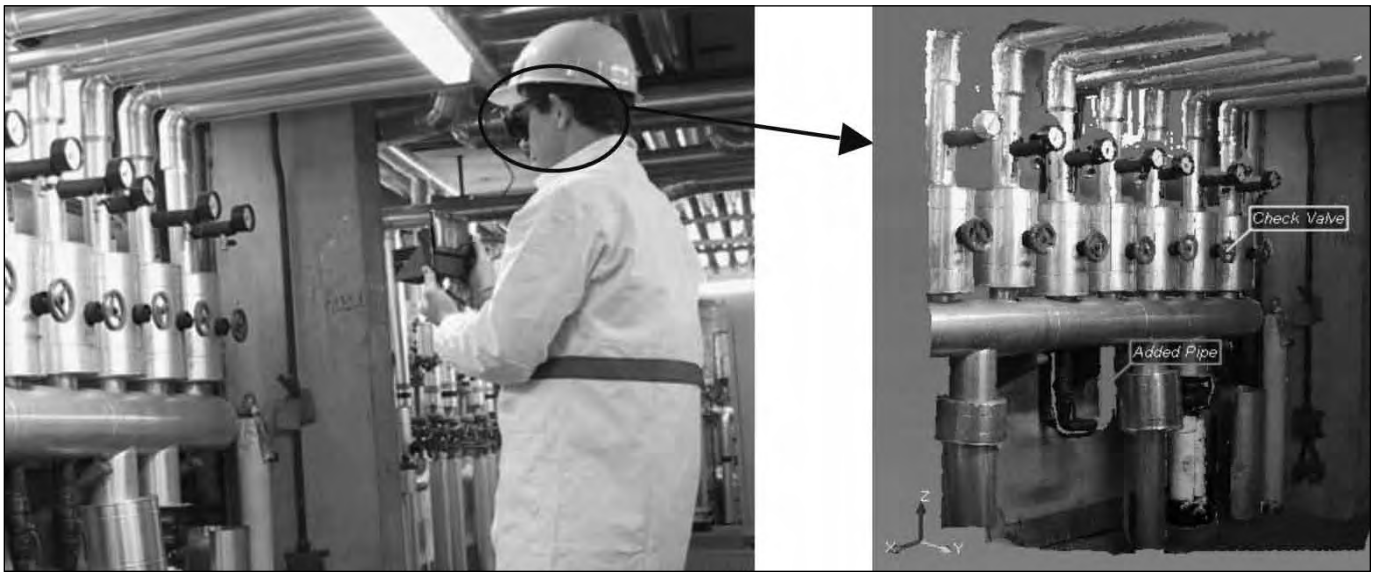

- *"Support the IAEA state evaluation process and improve understanding of a state's nuclear program."* Trade information on exports can support the assessment of a state's nuclear related industrial capabilities. Data on trade flows between states can be used to understand their international cooperation. Understanding mining-related activities can be improved by using data on the exports of raw materials and semi-finished products. Data on imports and exports of nuclear materials and equipment may also provide information on the development of the nuclear fuel cycle in general.
- *Verify import and export declarations made by states under Additional Protocols (APs)*, article 2.a.(ix) Trade data can prove useful to identify flows of raw material subject to safeguards. Trade categories (of the Harmonized System[16]) appear to be less specific than safeguards categories, but precise enough to be determined as safeguards-relevant. The identification of shipments of some AP Annex II equipment may represent a greater analytical challenge.
- *Identifying indicators of activities to be safeguarded or to be declared under APs,* article 2.a.(iv)—In this context it is foreseen that trade data can be used to verify hypotheses about the absence of undeclared activities. Commodities to serve as indicators and methodologies then need to be identified on a case by case basis and in a hypothesis-specific way.

The JRC supports the European Commission DG TRADE with different types of activities, such as technical and analytical consultancy for the harmonization of implementation and the amending of European Union (EU) regulation on dual use goods; development of software tools; contribution to International regimes and EU control lists review; training events, also in collaboration with the DOE's NNSA. These actions contribute to reinforce the EU barriers and resistance against weapons of mass destruction proliferation. Coordinated by JRC, a new export control activity has been launched within ESARDA to broaden its nonproliferation scope according to the findings and recommendations of the Reflection Group 2010.

Open Source Data Mining, Handling, and Interpretation

Open source information (including, but not limited to, media sources; government and non-governmental reports and analyses; commercial data; and scientific/technical literature available on the Internet) plays an important role in evaluating a state's nuclear program and verifying the compliance with its nuclear safeguards obligations.

However, the collection and analysis of the growing volume of open source information poses significant challenges to the analyst. Therefore, JRC is developing and operating a "Nuclear Security Media Monitor" (NSMM), which is a Web-based multilingual news aggregation system that automatically collects news articles from predefined Web sites.[17] NSMM is a domain specific version of the general Europe Media Monitor (EMM)[18] and monitors—additionally to the 2,500 general Web news sources targeted by EMM—more than 150 nuclear specific sites (including non-governmental organizations (NGOs), academic, inter-governmental, and scientific/technical sites). Filters remove articles not relevant to the nuclear domain and group them into various areas of interest, e.g., related to different steps of the nuclear fuel cycle or to relevant countries (see Figure 11).

NSMM has been established in a joint project with IAEA with the aim to streamline IAEA's acquisition and analysis of open source information and develop the current information collection/newsletter production process to a more efficient system. [19] In the meantime, NSMM is also available as a valuable resource to the wider nuclear security community.

Figure 11: Snapshot of the NSMM Web site

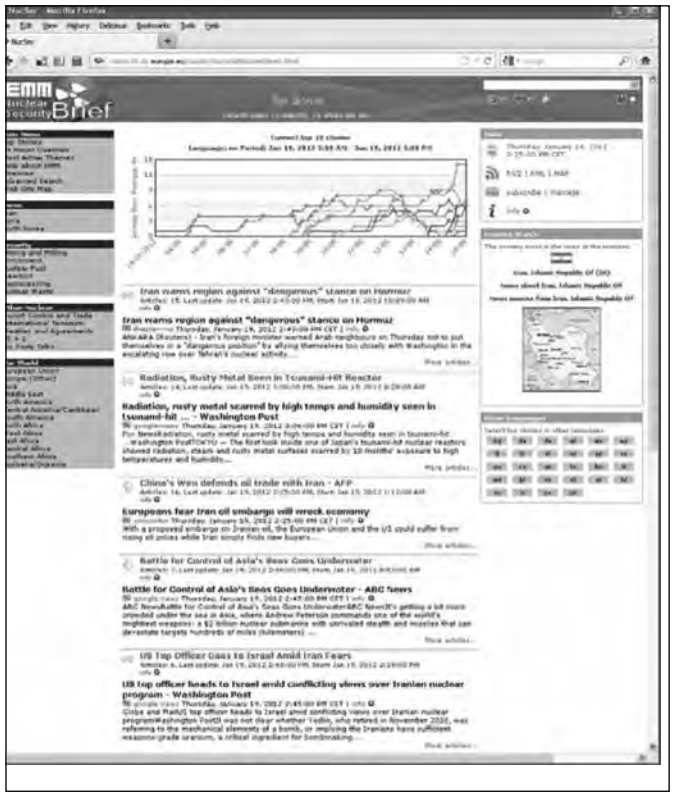

Integrated Safeguards Approaches and Nonproliferation Assessments

Safeguards By Design

Safeguarding the nuclear fuel cycle is a key aspect of proliferation resistance. The application of extrinsic measures to achieve the detection and timeliness goals has a strong relationship with the intrinsic design features of facilities.

By taking into account design features that facilitate the implementation of international safeguards very early in the design phase, a concept known as "safeguards by design" (SBD), the overall process can be made more effective and efficient with benefits to all the involved stakeholders. A few years ago the IAEA launched a task on "Guidance for Designers and Operators and Measures to Facilitate the Implementation of Safeguards at Future Nuclear Cycle Facilities" with contributions by EURATOM and member states' support programs, with the aim to formulate SBD Guidelines to designers and operators. The JRC has coordinated the EC and ESARDA contribution to the high level guidelines for safeguards by design, which are being finalized by IAEA. Papers were published linking SBD to safeguardability.[20]

Proliferation Resistance Methodologies

Proliferation resistance is defined by IAEA as: "*… that characteristic of a nuclear energy system that impedes the diversion or undeclared production of nuclear material or misuse of technology by States in order to acquire nuclear weapons or other nuclear explosive devices."*[21]

Proliferation resistance has been set, by the international initiative Generation IV International Forum (GIF), as one of the main goal areas, together with safety reliability, economics, and sustainability, relevant for the development of the new generation of nuclear energy systems (NES), the so called Generation IV, to be ready for deployment in the years 2020-2030.

The Proliferation Resistance and Physical Protection Working Group of GIF (PR&PP) has developed a methodology for the PR&PP evaluation of Generation IV NES. The mostly updated release the PR&PP Evaluation Methodology represents a framework available to the designers of Generation IV systems for the evaluation of the PR&PP at different design stages hence providing also a support to the design process.[22]

The project INPRO (International Project on Innovative Nuclear Reactors and Fuel Cycles), established under IAEA auspices, has also developed a methodology for the assessment of the proliferation resistance of innovative reactors. The INPRO PR methodology is more holistic and attempts to characterize nuclear system as a whole.[23] A joint harmonization activity between the two methodologies is ongoing.[24]

JRC as implementing agent of EURATOM is actively contributing to all GIF PR&PP activities and has participated in the INPRO projects in the areas of proliferation resistance, most recently, the PRADA (Proliferation Resistance: Acquisition/diversion Pathway Analysis), project which also set the stage for an update of the INPRO methodology.[25]

The new INPRO project PROSA (Proliferation Resistance and Safeguardability Assessment Tools) will further promote the harmonization of the two approaches by developing a set of coordinated tools. It will define the interface between the proliferation resistance and safeguardability assessment tools of both methodologies, at the different level of evaluation, namely facility, nuclear energy system, and state.

Linking Safeguards with Safety and Security

At the political level, safety, security, and safeguards remain in separate hands. Safeguards are implemented by international and national authorities through an international treaty, while security is an important national responsibility. Safety is the responsibility of the operator although the national safety authorities have the right to ensure the implementation by the operator of safety measures. Transparency remains at the heart of the safety principles to reassure the public of the safe operation of the nuclear installation, however security principles are based on confidentially avoiding any release of information that can fall in bad hands.

At a technical level the synergies between safeguards and security are now obvious and we have demonstrated at the JRC their possible integration allowing better optimization of the resources and important benefit from exchange of experience and expertise between the two systems.[26] We have demonstrated the synergies between non-destructive assay in nuclear safeguards and the detection and identification of illicit nuclear and radioactive materials, the synergy between destructive analysis (DA) and environmental sampling in nuclear safeguards with nuclear forensics for the determination of the origin of seized nuclear materials, the use of seals in nuclear security for containers benefits from the seals developed for safeguards, combined camera such as the 3D laser used for design verification and gamma/neutron source for source localization in luggage is another example of the synergy between security and safeguards, Open source information, export controls are also areas where the integration is possible.

In nuclear safety, mainly in the areas of radioprotection and emergency responses we believe that integration and synergies are also possible. The tools we are using at the JRC for monitoring and measuring the radioactivity in the environment can easily benefit from those developed for security and safeguards and vice versa. As an example we can mention the use for the characterization of environmental samples of low background gamma measures, Mass spectrometry techniques, particles analysis that are also tools—when adapted properly—are widely used in nuclear safeguards and security. The emergency response relies, in case of nuclear accident on the estimation by modeling of the geographical area of the radioactivity dispersion as well as its distribution level. In case of an incident involving radioactive materials (case of radio active dispersion devices) the same analyses are requested knowing that the models of prediction are more complicated in the case of a small scale event.

Conclusions

Safeguards and nonproliferation R&D continue to be a dynamic work area, also due to the new approaches that the IAEA has been putting forward in the recent year. A significant number of improvements can still be made at all different scales described in this paper: measurement of the materials, at the level of the facility and at the level of the state, whereby continued attention and improved skills are required to also detect clandestine activities, not necessarily operated by state actors. JRC is active in all these areas. Also at the level of the methodological concepts for safeguards and proliferation resistance, further improvements are being made. A noble goal for further R&D is to address the safeguards, safety and security concerns and challenges with a consistent and hopefully synergetic approach to the benefit of a peaceful, safe and secure civil nuclear fuel cycle. This will also inspire JRC R&D activities in this field in the future.

Acknowledgements

The authors would like to thank all staff working in the eight different sections of the JRC on nuclear safeguards and nonproliferation R&D, in Ispra, Karlsruhe, and Geel. They owe also particular thanks to those scientists who contributed significantly to some sections to this paper like G. Bosstroem, P. Richir, F. Sevini, M. Sironi, Z. Varga, C. Versino, M. Wallenius, and E. Wolfart.

References

1. http://irmm.jrc.ec.europa.eu/catalogue
2. http://irmm.jrc.ec.europa.eu/interlaboratory_comparisons/nusimep/Nusimep-7/Pages/index2.aspx
3. Looman, M., P. Peerani, and H. Tagziria. 2009. Monte Carlo simulation of neutron counters for safeguard applications, *Nuclear Instruments and Methods, Section A*, Volume 598, Issue 2, 542-550
4. Mortreau, P., E. Franke, and R. Berndt. 2010. ^{235}U enrichment or UF_6 mass determination on UF_6 cylinders with NDA methods, *Nuclear Instruments and Methods, Section A,* Volume 612, Issue 2, 309-319.
5. Varga, Z., M. Wallenius, and K. Mayer. 2010. Origin Assessment of Uranium Ore Concentrates Based on Their Rare-Earth Elemental Impurity Pattern, *Radiochimica Acta,* 98, 1–8.
6. Varga, Z., R. Katona, Z. Stefánka, M. Wallenius, K. Mayer, and A. Nicholl. 2010. Determination of Rare-Earth Elements In Uranium-Bearing Materials By Inductively Coupled Plasma Mass Spectrometry, *Talanta*, 1744–1749
7. Varga, Z., B.Öztürk, M. Meppen, K. Mayer, M. Wallenius, and C. Apostolidis. 2011. Characterization and Classification of Uranium Ore Concentrates (yellow cakes) using infrared spectrometry; *Radiochim. Acta* 99, 807–813 (2011)
8. Sequeira, V., Bostroem G., Goncalves J. 2009. 3D Laser-based System for Design Information Verification. *Proceedings of the 50th Annual Meeting of the Institute of Nuclear Materials Management.*
9. Blunsden, S., Versino, C. 2011. VideoZoom: Summarizing Surveillance Images for Safeguards Video Reviews. JRC68054
10. Carchon, R., L., Dechamp, L. G. Eklund, W. Janssens, G. Mercurio, P. Peerani, and P. Richir. 2011. Load Cell Monitoring in Gas Centrifuge Enrichment Plants: Potentialities for Improved Safeguard Verifications.
11. Wolfart, E. J. Goncalves, A. Ussorio, A. Patrono, K. Gutjahr, I. Niemeyer, P. Loreaux, P. Marpu, C. Listner. Integrated Analysis of Satellite Imagery for Treaty Monitoring - The LIMES Experience. *ESARDA Bulletin* (43); 2009. p. 40-56. JRC55181
12. Versino C., R. Chatelus, G. Cojazzi, F. Contini, M. Tarvainen, A. Tsois. 2010. Global Trade Data to Support IAEA Safeguards. *ESARDA Bulletin* (45), p. 14-22.

13. Versino, C., M. Tsukanova and G.G.M. Cojazzi 2010. *Catalogue of WEB Data Services on Global Trade.* EUR 24657 EN, ISBN 978-92-79-18919-7, JRC62363.
14. Versino, C., F. Contini, R. Chatelus, G.G.M. Cojazzi 2011. *The Big Table: A Software Tool for Nuclear Trade Analysis.* 2011.
15. 1997. IAEA, INFCIRC/540 (Corrected). Model Protocol Additional to the Agreement(S) Between State(S) and the International Atomic Energy Agency for the Application of Safeguards. 1997.
16. The Harmonized System by World Customs Organization. http://www.wcoomd.org/home_hsoverviewboxes_hsharmonizedsystem.htm
17. http://nsmm.jrc.ec.europa.eu/nucsec
18. Steinberger, R., B. Pouliquen, E. Van Der Goot. 2009. An Introduction to the Europe Media Monitor Family of Applications. *Proceedings of the SIGIR Workshop on Information Access in a Multilingual World* (SI GIR-CLIR2009), (July 2009)
19. Wolfart, E., G. Cojazzi, E. Van Der Goot, W. Hammond, F. Fuart, Z. Gastelum, Y. Feldman, M. Ferguson, R. Zarucki. 2011. Collection, Analysis and Dissemination of Open Source Safeguards-Relevant News Using Web Based Applications. *Proceeding of the Institute of Nuclear Materials Management Annual Meeting.*
20. F. Sevini et al., 2011. *ESARDA Bulletin* n.46, (2011)
21. IAEA STR-332, Proliferation Resistance Fundamentals for Future Nuclear Energy Systems, December2002.
22. IAEA-TECDOC-CD-1575, Guidance for the Application of an Assessment Methodology for Innovative Nuclear Energy System, INPRO Manuals Volumes 1-7, October 2007.
23. PR&PP WG of GIF, Evaluation Methodology for Proliferation Resistance and Physical Protection of Generation IV Nuclear Energy Systems, Revision 6, September 15 2011, GIF/PRPPWG/2011/003, http://www.gen-4.org/PDFs/GIF_PRPPEM_Rev6_FINAL.pdf
24. Pomeroy G., R. Bari, E. Wonder, M. Zentner, E. Haas, T. Killeen, G. Cojazzi and J. Whitlock. 2008. Approaches to Evaluation of Proliferation Resistance of Nuclear Energy Systems. *Proceedings of the INMM 49th Annual Meeting.*
25. H.L. Chang, R. Bari, H. Chayama, G.G.M. Cojazzi, E. Haas, T. Killeen, W.I. Ko, J.H. Park, G. Pomeroy, G. Pshakin, H. Qian, F. Sevini, J.K. Sprinkle,J. Whitlock, M.D. Zentner PRADA – Next Steps. *Proceedings of the 52nd Annual Meeting of the Institute of Nuclear Management,* July 17-21 2011, Palm desert, California, USA
26. S. Abousahl et al., Proceedings for the IAEA symposium on International Safeguards 2010, IAEA-CN-184/225 (2010).

Application of Safeguards-By-Design for the Pyroprocessing Facilities in the ROK

H. D. Kim, H. S. Shin, D.Y. Song, T. H. Lee, B.Y. Han, S. K. Ahn, and S. H. Park
Korea Atomic Energy Research Institute, Daejeon, South Korea

Abstract

The application of a Safeguards-By-Design (SBD) concept is now widely acknowledged as a fundamental consideration for the effective and efficient implementation of safeguards. The Republic of Korea (ROK) has implemented the SBD concept in nuclear fuel cycle facilities. Since the early 1990s, we have developed several nuclear fuel cycle facilities for research activities on spent fuel treatment. Such facilities include the DUPIC Fuel Development Facility (DFDF), the Advanced spent fuel Conditioning Process Facility (ACPF), and the PyRoprocessing Integrated inactive DEmonstration facility (PRIDE). The PRIDE, which is an engineering-scale pyroprocessing facility that deals with fresh natural or depleted uranium materials, is being constructed and will be completed in 2012. The safeguards system has been designed with a facility design team that has been involved since the pre-conceptual facility design step. Non-destructive assay (NDA) instruments, mostly hot-cell-operation neutron coincidence counters for determining the amount of bulk material present in dry-processing facilities, were also developed. Especially, the ROK has collaborated with the United States for many years to develop numerous state-of-the-art NDA techniques. Pyroprocessing technology is currently being developed, all over the world, and the Republic of Korea (ROK) is one of countries working most actively to realize this technology in the near future. The safeguards approach for the pyroprocessing facility, however, has yet not been established, especially from the viewpoint of nuclear material accountancy. The existing nuclear material accountancy technology for a wet reprocessing facility is difficult to apply. As part of a cooperative effort with the IAEA to find a safeguards approach for the pyroprocessing facility, the ROK has been involved in a member state support program (MSSP) since 2008. In the MSSP, the ROK designed a Reference Engineering-scale Pyroprocessing Facility (REPF) and developed a safeguards system for the REPF that was reviewed by the IAEA. The REPF serves as an example of implementing the SBD concept in the pre-conceptual design step.

Introduction

Korea Atomic Energy Research Institute (KAERI) has developed pyroprocessing technology since 1997.[1] Spent fuels are treated electro-chemically, and uranium and transuranium (TRU) are recovered during pyroprocessing. Pyroprocessing is completely different from conventional reprocessing technologies such as PUREX. Pure plutonium cannot be separated from the spent fuel via the pyroprocessing. This difference makes pyroprocessing significantly more proliferation resistant. The extracted materials can be directly used as metal fuel in a fast reactor, and the volume and heat load of the spent fuel can be drastically reduced by the pyroprocessing. Because the process materials in the pyroprocessing facility are very different from those in the reprocessing facility, safeguards technologies should be developed, and International Atomic Energy Agency (IAEA) safeguards criteria for the pyroprocessing facility are required.

Safeguards-By-Design (SBD) is an approach in which international safeguards requirements and objectives are fully integrated from the design stage of a nuclear facility.[2] By integrating all regulatory issues, including safeguards requirements, the project risks can be minimized. The Republic of Korea (ROK) has the experience of developing safeguards systems for nuclear fuel cycle facilities and is actively developing safeguards technologies for the pyroprocessing facility, using the SBD approach. In this paper, the main features of safeguards developments by the ROK, which include the nuclear fuel cycle facilities and its implemented safeguards system, the development of NDA instruments, and the study of reference pyroprocessing facility concept, are introduced and discussed.

Nuclear Fuel Cycle Facilities and Their Safeguards Systems

The nuclear fuel cycle facilities such as DFDF, ACPF, and PRIDE have been constructed in ROK, and the safeguards system for each facility was designed from the beginning of the facility design.

DFDF

DUPIC (Direct Use of PWR spent fuel In CANDU reactors) began to be developed at KAERI in the 1990s, and its proliferation-resistant characteristics were successfully proven.[3] A DUPIC R&D program has been carried out with international cooperation from Canada, the United States, and the IAEA. In 2000, a lab-scale DUPIC fuel fabrication campaign was started to

Figure 1. Working area of the DFDF

fabricate the DFDF hot cell. Based on the established qualification process of CANDU fuel design, DUPIC fuel pellets and elements were successfully fabricated with a low burnup spent fuel of 35,500 MWd/tU. An improvement in the DUPIC fabrication process has been made for the use of high burnup spent fuel, over 50,000 MWd/tU.

One of the most notable factors in the development of the DUPIC fuel cycle is that safeguards have been considered from the beginning of the R&D process. Since 1995, two aspects of its safeguards R&D technology have been developed and demonstrated. The first involves nuclear material accountancy in a hot cell with the DUPIC Safeguards Neutron Counter (DSNC), and the second involves containment and surveillance with an unattended image and radiation monitoring system.

The overall DUPIC process material balance is quantified by ^{244}Cm measurements using the neutron coincidence counting method. This recommended concept uses the spontaneous fission neutron emissions from ^{244}Cm to indirectly quantify the plutonium and uranium contents of fuel materials at the DUPIC facility. Because there is no chemical reprocessing involved in the DUPIC fuel cycle, the ratios of ^{244}Cm to plutonium and uranium should be constant at the input and output and during all of the DUPIC process steps. A coincidence neutron counter, the DSNC for material accounting of the DUPIC process, has been developed by the KAERI and Los Alamos National Laboratory (LANL) since 1995. The DSNC was installed at the DFDF at the beginning of 1999, and its performance test for nuclear material accounting was successfully completed by the IAEA in cooperation with the KAERI and LANL. Until 2004, the DSNC system was successfully used for material accounting of the IAEA safeguards in the DFDF.

The DSNC is a well-type neutron coincidence counter,[4] and the measurements can be performed remotely in a hot cell. Eighteen ^{3}He tubes were located in a high density polyethylene moderator, and each ^{3}He tube was connected to an individual preamplifier. Substantial shielding was added to protect the tubes and electronics from the intense gamma rays.

DSNC was installed in the M6b hot cell of the DFDF. Lead bricks and boron-lined high-density polyethylene bricks were placed around the DSNC to reduce the background. An IAEA safeguards instrument cabinet for monitoring DSNC data was also installed outside the hot cell to access the DSNC data.

There are two unsealed doors and one sealed door at the DFDF. Three CCD cameras were positioned at each door to monitor any activities related to the nuclear material movement to and from the doors. Two DSNMs (DUPIC Safeguards Neutron Monitors) were located near the unsealed doors to detect any transportation of nuclear material through the doors. The cameras and DSNMs installed on the outside surface of the DFDF were cabled to the surveillance server located in the working area of the DFDF. The personal computer received the image signal and the radiation signal periodically, analyzed them, and diagnosed the transportation status to report the result to the remote client.

ACPF

The advanced spent fuel conditioning process (ACP) has been developed by KAERI using simulated fuel and fresh fuel since 1997.[5] The ACP can be applied as a conditioning process for a long-term storage and eventual disposal of a PWR spent fuel. The heat, volume, and radioactivity of the spent fuel can be decreased with an oxide reduction and a selective isolation of high heat-load fission products. It may also serve as a preparation method for a metallic fuel for SFR. The ACP consists of several process steps such as slitting and voloxidation of spent PWR fuel rods, reduction of actinide oxides to metal, and smelting of metallic powder to an ingot.

During performing the mock-up test for the Li-based reduction process, KAERI developed and demonstrated an electrolytic reduction process. Also, an ACPF was designed for a hot demonstration of the ACP. Starting in 2004, KAERI designed and manufactured remotely operable process equipment capable of handling 20 kgU/batch size and installed it in the ACPF hot cell for a hot demonstration of the process. The ACPF construction was completed in July 2005. Since then several campaigns for cold tests using fresh U and simulated fuels have been completed. The ACPF consists of two hot cells. One is for the ACP process and the other one is for the maintenance of the process and the remote handling equipment.

Since 2002, KAERI has been developing, in cooperation with Los Alamos National Laboratory (LANL), a passive-mode neutron coincidence counter for material accounting of the ACP. This well-type neutron counter, the so-called ACP Safeguards Neutron Counter (ASNC), is for conducting NDA of the materials that exist during the ACP process. The ACPF's overall material balance is quantified by a ^{244}Cm measurement using the ASNC.

Figure 2. Working area and inside of hot cell of the ACPF

Figure 3. The ASNC for the material accountancy of the ACPF

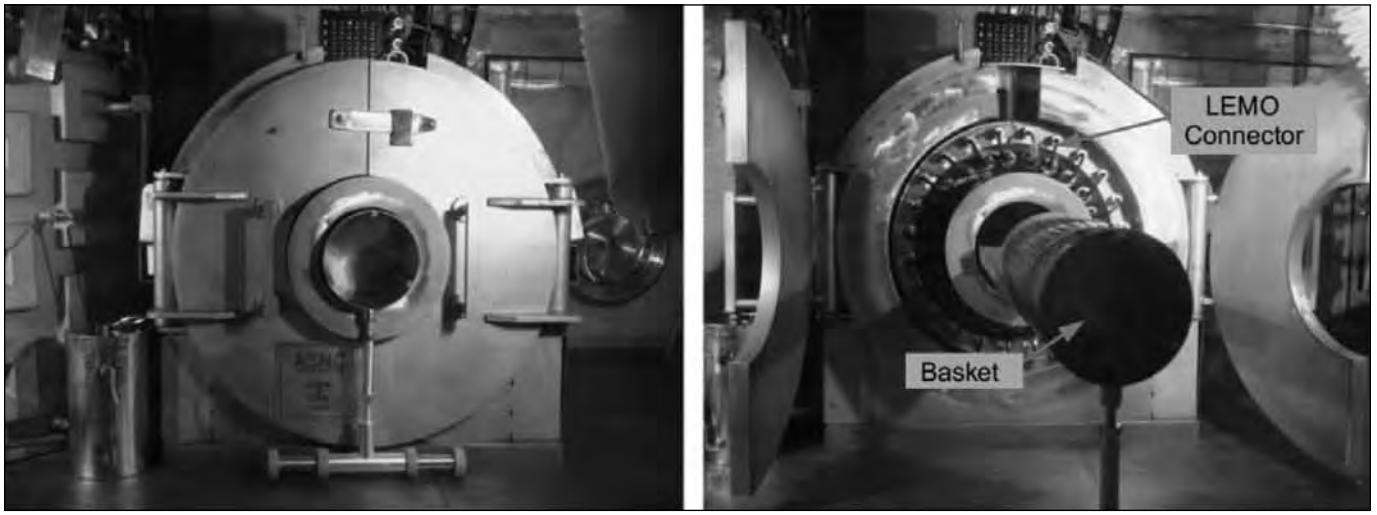

The basic concept of the ASNC is to measure the Cm mass by measuring the coincidence neutrons from the spent fuel.[6] The ASNC contains twenty-four ^{3}He tubes, which are symmetrically located in high-density polyethylene moderator. Each ^{3}He tube was connected to an individual amplifier. The twenty-four signals from the ASNC were divided into four groups, and each group was combined into one signal. The signal cable was designed to be replaced by remote manipulators. Lead shield was placed inside the ASNC to protect the ^{3}He tubes and electronics from the intense gamma rays of the process materials. Lead and HDPE shields were placed outside the ASNC to reduce the background gamma rays and neutrons in the hot cell condition.

The ASNC was installed inside the hot cell of the ACPF in 2005, and the performance tests were conducted with ^{252}Cf sources. A verification test using spent fuel rod-cuts was performed with experts from the IAEA and LANL in 2007.[6, 7] The singles (S), doubles (D), and triples (T) rates of the neutron distribution from spent fuel rod-cuts were measured and calibration curves were produced. MCNPX simulations were performed to compare them with the measurement results. The measured S/D and D/T ratio show excellent agreement with the MCNPX simulated ones. It could be seen that the ASNC is one of the most efficient neutron counters that has been applied to high burnup spent fuel rods, and the spent fuel could be measured with triple counts of the ASNC. The ASNC also has remote operation capabilities, and maintenance can be performed while the ASNC is in a hot cell.

In addition to the material measurement system, an automated nuclear material accounting system and an unattended continuous monitoring system were developed by KAERI in

Figure 4. The operation characteristics of the ASNC. High voltage plateau of the ASNC for the spent fuel rod-cuts (left) and D/T and S/D ratios vs. the singles rate of the ASNS (right).[6]

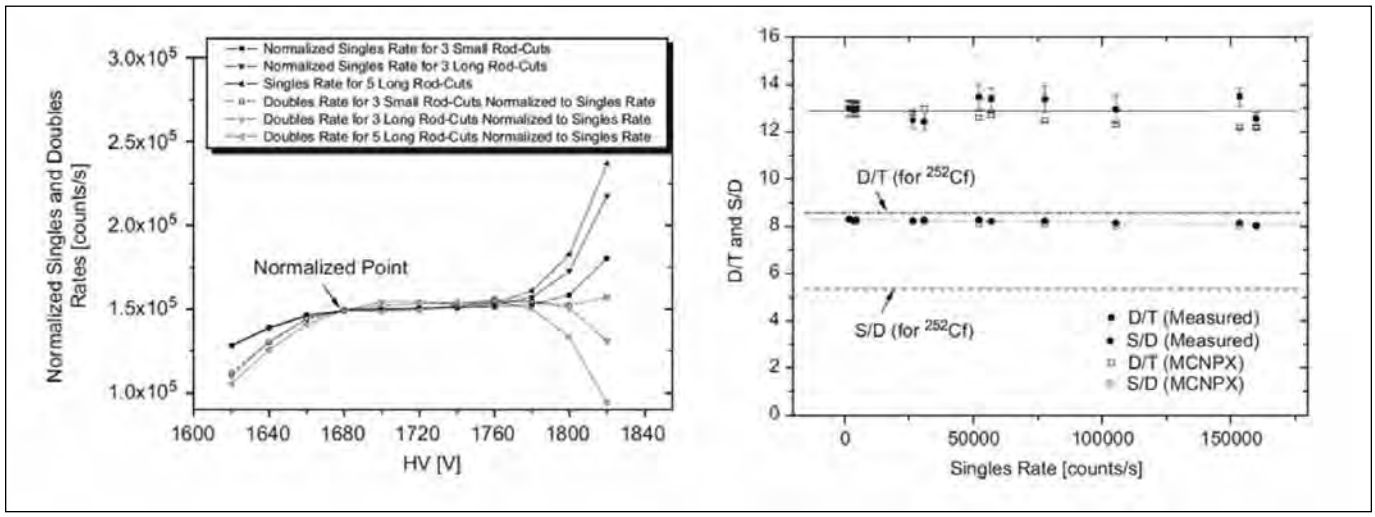

Figure 5. Safeguards system of the ACPF

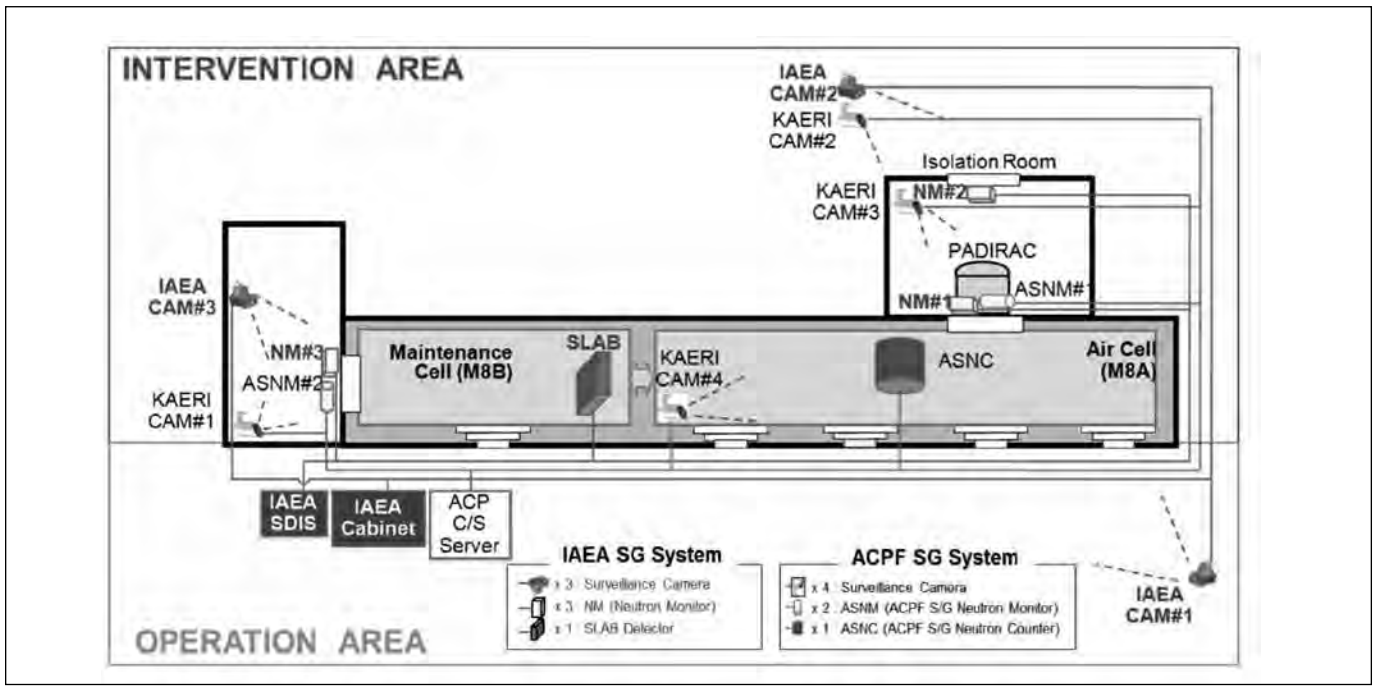

conjunction with LANL. Figure 5 shows the safeguards system installed in the ACPF including the operator's equipment as well as the IAEA's equipment. The ASNC is a key NDA device for nuclear material accounting. The accounting data of the ASNC are provided to the IAEA periodically. The IAEA's slab detector was used for independent verification of the nuclear material accountancy for the ACPF.

Three IAEA cameras and three IAEA neutron monitors were installed at the rear and side doors of the ACPF hot cells to monitor any activities related to the nuclear material movement through the doors. The cameras and neutron monitors were connected to the IAEA safeguards server located in the working area of the ACPF. On the purpose of safeguards R&D for the ACPF, the operator's three surveillance cameras and two ACP safeguards neutron monitors (ASNMs) were also installed at the two hot cell doors of the ACPF. The operator's surveillance system is able to identify spent fuel material movements to and from the ACPF hot cell system.

Figure 6. Front view and working area of the PRIDE facility

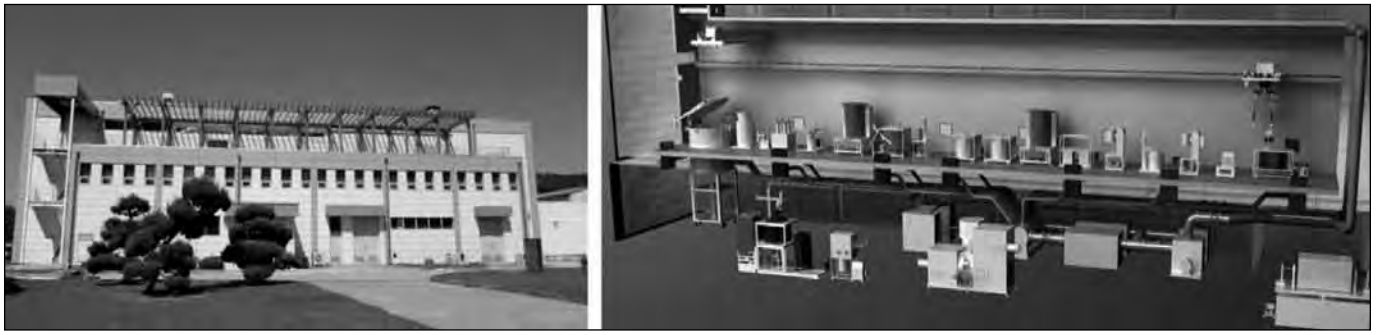

PRIDE

Since 1997, the laboratory-scale unit processes of pyroprocessing have been carried out, and the design and construction of an engineering-scale integrated system was developed by KAERI. PRIDE is the integrated engineering-scale mock-up pyroprocessing facility, and it will be constructed in early 2012. The purpose of the PRIDE is to test the unit process performance, the remote-equipment operability, the integrity of the unit process, the system operation under argon conditions and the safeguards technology. Only uranium and depleted uranium will be treated in the PRIDE. The processes in the PRIDE consist of voloxidation, oxide reduction, electrorefining, electrowinning, and waste treatment processes. Air-atmosphere processes such as fabrication of UCl_3, ingot production and voloxidation are carried out on the first floor and large argon cell is positioned on the second floor. The throughput of the facility is 10 tonU/yr.

A safeguards system of the PRIDE has been designed and is being developed. Because natural and depleted uranium are the process materials in the PRIDE, the mass measured at the key measurement point (KMP) is the most important parameters in the accounting system. The ^{235}U amounts will also be accounted for with a unified NDA system. This instrument is an integrated device with three independent techniques of neutron counting, gamma-ray spectroscopy, and weighing and called the 'Unified NDA' of PRIDE facility. Figure 7 shows an MCNPX model of the Unified NDA instrument. The Unified NDA instrument was designed to be flexible for several containers, which are largely different in their size. Thus the inner cylindrical neutron counter can be removed for larger containers to be accommodated. The basic principles of each technique will remain intact but some improvement in measurement error is expected by the synergy of the combined techniques. Although there will be only natural or depleted uranium materials to be used in the PRIDE facility, the Unified NDA concept could be applied to the nuclear material measurement for future pyroprocessing facilities.

Gamma detectors are installed inside the argon cell to evaluate the possibility of tracking the uranium process flow. Key measurement parameters such as current, voltage, temperature, and humidity will be monitored from process equipments.

Figure 7. MCNPX model of the Unified NDA instrument

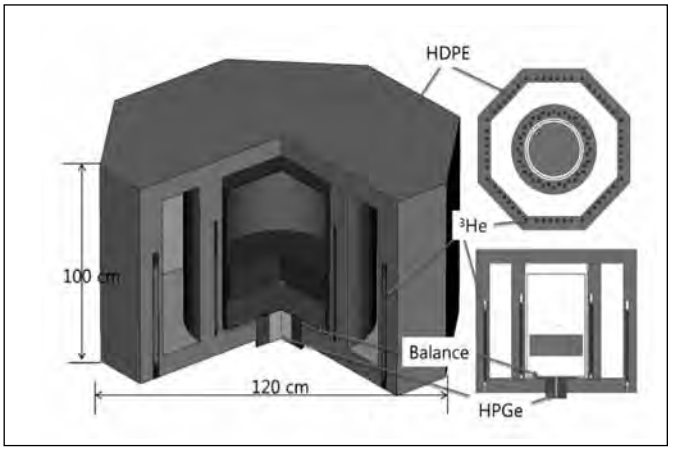

Cameras are installed to survey the movement of nuclear material. An integrated safeguards system, which combines the online NDA signals and process monitoring signals, is being developed to implement near-real-time accountancy (NRTA) at PRIDE.

Development of Other NDA Technologies

Laser-induced breakdown spectroscopy (LIBS) has been recognized as a promising technique for analyzing sensitive nuclear materials such as uranium, plutonium, and curium in a high-radiation environment and that can achieve a precision level similar to that of chemical analysis.[8] LIBS can conduct real-time quantitative analysis of nuclear materials at the processing sites because it does not require preparation of the sample and it can conduct distant measurement.[9] It is increasingly being used as a semi-nondestructive method of analyzing the sample by focusing a low-energy laser pulse (a few mJ) onto the sample, and basic studies of this technique are underway.[10]

KAERI has studied the LIBS technology to monitor and prevent the diversion of nuclear materials in an effort to strengthen the safeguards in the pyroprocessing facilities. The main purpose of the application of LIBS to the safeguards is to

Figure 8. Key measurement points in MBAs of the REPF

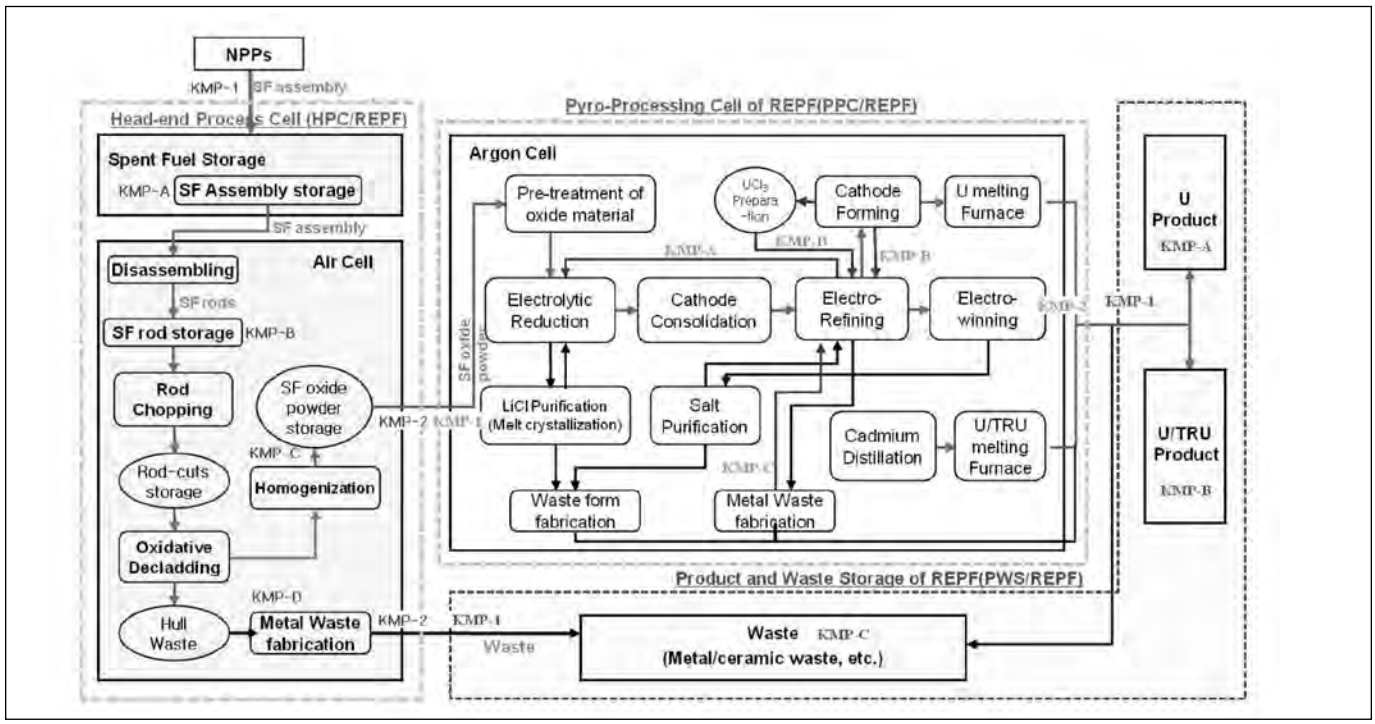

gain quantitative information regarding uranium and plutonium from the processing materials. Preliminary experiments on the materials to be handled in the pyroprocessing facilities have been conducted to optimize the hot cell application of the LIBS technology.

The albedo reactivity technology involved separating the primary emission neutrons from the induced fission neutrons using the neutron multiplicity counting and cadmium ratios. The cadmium ratio can be obtained from two measurements, with a cadmium liner and without the cadmium liner. To demonstrate the applicability of the Passive Neutron Albedo Reactivity (PNAR), a compact neutron counter was designed to measure the cadmium ratios from doubles and triples, which was carried out in the collaboration with LANL.[11]

In the United States, research efforts were started to develop a set of instruments capable of directly measuring the Pu content in spent fuel assemblies, and detecting the diversion of pins from these assemblies. Fourteen NDA techniques were identified that can provide information about the Pu composition.[12] KAERI has collaborated with LANL to carry out the performance tests of the prototype instruments, which include Self-interrogation Neutron Resonance Densitometry (SINRD), ^{252}Cf Interrogation with Prompt Neutron (CIPN) and Differential Die-away Self Interrogation (DDSI), with spent fuel assemblies at Post Irradiation Examination Facility (PIEF) of KAERI.

Safeguards System for Reference Pyroprocessing Facility

A member state supporting program for agency safeguards (MSSP) for the "Support for Development of a Safeguards Approach for a Pyroprocessing Plant" was contracted between the IAEA and the ROK in 2008. Six pyroprocessing facility concepts suggested by the U.S., Japan, and the ROK were analyzed, and the Reference Engineering-scale Pyroprocessing Facility (REPF) concept was developed.[13] The input material for the REPF is PWR spent fuel, and the output materials are U ingot and U/TRU ingot. The size of the process batch is 50 kgHM, the throughput per campaign is 500 kgHM, and the throughput per year is 10 MTHM.

The main processes performed in the REPF consist of receipt and storage of spent fuels, the head-end process, the electrolytic reduction process, the electro-refining process, the electro-winning process, and waste salt regeneration and solidification. The head-end process has five steps: disassembling and rod extraction, chopping, decladding, homogenization, and pretreatment of the oxide fuel. In the electrolytic reduction process, the oxide fuel is converted to a metallic form. The electro-refining system, which is composed of an electro-refiner, a salt distiller, and a melting furnace, recovers pure uranium from the electrolytically reduced fuel. The electro-winning system is able to recover actinides from salt after the electro-refining operation. The waste salts are fabricated into durable waste forms in the waste salt regeneration and solidification process.

Three material balance area (MBA)s were identified for the REPF, which consists of the spent fuel receiving area, the storage and head-end process area (MBA-1), the main pyroprocessing area (MBA-2), and the product and waste storage area (MBA-3). Key Measurement Point (KMP)s should be identified in which the nuclear materials are present to make it possible to measure them and determine the material flow or inventory.

Since the main nuclear materials that should be accounted for are uranium and plutonium in the REPF, and the most important KMPs for accounting these materials are the point before the main pyroprocessing, and two points where the final U ingot and U/TRU ingot products of the pyroprocessing are placed. A unified NDA equipment, a PNAR detector and a fission chamber were suggested as material accounting instruments at three KMPs.

A near-real time accountancy (NRTA) system will be established to timely detect a diversion during pyroprocessing. The NRTA system could be based on NDA equipment and a destructive assay (DA) would also be applied to the three important KMPs to increase the accuracy of material accounting. Considering the time required for a DA, a three-level method was suggested. In the first level, the DA samples are obtained at the three important KMPs, and the samples are analyzed by the DA method. In the second level, the NRTA equipments in the NRTA system are continuously performed at three important KMPs while the DA samples are analyzed. In the third level, the NRTA results from the NRTA system are updated and corrected by comparing with the DA results.

A simulation program called pyroprocessing material flow and material unaccounted for uncertainty simulation (PYMUS), has been developed to analyze the nuclear material flow in the REPF and to calculate the MUF uncertainty.[9] DA-based material accounting in the REPF can give accurate information for the necessary accountability, and the NDA-based accounting can also yield useful accounting information in a timely manner.

Although the REPF concept was mainly based on safeguards concerns and the analysis under these conditions may give limited results, the efforts to design a reference facility, and to develop a safeguards approach for pyroprocessing will be helpful in implementing the safeguards-by-design concept.

Conclusion

Pyroprocessing is a new and advanced proliferation-resistant technology that could help reduce the volume and the radioactivity of spent fuels and potentially allow the spent fuel to be recycled. The safeguards approach for pyroprocessing should be established to determine the Pu inventory accurately, track the nuclear material flow, and ensure that there is no diversion.

The ROK has successfully developed and implemented NDA instruments and safeguards systems for its nuclear fuel facilities. Currently, the R&D efforts to develop NDA measurement equipments, advanced C/S and process monitoring systems, and modeling and simulation for the safeguards of the pyroprocessing facilities continue. The SBD approach is based on these efforts. The safeguards system for the PRIDE is being designed to evaluate the safeguards technology of pyroprocessing facility. From the beginning of the design phase, these projects have proceeded in cooperation with facility designer. The REPF concept was established to develop the safeguards approach, and to analyze the safeguardability. A joint fuel cycle study (JFCS) was agreed between ROK and United States to explore the technical and economical feasibility and nonproliferation acceptability of the pyroprocessing. This study will be continued for ten years, and be composed of three phases. The study is currently at the phase 1, and the technical focus areas in the safeguards are safeguards technical direction and analysis, safeguards testing with irradiated material, technology for nuclear material accountancy, technology for containment and surveillance, safeguards and security by design, modeling and simulation for analysis of safeguards performance, and safeguards for fuel cycle alternatives. The application of SBD to these efforts will contribute to improving nuclear transparency and safeguards technology so that pyroprocessing technology can be realized in the future.

Acknowledgements

This work was supported by the nuclear research and development program sponsored by the Ministry of Education, Science and Technology of Korea.

References

1. Kim H. D. 2009. Progress and Prospects for System Engineering and Safeguards Technology Development of a Pyroprocessing Facility in Korea, *24th KAIF/KNS Annual Conference*.
2. 2009. Facility Design and Plant Operation Features That Faciliate the Implementation of IAEA Safeguards, 2009 IAEA, IAEA-STR-360.
3. DUPIC Fuel Fabrication Using Spent PWR Fuel at KAERI, 2007 KAERI, KAERI/AR-766/2007.
4. Kim H. D., H. R. Cha, W. I. Ko, D. Song, H. Y. Kang, D. Y. Kim, J.-Y. Hong, M. Yang, and H. Menlove. 1996. Technology Development on the DUPIC Safeguards System, LA-UR-01-0938, 1996.
5. 2011. Lab-scale Demonstration Plan of Advanced Spent Fuel Conditioning Process Using Irradiated Fuels at KAERI, KAERI/AR-888/2011.
6. Lee T.-H., H. O. Menlove, S.-Y. Lee, and H. D. Kim. 2008. Development of the ACP Safeguards Neutron Counter for PWR Spent Fuel Rods, *Nuclear Instruments and Methods in Physics Research A* 589, 57-65, 2008.

7. Lee T.-H, Y. S. Kim, H.-S. Shin, and H.-D. Kim. 2011. Hot-test Results of the Advanced Spent Fuel Conditioning Process Safeguards Neutron Counter for PWR Spent Fuel Rods, *Nuclear Technology* 176, 147-154.
8. Barefield J. E., S. M. Clegg, S. A. La Montagne, K. D. Veal, L. Le, and L. Lopez. 2010. Symposium on International Safeguards, Vienna, Austria, IAEA-CN-184/134.
9. Whitehouse A. I., J. Young, C. P. Evans, and A. Brown. 2003. Remote composition analysis of Spen-Fuel Residues Using Laser-induced Breakdown Spectroscopy, *Waste Management '03*.
10. Young J., I. M. Botheroyd, and A. I. Whitehouse. 1996. Remote Analysis of Nuclear and Non-nuclear Materials Using Laser-Induced Beakdown Spectroscopy (LIBS), *Conference on Electro-Optics and Lasers* (CLEO/Europe), Hamburg, Germany, 152.
11. Lee S. Y., Menlove H. O., Swinhoe M. T., and Marlow J. B. 2008. Development of a passive neutron albedo reactivity counter for a Korean advanced pyroprocessing facility, *Proceedings of 49th Annual Meeting of the Institute of Nuclear Material Management*.
12. Tobin S., S. Demuth, M. Fensin, J. Hendricks, H. Menlove and M. Swinhoe. 2008. Determination of plutonium content in spent fuel with NDA—why an integrated approach, *Proceedings of 49th Annual Meeting of the Institute of Nuclear Materials Management*.
13. Shin H. S., B. Y. Han, D. Y. Song, S. K. Ahn, S. H. Park, Y. P. Sitompul, and H. D. Kim. 2011. A Study on the MUF Uncertainty Estimation for an Engineering-scale Pyroprocessing Facility, *Proceedings of GLOBAL 2011*.

Advances in the Measurement Sciences for Verification Being Undertaken at LANL in Support of Nuclear Safeguards

Stephen Croft and Karen Miller
Los Alamos National Laboratory, Safeguards Science & Technology Group (N-1), Los Alamos, New Mexico USA

Abstract

The objective of international nuclear safeguards is the timely detection of the diversion of nuclear materials in peaceful nuclear programs for use in nuclear weapons or other explosive devices. In safeguarding nuclear materials, design information verification of facilities, establishment of a materials control and accountancy (MC&A) system, the implementation of a containment and surveillance system, along with an inspection regime are of fundamental importance to creating overall confidence in a nation's adherence to its international obligations. The MC&A activity is supported by nondestructive physical measurements. Los Alamos National Laboratory (LANL) has been at the forefront of research and development in nondestructive measurement techniques for identifying and quantifying key attributes of nuclear materials since the field of measurement sciences for verification began. Nondestructive assay (NDA) entails quantifying some attribute of nuclear material—such as enrichment, relative isotopic composition, or mass—using penetrating signatures so that the item can be measured intact with minimal or no preparation. In this paper, we review some of the work currently ongoing at LANL. Most of the examples we provide involve measuring neutrons, photons, or heat naturally emitted by the items under study. We conclude with thoughts on emerging challenges and opportunities such as the need for improvements in basic nuclear data.

Introduction

Verification of nuclear material by physical measurement is a scientific art inextricably linked to technology. At a basic level, nuclear material can be weighed on a scale, and the basic chemical form can be inferred from its color and material properties. However, in order to accurately verify the type and amount of nuclear material in a sample for modern applications, we measure the radiation emitted by the material. These applications include nuclear safeguards, noncompliance verification, treaty verification, nuclear event response, holdup and waste measurements, nuclear forensics, and the characterization of measurement standards. The focus of this paper is on nuclear safeguards, although the developments taking place across the verification application space are often cross-cutting and complementary.

Because radiation from nuclear materials is not readily seen, smelled, tasted, felt, nor heard, scientists and engineers have developed creative ways to detect and quantify it. In this paper, we describe the process of taking an idea for a new radiation detector from concept to design all the way through implementation in the field. This is a multidisciplinary and iterative process that relies not only on highly qualified professionals but also on tools such as predictive modeling codes, accurate nuclear data, and well-characterized calibration sources. We provide examples of cutting-edge technologies being developed at Los Alamos National Laboratory (LANL) for neutron, gamma-ray, and alpha measurements. These technologies are being used to solve some of the most pressing verification challenges of our day, and continuing to invest in research and development will help prepare the international community for the major verification challenges of the future.

The remainder of this article is structured as follows. We first discuss the technology development process that LANL uses to create solutions. Most of the article is dedicated to providing a review of key LANL projects in safeguards technology, and we close by highlighting several emerging challenges and opportunities.

The Technology Development Process

Throughout the history of innovation, the vast majority of breakthroughs have occurred in collaborative environments. The process of technology development for complex systems relies on the seamless operation of multidisciplinary teams. There is a method to taking an idea for a new radiation detector from concept to design all the way through implementation in the field. It is an organized process that always begins with deceptively simple step: identification of a problem. Physicists and nuclear engineers then develop the conceptual idea of how to solve that problem. They try to find harmony between the questions of "what attributes are we trying to determine?" and "what signatures can we measure?"

Most signatures of safeguards interest are reasonably well-understood at a fundamental level. In application space, physics phenomena may therefore be predicted by two methods. The first is experimental investigation, which is often expensive, time-consuming, and sometimes impossible. The second is theoretical calculation. We can write down a mathematical *model* for some

physical phenomena. Predictive modeling codes such as Monte Carlo N-Particle (MCNP)[1] and its variants can take user input (e.g., system geometry, material composition, source information), supplemented by data libraries that contain nuclear data, and estimate a detector response by evaluating the mathematical model of the physical phenomenon under consideration. They are used to determine if a detector will behave as expected, to optimize the physics design, and to conduct sensitivity studies. Implicit in modeling is that reliable predictions require realistic assumptions and accurate nuclear data.

At this point, the detector design usually iterates between physics, mechanical, and electrical design, each piece impacting the others. Optimization also involves achieving the measurement performance objective within a myriad of other constraints such as size, weight, lifetime cost of ownership, data security, reliability, and ease of maintenance. Once the design is finalized, it is manufactured and then characterized and tested in a laboratory environment. Laboratory experiments are done to benchmark the modeling, confirm estimated detector parameters such as the efficiency, and test the sensitivity of the instrument to environmental conditions such as moisture, temperature, and radiofrequency noise.

Finally, the instrument is ready to be taken into the field. It may be a prototype system, wherein field trials are used to assess the viability of the measurement technique and identify vulnerabilities in the design. The entire process, starting with the physics design, may need to be iterated several times. In some cases, laboratory personnel may collaborate with industrial partners with the ultimate goal of technology transfer to the commercial sector. In other cases, it may be a custom-built detector designed for installation in a nuclear facility. Once the detector is in the field, it must be calibrated. Uncertainty associated with the calibration source is folded into the total measurement uncertainty. As we push the limits of detection, we must necessarily increase our efforts in characterizing standards and reference materials.

The selection of emerging technologies described in the following section span the spectrum of this technology development process. Some of them have reached the realm of data collection and analysis, which marks the interface where verification begins. Technologies that enter service are not dormant, however, and important incremental refinements continue to take place. In other words, it is important to have a balanced portfolio of early research, capability development, focused demonstration, and implementation.

New and Emerging Radiation Detector Technologies

There is an enormous amount of research being done at LANL in measurement sciences for verification, specifically for safeguards applications. In this section, we provide summaries of some of the technologies currently under investigation. (One notable omission is the large Next Generation Safeguards Initiative (NGSI) Spent Fuel NDA project, which has evaluated fourteen different measurement techniques for quantifying plutonium in commercial spent nuclear fuel.[2] This project was covered in the spring 2012 issue of the *Journal of Nuclear Materials Management* on spent fuel measurements.[3])

- **ENMC:** The Epithermal Neutron Multiplicity Counter (ENMC) is the world's flagship correlated neutron counter. It is a passive well counter that contains 121 ^{3}He tubes with 10-atmospheres of gas pressure arranged in four concentric rings. The combination of high-efficiency and low die-away time make it especially well suited for high-precision coincidence and multiplicity counting.[4] Four variations of the ENMC have been built for nuclear facilities in Japan, and two Mini-ENMC units were built as smaller, more portable versions of the ENMC for field deployment. One of the Mini-ENMC units is currently in Vienna, Austria, on loan to the International Atomic Energy Agency (IAEA).

  The ENMC and Mini-ENMC are workhorse instruments. They are in high demand for a wide range of verification applications, one of which is in the field of metrology, or the science of measurement. One of the core concepts in metrology is traceability. It refers to the ability to trace a measurement result, through an unbroken chain of comparisons, to a recognized calibration standard. Recently, the Inventory Sample Coincidence Counter (INVS)[5] was re-introduced into the sample cavity of the ENMC. The integrated ENMC/INVS system has a total of 142 ^{3}He tubes, an efficiency of about 85 percent, and a die-away time of 19 ms. The precision that can be achieved with the ENMC/INVS is comparable to calorimetry (<0.2 percent) but with much shorter count times. In the short term, we plan to use the ENMC/INVS to cross-calibrate attributes of LANL's calibration sources, such as the absolute neutron emission rate, against the National Institute of Standards and Technology (NIST) certificates and study important parameters such as the mean number of neutrons emitted per fission and multiplicity distributions.

  The Mini-ENMC was used for two notable measurement campaigns in 2011. The first campaign demonstrated the capability to make high-mass plutonium measurements at LANL's Plutonium Facility.[6] The work was focused on measurement of a series of PuO_2 standards. The second campaign highlighted the versatility of the Mini-ENMC with the extension to uranium measurements at LANL's Sigma Facility.[7] Small UF_6 cylinders were measured in support of enrichment plant safeguards and nuclear noncompliance verification. In addition to testing measurement techniques for special nuclear materials, deployment of the Mini-ENMC to both the Plutonium and Sigma Facilities at LANL demonstrated the instrument's portability and reliability under field conditions.

- **AEFC:** The Advanced Experimental Fuel Counter (AEFC) was developed for the measurement of spent fuel rods and assemblies from research reactors (e.g., MTR, IRT, and Magnox reactors) for safeguards verification.[8,9] Specifically, it was designed to verify the residual ^{235}U mass, burnup, reactor power profile, and the initial enrichment of the fuel, and it can be used for both underwater and air applications. The measurement system contains components for active neutron interrogation, passive neutron totals counting, neutron coincidence counting, and gross gamma-ray counting. For measuring the ^{235}U fissile mass, the active neutron component has an AmLi source for neutron interrogation. The active assay mode uses two measurement methods: (1) neutron coincidence counting and (2) totals neutron differential transmission, in which the AmLi interrogation source has lower average neutron energy than the induced fission neutrons.

  Close collaboration with facility operators and international partners has been crucial to gaining field experience with the instrument. The first AEFC spent fuel measurements were obtained from the HIFAR reactor in Australia in 2006.[10] Recently, the AEFC was used for measurement of spent fuel arising from operation of the WWR-SM research reactor at the Institute of Nuclear Physics (INP) in Uzbekistan.[11] Twenty-four fuel assemblies were measured that covered a wide range of initial enrichments, burnups, and cooling times. Coming up in 2012, additional measurements are planned at Savannah River Site (SRS). With growing international interest in spent fuel verification, the experience gained from field deployment of the AEFC plays an important role in the development of new spent fuel measurement techniques.
- **PNEM:** The Passive Neutron Enrichment Meter (PNEM) was designed to determine ^{235}U mass and enrichment in UF_6 cylinders for uranium enrichment plant safeguards. It uses total neutron counting, coincidence counting, and cadmium subtraction to unfold key attributes of depleted, natural, and low-enriched UF_6 in 30B and 48Y cylinders.[12,13] The PNEM system consists of two briefcase-sized detector pods with polyethylene-moderated ^{3}He tubes and a removable cadmium cover. The measurement concept grew out of the success of the Uranium Cylinder Assay System (UCAS), which is an operator system installed at the Rokkasho Enrichment Plant (REP) in Japan that uses total neutron counting to determine ^{235}U mass in UF_6 cylinders.[14] By adding more efficiency for coincidence counting and a removable cadmium sheet, we can also make an enrichment measurement that is much less sensitive to heels and other heterogeneities than the traditional gamma-ray-based NDA method.

  The first field trial of the PNEM system occurred in 2011 at REP, where the joint U.S.-Japanese team measured thirty-six cylinders: twenty-six product, five feed, and five tails. It was a successful test and demonstrated the viability of the measurement technique. Additional field trials are planned for the near future, including one at the Westinghouse Fuel Fabrication Plant in South Carolina. Although the PNEM detector pods are portable and can be hand-carried to cylinders, the end state envisioned for this instrument is as a component in an unattended cylinder verification station at an enrichment plant.
- **AEM:** The Advanced Enrichment Monitoring (AEM) technology is based on the classical gamma spectroscopy measurement of the concentration of ^{235}U in UF_6 gas and a correction for gas density by use of a transmission measurement (active enrichment monitoring) or by use of temperature-corrected gas pressure information (passive enrichment monitoring). This technology is based on previous LANL experience with the Blend Down Monitoring System (BDMS) installed in various locations in Russia to monitor the conversion of highly enriched uranium to fuel for nuclear reactors.[15] It addresses typical challenges faced by implementation of this method: (1) periodic replacement of the decaying conventional radioactive source for transmission-based gas density corrections and (2) the necessity of empty pipe calibration of both transmission- and pressure-based corrections for gas density.

  To address the difficulties associated with the decaying radioactive transmission source, an X-ray tube and a notch filter are used to generate a transmission peak with flexible energy selection.[16] The X-ray source has a greater mean time between failures and does not degenerate with time. To address the calibration in presence of UF_6 gas, methods were developed for independent measurement of the pipe wall thickness[17] and pipe wall deposits.[18] The developed technology is undergoing tests at the URENCO Capenhurst gas centrifuge enrichment plant. The goals, equipment, measurement method, and calibration were described by Ianakiev *et al.*[19] The passive monitoring system was installed in August 2011, calibrated using LANL's pressure transient method, and has been compared with the operator's mass spectrometer enrichment values. Initial test results show good stability, and the system was able to track changes in enrichment with a fraction of a percent relative accuracy. The active monitoring system was scheduled for installation in April 2012.
- **IPCA 2:** The Improved Plutonium Canister Assay System 2 (IPCA 2) is a nondestructive assay system designed to measure incoming canisters of bulk mixed uranium-plutonium oxide (MOX) powders at the proposed Japan Nuclear Fuel Limited (JNFL) mixed-oxide fuel fabrication plant (J-MOX). The design evolved from the original IPCA, which is currently used to measure canisters of product MOX powder at Rokkasho Reprocessing Plant. Under the auspices of the Japan Safeguards Office (JSGO), the IPCA 2 was designed

jointly by the Nuclear Material Control Center (NMCC) and LANL.[20,21] The instrument will be installed in-line in the MOX receiving area and will operate in unattended mode. The data will be shared by Japan's domestic safeguards inspectorate and the IAEA.

The IPCA 2 consists of a ^{3}He-based passive neutron well counter with an integrated high-purity germanium (HPGe) gamma system comprised of three individual detectors, a load cell, and a camera. It is intended to make a bias defect level measurement of plutonium in full MOX canisters with a $^{240}Pu_{eff}$ neutron measurement uncertainty of less than 0.85 percent. The anticipated sample size is 18 kg plutonium in 50:50 U:Pu MOX powder. Achievement of this target uncertainty level is technically difficult due to the neutron emission rates in such high mass samples. It will also perform a gamma isotopic measurement on each sample with an accuracy of better than 2 percent for the $^{241}Pu/^{239}Pu$ and $^{240}Pu/^{239}Pu$ ratios. The IPCA 2 is a key measurement system for the new J-MOX plant and represents the future of international safeguards instrumentation, namely because it is a high-accuracy system that can be used in unattended mode.

- **^{3}HE Replacement:** The majority of the neutron-based NDA systems designed by LANL and deployed by the IAEA inspectorate for verification measurements of special nuclear material are based on ^{3}He gas-filled proportional counters. These can achieve the high-neutron detection efficiency necessary for correlated neutron counting (both coincidence and multiplicity). Further, these detectors are relatively insensitive to gamma radiation and possess excellent stability characteristics—both temperature and long-term stability—essential when operating in a nuclear facility. However, there is currently a worldwide shortage of ^{3}He. The supply of ^{3}He, which is produced via tritium decay, is in decline simultaneously with a dramatic increase in the demand for homeland security applications post 9-11.[22] As part of finding a viable alternative to ^{3}He for neutron detectors, LANL has developed a ^{3}He replacement detector test program[23,24] for the evaluation of safeguards-specific performance parameters, including: detection efficiency, die-away time, coincidence figure of merit for Doubles counting, gamma-ray discrimination, dead time (count rate capability), long-term stability, temperature stability, humidity response, scalability, physical size, and sensitivity. The test program provides detailed procedures to perform experimental characterization of ^{3}He alternative neutron detectors from various vendors.[25] The program also includes a novel simulation component in order to compare measured results from different size detectors with a ^{3}He-based reference system.[26] The test program has been completed for a range of prototype ^{10}B-lined detection technologies, which are considered to be a viable, near-term replacement for ^{3}He. The goal of the test activity is to identify a ^{10}B-lined detector to replace ^{3}He in a build of a full neutron safeguards counter based on the High Level Neutron Coincidence Counter (HLNCC). LANL will participate in this broader U.S. effort to build and test the system over the next few years.
- **^{6}LiSSND:** The ^{6}Li Scintillation Sandwich Neutron Detector (^{6}LiSSND) is an alternative detection technology for replacement of ^{3}He gas proportional counters that was proposed by LANL scientists and is currently being studied. It uses multiple layers of ^{6}Li foil placed between polymethylmethacrylate (PMMA) lightguide strips laminated with thin films of organic scintillator. When a neutron enters the detector volume, it traverses the sandwich layers of PMMA, scintillator film, and ^{6}Li foil repeatedly. It is moderated incrementally in the hydrogen-rich PMMA strips and organic scintillator film. It is then ca ptured in a ^{6}Li layer producing primary charged particles that escape the metallic lithium layer and deposit energy in adjacent organic scintillator films, producing photons. The multiple capturing layers of ^{6}Li film and double readout provided by two photomultiplier tubes positioned at the axial ends of the lightguide strips maximize intrinsic efficiency per layer while preserving a good pulse height distribution. Neutron-to-gamma-ray discrimination is based primarily on the difference of energies deposited by gammas and tritons in the thin scintillator film. MCNP modeling for the ^{6}LiSSND shows more than two times higher efficiency, up to three times shorter die-away time, and negligible dead time compared to the standard HLNCC-II.[27]

  The combination of high efficiency and good coupling between neutron moderation and capture makes this technology a good candidate for a thermal-well-geometry coincidence counter. The sandwich configuration ensures that neutrons can be captured at multiple locations as neutrons are incrementally moderated in the materials positioned between ^{6}Li layers, thereby increasing efficiency and detectability of neutrons across a broad energy spectrum. ^{6}Li foil with the desired thickness was manufactured and used in a small (2"×2"×18") proof-of-principle prototype, which has been fabricated and tested for characterization. The experimental results show ballpark efficiency of a 4-atmosphere ^{3}He tube of the same length and indicate good coupling between moderation and capturing. A full-sized well coincidence counter prototype based on ^{6}LiSSND was presented at the U.S.-Russian Radiation Detection Workshop.[28]
- **Statistical Challenges and Simulation:** Statistical challenges arise in several areas of safeguards technology development such as in characterizing measurement uncertainty, online decision making for process monitoring, and combining results from multiple experiments. Three ways in which LANL is actively addressing such challenges include the study of the following: (1) systematic effects of neutron multiplicity counting on uncertainty, (2) event marking,

and (3) meta-analysis and statistical modeling techniques. It is important to understand systematic effects in neutron multiplicity counting in order to accurately characterize total measurement uncertainty (i.e., random plus systematic uncertainties). In one study, MCNP simulations were used to estimate the effects of a range of MOX sample properties such as bulk density, sample positioning, heavy-metal-to-oxide fraction, and plutonium isotopic composition on the inferred plutonium mass. This type of modeling study is useful for understanding how variations in measurement conditions are projected into systematic uncertainties.[29] Process monitoring is increasingly important in nuclear safeguards as a complement to mass-balance-based nuclear material accounting, and automatic event marking is used in several process monitoring systems to locate the start and stop times and signal changes associated with key events. One LANL study evaluated different event marking methods with real and simulated data to find the most effective strategy for this type of time series safeguards applications.[30] Finally, some of the current work in statistical methods has used meta-analysis to combine results from multiple experiments[31] of nuclear reaction rate estimates needed in safeguards applications. For example, a neutron cross-section is typically measured in multiple experiments and a single estimate and associated uncertainty are provided as the estimated reaction rate. However, there can be important differences in experimental protocols among laboratories, making the synthesis of several estimates difficult. Burr et al.[31] are working on meta-analysis and statistical modeling techniques that can be used to discover inconsistencies that could result in more tightly controlled assay protocols and, therefore, more consistent assay results.

- **Microcalorimeter:** For several decades, HPGe detectors have been the state-of-the-art for NDA measurements that utilize gamma-ray spectroscopy. Now, cryogenic microcalorimeter arrays providing energy resolution up to ten times better than HPGe are further improving the accuracy and precision of nondestructive nuclear material measurements.[32,33,34,35] The improved resolution is well suited to the analysis of complex gamma-ray spectra with dense and overlapping photopeaks, such as the 100-keV region of mixed-isotope plutonium samples. The exceptional energy resolution of the microcalorimeter (as low as 22 eV full width half maximum (FWHM) at 100 keV) is derived from operation at low temperatures, typically near 100 mK. Although operation at such temperatures was at one time exotic, modern technology allows these temperatures to be reached routinely with commercially-available equipment. The core of the technology is a transition-edge sensor (TES) thermometer coupled to a bulk absorber with superconducting quantum interference device (SQUID) readout. Heat deposited by individual gamma rays is recorded to produce an energy spectrum. Signal readout of the detector array is through time-domain multiplexing circuitry. The past several years have seen rapid progress from a proof-of-principle device to a 256-pixel microcalorimeter array collecting data on nuclear samples in the laboratory. Recent results have demonstrated improved measurement precision for plutonium isotopics compared to HPGe data with equal total counts. Current work is focused on the fabrication and operation of high-yield arrays with counting rates in the kHz range, increasing multiplexing speed, and development of quantitative isotopic analysis code. A parallel research program is investigating the use of microcalorimeter detectors for high-energy-resolution alpha-particle spectroscopy, with applications in nuclear forensics. This technology has the potential to make high-fidelity basic nuclear data measurements.
- **WDS:** In the same genre of ultra-high-resolution techniques, there is a renewed interest in specialized wavelength dispersive spectroscopy systems that operate based upon Bragg diffraction from oriented single crystal analyzers.[36] These have several intrinsic advantages over energy-dispersive solid state detectors (cryogenic germanium) in the analysis of high-activity radioactive materials: (1) the diffracting crystals in a wavelength dispersive spectrometer (WDS) only direct photons in a very narrow energy range, equivalent to the resolution of the system, into the detector; (2) the photon detector does not require a line of sight to the source, which permits the detector to be well shielded from direct and background radiation; and (3) the energy resolution of a WDS can be more than an order of magnitude better than solid state detectors, which can significantly enhance the observed signal-to-noise ratio and result in increased analytical sensitivity. Diffractive optics can be implemented in both transmission and reflective geometries and custom-tailored for specific measurement challenges.[37,38] Two prototype WDS systems are currently being fabricated for safeguards applications. The first is a parallel-collection von Hamos spectrometer that uses a cylindrically bent crystal diffractor and a position sensitive detector. This spectrometer is being configured for characteristic L-series X-ray spectroscopy and is designed to simultaneously detect all actinide L-alpha lines at approximately 10-eV resolution. A second flat crystal spectrometer is being created as a test bed for the analysis of low-energy gamma rays and characteristic K-series X-rays.
- **FRAM:** The Fixed-Energy Response-Function Analysis with Multiple Efficiency (FRAM) code was developed at LANL to analyze high-resolution gamma-ray spectra to determine the relative isotopic composition of plutonium, uranium, and other actinides and fission products. Relative isotopic composition is important verification in its own right but is also needed to obtain quantitative results from correlated neutron counting and calorimetric measurements. It also allows total activity to be distributed between nuclides.

The FRAM code originated in the mid-1980s and, as operational experience accumulated and needs evolved, it has undergone continuous refinement. Today, FRAM is in routine use around the world and has become a benchmark in the field. In 2011, a decade after the last major release, FRAM Version 5 was distributed.[39] Some of the improvements in FRAM Version 5 include: ease of use; enhanced robustness; extensive auto-analysis; command-line operation mode; improved 100-keV region analysis; improved ^{236}U correlation; improved energy calibration peak search; error bars and error band for relative efficiency points and fit; provision for inclusion of systematic uncertainties in output results; maximum channel range extension to 32K channels; maximum energy range extension to about 10 MeV for physical model efficiency; interactive, real-time parameter editing; improved compatibility with commercial formats for multiple spectra; Microsoft Excel-compatible results file for multiple spectra analysis and comparison; improved parameter set version control; and fill and line spectrum display modes.

There are many other improvements and new features throughout the code. Most of these features have been available on in-house versions for some time and were also distributed for beta testing prior to release, which means that they have been tested extensively. Over a wide range of conditions, the performance results from FRAM 5.1 have been shown to be excellent.

- **Neutron Correlation Counting:** For more than forty years, correlated neutron counting has been used to assay special nuclear materials, namely plutonium via the passive spontaneous fission and induced signatures and uranium (mostly) via active interrogation methods. The predominant autocorrelation function method applied to the detected neutron pulse train is shift-register logic to extract multiplet information, and the only practical real-time inversion methods use algebraic point-model equations. Large, dense, multiplying items that couple to their surroundings and the detector violate the point-model assumptions.[40] Measurement scenarios that challenge existing count rate limits are being explored, and we have found that the current understanding of and compensation for rate loss effects are inadequate.[41] We currently have a program aimed at addressing both of these traditional weaknesses. The program addresses basic dead time correction models and alternative formalism. Furthermore, it also addresses the consolidation and comparison of correlation counting methods other than the traditional difference histogram shift register approach (e.g., early gate only, delayed gate only, and the Feynman variance-to-mean ratio approach using the fast accidental overlapping gate histogram).

Emerging Challenges and Opportunities

Technological development's enduring drivers include the ongoing need to reduce costs, miniaturize, cut power consumption, and simplify. The development of safeguards solutions may take many years, and the service life of equipment is typically decades. Thus, the safeguards field does not see the constant churning of new devices common in consumer markets. But, the need to have a nimble development process fully informed by current and emerging technologies is paramount; commercial entities and adversaries are not constrained by the established operational norms of the inspectorates. Advanced fuel cycle concepts will require new safeguards approaches. The shortage of ^{3}He for neutron detector fabrication is an example of a sudden step-like change to the development environment. The traditional challenge of how to verify software and system design continues to show incremental improvement in line with general engineering practice. In the safeguards domain, the influx of ideas from the consumer market also fuels expectations, especially with respect to intuitive and easy-to-use interfaces, interconnectivity of devices, user groups, and data sources. Data-collecting capability has increased enormously in recent years, and storing and mining this requires specialist skills in addition to those of the instrument designer/physicist. Technology development is moving towards smart instruments that continuously monitor their state of health and can recalibrate in the event of partial failure.

The list of improved nuclear data needs for safeguards is long. Instrument calibration requires well-characterized and representative standards and reference materials. Further, increasing reliance is being placed on simulation and modeling, which combines nuclear data with radiation transport models to predict physical phenomena. The accurate interpretation of nuclear material measurements rests on the availability of nuclear data that is fit for these purposes. For neutron detector characterization, ^{252}Cf has become a ubiquitous surrogate for plutonium, yet opportunities still exist to improve the data base on asymmetric neutron emission, spectrum-multiplicity and fission n-γ correlations, as well as yield estimates of reference ^{252}Cf sources. The experimental data base for the spontaneous fission isotopes of plutonium is remarkably sparse.[42,43] There are large discrepancies between measurements of certain reaction yields, such as the F(α,n) yields from uranium isotopes needed for UF_6 cylinder assay and hold-up measurements. In addition to improving the quality of measurements across the spectrum of verification applications, a program to advance the state of nuclear data today would provide an excellent training ground for the next generation of professionals in the field.

The safeguards budget for the IAEA is expected to remain flat at a time when the number and complexity of facilities under safeguards is expanding. Advanced technology is one way to do more with less. Remote, autonomous instruments connected to other sensors informing them about their environment will undoubtedly play a role. Making the most of the information and

data available will also be important, and using modern methods of inferential calculus and decision making can enrich safeguards technology development. The measurement sciences community will need to continue to be responsive as fuel cycles develop and change in the future. Retaining staff, facilities, reference materials, and knowledge is a structural issue that cannot be underestimated. The creation of regional centers of excellence with a mission to train the specialist skills needed is a response to this.

Perhaps the biggest challenge is how to deal with the increasing pace of change across an expanding canvas of possibilities. The safeguards community must, on the one hand, provide proven solutions with a long service life, commensurate with the nuclear facilities under safeguards, and yet it must also be nimble and flexible to take advantage of new ideas and innovations. Collaborative innovation networks may emerge as the essential element to delivering verification science solutions of the future.

Conclusion

Technology is the bridge that connects truth and verification. Whether that truth refers to the status of a state's compliance with its treaty obligations, the amount of nuclear material in a waste container, or the neutron emission rate of a calibration source, technologies provide observable signatures that scientists use to piece together complex systems and processes. The conclusions drawn from these signatures are used to inform policy makers, keep people safe, or provide the missing link for the next big technological breakthrough.

This paper provides a snapshot of some of the technological developments ongoing at LANL in support of measurement sciences for verification. LANL has been a constant force in the evolution of safeguards technology for more than forty years. As illustrated here, research in the field continues to be vibrant and many challenges and opportunities remain.

Acknowledgements

The authors would like to thank Louise Evans, Andrew Hoover, Tom Burr, Marcie Lombardi, Cliff Keller, and Rollin Lakis for contributing project summaries to this paper. The funding for many of the technologies highlighted here was provided by the Next Generation Safeguards Initiative (NGSI), Office of Nonproliferation and International Security (NIS), and the Office of Verification Research and Development, both of the National Nuclear Security Administration (NNSA).

References

1. X-5 Monte Carlo Team, *MCNP – A General N-Particle Transport Code, Version 5*, Los Alamos National Laboratory Code Package, Radiation Safety Information Computational Center (RSICC).
2. Tobin, S. J., H. O. Menlove, M. T. Swinhoe, and M. A. Schear. 2011. Next Generation Safeguards Initiative Research to Determine the Pu Mass in Spent Fuel Assemblies: Purpose, Approach, Constraints, Implementation, and Calibration, *Nuclear Instruments and Methods in Physics Research A*, Vol. 652, No. 1, 73-75.
3. Humphrey, M. A., S. J. Tobin, and K. D. Veal. 2012. The Next Generation Safeguards Initiative's Spent Fuel Nondestructive Assay Project, *Journal of Nuclear Materials Management*, Vol. 40, No. 3.
4. Stewart, J. E., D. G. Langner, F. A. Duran, C. D. Rael, H. O. Menlove, D. R. Mayo, K. E. Kroncke, and B. S. Cordova. 1999. The Epithermal Neutron Multiplicity Counter (ENMC): Faster Plutonium Assay by Factors of 5-20, *Proceedings of the 40th Annual Meeting of the Institute of Nuclear Materials Management.*
5. Menlove, H. O., J. E. Stewart, and D. R. Mayo. 1999. Advanced Performance Epithermal Neutron Detector for Measurement of Inventory Samples, *Proceedings of the Sixth International Conference on Facility Operation—Safeguards Interface.*
6. Lakis, R. E., M. T. Swinhoe, H. O. Menlove, and J. B. Marlow. 2011. Passive Neutron Multiplicity Measurements of High Mass Plutonium Samples, *Proceedings of the Institute of Nuclear Materials Management 52nd Annual Meeting.*
7. Lafleur, A. M., K. A. Miller and H. O. Menlove. 2011. Verification of Small UF_6 Cylinders Using Neutron Self-Interrogation and Multiplicity Counting, *Proceedings of the Institute of Nuclear Materials Management 52nd Annual Meeting.*
8. Swinhoe, M. T., H. O. Menlove, J. B. Marlow, et al. 2006. A Portable Spent Fuel Counter for Research Reactor Fuel," *Proceedings of the Institute of Nuclear Materials Management 47th Annual Meeting.*
9. Menlove, H. O., J. B. Marlow, M. T. Swinhoe, and C. D. Rael. 2008. Advanced Experimental Fuel Counter (AEFC) Calibration and Operation Manual, LA-14359-M, Los Alamos National Laboratory Manual.
10. Menlove, H. O., M. T. Swinhoe, A. Lebrun, et al. 2007. Field Application of a Portable Detector for the Verification of Research Reactor Spent Fuel, *Proceedings of the ESARDA Annual Meeting, Aix-en-Provence, France.*
11. Menlove, H. O., J. B. Marlow, K. A. Miller, et al. 2012. Field Tests of a Detector for the Verification of Research Reactor Spent Fuel at the WWR-SM Reactor at the Institute of Nuclear Physics in Uzbekistan," *Proceedings of the Institute of Nuclear Materials Management 53rd Annual Meeting.*
12. Miller, K. A., H. O. Menlove, M. T. Swinhoe, and J. B. Marlow. 2010. A New Technique for Uranium Cylinder Assay Using Passive Neutron Self-Interrogation, *Proceedings of the IAEA Safeguards Symposium.*

13. Miller, K. A., H. O. Menlove, M. T. Swinhoe, and J. B. Marlow. 2011. The Passive Neutron Enrichment Meter for Uranium Cylinder Assay, *ESARDA Bulletin*, No. 46.
14. Miller, K. A., H. O. Menlove, M. T. Swinhoe, et al. 2010. The Uranium Cylinder Assay System for Enrichment Plant Safeguards, *Journal of Nuclear Materials Management*, Vol. 39, No. 1.
15. Close, D. A., R. E. Anderson, W. S. Johnson, et al. 1999. Calibration of the Enrichment Monitor for HEU Transparency, *Proceedings of the 6th International Meeting on Facilities Operation—Safeguards Interface,* p. 111.
16. Ianakiev, K. D., B. D. Boyer, J. M. Goda, et al. 2009. Advanced Enrichment Monitoring Technology Based on Transmission Measurements with an X-Ray Source and NaI(Tl) Spectrometer, *Proceedings of the ANIMMA Conference.*
17. Lombardi, M. L., A. Favalli, J. M. Goda, et al. 2012. Determination of the Thickness of Aluminum Cascade Pipes in the Presence of UF_6 Gas During Enrichment Measurements, submitted to *Nuclear Instruments and Methods in Physics Research A.*
18. Favalli, A., K. D. Ianakiev, C. Keller, et al. 2011. Performance Evaluation of a Multi-Detector System for Unattended Uranium Enrichment Monitoring, *Proceedings of the Institute of Nuclear Materials Management 52nd Annual Meeting.*
19. Ianakiev, K. D., B. Boyer, A. Favalli, et al. 2011. On-Line Enrichment Monitor for UF_6 GCEP, *Proceedings of the ESARDA Meeting*, Budapest, Hungary (2011).
20. Marlow, J. B., M. T. Swinhoe, H. O. Menlove, et al. 2012. Design of the Improved Plutonium Canister Assay System 2 (IPCA 2), *Proceedings of the Institute of Nuclear Materials Management 53rd Annual Meeting.*
21. Miller, K. A., M. T. Swinhoe, J. B. Marlow, et al. 2012. Efficiency Profile Flattening Using Cadmium Tailoring for the Improved Plutonium Canister Assay System 2 (IPCA 2), *Proceedings of the Institute of Nuclear Materials Management 53rd Annual Meeting.*
22. Kouzes, R. T. 2009. The ^{3}He Supply Problem, PNNL-18388, Pacific National Laboratory Report.
23. Henzlova, D., L.G. Evans, H. O. Menlove, et al. 2011. Test Program to Compare Alternative Neutron Detectors for Potential ^{3}He Replacement for Nuclear Safeguards Applications, LA-UR 11-00098, Los Alamos National Laboratory Report.
24. Menlove, H. O., D. Henzlova, L. G. Evans, et al. 2011. ^{3}He Replacement for Nuclear Safeguards Applications—an Integrated Test Program to Compare Alternative Neutron Detectors, *ESARDA Bulletin*, No. 46.
25. Evans, L. G., D. Henzlova, H. O. Menlove, et al. 2011. ^{3}He Replacement for Nuclear Safeguards Applications Part I: Test Program and Experimental Results, *Proceedings of the Institute of Nuclear Materials Management 52nd Annual Meeting.*
26. Henzlova, D., L. G. Evans, H. O. Menlove, et al. 2011. ^{3}He Replacement for Nuclear Safeguards Applications Part II: Benchmarking and Simulation Results, *Proceedings of the Institute of Nuclear Materials Management 52nd Annual Meeting.*
27. Ianakiev, K. D., M. T. Swinhoe, A. Favalli, et al. 2011. ^{6}Li Foil Scintillation Sandwich Thermal Neutron Detector, *Nuclear Instruments and Methods in Physics Research A*, Vol. 652, No. 1.
28. Ianakiev, K. D., M. T. Swinhoe, A. Favalli, et al. 2012. ^{6}Li Foil Scintillation Sandwich Thermal Neutron Detector, *Proceedings of the U.S.-Russian Radiation Detection Workshop,* Moscow, Russia (to be published).
29. Evans, L. G., J. A. Favorite, and M. T. Swinhoe. 2010. Systematic Effects in Neutron Coincidence and Multiplicity Counting, *Proceedings of the Institute of Nuclear Materials Management 51st Annual Meeting.*
30. Burr, T., M. Suzuki, J. Howell, et al. 2011. Signal Estimation and Change Detection in Tank Data for Nuclear Safeguards, *Nuclear Instruments and Methods in Physics Research A*, Vol. 640, 200-212.
31. Burr, T., S. Croft, B. Williams and M. White. 2012. Meta-Analysis for Inconsistent Nuclear Measurements, LA-UR 11-06708, submitted to *Nuclear Science and Engineering.*
32. Hoover, A. S., N. Hoteling, M. W. Rabin, et al. 2011. Large Microcalorimeter Arrays for High-Resolution X- and Gamma-Ray Spectroscopy, *Nuclear Instruments and Methods in Physics Research A*, Vol. 652, No. 1, 302-306.
33. Bennett, D. A., R. D. Horansky, A. S. Hoover, et al. 2010. An Analytical Model for Pulse Shape and Electrothermal Stability in Two-Body Transition-Edge Sensor Microcalorimeters, *Applied Physics Letter*s, Vol. 97, 102504.
34. Hoover, A. S., M. K. Bacrania, M. K. Hoteling, et al. 2009. Microcalorimeter Arrays for Ultra-High Energy Resolution X- and Gamma-Ray Detection, *Journal of Radioanalytical and Nuclear Chemistry*, Vol. 282, No. 1, 227-232.
35. Doriese, W. B., J. N. Ullom, J. A. Beall, et al. 2007. A 14-Pixel, Multiplexed Array of Gamma-Ray Micro-Calorimeters with 47 eV Energy Resolution at 103 keV, *Applied Physics Letters*, Vol. 90, 191910.
36. Deslattes, R. D. 2000. High-Resolution Gamma-Ray Spectroscopy: The First 85 Years, *Journal of Research of the NIST*, Vol. 105, No. 1.
37. Seely, J. F., L. T. Hudson, G. E. Holland, et al. 2008. Enhanced X-Ray Resolving Power Achieved Behind the Focal Circles of Cauchois Spectrometers, *Applied Optics*, Vol. 47, No. 15, 2767.

38. Dumond, J. W. M. 1947. A High-resolving Power Curved-Crystal Focusing Spectrometer for the Short Wavelength X-Rays and Gamma-Rays, *Review of Scientific Instruments*, Vol 18, 626-638.
39. Vo, D. T. 2011. Operation and Performance of FRAM Version 5.1, *Proceedings of the Institute of Nuclear Materials Management 52nd Annual Meeting*.
40. Croft, S., L. G. Evans, M. A. Schear and M.T. Swinhoe. 2011. Feasibility of Classic Multiplicity Analysis Applied to Spent Fuel Assemblies*, Proceedings of the Institute of Nuclear Materials Management 52nd Annual Meeting.*
41. Hauck, D. K., S. Croft, A. Favalli, et al. 2011. Deployable Dead Time Corrections for Neutron Multiplicity Measurements Accounting for Neutron Correlations and Multiple Detector Chains*, Proceedings of the Institute of Nuclear Materials Management 52nd Annual Meeting.*
42. Santi, P., D. H. Beddingfield and D. R. Mayo. 2005. Revised Prompt Neutron Emission Multiplicity Distributions for Pu-236, Pu-238, *Nuclear Physics A*, Vol. 756, No. 3-4, 325-332.
43. Santi, P., and M. Miller. 2008. Reevaluation of Prompt Neutron Emission Multiplicity Distributions for Spontaneous Fission, *Nuclear Science and Engineering*, Vol. 160, No. 2, 190-199.

Assessing the Feasibility of Using Neutron Resonance Transmission Analysis (NRTA) for Assaying Plutonium in Spent Fuel Assemblies

David L. Chichester and James W. Sterbentz
Idaho National Laboratory, Idaho Falls, Idaho USA

Abstract

Neutron resonance transmission analysis (NRTA) is an active-interrogation nondestructive assay (NDA) technique capable of assaying spent nuclear fuel to determine plutonium content. Prior experimental work has definitively shown the technique capable of assaying plutonium isotope composition in spent fuel pins to a precision of approximately 3 percent, with a spatial resolution of a few millimeters. As a grand challenge to investigate NDA options for assaying spent fuel assemblies (SFAs) in the commercial fuel cycle, Idaho National Laboratory has explored the feasibility of using NRTA to assay plutonium in a whole SFA. The goal is to achieve a Pu assay precision of 1 percent. The NRTA technique uses low-energy neutrons from 0.1-40 eV, at the bottom end of the actinide-resonance range, in a time-of-flight arrangement. Isotopic composition is determined by relating absorption of the incident neutrons to the macroscopic cross-section of the actinides of interest in the material, and then using this information to determine the areal density of the isotopes in the SFA. The neutrons used for NRTA are produced using a pulsed, accelerator-based neutron source. Distinguishable resonances exist for both the plutonium (^{239,240,241,242}Pu) and uranium (^{235,236,238}U) isotopes of interest in spent fuel. Additionally, in this energy range resonances exist for six important fission products (^{99}Tc, ^{103}Rh, ^{131}Xe, ^{133}Cs, ^{145}Nd, and ^{152}Sm), which provide additional information to support spent fuel plutonium assay determinations. Based on extensive modeling of the problem using Monte Carlo-based simulation codes, our preliminary results suggest that by rotating an SFA to acquire two orthogonal views, sufficient neutron transmission can be achieved to assay a SFA. In this approach multiple scan information for the same pins may also be unfolded to potentially allow the determination of plutonium for sub-regions of the assembly. For a 17x17 pressurized water reactor SFA, a simplified preliminary analysis indicates the mass of ^{239}Pu may be determined with a precision on the order of 5 percent, without the need for operator-supplied fuel information or operational histories.

Introduction

Neutron resonance transmission analysis (NRTA) is a quantitative analytical technique capable of determining the mass of uranium, plutonium, higher-order actinides, and several fission products in spent fuel. In ad hoc testing the approach was experimentally demonstrated for commercial light-water reactor spent fuel pins more than thirty years ago; the measurement assay precision of the technique for quantifying plutonium was demonstrated in the range of 2 - 4 percent.[1, 2, 3] Recognizing the capabilities of this technique, in 2009 Idaho National Laboratory (INL) initiated a research program to explore the feasibility of using NRTA as a method for assaying a whole spent fuel assembly (SFA).[4, 5, 6, 7] The aim of this project was to understand the capabilities and limitations of NRTA for dealing with more massive objects (assemblies versus single fuel pins) and, in particular, to estimate the measurement precision that can be achieved. To make this estimate a system-level approach was used to consider the many different variables that impact mass estimation in NRTA measurements. Constraints were placed on this analysis to consider only currently-available technology. The ultimate goal was to see how close a conceptual design could come towards achieving the "grand challenge" goal for assaying Pu in a SFA of having a Pu assay precision of 1 percent or better. This analysis was entirely done based on simulation and modelling. Recognizing this limitation, effort was taken to model the earlier NRTA experimental work assaying fuel pins, to serve as a benchmark comparison for building confidence in the modelling.

INL's work to examine NRTA as a method for assaying Pu in spent fuel has been part of a larger program of research sponsored by the U.S. Department of Energy's Next Generation Safeguards Initiative (NGSI). The NRTA technique is just one of many technologies studied in the NGSI to investigate measurement techniques for determining Pu mass in commercial SFAs and for detecting the diversion of pins from commercial SFAs.[8,9]

Background Information

Neutron time-of-flight (TOF) measurements represent a well known set of tools for determining neutron-reaction cross sections of nuclei.[10,11] NRTA, in the simplest sense, is a cross-section

Figure 1. The total neutron interaction cross-section for four plutonium isotopes

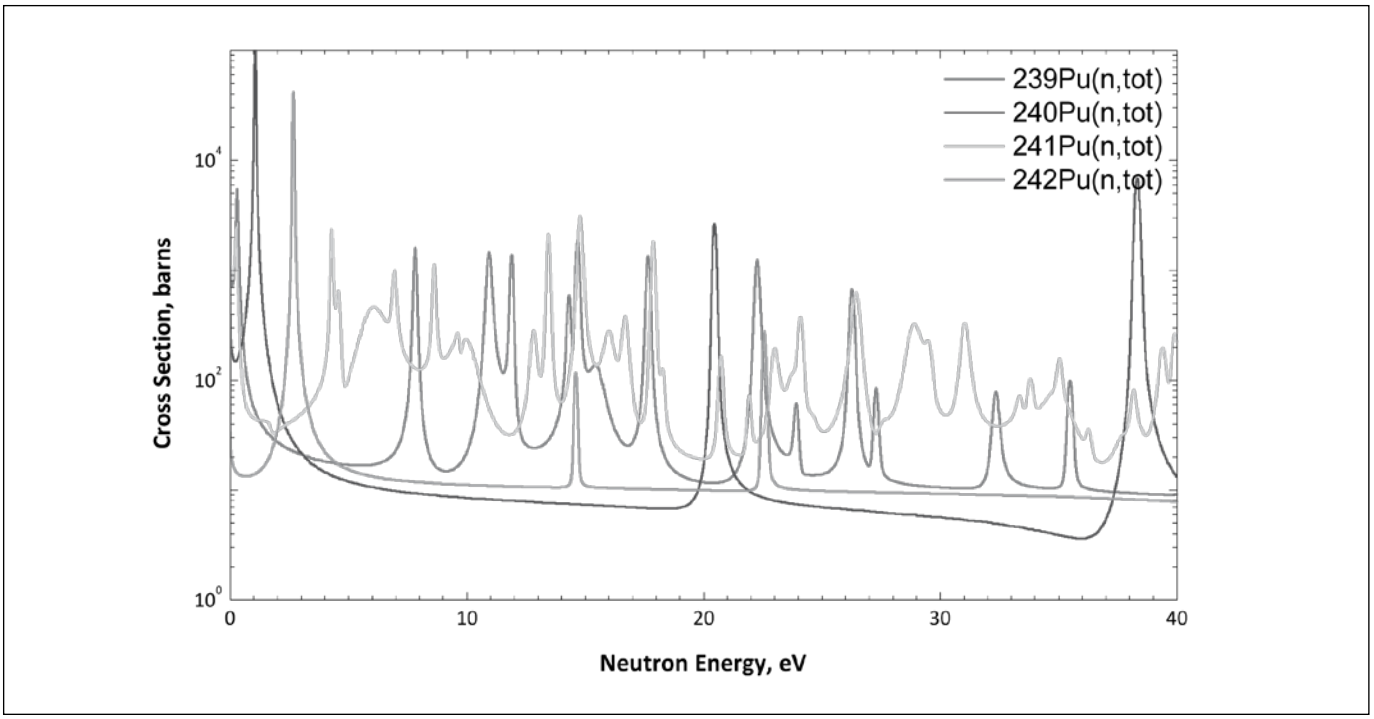

Figure 2. Schematic representation of the NRTA measurement approach

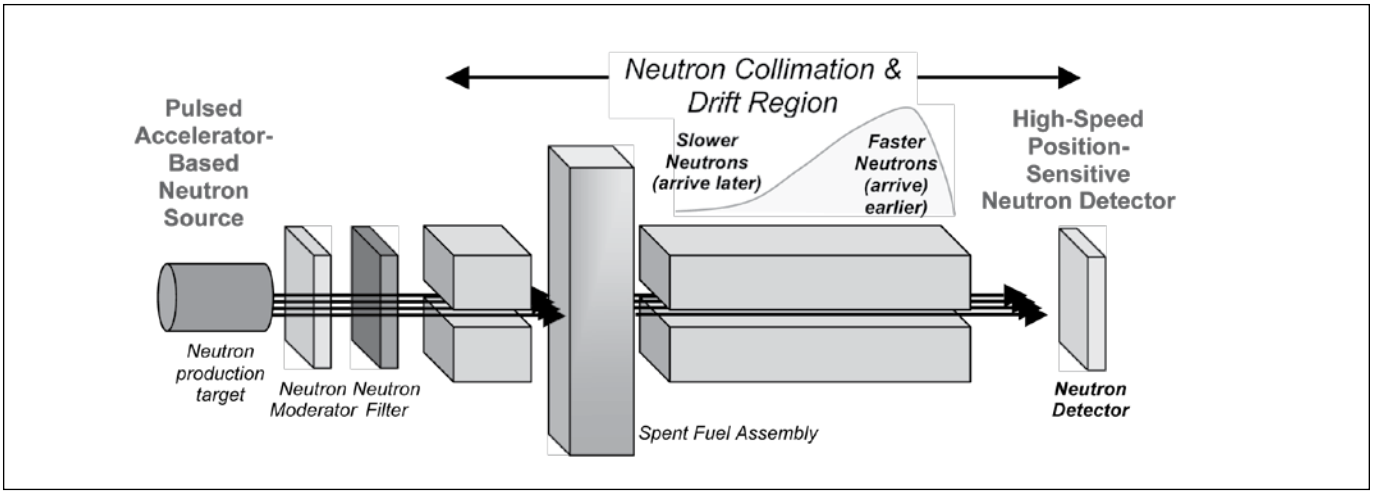

measurement in reverse where the cross-section is the known and the transmission-target mass is the unknown. It uses low-energy neutrons in the 0.1-40 eV energy range for quantifying plutonium (see Figure 1). This energy range is at the bottom end of the actinide-resonance range, where most actinides have one or more resonances. For most actinides in spent fuel these resonances are typically large in magnitude, narrow in breadth, and well separated, resulting in distinctive resonance transmission spectra.

NRTA Implementation

The neutrons may be generated using reactor neutron sources with a chopper wheel but, for implementation for safeguards measurements, accelerator-based sources are a more practical approach. Accelerator neutron production may be achieved using either electron or light-ion beams. A simplified approach using a pulsed electron accelerator, for example, would start by having a short duration pulse (lasting for a microsecond or less) of high-energy electrons impact a high-Z converter (e.g., tungsten or tantalum), producing a continuum of bremsstrahlung photons. It

is practical to consider using an accelerator having an endpoint energy in the range of ~10-12 MeV; higher energy systems are also suitable. The high-energy bremsstrahlung photons then pass through a low-Z photo-neutron converter (heavy water or beryllium) to produce high-energy neutrons. These high-energy neutrons pass through a low-Z neutron moderator (polyethylene, light or heavy water, or beryllium) where they scatter and lose energy (a process called thermalization). This scattering process yields a continuous distribution of neutrons, varying in energy from the starting energy down to approximately 0.025 eV, the thermal kinetic energy of nuclei. It is the portion of this continuum having thermal and epithermal neutrons that is of interest to the NRTA technique. The accelerator would be pulsed with a sufficiently long period to allow all of the thermal neutrons from one burst to exit the system prior to the start of the next pulse. Candidate pathways for producing neutrons using light-ions include the ^{7}Li(p,n) or ^{9}Be(p,n) reactions.

Once thermalized, irrespective of the production method, the neutrons need to be collimated to create a neutron beam directed at the SFA. The collimation process must also incorporate a minimum length of "drift space" to allow the multi-energy neutron beam to self-separate in time and space. High-energy neutrons traverse this drift space most quickly, arriving at the SFA sooner after the end of each beam pulse, while lower-energy neutrons arrive at later times after each burst of neutrons. A fraction of the 0.1-40 eV neutrons incident on the fuel assembly are removed from the beam as they interact with fuels pins in the SFA. The removal processes include elastic scattering, neutron-capture absorption, and neutron-capture fission. The rest of the neutrons pass through the spent fuel assembly unaffected, this is the transmitted signal. It is these transmitted neutrons–the modulated beam–that is measured in the NRTA technique. The transmitted signal is an integral scan through the assembly and is analogous to how a traditional X-ray radiograph is used to detect the presence of dense objects in the human body (bones) and the location of low density regions (bone cracks). The NRTA technique does not assay individual pins in a SFA, with the exception of the four corner pins. Measurements are made using a single-pixel or pixelated detector arrays that are sensitive to thermal neutrons. The time of arrival of the neutrons is recorded as a function of time following each burst of neutrons; the results from each successive burst are added together over the duration of a measurement. Since different energy neutrons travel at different speeds, the time of arrival can be related to the energy of the neutrons when the drift length is known. At neutron energies where there are resonances in isotopes present in the fuel the count intensity is observed to decrease. The magnitude of signal decrease is directly related to the areal density of the absorbing isotopes in the SFA. A schematic representation of the NRTA measurement approach is shown in Figure 2.

Table 1. Neutron energies and velocities, and transit times through a 5-m drift tube.

Neutron Energy [eV]	Velocity [cm/ms]	Neutron Flight Time over 5m [ms]
0.1	0.4377	1,142
0.9	1.313	380.8
1	1.384	361.2
9.9	4.355	114.8
10	4.377	114.2
19.9	6.174	80.98
20	6.190	80.78

Time and Energy Resolution: The Drift Length

For TOF measurements such as NRTA, the energy-resolution requirements for a measurement determine the drift tube length and the detector's timing-resolution requirement. Starting with a known detector resolving time, the drift tube length may be determined to ensure that the neutron energy spread (resolution goal) is less than the detector resolving time. Conversely, starting with a known drift tube length, a detector resolving time specification may be defined to achieve the desired energy resolution. A tabulation of neutron energies and velocities is shown in Table 1. If one were to assume a drift tube length of 5m, it is clear that a detector time resolution of 0.20 μs would be needed to have an energy difference of 0.1 eV between 20 eV and 19.9 eV. At lower energies though the detector timing requirements are reduced; between 1 eV and 0.9 eV the same 0.1-eV energy resolution would only require a detector time resolution of 19.5 μs. A neutron detector time resolution of 0.1 μs is reasonable using a ^{3}He-based detector, for example, but other detector options exist as well. Recognizing this, a drift-length of 5m has been the basis for most INL conceptual NRTA modeling to date. With a drift length of 5m the maximum permissible accelerator pulse rate may be determined by choosing a period so that the slowest neutrons of interest, 0.1 eV for NRTA, have sufficient time to reach the detector. For a 5-m drift tube the fastest permissible pulse rate is 876 Hz.

Competing Resonances in the 0.1 – 40 eV Range

Of the hundreds of fission-product isotopes found in spent fuel, only a half-dozen or so have a significant resonance structure in the 0.1-40 eV energy range (see Figure 3); both ^{235}U and ^{238}U have resonances in this region too (see Figure 4). However, for each of the actinide isotopes there is at least one clear resonance peak unobstructed by narrow-width interfering resonances (when the correct concentrations are accounted for). Other isotopes present in nuclear spent fuel—for example, oxygen in the UO_2 ceramic, and zirconium, tin, iron, chromium, oxygen, niobium, nickel, carbon, and silicon in the Zircaloy-4 clad—also have no

Figure 3. Total neutron interaction cross-sections for relevant fission products

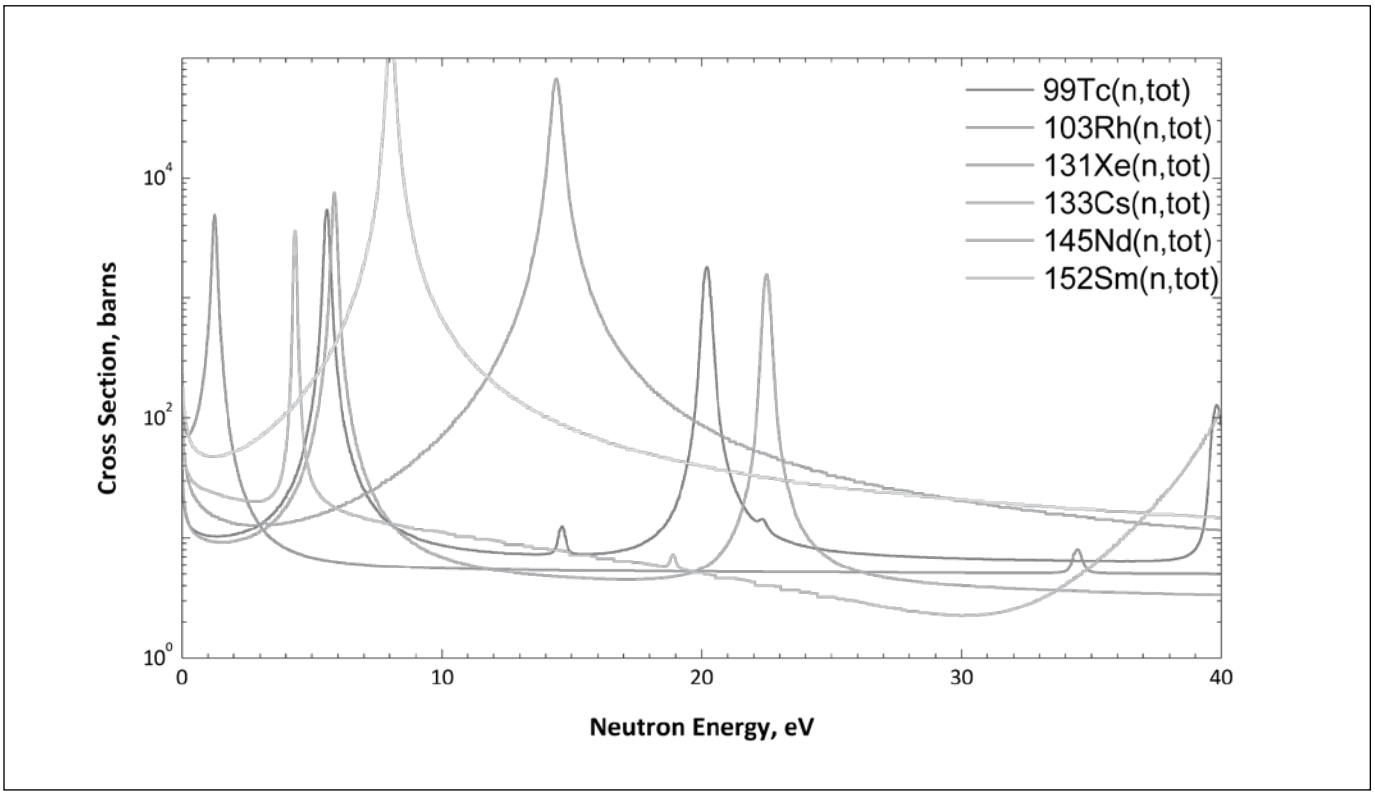

resonance structure in the 0.1-40 eV range. The same is true for the hydrogen impurity (hydration) in the clad and air isotopes.

Using Transmission to Determine Pu

Many advances have been made between the early NRTA work done in the 1980s and today. These advances help enable practical modeling and, potentially, the implementation of the NRTA technique. The most significant enabling advances have been improvements in the nuclear data needed to analyze NRTA data; neutron cross-sections and resonance parameters have been re-measured and evaluated and are now known with a much higher degree of accuracy.[12,13]

The NRTA technique grew out of cross-section measurement techniques; it is basically the inverse to the problem of measuring neutron cross-sections. In the case of neutron cross-section measurements the two known variables are (1) the sample isotopic content, or sample areal density N_i and (2) the transmission flux T_i through isotope i determined by the TOF measurement. A third variable, the total cross-section σ_{ti} for an isotope i, is the unknown variable and the desired quantity to be measured. The total cross-section is then calculable as a function of neutron energy, E, from Equation 1.

$$T_i(E) = e^{-N_i \sigma_{ti}(E)} \quad (1)$$

For NRTA, the unknown variable is the isotopic areal density N_i, and the two known variables are the total cross-section σ_{ti} and the measured neutron transmission flux T_i. Other known factors include the fuel pin and assembly geometry and dimensions, cladding material, and the fuel form (UO_2). Knowledge of these other factors helps to reduce systematic error and improve the overall NRTA measurement accuracy.

Calibrated reference standards, if available, can also play an important role in assessing the accuracy and precision of spent fuel assay measurements; the same would be true for an NRTA system. Unirradiated and irradiated fuel pins and assemblies with known dimensions and material compositions can be used as NRTA calibration standards. For example, pins containing (1) no fuel, (2) fresh UO_2 with 100 percent ^{238}U and various ^{235}U enrichments, (3) and spent fuel surrogate compositions (uranium and rare-earth elements) can all be fabricated with accurately known isotopic compositions.

High-fidelity burnup calculations can also play an important role to further support NRTA spent-fuel transmission measurements. NRTA transmission measurements can be compared to calculated transmission measurements. Agreement

Figure 4. Total neutron interaction cross-sections for uranium

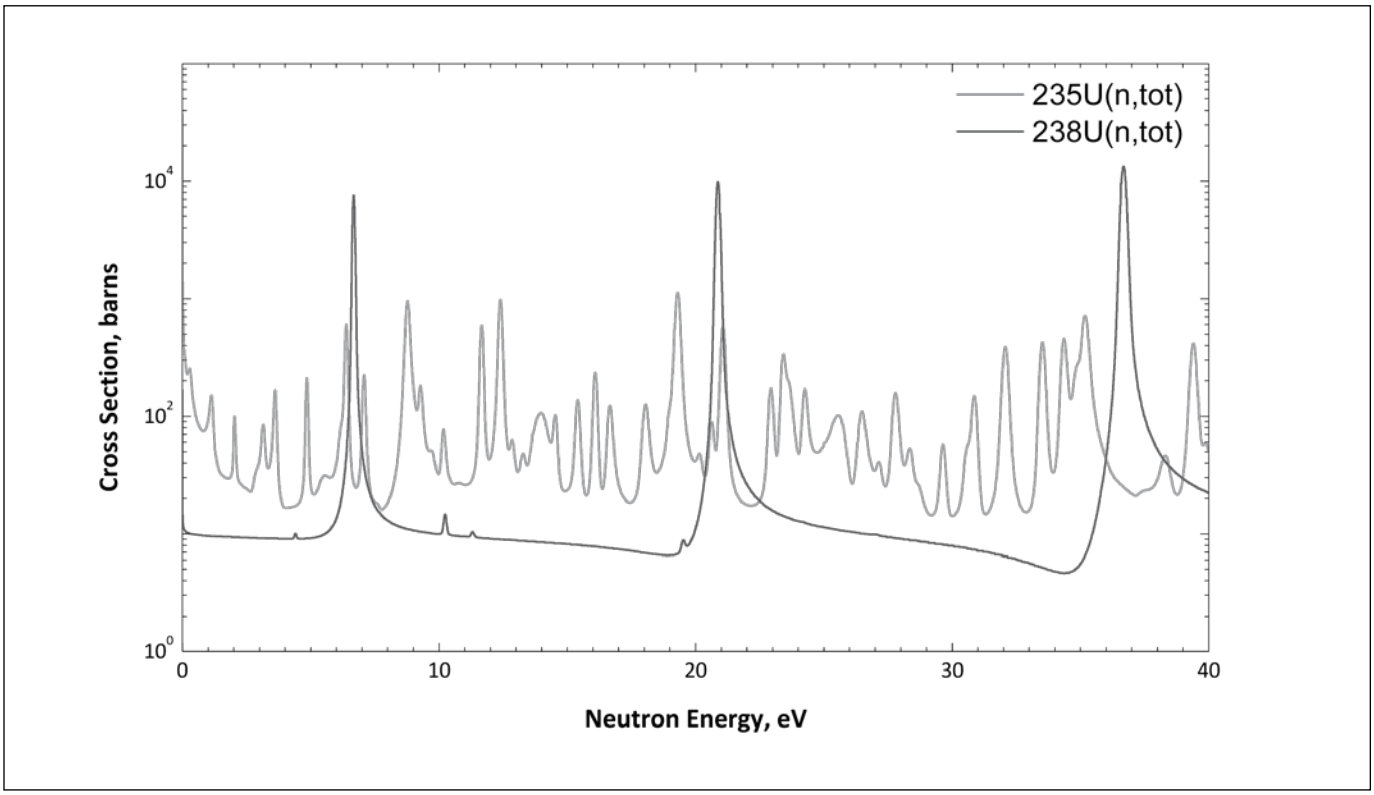

between measured and calculated spectra, and then comparison of the corresponding isotopic concentrations, can be used to confirm pin/assembly isotopic concentrations, burnup, and cooling times. This technique is uniquely applicable for NRTA spent fuel Pu assay due to the techniques proven capability (over thirty years ago) to perform absolute Pu measurements with better than 3 percent uncertainty for single pins, which would be possible for the four corner pins of a SFA.[1-3]

Understanding NRTA

Several MCNP (Monte Carle n-Particle) transport code models have been developed for NRTA feasibility studies, they were all relatively simple in geometry.[14,15] The simplest geometry models included a directed neutron source, a single fuel pin or line of pins, an evacuated flight tube, and flux-tally detector cells. More sophisticated models included a complete pressurized water reactor (PWR) 17 x 17 pin SFA, air-filled drift tubes, and a wide-area neutron beam. Some SFA models used for this project were based on models and libraries of irradiated UO_2 fuel developed at Los Alamos National Laboratory as a part of the U.S. Next Generation Safeguards Initiative.[16] The PWR spent-fuel pin geometry included a 0.82 cm UO_2 pellet diameter, 0.95 cm diameter clad (no gap), and a fuel pin pitch of 1.26 cm.

In all of the models the neutron source was uniformly sampled over the desired transmission neutron-energy range. In an actual physical NRTA system a slowing-down neutron source would be expected to exhibit some non-uniformity, in particular, slightly higher flux at higher energies. In the 0-40 eV energy range, however, with the use of a low-Z neutron moderator with low absorption, a relatively flat and uniform energy-flux distribution would be expected. The MCNP models used two different beam geometries: cylindrical beam and directed point-source beam. The cylindrical beam typically had a diameter less than the UO_2 pellet diameter (<0.82cm). The cylindrical-beam radius was also varied for some studies. The directed point source is essentially a cylindrical beam with zero radius: a point source directed in a particular direction creating a line of neutrons. The directed point source is useful in order to assess the effect of pellet curvature on the transmission signal. Evaluated Nuclear Data File VII (ENDF-7) was used for most of the numerical simulations.[12] ENDF-5 and ENDF-6 data were used initially and results calculated with these data compare well with the ENDF-7 data.

Benchmark Study

Without the ability to perform a new set of experiments it was important to validate the performance of the MCNP modeling approach. To do this, a model was developed to simulate the

Figure 5. Measured resonance transmission spectra as a function of neutron energy for the NBS UO_2 spent fuel samples. (Spectrum A is for fuel cut from the center of the fuel pin and spectrum B is cut from one end of the fuel pin.)

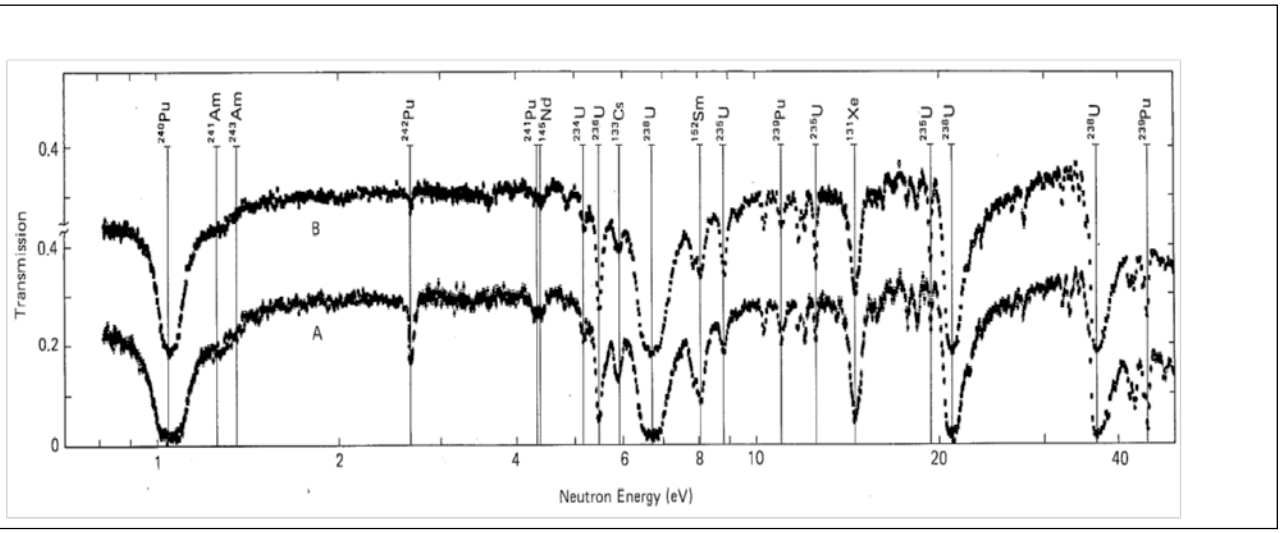

first NRTA experiments with spent fuel pins performed in the 1980s.[2] These early experiments used two segments of a single UO_2 fuel pin taken from a commercial SFA. The samples were approximately 1.0 cm in diameter and 2.5 cm in length (probably a PWR fuel pin); one sample was from the vertical center of the SFA, the other sample was from near an end. The fuel had an estimated burnup of approximately 25 GWD/MTU. No initial enrichment or cooling time was given, but prior experience indicates that a PWR assembly with approximately 25 GWD/MTU back in the 1970s timeframe was probably around 3.2 wt percent ^{235}U. For the model an external pin from a SFA in the NGSI library with an initial enrichment of ^{235}U 3.0 wt percent, a burnup of 30 GWD/MTU, and a five-year cooling time was used.

NRTA-measured transmission spectra measured for the two samples are shown in Figure 5. The spectrum at the bottom of the figure is for the sample cut from the center of the fuel pin, and spectrum B, the upper spectrum, is for the sample taken from the end of the fuel pin. Note the ordinate axis discontinuity in this figure. The resonance depressions correspond to specific actinide and fission product isotopes and have been marked in the figure. It is interesting to note the deeper depression in spectrum A for the ^{242}Pu resonance at 2.65 eV. This is due presumably to the higher burnup in the middle of the spent fuel pin, due to the typical PWR-reactor cosine-like vertical power distribution, and thus correspondingly higher ^{242}Pu concentration. Also, the ^{235}U depression at 8.8 eV is deeper for spectrum B relative to A, due to the higher ^{235}U concentration remaining in the fuel at the ends of the pin relative to the center (again, due to the lower burnup at the ends of the fuel pin). A key observation from this simple set of measurements is the natural axial variation in burnup in a SFA having some average 'declared' burnup. For Pu analysis of a whole SFA this must be accounted for if a measurement precision on the order of 1 percent is desired.

These measured transmission spectra are compared with the simulated NRTA response shown in Figure 6. This simulated spectrum was calculated with the MCNP5 code and models described above. In the NGSI spent fuel library the spent fuel composition is assumed to be axially uniform, hence the calculated spectrum represents an average over the length of the fuel pin. One might expect the magnitude of the resonance depressions to lie between the two measured spectra. Comparing Figure 5 and Figure 6, it is readily visible that the simulated transmission spectrum bears the same shape and includes all of the important actinide transmission depressions as the measured spectra. The measured depressions are proportional in depth to the simulated spectrum although the ordinate axis in Figure 6 is plotted over a larger range.

Accessibility of High-Yield Neutron Sources

An intense neutron source would be required to achieve reasonable count times for NRTA SFA measurements. Estimates on the order of 10^{12} n s^{-1} (4π emission) are projected due to the basic physics of the NRTA technique.[4,7] Multiple accelerator options exist to meet this need. In addition to the electron-accelerator based sources which this project has considered, light-ion accelerators may also be used. Specific examples of fielded accelerator systems that meet this neutron-intensity requirement need include the following.[17]

1. Compact pulsed hadron source, Tsinghua University, China
   E_p = 13.0 MeV, I_{ave} = 1.25 mA, rate = 50 Hz
2. Low energy neutron source, Indiana University, United States
   E_p = 13.0 MeV, Y ≈ 4.2 x 10^{13} n s^{-1}
3. KUURI-FFAG, Kyoto University, Japan
   E_p = 11.0 MeV, Y ≈ 5.0 x 10^{13} n s^{-1}, rate = 200 Hz, pulse width = 200 μs
4. KUURI-eLINAC, Kyoto University, Japan

Figure 6. MCNP-calculated relative transmission spectrum as a function of neutron energy through a single UO_2 spent fuel pin; important isotopes have been highlighted

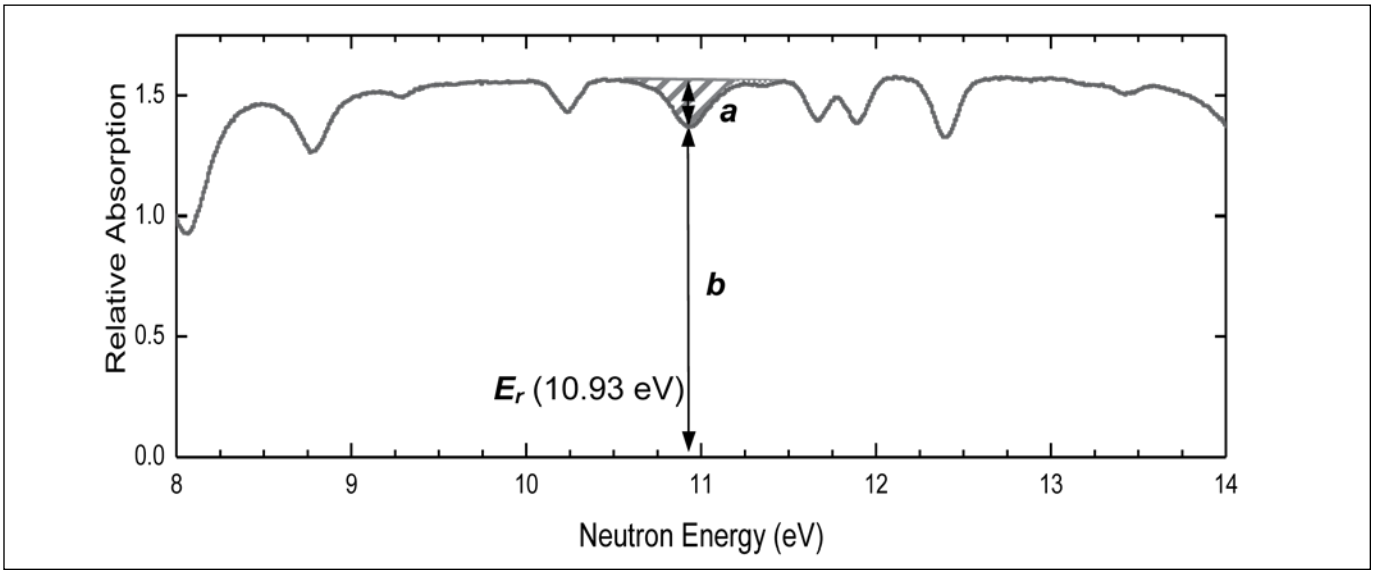

E_e = 30.0 MeV, Y ≈ 8.0 x 10^{12} n s^{-1}, I_{ave} = 200 μA, rate = 300 Hz

Count Time Estimates

The baseline neutron source used for modeling in this project has been a 10-MeV electron accelerator producing photoneutrons using a tungsten/beryllium converter/moderator; its neutron source yield is 2.7 x 10^{11} n s^{-1} (4π emission). With this model, counting times have been estimated for a single PWR pin transmission as well as transmission through a diagonal cross-section through the SFA of 8 pins.

The following assumptions are used in the count time estimates:

1. Linear electron accelerator with maximum electron energy of 10 MeV
2. Optimal tungsten converter thickness of 1.45 cm for 10-MeV operation
3. Neutron energy range of interest: 1.0 - 40 eV
4. Tungsten-beryllium (W/Be) converters
5. 5-meter flight tube distance to detectors
6. 100-μA average beam current
7. Detector active area of π cm^2 (1 cm radius) perpendicular to beamline axis
8. Neutron detector efficiency ε = 20 percent

For assaying through a section of a single pin with this baseline neutron source the counting time needed to resolve one resonance absorption line with counting statistics of better than one percent, including accounting for background events due to spontaneous neutrons emitted from the SFA, has been calculated to be approximately 1.8 hours.[7] For an eight-pin row assay the count time goes up to approximately 13.4 hours. For a single detector this may be too long for a safeguards-relevant measurement. However, if multiple detectors are used to allow complete assay of multiple sections of an assembly simultaneously, this may be acceptable. If faster counting times are desired, e.g., to reduce the eight-pin count time from 13.4 hours to approximately twenty minutes, the neutron source strength would need to be increased by a factor of 40; as illustrated above higher yield systems are well-proven. There are several ways to get this factor of 40 increase in the neutron intensity, considering modifications to the base-line model. These include a) increasing the accelerator electron energy, b) increasing the average beam current, c) changing out the tungsten converter for a depleted uranium converter, and c) optimizing the converter materials and dimensions.

Assaying Pu in a SFA

The simplest approach for estimating the Pu content in an NRTA measurement is to determine the neutron removal fraction of each Pu isotope at a single resonance energy. For each resonance a straight line is drawn over the top of the depression from the high points on each side of the depression and then the attenuation from the point on the line corresponding to the resonant energy to the bottom of the depression is measured and recorded as the b value, in counts. The other important variable to be measured is the distance from the bottom of the depression to zero on the ordinate axis (number of detector counts). The transmission factor (T) is then estimated to be the ratio of b divided by a+b. The mass can then be derived from the transmission factor, T.

To demonstrate how the transmission approach above can be used to estimate the total ^{239}Pu mass in a SFA, the single ^{239}Pu resonance at 10.93 eV will be used; no interfering resonances (e.g. ^{235}U) have been accounted for. While this particular resonance

Figure 7. Estimation of the transmission factor (T) using the 10.93 eV resonance depression from ^{239}Pu. The transmission factor T is simply given by T = b/(a+b).

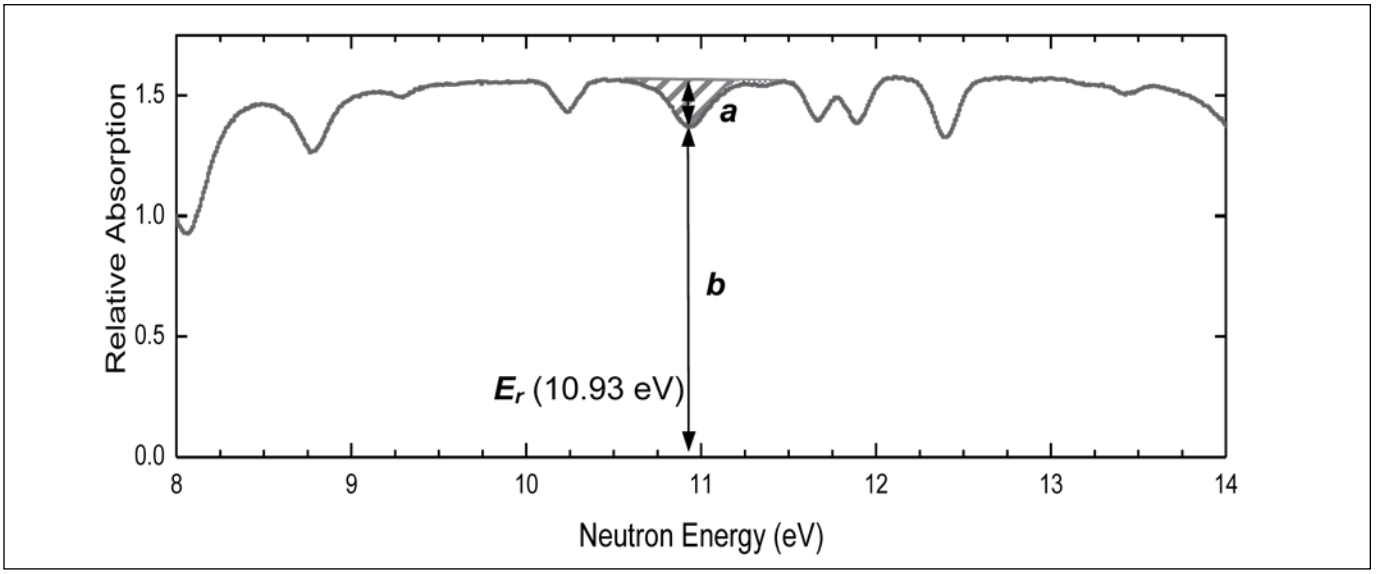

is relatively well isolated other resonance interferences still affect the analysis. The simulations for this example involved a PWR spent fuel assembly with a burnup of 45 GWD/MTU, initial enrichment of 3 wt percent ^{235}U, and a one-year cooling time. The fuel composition is taken directly from LANL spent fuel library #1, where each of the 264 fuel pins in the assembly has been divided into four radial fuel-pin depletion regions, with a single axial value over the full length of each fuel pin. The depleted fuel assembly has thirty-nine different depleted fuel pins and a total of 156 different fuel compositions. In LANL library #1 the SFAs have depleted fuel pin symmetry about the horizontal and vertical axes through the center of the assembly, as well as symmetry about the two diagonal axes through the corners and center of the assembly.

The total ^{239}Pu mass in the library SFA (45 GWD/MTU) is 2,610.45 grams. In an ideal situation, an estimation of the ^{239}Pu mass using this simple approach should equal this value. However, in practice curve-fitting the transmission depression signals, and accounting for additional resonances, would be needed to best measure the transmission factor. For the example here, however, only the single time-bin value at the center of the resonance (and only the ^{239}Pu resonance cross-section) is used to calculate the transmission factor. This is illustrated in Figure 7, which shows the resonance absorption method being used to determine the transmission factor T. The transmission spectrum in the figure is the 8-14 eV portion of the energy range which includes the ^{239}Pu resonance depression of interest at 10.93 eV; the hatched area is this transmission depression. The values a and b are shown and estimated by simply drawing a straight line across the top of the depression and measuring the "a" and "b" distances. The transmission factor T is then given by the formula: T = b/(a+b).

The transmission factor (T) is related to the average ^{239}Pu number density (N) in the transmission path by the following attenuation formula

$$T(E_r) = \frac{b}{a+b} = e^{-N\sigma_t(E_r)x} \qquad (2)$$

where $T(E_r)$ is the transmission factor at the resonant energy, σ_t is the magnitude of the ^{239}Pu total neutron interaction cross-section at the resonant energy (10.93 eV), and x the average chord length of the transmission path through the fuel pin(s) in an assay row. With this approach, the ^{239}Pu mass was estimated for fifteen of sixteen paths (d1-d15) through the SFA. These paths correspond to the labeled diagonal lines in Figure 8. The sixteenth scan (d16) was not calculated. The results of the calculations are shown in Table 2, which gives the calculated mass estimate (Calc. Mass) in grams along with the true mass from the LANL library fuel compositions (Lib. Mass) for scan numbers d1 through d15. The last column is the percent difference between the calculated mass and the LANL library mass. The percent difference is always negative, meaning that the calculated mass using this approach always slightly under predicts the library values. The under prediction is believed to be due to the presence of the overlapping resonances of the other material in the fuel. It is also possible that small fission product or actinide resonances may be present inside the ^{239}Pu 10.93-eV resonance but a search for these has not yet been performed.

Figure 8. The 15-pin rows (d1-d15) used in the transmission spectra calculations

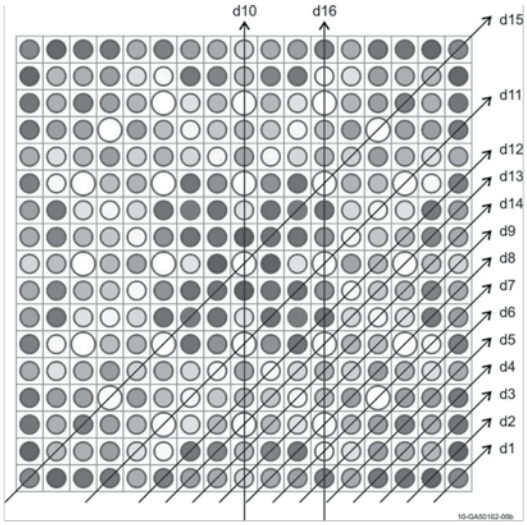

Table 2. Results of the ^{239}Pu estimate by scan row

Scan No.	No. of Pins	Lib. Mass [g]	Calc. Mass [g]	Diff. [percent]
d1	1	10.86	10.49	-3.4
d2	2	21.62	20.82	-3.7
d3	3	31.96	30.51	-4.5
d4	4	41.92	41.04	-2.1
d5	5	51.27	48.61	-5.2
d6	6	60.20	57.40	-4.7
d7	6	59.52	57.41	-3.5
d8	6	59.48	57.29	-3.7
d9	9	87.82	83.02	-5.5
d10	12	115.49	103.55	-10.3
d11	10	98.37	89.04	-9.5
d12	12	116.95	105.75	-9.6
d13	8	78.45	73.75	-6.0
d14	10	97.51	89.42	-8.3
d15	12	120.46	110.51	-8.3
d16	12	---	---	---

These values may be used to develop estimates of the total ^{239}Pu mass in the assembly. First, limiting the discussion to a set of scans only reaching a total thickness of eight pins in a row (the d1-d8 and d13 scans, which may be the practical limit for attenuation assays), then 156 of 264 (59 percent) of all the fuel pins are assayed directly. For an estimate one uses the directly measured fuel masses from scans d1-d8 and d13 and then, for the remaining internal pins which are not included, an average ^{239}Pu mass was derived from the average value of the d13 scan. The final calculated SFA ^{239}Pu mass is then 2,511 grams, which should be compared with the MCNP library mass of 2,610.45 g. The -3.80 percent difference is directly attributable to the simplified peak fitting approach which omits known resonance interferences from uranium and fission products. This is a systematic error, it could likely be improved upon by using more sophisticated assay analysis techniques beyond the 'peak height' analysis used here. If a counting statistics error of 2.5 percent is acceptable then a measurement would take 13.4 x 2 = 26.8 hours using a 2.7 x 10^{11} n s^{-1} neutron source or 20 x 2 = 40 minutes using a 1.1 x 10^{13} n s^{-1}. The total uncertainty would be approximately 4.3 percent.

Table 3. Estimated average ^{239}Pu pin content by transmission scan

Scan No.	Average ^{239}Pu mass [g]
d1	10.5
d2	10.4
d3	10.2
d4	10.2
d5	9.72
d6	9.57
d7	9.57
d8	9.55
d9	9.22
d10	8.63
d11	8.90
d12	8.81
d13	9.22
d14	8.94
d15	9.21

If twelve pins per row can be assayed (e.g., if more time is allocated for measurements) then all fifteen scans (d1-d15) can be used in the total ^{239}Pu assembly estimate. The total mass of ^{239}Pu in the assembly is then estimated to be 2,488 grams. Compared to the 'true' total ^{239}Pu assembly mass, this is now a -4.68 percent difference. The difference has grown slightly due to resonance interferences but it is also impacted by more overall signal degradation due to the notably larger UO_2 distance traversed in the scanning of nine to twelve pins in a row. Note the percent difference in Table 2 tends to increase with the number of pins in a row. The lower total inventory estimate of 2,488 grams is also due to the generally lower average ^{239}Pu pin content of the interior pins relative to peripheral pins, as shown in Table 3 (which indicates a more sophisticated averaging approach must be used to estimate Pu in the inner region of the SFA).

An NRTA measurement with twelve-pin scan capability would allow every pin in the assembly to be part of one or more scans. Because of this it may prove possible that the measurement precision can be improved on by developing an approach to optimize the assignment of average ^{239}Pu pin mass determinations using data from the sixteen integral transmission scans (rather

than the single average value assigned to all pins as used in this discussion). Starting with the corner pins and moving inward, for example, it might be possible to determine the ^{239}Pu mass content of each pin in the assembly to a higher degree of accuracy using an iterative approach. Ultimately some approximations may be required for the interior pins but, as recently described elsewhere, the interior pins have a fairly uniform and predictable ^{239}Pu distribution that may support this extrapolation.[18]

Pin Diversion

Although a large neutron source strength and perhaps long count times would be needed to perform a quantitative NRTA twelve-pin scan, lower system requirements would be needed to quickly detect diversion of a pin in the assembly. This would be true even if the neutron intensity only allowed sufficient transmission to support quantitative measurements for scans through a depth of 8 pins. This analysis would involve examination of the uranium isotopes as well as the fission products ^{99}Tc, ^{103}Rh, ^{131}Xe, ^{133}Cs, ^{145}Nd, and ^{152}Sm in the assembly. Use of ^{131}Xe is a particularly valuable indicator in this case.

Discussion

As a measurement technique for performing high-precision plutonium assays the NRTA technique has a number of strengths in comparison with other nondestructive assay approaches.

1. NRTA has the potential for accurate assay measurements with a precision in the range of 5 percent uncertainty or better.
2. NRTA produces distinctive resonance-transmission spectra that can uniquely identify specific actinide and fission product isotopes. The method detects and measures plutonium isotopes directly; it does not rely on correlations or the "effective ^{240}Pu" concept.
3. In addition to ^{239}Pu, NRTA can identify and assay several important fissionable isotopes and spent-fuel actinides directly, including ^{235}U, ^{236}U, ^{238}U, ^{240}Pu, ^{241}Pu, and ^{242}Pu.
4. NRTA can identify the presence of ^{234}U, ^{241}Am, and ^{243}Am. Americium-241 is of particular relevance in higher burn-up fuels (45-60 GWD/MTU) with large cooling times (>5 years).
5. NRTA can identify six resonant fission-product isotopes (^{99}Tc, ^{103}Rh, ^{131}Xe, ^{133}Cs, ^{145}Nd, and ^{152}Sm), which can potentially be used to estimate assembly burnup, cooling time, and diversion and to verify operator-reported burn-up values.
6. The neutron resonance transmission analysis technique is a mature technology with a solid foundation in theoretical physics.
7. NRTA system calibrations with pin/assembly standards can be straightforwardly used to reduce NRTA systematic errors.
8. An NRTA system can be designed to be insensitive to spent-fuel gamma radiation.

The NRTA technique may require temperature control equipment for the spent fuel assembly. For NRTA, the fuel assembly will necessarily be assayed in air (or vacuum) but not in water. An assembly suspended in vacuum will tend to heat up due to lack of conduction and convection heat-transfer pathways. An assembly suspended in air, however, can be air-cooled through forced convection. In the latter case of forced-air cooling a temperature measurement may not be needed but in vacuum the assembly may heat up, particularly true for assemblies with short cooling times. Heat up of the UO_2 fuel that would be expected in an evacuated system will Doppler-broaden the resonances; this must be compensated for in the cross-section data that are part of the analytical computer tools.

Low-energy neutron penetrability, or the maximum number of PWR pins that can be assayed in a given row, is limited by the physics of the problem. Accelerator systems used in neutron cross-section measurements are large, high-power systems that typically use 100-MeV or higher electron energies, a 700-800 Hz repetition rate, and flight-tube lengths up to 200-meters or longer. They operate at powers ranging from 1.5-14.0 kW.[19,20] An optimized NRTA system may operate in the same repetition rate and power range, but at much lower electron energies. The relatively low-energy electrons required when using an electron-accelerator-based neutron source may be of particular value to reduce the size of the accelerator. To optimize performance the NRTA technique will require an intense source of pulsed low-energy neutrons in the range of 10^{12}-10^{13} n/s; commercial electron accelerators are available to meet this requirement, generally operating with a relatively low electron endpoint energy in the 10-20 MeV. Charged-particle accelerators may also be suitable for use in an NRTA system, instead of using an electron accelerator. Commercial accelerators using deuteron and proton beams that can generate neutron yields up to 10^{13} neutrons per second are currently available.[21]

Determination of the flight tube length is based primarily on the energy range of interest for the transmission neutrons. For the NRTA technique and plutonium assay, neutrons of energy 0.1-40 eV should be sufficient. This relatively narrow energy range includes one or more resonances for ^{234}U, ^{235}U, ^{236}U, ^{238}U, ^{239}Pu, ^{240}Pu, ^{241}Pu, ^{242}Pu, ^{241}Am, and ^{243}Am isotope, plus the six resonant fission products ^{145}Nd, ^{133}Cs, ^{99}Tc, ^{152}Sm, ^{131}Xe, and ^{103}Rh. Energies from 20-40 eV provide redundant resonances for some of these actinides and therefore it may be possible to restrict the analysis to a maximum energy of 20 eV. (Higher energies also require longer flight tubes for good energy resolution.) The NRTA system as proposed here is for a 0.1- to 20-eV energy range would minimize the flight tube length to approximately 5m and reduce the overall NRTA system footprint from previous work.

Multiplexing

Use of a high-power, accelerator-based neutron source may be perceived as a significant drawback of the NRTA technique.

However, it may be possible to take advantage of the isotropic nature of this type of neutron source to permit the simultaneous analysis of multiple fuel assemblies. The first concept for analyzing an assembly would be to scan one section of the fuel, and then rotate it to get the orthogonal view. This would allow an assembly to be assayed at one axial location, perhaps 5cm to 10cm in width. However, if it was required to assay the complete assembly top-to-bottom this approach would be time consuming. An alternate approach would be to simultaneously collect data at multiple elevations on the assembly at the same time. Secondly, the isotropic neutron sources proposed for NRTA would permit measuring multiple assemblies in parallel. Based on size limitations and estimates of beam-tube length, it may be possible to analyze up to one dozen assemblies in parallel using one accelerator if desired. It is worth noting that any system designed to comprehensively assay SFAs will, by necessity, be technically complicated. It is difficult to handle spent fuel. As a measurement technique for spent fuel NRTA is most relevant for large scale, national facilities expected to process large numbers of SFA in an assembly-line fashion. One application where NRTA might be used, for example, would be to verify shipper inventory declarations at a large-scale fuel reprocessing facility. Another application would be as a receipt inspection tool at a longer-term storage facility or a geological repository.

Other Applications Beyond Safeguards SFA Analysis

In addition to using NRTA for safeguards measurements, the approach might also be of relevance as a tool for basic scientific research related to the development and understanding of how nuclear fuel behaves. NRTA-type measurements of small samples or single pins have the potential to generate two-dimensional isotopic composition images of the actinide and fission production distributions in fuels with a spatial resolution of 1 mm or better. Taking multiple images, tomography methods could further allow the reconstruction of three-dimensional distribution maps of these isotopes in fuel. This information would be valuable for understanding the migration and diffusion of elements in nuclear fuel, and for understanding rim-effects in the radial burnup distribution of commercial light-water reactor fuels.

The NRTA measurement approach may also be applicable as a non-contact, non-destructive assay measurement approach for analyzing and categorizing debris materials that will someday be collected from the remains of the Fukushima-Daiichi complex in Japan. These materials will be non-uniform in size and will be intimately comingled with structural materials from the reactors. Traditional NDA methods which might be applied to these analyses will be limited in applicability due to high radiation fields and the inability to readily make geometric and form-factor corrections. The absolute Pu-assay approach of the NRTA technique, as originally illustrated thirty years ago, is ideally suited for addressing these challenges.

Acknowledgements

The work in this report was supported by the U.S. Department of Energy's Next Generation Safeguards Initiative (NGSI), Office of Nonproliferation and International Security (NIS), National Nuclear Security Administration (NNSA).

This manuscript has been authored by Battelle Energy Alliance, LLC under Contract No. DE-AC07-05ID14517 with the U.S. Department of Energy. The U.S. government retains and the publisher, by accepting the article for publication, acknowledges that the U.S. government retains a nonexclusive, paid-up, irrevocable, worldwide license to publish or reproduce the published form of this manuscript, or allow others to do so, for U.S. government purposes.

This information was prepared as an account of work sponsored by an agency of the U.S. government. Neither the U.S. government nor any agency thereof, nor any of their employees, makes any warranty, express or implied, or assumes any legal liability or responsibility for the accuracy, completeness, or usefulness of any information, apparatus, product, or process disclosed, or represents that its use would not infringe privately owned rights. References herein to any specific commercial product, process, or service by trade name, trademark, manufacturer, or otherwise, does not necessarily constitute or imply its endorsement, recommendation, or favoring by the U.S. government or any agency thereof. The views and opinions of authors expressed herein do not necessarily state or reflect those of the U.S. government or any agency thereof.

References

1. Schrack, R.A. 1981. Resonance Neutron Radiography Using an Electron Linac, *IEEE Transactions in Nuclear Science,* 28, 1640-1643.
2. Bowman, C.D. 1983. Neutron Resonance Transmission Analysis of Reactor Spent Fuel Assemblies, *Neutron Radiography,* Barton, J. P. and von der Hardt, P., eds., ECSC, EEC, EAEC, Brussels, Belgium and Luxembourg, 503-511.
3. Behrens, J. W., R. G. Johnson, and R. A. Schrack. 1984. Neutron Resonance Transmission Analysis of Reactor Fuel Samples, *Nuclear Technology,* 67, 162-168.
4. Sterbentz, J. W., and D. L. Chichester. 2010. Neutron Resonance Transmission Analysis (NRTA): A Nondestructive Assay Technique for the Next Generation Safeguards Initiative's Plutonium Assay Challenge, Report INL/EXT-10-20620, Idaho National Laboratory, Idaho Falls, Idaho.
5. Chichester, D. L., and J. W. Sterbentz. 2011. Neutron Resonance Transmission Analysis (NRTA): Initial Studies of a Method for Assaying Plutonium in Spent Fuel, Report INL/CON-10-20684, Idaho National Laboratory, Idaho Falls, Idaho.

6. Chichester, D. L., and J. W. Sterbentz. 2011. A Second Look at Neutron Resonance Transmission Analysis as a Spent Fuel NDA Technique, Report INL/CON-11-20783, Idaho National Laboratory, Idaho Falls, Idaho.
7. Sterbentz, J. W., and D. L. Chichester. 2011. Further Evaluation of the Neutron Resonance Transmission Analysis (NRTA) Technique for Assaying Plutonium in Spent Fuel, INL/EXT-11-23391, Idaho National Laboratory, Idaho Falls, Idaho.
8. Veal, K. D., S. Tobin, and S. A. LaMontagne. 2010. NGSI Program to Investigate Techniques for the Direct Measurement of Plutonium in Spent Fuel LWR Fuels by Non-Destructive Assay, *Proceedings of the Institute of Nuclear Materials Management 51st Annual Meeting.*
9. Tobin, S. J., et al. 2011. Next Generation Safeguards Initiative Research to Determine the Pu Mass in Spent Fuel Assemblies: Purpose, Approach, Constraints, Implementation, and Calibration, *Nuclear Instruments and Methods in Physics Research A,* 652, 73-75.
10. Fermi, E., J. Marshall, and L. Marshall. 1947. A Thermal Neutron Velocity Selector and Its Application to the Measurement of the Cross Section of Boron, *Physics Review* 72, 193-196.
11. Copley, J. R. D., and T. J. Udovic. 1993. Neutron Time-of-Flight Spectroscopy, *Journal of Research of NIST* 98, 71-87.
12. Chadwick, M. B., et al. 2006. ENDF/B-VII.0: Next Generation Evaluated Nuclear Data Library for Nuclear Science and Technology, *Nuclear Data Sheets* 107, 2931-3060.
13. Mughabghab, S. F. 2006. *Atlas of Neutron Resonances Resonance Parameters and Thermal Cross Sections,* Z = 1 – 100, Fifth Ed., Elsevier BV, Amsterdam, The Netherlands.
14. 1987. MCNP—A General Monte Carlo N-Particle Transport Code, Version 5. 2003. X-5 Monte Carlo Team, Report LA-UR-03-1987, Los Alamos National Laboratory, Los Alamos, New Mexico USA.
15. MCNPX—A General Purpose Monte Carlo Radiation Transport Code, Version 2.5.0., MCNPX User's Manual. 2005. LA-UR-05-0369, Los Alamos National Laboratory.
16. Conlin, J. L., and S. J. Tobin. 2010. Spent Fuel Library Report, Report LA-UR-10-07894, Los Alamos National Laboratory.
17. References for this section may be found at: www.indiana.edu/~lens/UCANS/.
18. Freeman, C., et al. 2010. Using X-Ray Fluorescence for Quantifying Plutonium in Spent Fuel Assemblies, Report LA-UR-11-00513, Los Alamos National Laboratory.
19. The Geel Electron Linear Accelerator (GELINA) neutron time-of-flight facility: irmm.jrc.ec.europa.eu/about_IRMM/laboratories/Pages/gelina_neutron_time_of_flight_facility.aspx
20. The Oak Ridge Electron Linear Accelerator (ORELA) pulsed neutron source: www.phy.ornl.gov/orela/orela.html/
21. See, for example, the Lansar Neutron Generator from Accsys Technologies, Inc. (www.accsys.com/products/lansar.html).

Construction and Development of a BF_3 Neutron Detector at Brookhaven National Laboratory

C. Czajkowski, C. Finfrock, P. Philipsberg, and V. Ghosh
Brookhaven National Laboratory, Upton, New York USA

Abstract

Most current radiation portal monitors (RPMs) use neutron detectors based upon ^{3}He-filled gas proportional counters. ^{3}He is in short supply in the world and continues to decline in availability. Concurrent with the decline in gas is a disproportionate increase in the cost of available gas. It is therefore desirable to find substitutes for the ^{3}He with technologies that will effect minimal changes to currently deployed systems and provide equivalent effectiveness in neutron detection. This project investigates the feasibility of BF_3 as a substitute for the ^{3}He in configurations that can be readily installed in currently deployed systems.

In response to this ^{3}He shortage, the U.S. Department of Homeland Security's (DHS), Domestic Nuclear Detection Office (DNDO), Product Acquisition and Deployment Directorate (PADD) commissioned Brookhaven National Laboratory (BNL) to construct and test a boron tri-fluoride (BF_3) based neutron detection module (NDM). The NDM was required to meet specific criteria as outlined in a DNDO Functional Requirements Document (FRD).[1] The detector was to be built utilizing (as much as practicable) off the shelf components and have the same exterior dimensions as current NDMs so that they can fit into existing portal monitor enclosures.

The module was mounted in the standard Radiation Portal Monitor (RPM) NEMA enclosure inside the standard steel shroud, and shipped to the Nevada National Security Site (N2S2) for testing. Concurrently, a full-scale surrogate "BF_3 detector," fabricated with air replacing the BF_3, was constructed for the purpose of evaluating the ability of the design to survive being dropped from a height that would be typical when performing a field replacement of an NDM on the tallest portal monitor configuration. This height corresponds to a condition such that the bottom of the NDM is at an elevation of 15 feet, or 457cm, above ground level.

This paper discusses the design features of the detector system, mitigation techniques developed to ameliorate the hazards posed by the BF_3 gas, drop test results, and discussion of neutron detection efficiency for the constructed detector system. BF_3 detectors potentially have direct applications to international safeguards where ^{3}He neutron detectors are typically deployed.

Background

In September 2010, the U.S. Department of Homeland Security's (DHS), Domestic Nuclear Detection Office (DNDO), Product Acquisition and Deployment Directorate (PADD) commissioned Brookhaven National Laboratory (BNL) to construct and test a boron tri-fluoride (BF_3) neutron detector. The detector was designed to meet the specific criteria outlined in a DHS Functional Requirements Document (FRD).

The module was then mounted in the standard RPM NEMA enclosure inside a standard steel shroud, and shipped to the Nevada National Security Site (N2S2) for testing (Note: NNSS is the U.S. Department of Energy reservation located in southeastern, Nevada, approximately sixty-five miles northwest of Las Vegas, formerly known as the Nevada Test Site).

This paper is a compilation of the work performed in the execution of the DHS project and the results of the BNL efforts to build and test a neutron detector that has significant potential applications in the safeguards and security arena as a substitute for ^{3}He.

The following tasks were performed for this project:

Task 1. Design of the BF_3 Detector-based Neutron Detection Module (NDM)

Los Alamos National Laboratory (LANL) and Brookhaven National Laboratory collaborated on developing the design of the BF_3 detector-based NDM. The NDM design requirements were specified in a DNDO FRD.[1] The primary design requirements were that:

1. the NDM should have an absolute detection efficiency greater than 2.5 c/s for a ^{252}Cf source emitting 2100n/s placed at 2m from the NDM;
2. the NDM should fit into existing envelope dimensions (5 inches thick by 12.5 inches wide by 85 inches tall);
3. the NDM should contain hazard mitigation for BF_3; and
4. a passive indicator for BF_3 leak annunciation.

MCNP[2] simulations were performed to develop and optimize the NDM design. Many different tube sizes and configurations were modeled and compared. In the final analysis the simplest design meeting the sensitivity criteria was selected in order to minimize cost and increase reliability.

The final design incorporated three stainless steel BF_3 tubes filled to a pressure of one atmosphere, with BF_3 enriched to 96

Figure 1. This is a photograph of the full assembly, showing the machined one-piece cavity with o-ring seal, the tubes with electronics modules, and the alumina and poly bead blend, just prior to assembly. The top cover can be seen leaning against the wall at the top of the photo.

percent ^{10}B. The tube dimensions were 5.08cm in diameter, by 183cm active length. The thicknesses of the front, back, and sides of the high-density polyethylene (HDPE) moderator cavity were optimized within the constraints of the specified envelope dimensions. Details of the design development and optimization are discussed in Reference 3.

The design specifications also required the inclusion of several layers of mitigation to ameliorate the potential hazards presented by the BF_3, which is a hazardous corrosive gas. The tubes themselves were constructed of high-quality stainless steel, subjected to rigorous cleaning, manufacture, and quality control by the vendor (LND, Inc.), who has decades of experience making BF_3 tubes. The HDPE moderator cavity was fabricated from one monolithic billet of HDPE, with an o-ring sealed cover. Sealed electrical feed-throughs were incorporated in the design (Figures 1 and 2). These features provide a robust barrier to leakage of gas. Typical cavities are built from a number of flat slabs, with no regard to hermetic sealing. As an additional barrier to leakage, the entire moderator cavity was placed inside a welded stainless steel *envelope* with a sealed cover.

A *gettering* material (alumina) was distributed in the interstitial spaces between the BF_3 tubes to react with the BF_3, preventing its migration outside the moderator cavity. Alumina (Al_2O_3) beads were mixed with HDPE beads, which provide some additional neutron moderation and increase the efficiency of the detector.

Given the short timeframe of the project, commercial neutron detector electronics were ordered and incorporated in the design. These electronics modules will most probably not be used in any final production device since it is envisioned that the electronics will need to be more tightly integrated into the current overall electronics design of the RPM.

Figure 2. This is a photograph of the layout of the stand-alone electronics modules used in the detector prior to final assembly and shipment to Nevada.

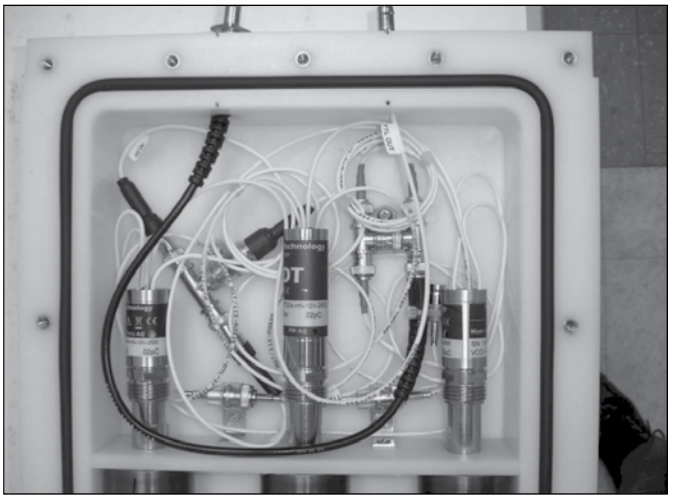

Task 2. Drop tests to validate the primary and secondary containment function with surrogate gas and/or BF_3 within the detector assembly.

A full-up surrogate "BF_3 detector" was constructed for the purpose of evaluating the ability of the design to survive being dropped from a height that would be typical when performing a field replacement of an NDM on the tallest portal configuration. This height corresponds to a condition such that the bottom of the NDM is at an elevation of 15 feet, or 457cm, above ground level. The criterion for success in this test was not that the detector remain functional, but rather that there is no release of BF_3 gas to the environment. The drop test surrogate was constructed

Figure 3. This is a photograph of the full detector assembly dropped onto concrete from a height of fifteen feet. Picture is taken just after initial impact. After impact, visible deformation of the outer stainless steel envelope is evident at the lower edge, as can be seen in Figures 4 and 5. Upon inspection, no breach of the stainless steel envelope was detected. The drop test surrogate actually bounced on its end twice before falling over on its side.

precisely as the actual NDMs were constructed, except for the following details. The three tubes used in the drop test surrogate were manufactured by the BF_3 tube vendor precisely as if they were going to be filled with BF_3, except that they were equipped with valves where they would have had sealed pinch-offs, and they were filled with air to one atmosphere. In addition, the blend of polyethylene and alumina beads that was used in the actual NDM was replaced by polyethylene beads only.

The drop test was performed in a "high bay" laboratory space equipped with an overhead crane. A layer of solid concrete blocks was arranged on the concrete floor underneath the impact area, primarily to protect the floor tiles from impact damage. The drop test surrogate was also equipped with a lifting eye bolted into the top of the detector such that when suspended from the crane, the detector hung vertically, with the bottom face parallel to the floor. A "special effects" quick release device was used between the surrogate detector and the crane to initiate a free-fall drop of the surrogate from the test elevation of 15 feet above the floor. Figure 3 illustrates the impact area and also the surrogate drop test detector just after the moment of impact. The drop test surrogate was observed to bounce upward after impact with the concrete floor, to a height of about 29 inches, estimated from video taken during the drop test. The calculated velocity at impact (v=sqrt(2gd), where g= -9.8 m/sec^2) is -9.47 m/sec, or -21.1mph. Measurements made by scaling the displacement of the detector in progressive frames of video resulted in measurements of velocity ranging from -18.5 to -21 mph.

The drop test surrogate was recovered and disassembled. The deformation of the outer stainless steel envelope was mild enough that the envelope could still be slid off of the sealed polyethylene

Figure 4. This photograph (after impact) depicts the damage to the concrete bricks and the damage to the stainless steel case for the detector assembly. The stainless steel case was not breached.

cavity by having two people pull in opposite directions. The polyethylene cavity can be seen in Figure 6. When the screws were removed from the polyethylene cover, it was observed that several of the brass threaded inserts installed in the plastic had been slightly lifted out of the plastic. This was not sufficient to allow any of the polyethylene beads inside the cavity to fall out. Inspection of the three surrogate tubes revealed that differing amounts of damage had occurred. Tube number one suffered almost no discernible damage. Tube number two suffered some mushrooming distortion near the bottom end, similar to the bare-tube drop test. Tube three suffered similar damage, but slightly larger in magnitude. The tubes can be seen in Figures 7 and 8. Each of the tubes from the drop-test surrogate were evacuated

Figure 5. This is a side view of the assembly after impact, showing deformation of the case.

Figure 6. The polyethylene cavity after being slid out of the stainless steel envelope

to roughing pump vacuum and then valved off for periods of time ranging from twenty-four to seventy-two hours. None of the three tubes that were used in the drop test surrogate experienced any change in pressure over the time that they were evacuated, indicating that none of the tubes had been breached.

Task 3. Assemble a "Full-up" BF_3 Detector

Besides optimizing the neutron sensitivity, the detector was fabricated in order to incorporate several BF_3 leak mitigation strategies. The polyethylene moderator cavity was fabricated by machining the recess which the BF_3 tubes occupy, out of a solid billet of plastic. This was done to minimize the number of seams and joints that the cavity would have, all of which would be potential leak paths. The cover for this cavity was sealed to the cavity by an o-ring installed in a machined groove in the top edge of the cavity. The cover was screwed to the cavity, compressing the o-ring, by an array of stainless steel screws that threaded into brass inserts that were installed in the cavity. The brass inserts provided a higher quality thread for attachment as opposed to threading directly into the plastic. The thickness of the back of the cavity, behind the tubes, was 5.08cm (2 inches). The depth of the recess in which the tubes were installed was also 5.08cm (2 inches). The

Figure 7. This is a photograph of the ends of the BF_3 tubes showing only minimal distortion of the two tubes on the right and no discernible damage to the third tube. (Tube diameter is 5.08cm).

Figure 8. A close-up view of the most damaged tube from the drop test mock-up. While wrinkled, the tube has not been breached. The tube is being held above its installed position in the mockup for this photo.

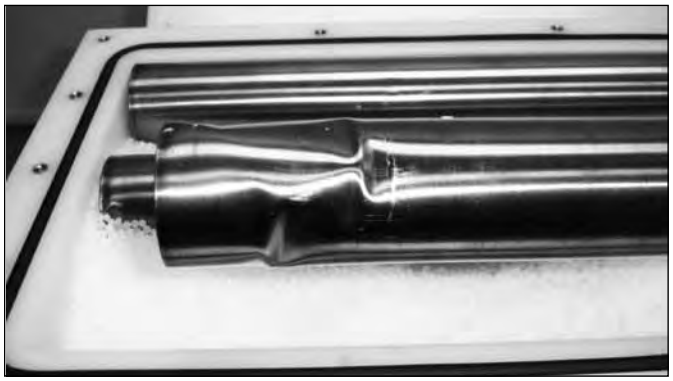

thickness of the front polyethylene cover was 1.9cm (0.75 inch).

Three stainless steel BF_3 tubes were installed into the cavity. The tubes were manufactured by LND Inc., and were filled with BF_3 at 96 percent ^{10}B enrichment, to one atmosphere. The tubes have a 5.08cm (2 inches) diameter, and a 183cm (72 inches) active length. In order to minimize the risk associated with developing custom electronics at this time, commercial-off-the-shelf electronics were used. Compact neutron electronics modules were obtained from Precision Data Technology. These modules provided tube bias voltage and signal conditioning in one small package that could be mounted directly onto the BF_3 tubes' HN fittings. The modules from each tube were connected in daisy chain fashion and provided a TTL pulse train with one pulse corresponding to one neutron event in the aggregate detector. The modules only require 12VDC power to operate.

After the tubes were installed in the cavity, the interstitial space was filled with a blend of poly and alumina (Al_2O_3) beads (Figure 1). The alumina provided another level of mitigation for

Table 1. BF_3 NDM neutron sensitivity test data

BF_3 NDM Replacement Neutron Sensitivity Test Data					
Measurement Type	Time (sec)	Total Counts	Count Rate (N/sec)	Net Count Rate (N/sec) (source – bkg)	Sensitivity (N/sec/ng of ^{252}Cf at 2 meters) Target = 2.5
background	4,000	10,641	2.66	-	-
Cf source	300	8,574	29.1	26.44	2.59
Cf source	300	8,832	29.4	26.74	2.61
Cf source	300	8,785	29.3	26.64	2.605
Sum of three	900	26,371	29.3	26.64	2.605

the BF_3 hazard. The alumina reacts irreversibly with the BF_3 and sequesters it, so it is not freely released to the environment. A 3mm bead size was decided on for the materials as a compromise between providing a large bed surface area and still allowing flow of gas to permeate the bed without requiring significant driving pressure. The alumina and poly beads were mixed 50/50 percent by weight, and the space between the tubes was completely filled with the blend. The poly beads added slightly to the neutron moderation, and were taken into account in the MCNPX modeling.

As a final layer of mitigation, the entire detector was installed inside a stainless steel envelope. This was fabricated from 16-gauge type 304 stainless steel. All seams were welded over their full length. The detector slides into the envelope from one end and a stainless steel cover is then sealed with silicone, and screwed in place. Two sealed bulkhead penetrations exit the top of the detector, and provide connections for 12 VDC input, and the TTL pulse output.

Task 4. Developmental Tests of the BF_3 Detector at BNL

Neutron detection sensitivity was evaluated at the site of BNL's, former RAdiation Detector Test and Evaluation Center (RADTEC). This area provided a section of paved roadway along which concrete footings for mounting portal monitors were available for detector mounting. The module, without its stainless steel envelope, and not installed in its NEMA 4 enclosure or steel shroud, was mounted on a footing. The detector module, mounted on a footing, can be seen in Figure 9, below. DNDO Functional Requirements Document (FRD) for Radiation Portal Monitor System (RPMS) ^{3}He Neutron Detection Module (NDM) Replacement," delineates some performance criteria for the prototype NDM replacement. The neutron sources used for evaluation of this detector contain a mixture of ^{252}Cf and ^{250}Cf, and have a fair fraction of their neutron emission attributed to their ^{250}Cf content. The neutron flux of these sources is well understood. The sources used produced a neutron flux of 21,475 N/sec at the time of the testing. The current assumption of one nanogram of ^{252}Cf producing an emission rate of 2,100 N/sec implies that the equivalent ^{252}Cf mass that our sources represent is 10.226 nanograms. Table 1 contains the results of the final testing of the NDM. The measurements indicate the module's sensitivity to this source.

The insensitivity of the neutron detector to gamma ray-induced neutron counts was also evaluated. Requirement of the FRD states, "The NDM shall not cause the RPMS to alarm on neutrons when exposed to gamma radiation at an exposure rate of up to 20 mR/h (threshold) [goal of 50mR/h]." This behavior was evaluated in BNL's Low Scatter Irradiation (LSI) facility, where a gamma source of an appropriate magnitude was available. Due to the presence of other neutron sources in the facility that cannot be removed, the neutron background reported is significantly higher than the background at the former RADTEC site. The module was moved into the LSI and placed horizontally on the remote controlled positioning stage such that the detector centerline was aligned with the "source-deployed" location (the vertical tube seen on the left in Figure 10). A 196 millicurie ^{137}Cs source was remotely deployed, and the detector position remotely adjusted to produce a 20 mR/hr field at the center of the detector face. Several sets of count rate data were collected. The ^{137}Cs source was retracted, and a set of *background* neutron count rate measurements was collected. Table 2 presents some of the data that was collected. There is no evidence of any increase in the measured neutron count rate when the detector was exposed to a gamma field of 20mR/hr from ^{137}Cs.

Task 5. Performance Tests

An assembly of the completed detector, a NEMA 4 enclosure, and a standard portal monitor steel shroud was shipped to the Nevada National Security Site (NNSS) for inclusion in a DNDO test of alternative neutron detection modules. The equipment shipped to NNSS can be seen in Figure 11.

Figure 9. The detector module is seen here mounted on a footing at the former RADTEC site, for sensitivity tests.

Table 2. BF_3 NDM module gamma insensitivity test data

BF3 NDM Replacement Module Gamma Insensitivity Test Data			
Measurement Type	**Time (sec)**	**Counts**	**Count Rate (N/sec)**
20 mR/hr 137Cs	300	15,172	50.573
20 mR /hr 137Cs	300	15,023	50.077
20 mR /hr 137Cs	300	14,978	49.927
sum	900	45,173	50.192
LSI background	300	15,192	50.64
LSI background	300	15,073	50.24
LSI background	300	15,120	50.4
sum	900	45,385	50.428

Figure 10. A view of the module on the test stage in the LSI facility, looking from behind the "source-deployed" location (the vertical tube without the wire).

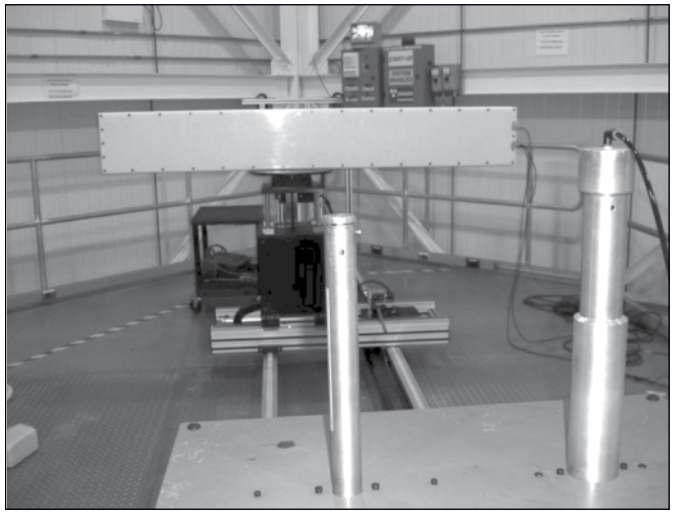

Figure 11. The completed NDM, installed in its stainless steel envelope, can be seen in place inside the open NEMA 4 enclosure, which is inside of the steel shroud.

Results of Testing

The BNL detector performed without mishap during the DNDO Test campaign in Nevada. It met all of the functional and dimensional requirements specified by DNDO; and is considered (by BNL) to be a viable alternative to ^{3}He for neutron detection.

Continuation Work at BNL

After the independent Government Test Campaign and drop tests were completed, BNL was tasked (by DNDO) to re-evaluate the design using MCNP calculations to continue to optimize performance and cost. This optimization process for the BF_3 design was to encompass the following design considerations: the tube pressure, operating voltage, design of the indicator for the BF_3 leak detection on the secondary containment (if any), survivability in the drop test, reduce electronic costs, and location and amount of "Getter Material" to neutralize the gas within the secondary containment.

Unfortunately, the funding for these tasks was "zeroed out" by the funding agency after only a partial fulfillment of the tasks could be accomplished by BNL.

These additional data will be presented at a later time.

Acknowledgements

The authors would like to thank the U.S. Department of Homeland Security (DHS)'s Domestic Nuclear Detection Office (DNDO), Product Acquisition and Deployment Directorate (PADD) for funding this work, the excellent folks at LND, Inc. for their help in understanding the intricacies of BF_3 neutron detector construction and design, and our collaborators at Los Alamos National Laboratory for their help in the design phase of the NDM.

References

1. U.S. Department of Homeland Security Domestic Nuclear Detection office (DNDO) Functional Requirements Document (FRD) for Radiation Portal Monitor System (RPMS) ^{3}He Neutron Detection Module (NDM) Replacement. Document Number 600-NDRP-113410 V2.07.
2. X-5 Monte Carlo Team, 2003. MCNP – A General Monte Carlo N-Particle Transport Code, Version 5, LA-UR-03-1987, 2003.
3. Ghosh, V. J. C. Czajkowski, C. Finfrock, M. Schear, F. H. Stephens, and C. K. Cheslan. Design of a Neutron Detection Module based on BF_3 Detectors, BNL Report.

Applications of Accelerator Mass Spectrometry in Nuclear Verification

M.A. C. Hotchkis, D. P. Child, and K. Wilcken
Australian Nuclear Science and Technology Organisation, Sydney, New South Wales, Australia

Introduction

The reduction and eventual elimination of nuclear threats to global peace and security remains a high priority for governments around the world.[1] The approach towards this goal involves multiple paths, including through existing treaties, such as the Non-proliferation Treaty (NPT), through bringing into force treaties and agreements such as the Additional Protocol and the Comprehensive Test Ban Treaty, and through the negotiation and enactment of new arms reduction measures and treaties such as the Fissile Material Cut-off Treaty. In all cases, trust between the parties to these agreements is built on sets of arrangements for verification.

Verification entails credible quantification and gathering of sound evidence, using scientifically proven methods. Not only must the best available methods be brought to bear, but also new methods must be researched, proven and implemented. Thus agencies responsible for nuclear verification provide drivers for development and innovation in the sciences and technologies applicable to verification. This does not necessarily involve the development of novel technologies from scratch, but rather through interaction with those parts of the scientific community who already utilise methods which can be adapted for verification purposes.

One such example is Accelerator Mass Spectrometry (AMS).[2,3] AMS was originally demonstrated in the late 1970s as a means for detection of radiocarbon at natural abundance levels. The technique quickly expanded to a number of other long-lived radioisotopes, and now stands as the most sensitive method available for the detection of long-lived radioisotopes at ultra-trace levels. In the next section we will introduce the AMS technique, and then review its application to verification science.

Accelerator Mass Spectrometry

AMS: introduction

AMS was originally developed for radiocarbon (^{14}C) dating. 'Modern' carbon – that is, in equilibrium with atmospheric carbon – contains one part in 10^{12} ^{14}C atoms. With a half-life of 5,700 years, it is possible to use radiocarbon for dating to ages of around 50,000 years before present. This requires measurement of the $^{14}C/^{12}C$ ratio down to one part in 10^{15} or better. While this was already achievable with decay counting, large samples of carbon were required (several grams), and needed many days of counting time.

In AMS, atoms are identified and counted directly, without waiting for their decay. This permits measurements to be performed quickly and with much smaller samples. In 1989 it was famously applied to the dating of the Shroud of Turin.[4] AMS is now routinely performed with 100µg of carbon, and has been applied with as little as 5µg.[5] These capabilities have opened up a vast array of applications,[6] in archaeological, environmental, earth, biomedical and forensic sciences.

For radiocarbon dating, the carbon must first be extracted from the sample material. It is then formed as graphite and placed in a high output sputter ion source: see Figure 1, which shows a schematic of part of the ANTARES accelerator system at ANSTO. The ion source generates carbon beams as negative ions for injection into a tandem accelerator. The negative ion beam is mass-analysed prior to injection. Energy analysis is frequently also incorporated at this stage. For radiocarbon, mass 14 is injected. At mass 14, a number of molecular species may accompany the radiocarbon beam. However, the isobaric species ^{14}N is absent, as nitrogen does not form a negative ion. At the accelerator terminal, the beam is converted from negative to positive ions by passage through a canal containing a 'stripper' gas, typically argon (sometimes a thin foil is used). This process also causes the break-up of molecular species. After acceleration, the beam emerging from the accelerator is subject to a combination of electrostatic and magnetic analysers, which are set to select the mass 14 ions and reject the molecular fragments. In addition, the ion energy and rate of energy loss (characteristic of the element) are measured by the ion detector—these further measures are not possible with low energy ions used in other mass spectrometry systems.

The end result is the ability to count the ions of the isotope of interest, with a background rate (or dark current) typically less than 0.001 per second.[7] Systems are implemented to concurrently measure the beam currents of the stable isotopes (e.g. ^{12}C), allowing precise measurement of isotopic ratios. While other mass spectrometry systems can measure isotopic ratios, only AMS can measure ratios below 10^{-9}, reaching its limit at around 10^{-16}. Such low ratios (i.e., high abundance sensitivity) are achieved through the combination of low dark current and effective elimination of both molecular and atomic isobaric interferences.

The AMS technique, as outlined above, can be used to

advantage in the detection of any long-lived radioisotope. It is not normally used for short-lived radioisotopes ($T_{½}$ < 1 year), which can usually be measured efficiently by radiometric means. In some situations, AMS may also be useful for trace element and stable isotope analysis[8]. The AMS technique is routinely applied to the measurement of ^{14}C, ^{10}Be, ^{26}Al, ^{36}Cl, ^{41}Ca, ^{129}I, ^{236}U, $^{239,240,242}Pu$, and has been developed for numerous other long-lived species including ^{99}Tc, ^{231}Pa and ^{237}Np. As for radiocarbon, molecular interferences are eliminated in the tandem accelerator terminal stripper. In some of these cases, and also in common with radiocarbon, the atomic isobar is absent due to the instability of the corresponding negative ion. These cases include ^{26}Al and ^{129}I; the relevant isobars are isotopes of magnesium and xenon, neither of which form negative ions. In the cases of ^{10}Be and ^{36}Cl, the atomic isobars (^{10}B and ^{36}S respectively) are separated from the isotope of interest by means of their different stopping characteristics in the detection system. Chemical separation (to remove boron from ^{10}Be samples, or sulphur from ^{36}Cl) is applied, but is not by any means sufficient to enable detection of ^{10}Be and ^{36}Cl at natural levels.

AMS of heavy elements

Application of AMS to the actinides has been reviewed recently by Fifield[9] and by Steier et al.[10] The long-lived actinides radioisotopes of interest are usually the most abundant species of that mass and radiochemical separation is sufficient to remove atomic isobars if they are present. However, it has proven to be a significant challenge for actinides analysis to approach the high abundance sensitivity ($<10^{-15}$) which is readily achieved for ^{14}C and others. Higher resolution mass analysers are required for actinides to separate neighbouring masses effectively. This needs to be implemented for both the low energy (prior to acceleration) and high energy mass analysers.

For high mass ions, energy loss measurements cannot be made with sufficient resolution to separate, for example, uranium from plutonium. This is also the case at intermediate mass, such as ^{129}I, which may be subject to interference from ^{128}Te[11]. The practical upper limit for use of energy loss to resolve the atomic number occurs at around mass 80.[12] For higher masses, it is useful to include a time-of-flight (TOF) measurement to the detection system. This exploits the small velocity differences between ions of neighbouring mass, such as ^{128}Te:^{129}I or ^{235}U:^{236}U. TOF can be measured with sufficient resolution to improve abundance sensitivities significantly. This method has enabled the measurement of $^{236}U/^{238}U$ ratios down to 10^{-12}.[13,14] limited not by instrument sensitivity but rather by the sample material.

The key advantage of accelerator mass spectrometry (AMS), compared to other forms of mass spectrometry, is its exceptional abundance sensitivity. This translates also to a very high absolute sensitivity. In the measurement of actinides at trace levels, the kinds of molecular interferences that can affect, for example, ICPMS,[15] are eliminated in the AMS technique.

It is instructive to make some comparison between AMS and the more commonly used methods, TIMS and ICPMS, for detection of actinides at trace levels (see Table 1). In terms of efficiency and count rate, AMS does not appear to have an advantage. Where it tends to have an advantage is in the low 'dark current' and elimination of backgrounds, hence good abundance and absolute sensitivities. The superior elimination of backgrounds makes AMS analysis much less sensitive to matrix effects and/or residues from sample treatment.

AMS efficiency ε_{AMS} is a combination of two factors:

$$\varepsilon_{AMS} = \varepsilon_i \times \varepsilon_t$$

with ionisation efficiency ε_i (i.e., formation of the negative ion in the ion source) and accelerator transmission efficiency ε_t. The latter depends on the selection of a suitable positive ion charge state, from the range of charge states formed in the stripping process. For higher energy AMS systems, it has been necessary to select the 5+ charge state for analysis, leading to ε_t not better than around 4 percent.[16,10] However, it has been found recently that yields of 15 percent or better can be obtained with lower energy accelerators using 3+ ions, at 0.3 to 1.0MV.[17-19] This is discussed further in the final section below. For carbon, negative ions can be formed with high efficiency, up to 30 percent for high-output sources.[20,21] This is not the case for most metals, including the actinides. In fact, the greatest ion source yields for actinides are achieved using actinide oxide target material and selection of negative oxide ions, as the yields are about 20 times greater than the corresponding atomic ions.[22] Even then, the ionisation efficiency is low, of the order of 0.5 percent.[23]

Table 1. Comparison of performance characteristics of mass spectrometric methods used for analysis of actinides at trace levels.[10, 24] The sensitivities quoted are the best reported and may not be achievable for all systems or all sample types.

	AMS	TIMS	ICP-MS
Efficiency*	0.02 – 0.2 percent	0.1 – 2 percent	0.1 – 1 percent
Typical count rate	100 c/s per pg/mg	1000 c/s per pg	1000 c/s per pg/ml
Isotope ratio sensitivity**	£10-12	³ 2×10-10	10-8
Absolute sensitivity (fg)***	0.2	0.6	10

*ratio of ions detected to atoms in the sample, for actinides;
**as demonstrated for $^{236}U/^{238}U$ measurement;
***as demonstrated for ^{239}Pu concentration.

Applications of AMS

Mass spectrometric methods are used widely in nuclear verification. High sensitivity analysis at ultra-trace levels are of particular interest and it is here we find applications for AMS. As we have seen, AMS is good for interference-free detection of a wide range of long-lived radioisotopes; among these are fission products, activation products, actinides and radiogenic daughter products.

History of AMS Involvement in Verification

From the early 1990s, the nuclear safeguards program run by the IAEA for monitoring compliance with the Nonproliferation Treaty was required to expand its role from mainly verification of declared activities, to also include detection of undeclared activities. Among a range of measures, environmental sampling was introduced, and the powers to use such methods were expanded by the introduction of the Additional Protocol. At that time, investigations were conducted to determine the kinds of technologies that could contribute to detection of undeclared activities, whether they be occurring (or had occurred in the past) within declared sites or at undeclared facilities.

One concept investigated at that time involved wide area environmental sampling (WAES); that is, seeking nuclear signatures in the environment as indicators of the presence and nature of an undeclared facility. A variety of environmental sample types were considered, including soil, water, sediment and air filters. A number of laboratories were involved in field trials to test the concept, including use of AMS for detection of the fission product ^{129}I. At ANSTO we also investigated the detection of ^{236}U in environmental samples as a signature of irradiated uranium.[16,25] At that time, the IAEA commissioned an investigation into the possible routes for implementation.[26-28] Aerosol sampling was implemented briefly in Baghdad, Iraq.[29] Although not pursued for routine safeguards monitoring, the use of wide-area samples remains an option for the IAEA under special circumstances and for other verification agencies.

Sample Analysis for Nuclear Safeguards and Forensics

The nuclear safeguards system operated by the IAEA includes routine collection and analysis of environmental samples[30]. Cotton wipes (swipes) are used to collect surface dust from facilities and these swipes are analysed. Analysis of individual dust particles is performed by TIMS, following hot particle identification by the fission track method, or by SIMS. Bulk analysis of the samples can also be performed, using ICP-MS, TIMS, or AMS. Bulk analysis provides an 'average' as individual particles are combined; however, it provides better absolute sensitivity. A recent overview of methods with references has been published by Sturm.[31] Our recently updated method, using AMS, is described in Hotchkis et al.[32]

The primary signatures sought in such analyses are the enrichment of uranium in ^{235}U and the isotopic ratio of plutonium (^{240}Pu/^{239}Pu) – these are the keys to distinguishing weapons-grade from power reactor nuclear materials. However, much more information can be obtained, and indeed is required, to verify safeguards declarations and to seek evidence of undeclared activities. Axelsson et al.[33] give an example illustrating the usefulness of the minor isotopes, ^{234}U and ^{236}U, to elucidate the full story, revealed by environmental sampling and careful data evaluation.

The importance of minor isotopes in data interpretation provides a challenge for analysts to ensure the reliability of results for small isotopic ratios in very small samples. Swipes and other materials used for sampling may contain only nanograms of uranium and femtograms (10^{-15}g) of plutonium. For uranium, the minor isotope component is at the 10^{-5} level or below, putting the isotope concentration into the low femtogram range. Ten years ago, only AMS could achieve these levels;[34] however, the gap has narrowed more recently, especially with improvements to ICP-MS. At the same time, considerable progress is being made with improvements to AMS.[10]

The same methods are also applicable to nuclear forensic investigations.[35] A wide variety of samples may be required as evidence in cases of illicit trafficking. Seized materials may or may not form part of that evidence; additionally, or alternately, swipes and other sample types may be collected to trace people and locations involved in the trafficking. Analysis of seized material may need to include age dating[36] to assist in attribution of material to a particular source. It is the minor actinide isotopes such as ^{234}U, ^{236}U, ^{231}Pa, ^{230}Th and others that assist with age dating of nuclear materials, revealing the time since the material was last processed. Dating is also relevant for safeguards analyses, for example where existing facilities have traces of contamination from early research work performed prior to safeguards agreements. There could be a role, too, for age dating in the monitoring of a Fissile Material Cut-off Treaty.[37]

Fingerprinting Ores and Yellowcake

For both safeguards and forensic investigations, there is a need to identify sources of materials. Key to this is the identification of 'nuclear fingerprints'[38] for materials at various stages in the fuel cycle. Characteristics which could be useful fingerprints include chemical form, morphology, elemental composition, impurities and isotopic composition of various constituents.

To 'fingerprint' uranium ores various approaches have been used: oxygen and lead isotopes[39-41] and rare earth and other elements.[42-45] Alternatively one may look for isotopic differences between uranium isotopes as a 'fingerprint'.[46] This in principle has the benefit of looking directly at the material of interest, that is, the uranium. The uranium isotopic composition should be unchanged through ore processing steps, unlike the trace element composition that might vary depending on the level of processing of the material. It has been shown that the impurity concentrations may be successfully applied to trace back the origin of uranium ore concentrate if sufficient data libraries are in place.[44] In the case of the uranium isotopic composition, the observed differences between ^{234}U, ^{235}U, and ^{238}U are small, thus making their application for fingerprinting difficult.[46] However, the rare isotope ^{236}U may offer a solution. Due to spontaneous fission of ^{238}U and (α,n) reactions it follows that there is naturally a certain level of neutron flux present in uranium ore bodies. This results in production of ^{236}U via neutron capture on ^{235}U (as well as producing other radioisotopes such as ^{239}Pu and ^{36}Cl). It is present at extremely low levels, but well within the measurement capabilities of AMS.[13,14,47,48]

An example of a set of $^{236}U/^{238}U$ ratio measurements of uranium ores is shown in Figure 2. The two key features apparent from the figure are: (i) $^{236}U/^{238}U$ ratios range over 2 orders of magnitude demonstrating a potentially valuable signal for fingerprinting; (ii) there is a large amount of scatter in the data and ^{236}U content does not follow a simple correlation with uranium concentration. The ^{236}U content is in fact a complex function of the minor and major element concentrations as well as water content.[13] The production can be predicted reasonably well by carefully mapping the ore deposit and then calculating the neutron flux within it.[49,50] However, a simple assumption of homogeneous or 'representative' ore is not suitable[13] and in fact there can be a large range of rare isotope concentrations present within a single borehole as shown for ^{36}Cl and ^{239}Pu.[49,50]

Despite the difficulty of establishing a clear ^{236}U fingerprint for a particular ore body, there may be an alternative way to utilize the ^{236}U signal. Even though the range of neutrons within the deposit is too short to result in homogeneous neutron flux and a common $^{236}U/^{238}U$ ratio, it is possible that the mining operations and production of yellowcake causes sufficient averaging of the varying $^{236}U/^{238}U$ ratios. Subsequently a typical $^{236}U/^{238}U$ ratio may be assigned for the yellowcake from a particular mill. First experimental results are encouraging.[51] However, one needs to bear in mind that some mills use ore from different deposits that might mix the signal or contribute to variability, but this is clearly a challenge for any method trying to establish a link between yellowcake and its source material.

Anthropogenic Radionuclides in the Environment – A Growing Knowledge Base

The utility of wide area environmental sampling for safeguards depends on having well established baseline data, so that if a signal is observed its significance can be determined. Other verification measures or nuclear forensic investigations (for example, post-detonation investigations), which may seek to use wide-area type samples would face the same issue. If evidence is sought from signatures with ultra-trace analysis of environmental media, then there must be fore-knowledge of the expected background levels of that signature. Background levels may be naturally occurring or, more frequently, of anthropogenic origin. With new analytical capabilities becoming available, there have been a growing number of studies which are providing this background data. We will highlight here some recent work that has used AMS.

The AMS technique is capable of providing concentration measurements of global fallout plutonium in small-sized samples and has been applied recently in several studies.[52-55] In these works, global fallout plutonium provides an age marker in environmental media such as sediments and soils. Plutonium is approximately 6 times more abundant than ^{137}Cs, which has been used widely in the past for erosion and sedimentation research. The long half-lives of the most abundant isotopes of plutonium, 24,110 years and 6,561 years respectively for ^{239}Pu and ^{240}Pu, mean that no significant decay has occurred since its release into the environment, in contrast to ^{137}Cs ($T_{½}$ = 30.1y).

Furthermore, unlike alpha spectrometry, AMS also provides isotopic information. A study of the Herbert River catchment in Queensland, Australia,[52] reported an average $^{240}Pu/^{239}Pu$ ratio of 0.149, lower than the Southern Hemisphere average of 0.172,[56] hinting at regional contributions in addition to stratospheric fallout. Fallout plutonium in a bushfire-affected catchment[54] in eastern Victoria, Australia, also shows a lower than average plutonium ratio. A sedimentation study of Bathurst Harbour in Tasmania, Australia by Harrison et al.[55] showed variations in the plutonium ratio corresponding to different dates of deposition. Potential regional influences on fallout within Australia are the British nuclear weapon test sites at Maralinga, Emu Junction and Monte Bello islands. AMS has been used to characterise the contamination at the test sites[57] and examine the impact of these tests around the Australian mainland.[58] Similar studies have also been performed at other nuclear weapon test sites such as Bikini Atoll,[59] Amchitka Island, Alaska[60] and in French Polynesia.[61] Studies such as these provide information on the geographic (local/regional/global) and time-dependent variability of fallout plutonium, both for concentrations and isotopic ratios.

^{236}U may be produced during nuclear weapon detonations by neutron capture within the uranium tamper. As a result, it is expected to be present in global fallout and this has recently been confirmed in Japan[62] and in the Canary Islands[63]. The observed ratio of ^{236}U to ^{239}Pu is between 0.212 and 0.253 at the Japanese site. These observations open up the possibility of using global fallout uranium as a tracer. Local sources of ^{236}U have also been studied. As discussed for plutonium, nuclear weapon detonations are local sources of ^{236}U contamination, and this isotope has been observed at Hiroshima[64] and at test sites in Australia.[57] ^{236}U is also produced by neutron capture on ^{235}U in nuclear reactors and has been measured in environments affected by Chernobyl,[16,65] near an Italian nuclear power plant site[66] and near a reprocessing facility.[16,67,68] Depleted uranium contains ^{236}U due to the practice of using recycled uranium at some enrichment facilities. As a result, it is observed at locations where DU contamination exists, for example in Kosovo[69] and Kuwait.[70]

^{233}U may also be formed during nuclear detonations, both in the uranium tamper from (n,2n) reactions on ^{234}U and in the surrounding soil by neutron capture on ^{232}Th. This isotope has been measured in an unspecified contaminated site,[71] and in-situ production in soil has been measured at the former British nuclear test sites in Australia.[57] A number of other rare actinides have also been measured by AMS in environmental samples such as ^{237}Np[72] and ^{231}Pa.[73] ^{233}U, ^{237}Np and ^{231}Pa are all of potential interest in nuclear verification, either as alternative fissile materials or as daughter radionuclides relevant to nuclear material dating.

The fission product ^{129}I has had widespread release throughout the environment both from civil nuclear facilities, predominantly from reprocessing activities, and nuclear weapons

Table 2. AMS laboratories with current and planned facilities for heavy element analysis

Accelerator	Institute	Location	Max. Voltage†
ANTARES	ANSTO	Sydney, Australia	8MV, 1MV*
Atlas	ANL	Argonne, USA	linac
14UD	ANU	Canberra, Australia	14MV
CCAMS	Univ. of Ottawa	Ottawa, Canada	3MV*
HI-13	CIAE	Beijing, China	13MV
CIRCE	Seconda Univ. di Napoli	Caserta, Italy	3MV
1MV AMS	CNA	Seville, Spain	1MV
Tandy	ETH	Zurich, Switzerland	0.6MV
CAMS	LLNL	Livermore, USA	8MV
MP tandem	Tech. Univ. München	Munich, Germany	12MV
VERA	Univ. of Vienna	Vienna, Austria	3MV

† indicates size of accelerator; the operating voltage for heavy elements may be lower than this value due to magnetic analyser limitations.
* under construction.

Figure 1. A schematic of the ANTARES accelerator at ANSTO, including those components used for actinide analysis

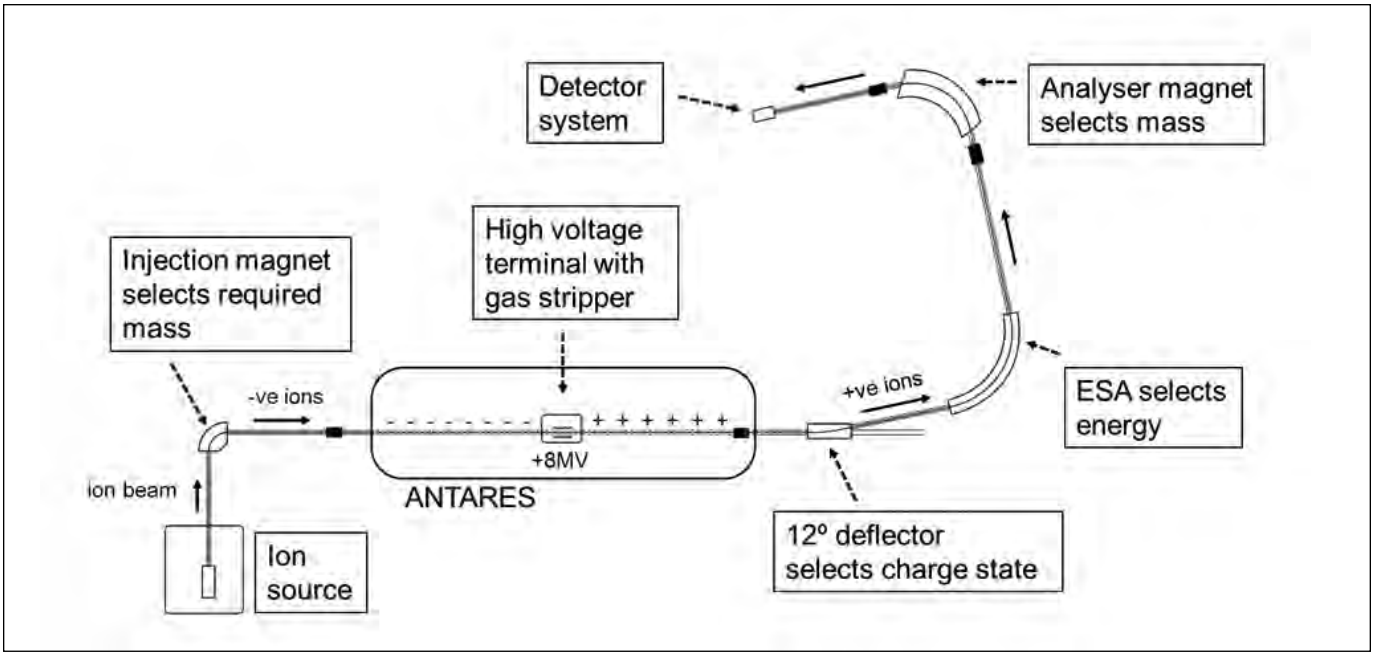

detonation. There has been substantial work done to establish baseline concentrations for ^{129}I through the environment (see, for example, Snyder and Fehn[74]). This isotopic marker has also been used to model the source contribution for radiological contamination found in lake sediments.[75] Of particular relevance to its potential application in wide area monitoring, the ^{129}I signal from reprocessing facilities has been observed in aerosols across Europe.[76,77]

Future Prospects for AMS of Heavy Elements

The range of investigations highlighted in the previous sections represents only a sample of the research being pursued at AMS facilities with the capability to analyse heavy elements. Eleven laboratories (see Table 2) have AMS facilities used for heavy element analysis and are involved in the kinds of environmental studies outlined above, and several are actively involved with nuclear

Figure 2. AMS measurements of $^{236}U/^{238}U$ ratios from various ore bodies as a function of uranium concentration[13,48]

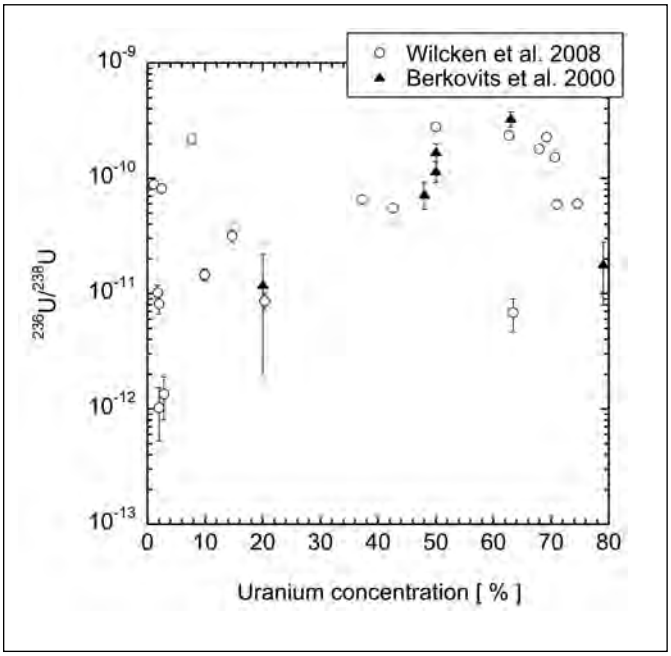

verification activities.

Recent innovations in the AMS technique are delivering even better performance. Two laboratories have been pursuing the potential for enhanced efficiency with alternative accelerator stripper gases.[19,78] The Ion Beam Laboratory of ETH, Zurich, has recently demonstrated radiocarbon analysis at only 50kV accelerating voltage[79]—this made practical through the use of helium as a stripper gas. Helium stripping has also been shown to deliver enhanced yield for actinides, delivering up to 35 percent accelerator transmission efficiency[19] at 325kV accelerating voltage. In contrast, a heavy molecular gas stripper has been shown to deliver yield benefits for higher energy accelerators[80]. Improved efficiency translates into higher counting rates and therefore better precision for ultra-trace level measurements, where the precision is frequently limited by counting statistics.

Poor ion source efficiency remains a weakness for AMS analysis of actinides and some other species. Investigations of source efficiency[23] have not so far delivered any breakthroughs. However, interesting new developments by Zhao et al.[81] have shown that there may be a way forward using fluoride molecular species.

At ANSTO we will take delivery of a new 1MV AMS system early in 2013 from NEC.[82] Its design is tailored to deliver high efficiency, high sensitivity and high throughput both for radiocarbon and for actinides. The system beam optics are engineered to work with a high output ion source and alternate stripping gases to maximise efficiency. Also, the system will include a second high-resolution analysing magnet in the high energy beamline for improved background suppression. The ETH laboratory has recently demonstrated the efficacy of this measure,[83] which also has advantages for other isotopes such as ^{10}Be for small systems operating at <1MV.

The growing activity in this area, coupled with improving AMS performance, point to a bright future.

References

1. Evans, G., Y. Kawaguchi, and Co-Chairs. 2009. *Eliminating Nuclear Threats: A Practical Agenda for Global Policymakers,* Canberra/Tokyo: International Commission on Nuclear Nonproliferation and Disarmament.
2. Tuniz, C., J.R. Bird, D. Fink, and G.F. Herzog. 1998. *Accelerator Mass Spectrometry.* Boca Raton: CRC Press.
3. Hellborg, R., and G. Skog. 2008. Accelerator Mass Spectrometry,*Mass Spectrometry Reviews* 27, 398-427.
4. Damon, P. E., D. J. Donahue, B. H. Gore, A. L. Hatheway, A. J. T. Jull, T. W. Linick, P. J. Sercel, L. J. Toolin, C. R. Bronk, E.T. Hall, R. E. M. Hedges, R. Housley, I. A. Law, C. Perry, G. Bonani, S. Trumbore, W. Woelfli, J.C. Ambers, S. G. E. Bowman, M.N. Leese, and M. S. Tite. 1989. Radiocarbon dating of the Shroud of Turin, *Nature* 337, 611-15.
5. Smith, A. M., Q. Hua, A. Williams, V. Levchenko, and B. Yang. 2010. Developments in micro-sample 14C AMS at the ANTARES AMS facility. *Nuclear Instruments and Methods in Physics Research Section B: Beam Interactions with Materials and Atoms* 268, 919-23.
6. See, for example, the Proceedings of the 20th International *Radiocarbon* Conference, *Radiocarbon* 52 no. 2-3 (2010), and other issues of the journal *Radiocarbon.*
7. Fifield, L. K., R. G. Cresswell, M. L. Di Tada, T. R. Ophel, J. P. Day, A. P. Clacher, S.J. King, and N.D. Priest. 1996. Accelerator mass spectrometry of plutonium isotopes, *Nuclear Instruments and Methods in Physics Research Section B: Beam Interactions with Materials and Atoms* 117, 295-303.
8. Matteson, S. 2008. Issues and opportunities in accelerator mass spectrometry for stable isotopes, *Mass Spectrometry Reviews* 27, 470-84.
9. Fifield, L.K. 2008. Accelerator mass spectrometry of the actinides, *Quaternary Geochronology* 3, 276-90.
10. Steier, P., F. Dellinger, O. Forstner, R. Golser, K. Knie, W. Kutschera, A. Priller, F. Quinto, M. Srncik, F. Terrasi, C. Vockenhuber, A. Wallner, G. Wallner, and E.M. Wild. 2010. Analysis and application of heavy isotopes in the environment, *Nuclear Instruments and Methods in Physics Research Section B: Beam Interactions with Materials and Atoms* 268, 1045-49.
11. Wagner, M.J.M., B. Dittrich-Hannen, H.A. Synal, M. Suter, and U. Schotterer. 1996. Increase of ^{129}I in the Environment, *Nuclear Instruments and Methods in Physics Research*

Section B: Beam Interactions with Materials and Atoms 113, 490-94.
12. Wang, W., Y. Guan, M. He, S. Jiang, S. Wu, and C. Li. 2010. A Method for Measurement of Ultratrace 79Se with Accelerator Mass Spectrometry, *Nuclear Instruments and Methods in Physics Research Section B: Beam Interactions with Materials and Atoms* 268, 759-63.
13. Wilcken, K.M., L.K. Fifield, T.T. Barrows, S.G. Tims, and L.G. Gladkis. 2008. Nucleogenic ^{36}Cl, ^{236}U and ^{239}Pu in Uranium Ores. *Nuclear Instruments and Methods in Physics Research Section B: Beam Interactions with Materials and Atoms* 266, 3614-24.
14. Steier, P., M. Bichler, L.K. Fifield, R. Golser, W. Kutschera, A. Priller, F. Quinto, S. Richter, M. Srncik, P. Terrasi, L. Wacker, A. Wallner, G. Wallner, K.M. Wilcken, and E.M. Wild. 2008. Natural and Anthropogenic ^{236}U in Environmental Samples. *Nuclear Inst. and Methods in Physics Research, B* 266, 2246-50.
15. Pointurier, F., P. Hemet, and A. Hubert. 2008. Assessment of Plutonium Measurement in the Femtogram Range by ICP-MS; Correction From Interfering Polyatomic Species, *Journal of Analytical Atomic Spectrometry* 23, 94-102.
16. Hotchkis, M.A.C., D. Child, D. Fink, G.E. Jacobsen, P.J. Lee, N. Mino, A.M. Smith, and C. Tuniz. 2000. Measurement of U-236 in Environmental Media, *Nuclear Instruments & Methods in Physics Research Section B: Beam Interactions with Materials and Atoms* 172, 659-65.
17. Wacker, L., E. Chamizo, L.K. Fifield, M. Stocker, M. Suter, and H.A. Synal. 2005. Measurement of Actinides on a Compact AMS System Working at 300kV, *Nuclear Institute and Methods in Physics Research, B* 240, 452-57.
18. Chamizo, E., J.M. López-Gutiérrez, A. Ruiz-Gómez, F.J. Santos, M. García-León, C. Maden, and V. Alfimov. 2008. Status of the compact 1MV AMS Facility at the Centro Nacional de Aceleradores (Spain), *Nuclear Institute and Methods in Physics Research, B* 266, 2217-20.
19. Vockenhuber, C., V. Alfimov, M. Christl, J. Lachner, T. Schulze-König, M. Suter, and H. A. Synal. The Potential of He Stripping in Heavy Ion AMS, *Nuclear Instruments and Methods in Physics Research Section B: Beam Interactions with Materials and Atoms.*
20. Southon, J., and G. M. Santos. 2007. Life with MC-SNICS. Part II: Further ion Source Development at the Keck Carbon Cycle AMS Facility, *Nuclear Instruments and Methods in Physics Research Section B: Beam Interactions with Materials and Atoms* 259, 88-93.
21. Fallon, S. J., T. P. Guilderson, and T. A. Brown. 2007. CAMS/LLNL ion source efficiency revisited, *Nuclear Instruments and Methods in Physics Research Section B: Beam Interactions with Materials and Atoms* 259, 106-10.
22. Zhao, X. L., M. J. Nadeau, M. A. Garwan, L. R. Kilius, and A. E. Litherland. 1994. Radium, Actinides, and Their Molecular Negative Ions From a Cesium Sputter Ion Source, *Nuclear Instruments and Methods in Physics Research Section B: Beam Interactions with Materials and Atoms* 92, 258-64.
23. Child, D. P., M. A. C. Hotchkis, K. Whittle, and B. Zorko. 2010. Ionisation Efficiency Improvements for AMS Measurement of Actinides, *Nuclear Institute and Methods in Physics Research, B* 268, 820-23.
24. Hou, X., and P. Roos. 2008. Critical Comparison of Radiometric and Mass Spectrometric Methods for the Determination of Radionuclides in Environmental, Biological and Nuclear Waste Samples, *Analytica Chimica Acta* 608, 105-39.
25. Tuniz, C., M.A.C. Hotchkis, D. Donohue, R. Perrin, and S. Vogt. 2000. ^{236}U *Analysis by AMS: A New Tool for Strengthening Nuclear Safeguards. In 22nd Annual Meeting of ESARDA.* Dresden, Germany.
26. Swindle, D.W., R.L. Pearson, N.A. Wogman, and P.W. Krey. 2001. Screening of Potential Sites for Undeclared Nuclear Facilities in Environmental Monitoring for Nuclear Proliferation, *Journal of Radioanalytical and Nuclear Chemistry* 248, 599-604.
27. Krey, P.W., and K.W. Nicholson. 2001. Atmospheric Sampling and Analysis for the Detection of Nuclear Proliferation, *Journal of Radioanalytical and Nuclear Chemistry* 248, 605-10.
28. Wogman, N.A., M.S. Wigmosta, D.W. Swindle, and P.W. Krey. 2001. Wide-area Aquatic Sampling and Analysis for the Detection of Nuclear Proliferation, *Journal of Radioanalytical and Nuclear Chemistry* 248, 611-15.
29. Valmari, T., M. Tarvainen, J. Lehtinen, R. Rosenberg, T. Honkamaa, A. Ossintsev, M. Lehtimäki, A. Taipale, S. Ylätalo, and R. Zilliacus. 2002. Aerosol Sampling Methods for Wide Area Environmental Sampling (WAES). Helsinki: STUK-YTO-TR 183.
30. Donohue, D.L. 1998. Strengthening IAEA Safeguards Through Environmental Sampling and Analysis. *Journal of Alloys and Compounds* 271-273, 11-18.
31. Sturm, M. 2010. Destructive Analysis: Effective Analytical Support to Nuclear Safeguards and Non-Proliferation, *ESARDA Bulletin* 45, 56-65.
32. Hotchkis, M.A.C., D.P. Child, and B. Zorko. 2010. Actinides AMS for Nuclear Safeguards and Related Applications. *Nuclear Instruments and Methods in Physics Research, Section B* 268, 1257-60.
33. Axelsson, A., D.M. Fischer, and M.V. Penkin. 2009. Use of Data from Environmental Sampling for IAEA Safeguards. Case Study: Uranium with Near-natural ^{235}U Abundance, *Journal of Radioanalytical and Nuclear Chemistry* 282, 725-29.
34. Hotchkis, M., D. Child, and C. Tuniz. 2003. Application of Accelerator Mass Spectrometry for ^{236}U Analysis, *Journal of Nuclear Science and Technology* 39, 532-36.
35. Mayer, K., M. Wallenius, and T. Fanghänel. 2007. Nuclear

Forensic Science-From Cradle to Maturity, *Journal of Alloys and Compounds* 444-445, 50-56.
36. Mayer, K., M. Wallenius, M. Hedberg, and K. Lützenkirchen. 2009. Unveiling the History of Seized Plutonium Through Nuclear Forensic Investigations, *Radiochimica Acta* 97, 261-64.
37. Glaser, A., and S. Burger. 2009. Verification of a Fissile Material Cutoff Treaty: The Case of Enrichment Facilities and the Role of Ultra-trace Level Isotope Ratio Analysis, *Journal of Radioanalytical and Nuclear Chemistry* 280, 85-90.
38. Mayer, K., M. Wallenius, and I. Ray. 2005. Nuclear Forensics-a Methodology Providing Clues on the Origin of Illicitly Trafficked Nuclear Materials, *Analyst* 130, 433-41.
39. Fayek, M., J. Horita, and E.M. Ripley. 2011. The Oxygen Isotopic Composition of Uranium Minerals: A Review, *Ore Geology Reviews* 41, 1-21.
40. Pajo, L.P., K.M. Mayer, and L.K. Koch. 2001. Investigation of the Oxygen Isotopic Composition in Oxidic Uranium Compounds as a New Property in Nuclear Forensic Science. Fresenius' *Journal of Analytical Chemistry* 371, 348-52.
41. Redermeier, A. 2009. Fingerprinting of Nuclear Material for Nuclear Forensics. *ESARDA Bulletin* 43.
42. Richard, A., D.A. Banks, J. Mercadier, M.-C. Boiron, M. Cuney, and M. Cathelineau. 2011. An Evaporated Seawater Origin for the Ore-forming Brines in Unconformity-related Uranium Deposits (Athabasca Basin, Canada): Cl/Br and δ37Cl Analysis of Fluid Inclusions, *Geochimica et Cosmochimica Acta* 75, 2792-810.
43. Svedkauskaite-LeGore, J., G. Rasmussen, S. Abousahl, and P. van Belle. 2008. Investigation of the Sample Characteristics Needed for the Determination of the Origin of Uranium-bearing Materials, *Journal of Radioanalytical and Nuclear Chemistry* 278, 201-09.
44. Keegan, E., S. Richter, I. Kelly, H. Wong, P. Gadd, H. Kuehn, and A. Alonso-Munoz. 2008. The Provenance of Australian Uranium Ore Concentrates by Elemental and Isotopic Analysis, *Applied Geochemistry* 23, 765-77.
45. Mercadier, J., M. Cuney, P. Lach, M.C. Boiron, J. Bonhoure, A. Richard, M. Leisen, and P. Kister. 2011. Origin of Uranium Deposits Revealed by Their Rare Earth Element Signature, *Terra Nova* 23, 264-69.
46. Richter, S., A. Alonso, W. De Bolle, R. Wellum, and P.D.P. Taylor. 1999. Isotopic "fingerprints" for Natural Uranium Ore Samples, *International Journal of Mass Spectrometry* 193, 9-14.
47. Zhao, X.L., M.J. Nadeau, L.R. Kilius, and A.E. Litherland. 1994. The First Detection of Naturally-occurring ^{236}U with Accelerator Mass Spectrometry, *Nuclear Instruments and Methods in Physics Research Section B: Only-Beam Interaction Materials Atoms* 92, 249-53.
48. Berkovits, D., H. Feldstein, S. Ghelberg, A. Hershkowitz, E. Navon, and M. Paul. 2000. ^{236}U in Uranium Minerals and Standards, *Nuclear Instruments and Methods in Physics Research Section B: Beam Interactions with Materials and Atoms* 172, 372-76.
49. Curtis, D., J. Fabryka-Martin, P. Dixon, and J. Cramer. 1999. Nature's Uncommon Elements: Plutonium and Technetium, *Geochimica et Cosmochimica Acta* 63, 275-85.
50. Cornett, R.J., J. Fabryka-Martin, J.J. Cramer, H.R. Andrew, and V.T. Koslowsky. 2010. 36Cl Production and Mobility in the Cigar Lake Uranium Deposit, *Nuclear Instruments and Methods in Physics Research Section B: Beam Interactions with Materials and Atoms* 268, 1189-92.
51. Srncik, M., K. Mayer, E. Hmecek, M. Wallenius, Z. Varga, P. Steier, and G. Wallner. 2011. Investigation of the (236) U/(238)U Isotope Abundance Ratio in Uranium Ores and Yellow CakeSamples, *Radiochimica Acta* 99, 335-39.
52. Everett, S. E., S. G. Tims, G. J. Hancock, R. Bartley, and L.K. Fifield. 2008. Comparison of Pu and 137Cs as Tracers of Soil and Sediment Transport in a Terrestrial Environment, *Journal of Environmental Radioactivity* 99, 383-93.
53. Tims, S. G., S. E. Everett, L. K. Fifield, G. J. Hancock, and R. Bartley. 2010. Plutonium as a Tracer of Soil and Sediment Movement in the Herbert River, Australia, *Nuclear Instruments & Methods in Physics Research Section B: Beam Interactions with Materials and Atoms* 268, 1150-54.
54. Smith, H. G., G. J. Sheridan, P. Nyman, D. P. Child, P. N. J. Lane, M. A. C. Hotchkis, and G. E. Jacobsen. 2012. Quantifying Sources of Fine Sediment Supplied to Post-fire Debris Flows Using Fallout Radionuclide Tracers, *Geomorphology* 139–140, 403-15.
55. Harrison, J., K. Saunders, D. P. Child, and M. A. C. Hotchkis. 2011. Modern Sedimentation Patterns in World Heritage Bathurst Harbour, Tasmania, Australia Inferred Using ^{210}Pb dating, ^{239}Pu and ^{240}Pu. To be published.
56. Krey, P. W., E. P. Hardy, C. Pachucki, F. Rourke, J. Coluzza, and W. K. Benson. 1976. Mass Isotopic Composition of Global Fall-out Plutonium in Soil. Paper Read at Transuranium Nuclides in the Environment, at Vienna, Austria.
57. Child, D. P., and M. A. C. Hotchkis. 2011. Plutonium and Uranium Contamination in Soils from the Former Nuclear Weapon Tests in Australia. Paper read at 12th International Conference on Accelerator Mass Spectrometry, at Wellington, New Zealand.
58. Tims, S., L. K. Fifield, R. Lal, and W. Hoo. 2011. Plutonium Isotope Measurements from Across Continental Australia. Paper read at 12th International Conference on Accelerator Mass Spectrometry, at Wellington, New Zealand.
59. Lachner, J., M. Christl, T. Bisinger, R. Michel, and H. A. Synal. 2010. Isotopic Signature of Plutonium at Bikini atoll. *Applied Radiation and Isotopes* 68, 979-83.
60. Hamilton, T. 2005. Determination of Plutonium Activity Concentrations and ^{240}Pu/^{239}Pu Atom Ratios in Brown Algae (Fucus distichus) Collected From Amchitka Island,

Alaska. Final Report, Lawrence Livermore National Laboratory, Livermore CA, UCRL-SR-212129.
61. Hrnecek, E., P. Steier, and A. Wallner. 2005. Determination of Plutonium in Environmental Samples by AMS and Alpha Spectrometry, *Applied Radiation and Isotopes* 63, 633-38.
62. Sakaguchi, A., K. Kawai, P. Steier, F. Quinto, K. Mino, J. Tomita, M. Hoshi, N. Whitehead, and M. Yamamoto. 2009. First Results on ^{236}U Levels in Global Fallout, *Science of the Total Environment* 407, 4238-42.
63. Srncik, M., P. Steier, and G. Wallner. 2011. Depth profile of 236U/238U in soil samples in La Palma, Canary Islands. *Journal of Environmental Radioactivity* 102, 614-19.
64. Sakaguchi, A., K. Kawai, P. Steier, T. Imanaka, M. Hoshi, S. Endo, K. Zhumadilov, and M. Yamamoto. 2010. Feasibility of Using ^{236}U to Reconstruct Close-in Fallout Deposition From the Hiroshima Atomic Bomb, *Science of the Total Environment* 408, 5392-98.
65. Mironov, V., S. Pribylev, V. Zhuravkov, J. Matusevich, M. Hotchkis, and D. Child. 2009. "The Use of ^{236}U as a Tracer of Irradiated Uranium." In *Radioactive Particles in the Environment,* edited by Deborah H. Oughton and Valery Kashparov, 221-32. Springer Netherlands.
66. Quinto, F., P. Steier, G. Wallner, A. Wallner, M. Srncik, M. Bichler, W. Kutschera, F. Terrasi, A. Petraglia, and C. Sabbarese. 2009. The First Use of ^{236}U in the General Environment and Near a Shutdown Nuclear Power Plant, *Applied Radiation and Isotopes* 67, 1775-80.
67. Marsden, O. J., F.R. Livens, J. P. Day, L. K. Fifield, and P.S. Goodall. 2001. Determination of U-236 in Sediment Samples by Accelerator Mass Spectrometry, *Analyst* 126, 633-36.
68. Srncik, M., E. Hrnecek, P. Steier, and G. Wallner. 2011. Determination of U, Pu and Am Isotopes in Irish Sea Sediment by a Combination of AMS and Radiometric Methods, *Journal of Environmental Radioactivity* 102, 331-35.
69. Danesi, P. R., A. Bleise, W. Burkart, T. Cabianca, M. J. Campbell, M. Makarewicz, J. Moreno, C. Tuniz, and M. Hotchkis. 2003. Isotopic Composition and Origin of Uranium and Plutonium in Selected Soil Samples Collected in Kosovo, *Journal of Environmental Radioactivity* 64, 121-31.
70. Salbu, B., K. Janssens, O.C. Lind, K. Proost, L. Gijsels, and P.R. Danesi. 2004. Oxidation States of Uranium in Depleted Uranium Particles from Kuwait, *Journal of Environmental Radioactivity* 78, 125-35.
71. Tumey, S. J., T. A. Brown, B. A. Buchholz, T. F. Hamilton, I. D. Hutcheon, and R. W. Williams. 2009. Ultra-sensitive Measurements of ^{233}U by Accelerator Mass Spectrometry for National Security Applications, *Journal of Radioanalytical and Nuclear Chemistry* 282, 721-24.
72. Keith-Roach, M. J., J. P. Day, L. K. Fifield, and F.R. Livens. 2000. Measurement of ^{237}Np in Environmental Water Samples by Accelerator Mass Spectrometry, *Analyst* 126, 58-61.
73. Christl, M., L. Wacker, J. Lippold, H. A. Synal, and M. Suter. 2007. Protactinium-231: A New Radionuclide for AMS, *Nuclear Instruments and Methods in Physics Research Section B: Beam Interactions with Materials and Atoms* 262, 379-84.
74. Snyder, G., and U. Fehn. 2004. Global Distribution of 129I in Rivers and Lakes: Implications for Iodine Cycling in Surface Reservoirs, *Nuclear Instruments and Methods in Physics Research Section B: Beam Interactions with Materials and Atoms* 223-224, 579-86.
75. Englund, E., A. Aldahan, G.r. Possnert, E. Haltia-Hovi, X. Hou, I. Renberg, and T. Saarinen. 2008. Modeling Fallout of Anthropogenic 129I, *Environmental Science & Technology* 42, 9225-30.
76. Santos, F. J., J. M. Lopez-Gutierrez, E. Chamizo, M. Garcia-Leon, and H. A. Synal. 2006. Advances on the Determination of Atmospheric I-129 by Accelerator Mass Spectrometry (AMS), *Nuclear Instruments & Methods in Physics Research Section B: Beam Interactions with Materials and Atoms* 249, 772-75.
77. Englund, E., A. Aldahan, X. L. Hou, G. Possnert, and C. Söderström. 2010. Iodine (129I and 127I) in Aerosols from Northern Europe, *Nuclear Instruments and Methods in Physics Research Section B: Beam Interactions with Materials and Atoms* 268, 1139-41.
78. Hotchkis, M. A. C., D. Child, D. Fink, V. Levchenko, and A. Wallner. Investigation of Gas Stripping at 4.1 MeV for High Mass Negative Ions, *Nuclear Instruments and Methods in Physics Research Section B: Beam Interactions with Materials and Atoms.*
79. Synal, H. A., T. Schulze-König, M. Seiler, M. Suter, and L. Wacker. Mass Spectrometric Detection of Radiocarbon for Dating Applications, *Nuclear Instruments and Methods in Physics Research Section B: Beam Interactions with Materials and Atoms.*
80. Hotchkis, M. A. C., D. Child, D. Fink, V. Levchenko, and K. Wicken. 2012. To be published.
81. Zhao, X.-L., W. E. Kieser, X. Dai, N. D. Priest, S. Kramer-Tremblay, J. Eliades, and A. E. Litherland. Nuclear Instrument Methods in Physics Research B, submitted.
82. National Electrostatics Corporation, Wisconsin, USA, http://www.pelletron.com.
83. Vockenhuber, C., M. Christl, C. Hofmann, J. Lachner, A.M. Müller, and H.-A. Synal. 2011. Accelerator Mass Spectrometry of ^{236}U at Low Energies, *Nuclear Instruments and Methods in Physics Research Section B: Beam Interactions with Materials and Atoms 2*69, 3199-203.

Safeguards Verification Measurements Using Laser Ablation, Absorbance Ratio Spectrometry in Gaseous Centrifuge Enrichment Plants

Norm C. Anheier, Bret D. Cannon, H. Amy Qiao, and Jon R. Phillips
Pacific Northwest National Laboratory, Richland, Washington USA

Abstract

Laser Ablation, Absorbance Ratio Spectrometry (LAARS) is a new verification measurement technology under development at the U.S. Department of Energy's (DOE) Pacific Northwest National Laboratory (PNNL). LAARS uses three lasers to ablate and then measure the relative isotopic abundance of uranium compounds. An ablation laser is tightly focused on uranium-bearing solids, producing a small plasma plume containing uranium atoms. Two collinear wavelength-tuned spectrometry lasers transit through the plume and the absorbance of U-235 and U-238 isotopes are measured to determine U-235 enrichment. The measurement has high relative precision and detection limits approaching the femtogram range for uranium. It is independent of chemical form and degree of dilution with nuisance dust and other materials. High speed sample scanning and pinpoint characterization allow measurement rates approaching one million particles/hour to detect and analyze the enrichment of trace uranium in samples. The spectrometer is assembled using commercially available components and features a compact and low-power design. Future designs can be engineered for reliable, autonomous deployment within an industrial plant environment.

Two specific applications of the spectrometer are under development: 1) automated unattended aerosol sampling and analysis and 2) on-site small sample destructive assay measurement. The two applications propose game-changing technological advances in gaseous centrifuge enrichment plant (GCEP) safeguards verification. The aerosol measurement instrument, LAARS-environmental sampling (ES), collects aerosol particles from the plant environment in a purpose-built rotating drum impactor and then uses LAARS-ES to quickly scan the surface of the impactor to measure the enrichments of the captured particles. The current approach to plant misuse detection involves swipe sampling and offsite analysis. Though this offsite analysis approach is very robust, it generally requires several months to obtain results from a given sample collection. The destructive assay instrument, LAARS-destructive assay (DA), uses a simple purpose-built fixture with a sampling planchet to collect adsorbed UF_6 gas from a cylinder valve or from a process line tap or pigtail. A portable LAARS-DA instrument scans the microgram quantity of uranium collected on the planchet and the assay of the uranium is measured to ~0.16 percent relative precision. Currently, destructive assay samples for bias defect measurements are collected in small sample cylinders for offsite mass spectrometry measurement.

Introduction

Application of International Atomic Energy Agency (IAEA) safeguards in Gaseous Centrifuge Enrichment Plants (GCEPs) is a growing challenge. Gaseous Diffusion Plants (GDPs) are moving into retirement and the global nuclear reactor fleet continues to grow. The increasing demand for enrichment services, combined with GDP retirement, implies significant growth in GCEP capacity. Therefore, a robust IAEA safeguards approach for GCEPs is critical. Given the desire of the operator to protect proprietary information and sensitive technology, the enduring challenge of GCEP safeguards remains independent verification of plant declarations in the absence of full access to the facility. To understand the path forward in GCEP safeguards requires detailed comprehension of this significant and unavoidable context.

Current GCEP Safeguards Measures

The IAEA safeguards approach for GCEPs is to verify the uranium and U-235 mass balance of the uranium hexafluoride (UF_6) flows. A basic set of safeguard inspections focus on physical inventory verification (PIV) of UF_6 cylinders (mass and enrichment) in the storage yards and in the feed and withdraw processing stations. The gas and solid phase holdup in the cascade is usually small and verification limited due to cascade hall access restrictions. Safeguards inspectors generally perform monthly inspections and randomly select feed, product, and tails cylinders for verification by weighing selected cylinders and measuring the U-235 abundance by non-destructive assay (NDA) or by sampling and destructive analysis (DA). These verified results are compared with the GCEP operator declaration to provide a monthly accounting of the flow of U-235 in and out of both the facility and enrichment process.

Within the statistical mass accountancy sampling plan, a certain number of bias defect measurements are required to detect protracted diversions of nuclear material (the so-

called "trickle diversion" scenario). Moreover, bias defect measurements validate a larger number of less precise partial defect measurements (gamma NDA) that seek to detect missing material (e.g., uranium, U-235) in a cylinder. Simple calculations demonstrate that as plant capacity increases so do the number of required bias defect measurements. (This is also true of partial defect measurements, indicating significant increases in the safeguards resources required to verify declarations at large GCEPs. In fact, such increases may require either larger inspection teams or resident inspectors.) Bias defect measurements currently require collection of a material sample followed by shipment under chain of custody to the IAEA Seibersdorf Analytical Laboratory (SAL). Bias defect measurements of product assay are based on gas source mass spectrometer (GSMS) measurements on samples collected from process line taps in a small standard UF_6 sample cylinder. The requirement for bias defect measurements is 0.1 percent relative precision (LEU). Since DA involves physical collection of multi-gram gas samples followed by chain of custody shipping and laboratory analysis, the cost of each measurement, and the time required for analysis, is significant.

Another powerful safeguards verification tool is environmental sampling (ES) and analysis. The current practice of ES in GCEPs includes swipe sampling of surfaces in process areas and on occasion within the cascade halls during a low-frequency unannounced access (LFUA). Swipe samples are shipped by formal chain of custody to the SAL, where, depending on the type and number of samples, they are parsed, blinded and shipped to various laboratories in the Network of Analytical Laboratories (NWAL).

The IAEA evaluates the ES data (including SAL and NWAL reports) to determine whether particulate assays are fully consistent with facility declarations. Swipe samples are received at SAL or NWAL and processed in a Class 100 clean room. The ES particles are recovered from swipes by ashing, or physical removal using ultrasonication in solvent, or by hand using a vacuum impactor. The fusion track method is used to irradiate particles mounted on a Lexan plate in a reactor using thermal neutrons. Fissile particles produce damage tracks that are evaluated by a trained analyst. Particles of interest are selected and mounted onto a filament to produce ions for element identification and enrichment analysis using thermal ionization mass spectrometry (TIMS). Secondary ion mass spectrometry (SIMS) is also routinely used for measuring isotopic composition of ES particles. Both TIMS and SIMS analysis can achieve excellent relative abundance precision for micron and submicron diameter ES uranium particles, providing a certain indicator of facility misuse, but the process of collection, shipping, and analysis is self-limiting since it is expensive, time-consuming and resource-intensive.

Despite these well-thought-out safeguard ambitions, serious GCEP verification gaps remain. First, current safeguards activities do not permit direct and adequate verification of U-235 flows in and out of the enrichment process. This situation is unlikely to change without development of new safeguards technology and adoption of new safeguards approaches that enable a comprehensive and robust statistical mass accountancy sampling plan, while streamlining verification cost and workforce requirements. Another important factor is that misuse detection through ES typically requires several months between sample collections and analysis reporting. One potential means of GCEP misuse is undeclared production of high-enriched uranium (HEU). The goal for detection of undeclared HEU production is one month, therefore more timely approaches would be helpful.

The current paper explores the application of a new technology, called Laser Ablation, Absorbance Ratio Spectrometry (LAARS), to measure trace uranium aerosols emitted during GCEP operations and destructive analysis of cylinder samples to detect bias defect measurements required to affect the mass balance. This technology offers the promise of more timely and cost-efficient GCEP safeguards analysis.

Laser-induced Breakdown Spectroscopy, (LIBS)

Prior research in the area of laser isotope analysis includes Laser-induced Breakdown Spectroscopy (LIBS) and research conducted by Pacific Northwest National Laboratory (PNNL) based on laser ablation, followed by either laser-induced fluorescence or direct absorbance measurements. There are distinct differences between LIBS and LAARS that sets LAARS apart. Both techniques use a pulsed laser to create a laser-induced plasma. The laser pulse dissociates and ionizes solid and molecular components into a dense atomic plasma, which rapidly expands and cools to produce excited atomic constituents. LIBS measures characteristic atomic optical emission as these excited atoms make transitions to lower energy states. A high-resolution monochromator collects the emission spectra from the entire atomic ensemble. Individual emission lines can then be correlated to atomic elements assuming no overlapping emissions are present. LIBS has the advantage that little or no sample preparation is required (laser ablation atomizes the sample), analysis is near-real-time, the technique is sensitive (down to the level of parts-per-million), and it has the potential to measure isotopes in some cases. With an ultra-high resolution monochromator, LIBS has been used to determine the isotopic ratios of many elements, including uranium[1] and plutonium[2] through direct observation of atomic emission in a laser-induced plasma. However, LIBS isotope assay performance is subject to limitations of small isotope-shifts and large linewidths. For example Pietsch[1] observed a linewidth of 0.67 cm^{-1} (20.1 GHz) for uranium, yet the U-235:U-238 isotope shift was only 1.39 cm^{-1} (41.7 GHz). Smith[2] observed a linewidth of 0.19 cm^{-1} (5.7 GHz) for plutonium using a transition with one of the largest isotope shifts, namely 0.355 cm^{-1} (10.6 GHz) for Pu-239:Pu-240. Because the isotope shifts for uranium and plutonium are only roughly twice their emission linewidths, it is extraordinarily challenging to separately quantify the emissions of the two isotopes. Smith used a large two-meter double monochromator coupled to

an intensified CCD camera, with plutonium metal samples having a Pu-239:Pu-240 isotope ratio of 49/51, to produce clearly separated emissions (see Figure 2 in Reference 2). Unfortunately, when a more challenging and realistic isotope ratio (93/6) is measured, the minor isotope is barely distinguishable in the presence of the intense major isotope (see Figure 1 in Reference 2). In addition, significant emission signal averaging is required to generate each isotopic spectra (900 lasers shots for Pu and 20,000 for U). These results show promise, but also suggest that LIBS-based isotopic analysis may have limited dynamic range and poor performance when applied to non-metallic inhomogeneous samples, where intense atomic emission from non-target materials could dominate the spectral data.

Laser Ablation, Absorption Ratio Spectrometry (LAARS)

During the early 1990s, PNNL conceived of a new laser-based concept for uranium enrichment analysis. This program began out of a need for a field-portable, uranium-isotope analysis capability. In 1991, when the Gulf War ended, UN Resolution 687 required Iraq to "unconditionally accept under international supervision the destruction, removal, or rendering harmless of its weapons of mass destruction." This technology targeted the "lessons learned" during the attempt to implement UN Resolution 687 by providing to the UNSCOM inspection teams rapid, onsite identification and isotopic assay of uranium in milligram samples (e.g., dust, metal shavings). This early work forms the technical basis of our current technology. Over the past two decades, continuous technological advances in commercially available laser sources, optoelectronics, and microelectronics have enabled significant performance gains in this laser-based isotopic measurement technique and instrument designs that are robust, compact, precise and comparatively affordable.

In contrast to LIBS, LAARS uses the high spectral resolution and high brightness of a pair of probe lasers, which avoids the need for an ultra-high resolution monochromator, to probe the more abundant and longer lived ground state uranium atoms rather than short-lived excited states of uranium atoms. A simplified schematic of the LAARS experimental laboratory apparatus is shown in Figure 1. A miniature commercial pulsed Nd:YAG laser source is used to vaporize a pinpoint region of the sample, shown here mounted on a flat substrate. The sample chamber contains windows for the ablation laser beam and entrance and exit of the probe diode laser beams. LAARS samples are acquired as collected aerosol particles, swipes, or adsorbed UF_6 vapor, then loaded into the reduced-pressure sample chamber. Specific details of sample collection and conveyance to LAARS are given later in this paper. The vaporized sample (and substrate) material is ejected from the sample surface to form a high temperature (~50,000 K) plasma through interaction with the intense (~32 GW/cm^2) pulsed laser radiation. Laser vaporization of the sample serves two important functions. First the high-temperature plasma effectively dissociates and ionizes all molecular species of uranium into atomic components, regardless of their original composition. No further manipulation or chemical processing is required. The focused ablation laser spot size also defines the sampling spatial resolution and the subsequent stepwise scanning leads to high spatial resolution isotope analysis across the entire sample surface. This characteristic provides LAARS with the ability to detect and analyze trace assemblages of uranium particles intermixed in an ocean of background particles, as discussed further in the LAARS-ES section.

Shortly after vaporization, the plasma quickly (~ 1 µs) cools though supersonic expansion and more slowly (~10 µs) through conduction with the surrounding cover gas (argon, ~1,300 Pa) to form a ~3 mm diameter hemispherical plume containing neutral uranium atoms. Two wavelength-tunable diode lasers, having linewidths ~ 20 MHz, are directed through the plume of neutral uranium atoms and selectively probe (via precise wavelength tuning) the U-235 and U-238 isotopes in two different atomic transitions. Each laser beam is then directed to a compact photodetector that measures the transmitted laser intensity. Comparison of the intensity immediately prior to the ablation pulse with the intensity at the time of maximum atomic column density, typically 15 µs after the ablation pulse, yields a precise absorbance signal that is directly proportional to the atom concentration of each isotope. The measured absorbance signals are processed to provide the U-235 relative abundance determinations each time the ablation laser fires.

Under LAARS pressure and plasma measurement conditions, the isotope linewidths are nominally ~1 GHz FWHM and the U-235 isotope shift is ~20 GHz. The isotope shift is due to subtle differences in atomic energy levels that arise from differences in each isotope's nuclear mass, volume, and spin. Unlike LIBS, the narrow probe laser linewidths and large separation between probe wavelengths are distinctive to LAARS analysis, providing resilience to major-minor isotope channel crosstalk, which would otherwise skew the enrichment result.

A small vacuum pump maintains reduced pressure in the sample chamber under a low flow of argon cover gas. Optimum ablation plume conditions are obtained using a cover gas of 99.95 percent pure argon that contains the uranium atoms in a suitable volume, provides conductive cooling and flow to carry away sample outgassing and residual contamination from the laser ablation process. A system of optical components shapes and combines the output of the two probe lasers into a single, dual-wavelength beam and directs it through the ablation chamber. The laser light that passes through the plume exits the chamber, and the two laser wavelengths are separated using a small holographic diffraction grating. Each laser line is then directed to a compact photodetector that measures the transmitted laser intensity from which the enrichment can be determined for each ablation laser pulse. A wavemeter provides feedback for wavelength stabilization for both probe lasers with 10^{-7} relative accuracy, which is sufficient to lock each laser to the center of the

Figure 1. The basic components of the LAARS instrument, including a compact Nd:YAG laser, two external cavity diode lasers, the LAARS sample chamber, and the absorbance detectors

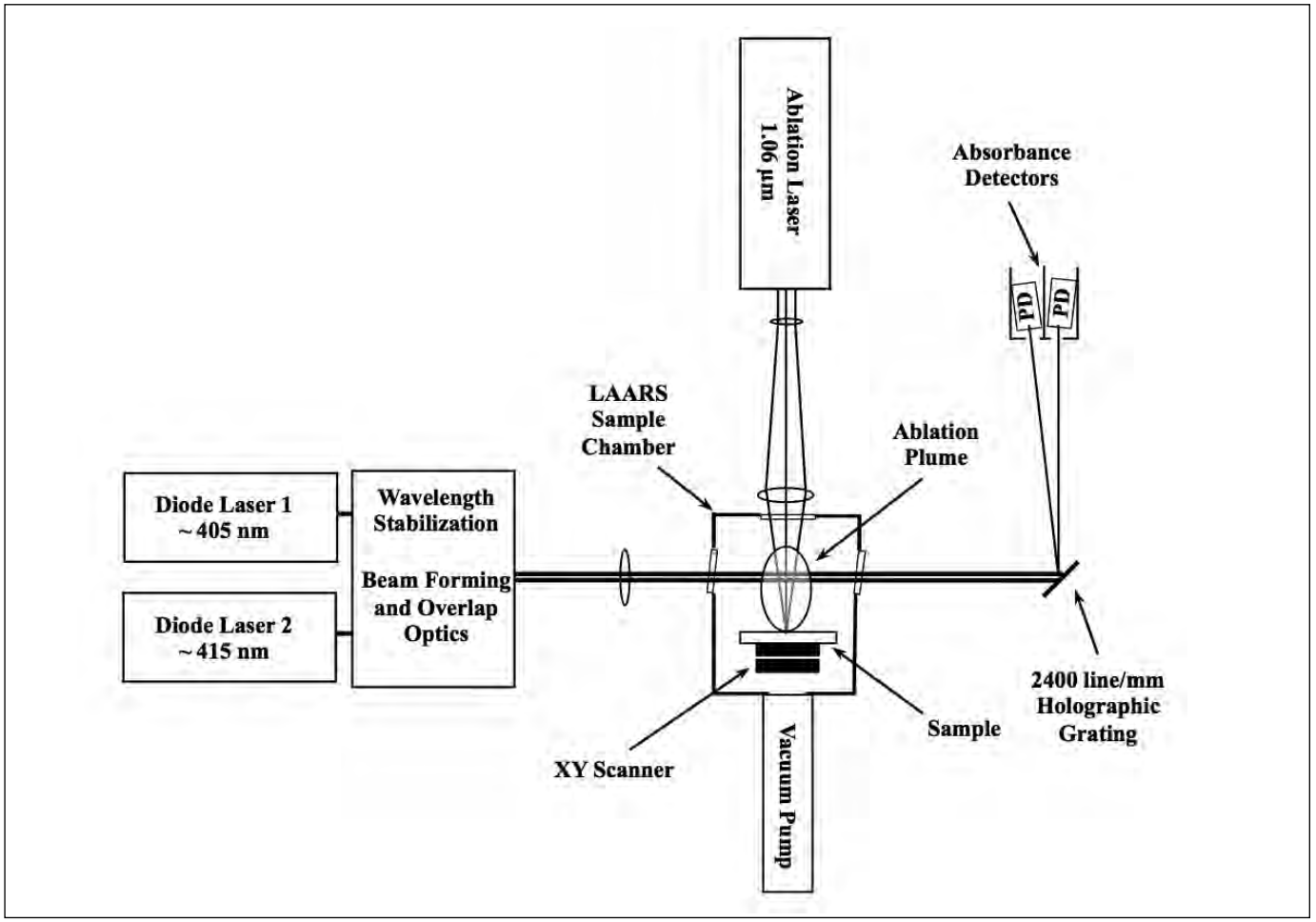

respective isotopic transitions. The sample substrate is mounted to a miniature XY translation system that scans the sample at the focal plane of the focused ablation laser. The laser pulse repetition is synchronized to the X-axis translation to sample a ~20 µm spot at ~30 µm step increments at 200 samples/sec. At this sampling rate, 120,000 discrete enrichment measurements can be completed in 10 min. Further details of LAARS operation are given in prior papers.[3-6]

GCEP Misuse Detection by LAARS-ES

IAEA ES and offsite laboratory analysis has been an effective GCEP misuse deterrence tool, providing assurances regarding the absence of uranium enrichment to undeclared levels. Unfortunately the timeliness to reach a safeguards conclusion could be improved, and this approach will be sustainable under the continued expansion of GCEP production capacity.

PNNL is developing a new GCEP safeguards technology that addresses these problems by conducting onsite ES and sample analysis using LAARS. Automated ES targets micron-size uranyl fluoride aerosol particulates produced during atmospheric hydrolysis of trace UF_6 process emissions. Emissions occur from minor leaks or maintenance within the cascade hall, process service area, and feed and withdrawal area. Continuous collection allows the acquisition of samples when and where they are generated (before loss or diffusion) and also provides the ability to timestamp and pre-concentrate samples prior to analysis. This approach also significantly relaxes the analysis detection sensitivity requirements and provides a pathway to enable onsite sample analysis.

The LAARS-ES aerosol collector is based on a rotating drum impactor (RDI). The RDI is a well-proven design, originally developed for remote long-term deployment to collect atmospheric particles for atmospheric science interests, such as global climate change.[8] The onsite LAARS-ES concept is based on an integration of the RDI aerosol collector and the LAARS uranium enrichment instrument, and is shown conceptually in Figure 2.

Figure 2. A cross-section view of the integrated LAARS-ES instrument

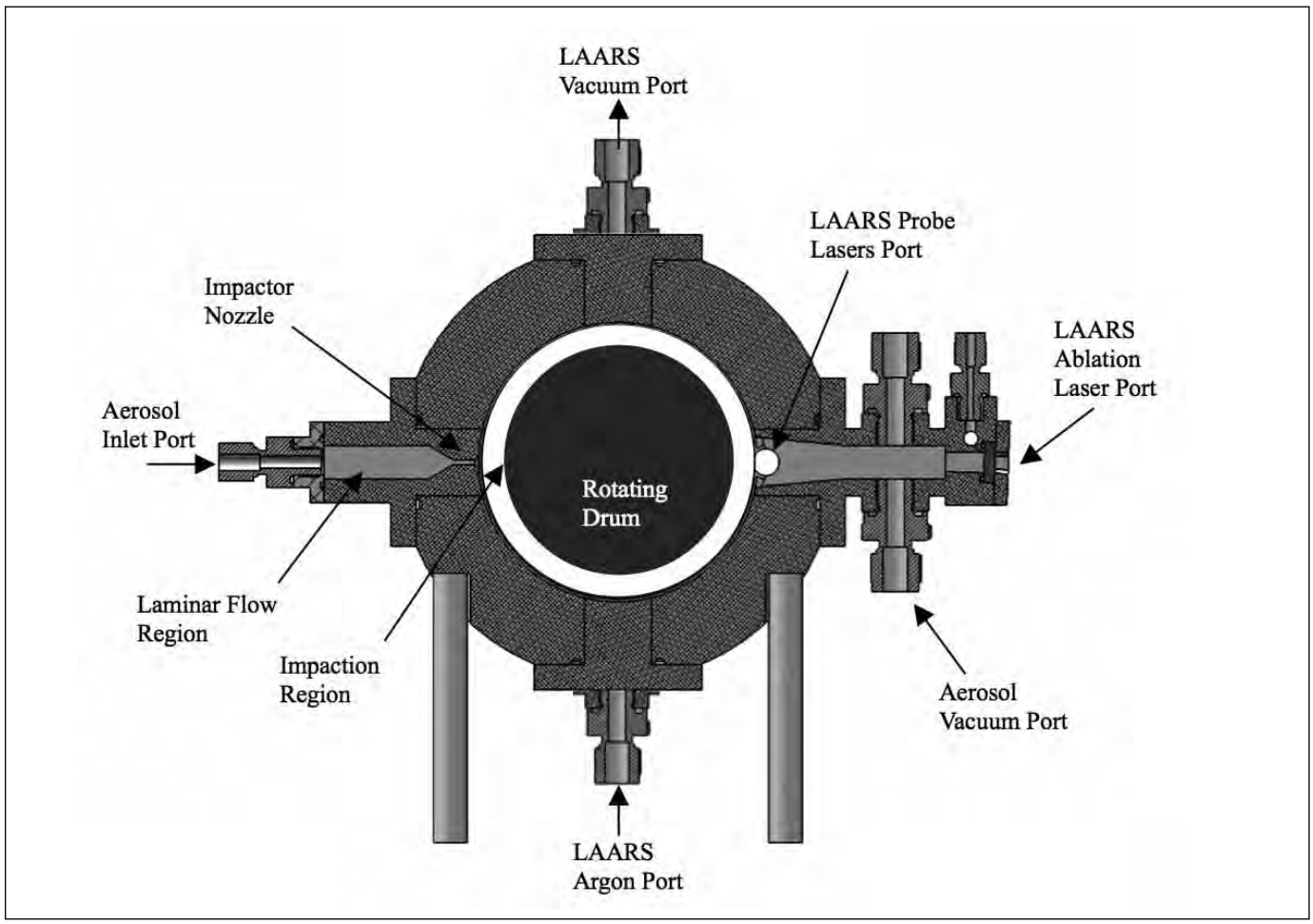

Referring to Figure 2, an aerosol sampling tube connects the Aerosol Inlet Port to a remote ES inlet located at a likely gaseous UF_6 emission point, such as the GCEP feed or withdraw station. An external vacuum pump is connected to the Aerosol Vacuum Port and serves to draw aerosols from the remote ES inlet, through the sampling tube, where they are collected by impaction onto the rotating drum. Smaller particles, below the particle size cutoff, will not have enough inertia to strike the impaction surface, but rather follow the airflow around the drum surface to be exhausted from the collection system. The particle size distribution captured by impaction is determined by the flow rate through the RDI and by the Impactor Nozzle width and the gap between the rotating drum and RDI internal sidewall. Computational fluid dynamics simulations were used to evaluate the interdependencies of these parameters and are described in detail in a prior paper.[6] The design was optimized to collect expected particle size distributions resulting from a fugitive UF_6 release. The uranyl fluoride aerosol size distribution is principally driven by the ambient relative humidity.[9] Individual particles are generally formed as roughly spherical 100 nm diameter elements and tend to agglomerate to several microns in diameter. Not shown in the design is a cyclone extractor to remove larger background aerosols just prior to the RDI Aerosol Inlet Port.

Under automated operation, the system collects airborne particles for a preset time interval, at which point the drum rotates to expose a new rectangular strip on the drum. A drum having a modest diameter and length could provide time-resolved particle sampling and integration on a daily or weekly basis over a period of one year. The drum could also be segmented along the axial dimension to separate the collected samples into three equivalent regions, one each for the onsite LAARS measurement, for offsite analytical laboratory analysis, and for host state confirmation if required.

After a prescribed ES integration period (e.g., day, week), ES is paused and the sample chamber is evacuated and then backfilled to ~1,300 Pa with argon. The rectangular impaction strip is raster scanned using LAARS to detect and analyze the spatial distribution for enriched uranium particles. The drum is

Figure 3. Measurement of Gd-152 isotopic abundance in micron-sized particles of $GdCl_3$. The particle spatial distribution map is shown for an 8 mm by 10 mm LAARS scan. The zoomed area (1 mm^2) shows individual particles of natural and low enriched Gd-152. The Gd-152 relative abundance plots show the distributions before and after spiking with 43 percent enriched Gd-152.

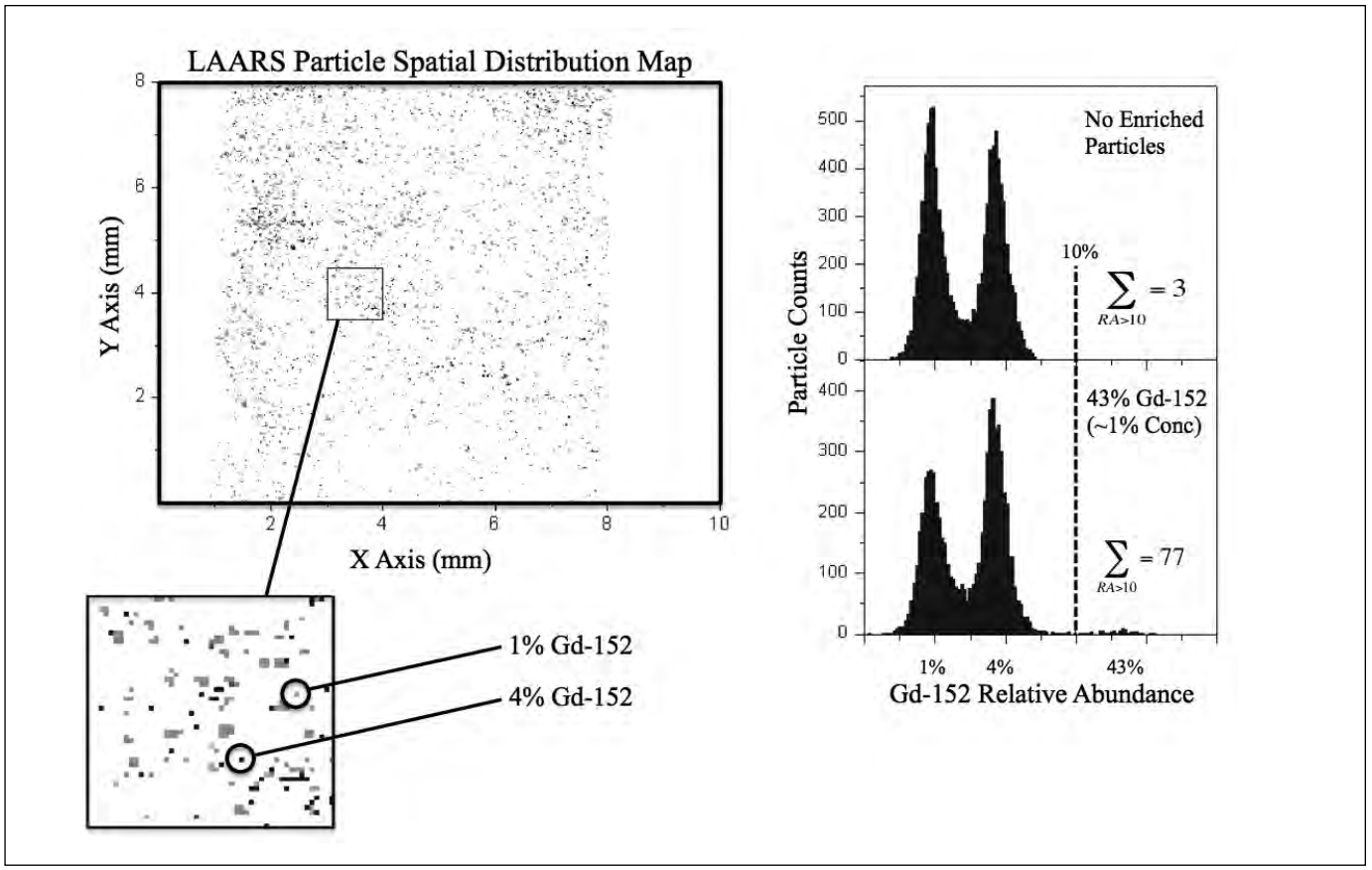

rotated one measurement resolution unit (typically 1 to 4 ablation laser spot diameters) and the next line is scanned. This process is repeated until the entire impaction strip is analyzed. Within ten to twenty minutes, the entire impaction strip is scanned and the U-235 abundance distribution is determined. The sample chamber is then returned to atmospheric pressure to begin the next ES cycle.

The LAARS-ES concept is predicated on the ability to detect and assay enrichment on trace uranium aerosol particles mixed in a large excess of background aerosols (e.g., dust, minerals). Prior LAARS feasibility studies were conducted using Gadolinium isotopes to study this question. Gd-160 and Gd-152 isotopes served as analogs for U-238 and U-235. Isotopically enriched $GdCl_3$ particles were prepared with relative abundances 1 percent, 4 percent, and 43 percent, serving as natural, low-enriched uranium, and highly enriched uranium enriched simulants. The particles were ground and sieved to 5 µm. A sample was prepared containing an approximately 1:1 mix of 1 percent and 4 percent enriched Gd-152. A sparse sample quantity was sprinkled onto a substrate covered with double-sided tape, then measured by LAARS. The particle spatial distribution map is shown in Figure 3. The zoom area shows single particles assayed at 1 percent and 4 percent G-152 enrichment. The Gd-152 relative abundance distribution is shown in the upper right figure, plotted as a function of particle counts. Only three particles, exceeding the absorbance discriminator threshold, were detected above the 10 percent enrichment level. The same sample was then spiked with 43 percent enriched Gd-152 at 1 percent concentration to simulate trace HEU entrained in GCEP background aerosol samples. The sample was measured by LAARS and the Gd-152 relative distribution is shown in the lower right figure. This time seventy-seven particles were detected above the 10 percent enrichment level, demonstrating the feasibility of LAARS to detect trace HEU particles in a distribution of lower-enriched (i.e., *declared*) particles. Follow-on studies were conducted to assess LAARS false alarm probability and performance with heavily loaded soil particles sample, and are summarized in a number of prior papers.[3-6]

Current LAARS-ES studies are underway using prepared uranium particle samples. This study evaluated the effects of heavy sample loading and particle retention on the surface of the substrate. The motivation of the study is two-fold. First, high

Figure 4. A study of uranium particle sample preparation in grease. The U-235 abundance distribution for sample #1 shows a broad and poorly defined abundance peak (left). A large non-resonant absorption peak is seen near 65 percent, as well as significant non-valid absorbance signal above the discriminator. Sample #2 produced a sharp, well-defined abundance peak, with a small residual absorbance tail at higher abundances (right).

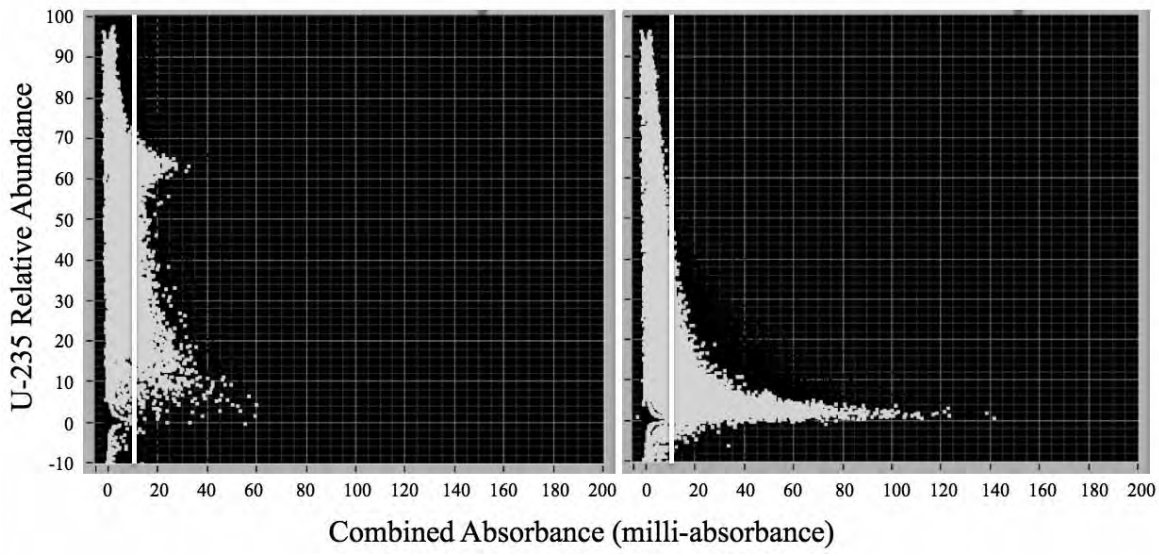

particle loading has the potential to liberate particles around the ablation region, due to the shock wave produced during the vaporization process. These particles can cross the laser probe beams during the absorbance sampling time to produce undesirable non-resonant absorbance interference signals. Non-resonant events produce absorbance (scaled by the relative transition strengths) on both isotope channels and are manifested as a false distribution near 65 percent relative abundance. Our second motivation is to evaluate the effects of impactor drum surface preparation. Prior literature reports have demonstrated that Apiezon grease was effective at minimizing particle bounce during impaction[10] and our prior LAARS studies have shown that this grease has no effect on the enrichment measurement. Therefore we plan to use a greased impactor drum to minimize particle loss during impaction, as well as maximize the particle loading during long ES integration periods.

Natural UO_3 powders with a mean particle distribution of 10 microns were prepared on 25 mm diameter glassy carbon (same material as the impactor drum) planchet. The surface of the planchet was roughened using 360 grit sandpaper to approximate the machined impactor drum surface finish. Two samples were prepared with different grease application steps. The first sample used a thin layer of grease applied to the entire surface. A single-sided razor blade was used to smooth the grease into a roughly uniform film. The UO_3 powder was suspended in a carrier solution of deionized water (10 mg/ml) with a drop of surfactant (soap) to minimize particle agglomeration. Sample #1 contained approximately 850 µg total uranium mass (244 µg/cm^2). This high concentration represented a heavy loading, as expected during long ES integration. The solution was pipetted across the surface of the grease layer and then allowed to dry. A sheet of wax paper was placed on top of the substrate and a small roller was used to press the particles into the grease to simulate particle impaction. The wax paper was removed and the sample was then measured by LAARS. Sample #2 was prepared with the same UO_3 solution. This time the grease was applied using a cotton-tipped applicator and then wiped using a lens tissue, leaving a very thin grease film on the substrate surface. The sample solution was applied at a similar areal concentration onto the grease layer. The particle solution was air dried, then pressed into the thin grease layer using wax paper.

The LAARS U-235 relative abundance distributions for these samples are plotted as a function of the combined U-235 and U-238 absorbance, as shown in Figure 4. The vertical line near 10 milli-absorbance is a typical discriminator threshold used to reject the zero-point absorption distribution from subsequent enrichment analysis.[3] Sample #1 had 3,820 particles detected (out of 24,500 total measurements) and Sample #2 had 2,821 particles detected (out of 12,500 total measurements) above the discriminator set point. It is readily apparent that the natural abundance peak is broad and poorly defined in Sample #1 (Figure 4, left). Also present is a peak located at near 65 percent abundance that likely corresponds mostly to non-resonant absorption of non-vaporized grease material and some uranium particles. Significant absorbance is seen above the discriminator level at abundances up to 70 percent. Clearly this sample

Figure 5. Conceptual LAARS-DA gaseous UF_6 sampling device

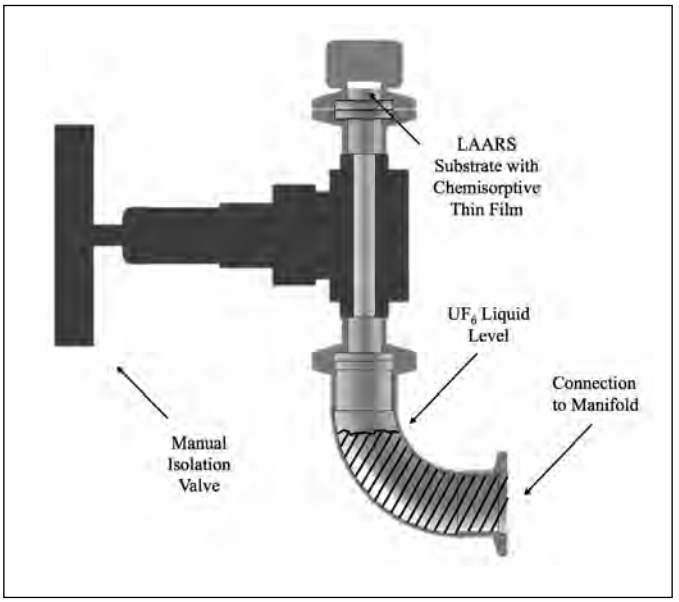

preparation method produces poor peak characteristics and target particle loss to a non-vaporization process. In contrast, LAARS analysis of Sample #2 produced a sharp abundance peak centered near 0.7 percent (Figure 4, Right). A tailing absorbance signal is present that extends to the zero-point, but the non-resonant peak is absent. The tailing absorbance mechanism is currently under investigation and may be due to systematic measurement factors; nevertheless these initial LAARS-ES studies of heavy-loaded uranium particle samples are very encouraging. Future studies include LAARS analysis on prepared particle samples containing mixed natural, LEU, and trace HEU and uranium particles entrained in heavy soil loadings.

GCEP Bias Defect Detection by LAARS-DA

The IAEA safeguards approach for gaseous centrifuge enrichment plants includes measurements of gross, partial, and bias defects in a statistical sampling plan. These safeguard methods consist principally of mass and enrichment NDA verification. DA samples are collected from a limited number of cylinders to quantify bias defects in the GCEP material balance. Under current safeguards measures, the inspector requests a DA sample from a particular cylinder, most frequently a product cylinder. In this case, the operator places a filled 30B product cylinder in a liquid sampling autoclave. Typically, the autoclave will have an internal sampling manifold with electric control valves and connections to the cylinder and sampling bottle. IAEA DA samples are collected in a 2926 UF_6 sample bottle. The autoclave is heated to 70°C and the contents of the cylinder are homogenized for about sixteen hours, at which point the sampling process is initiated. The autoclave is tilted to fill the sampling manifold with liquid UF_6. The 30B cylinder manifold electric valve is closed and the autoclave is returned to the horizontal position. Next the sample bottle connection electric valve is opened to collect the sample in the bottle. The valve is then closed and the autoclave is cooled to room temperature. The autoclave is vented, opened, and the bottle removed following manual bottle valve closure and connection line venting. The sample bottle is then transferred to IAEA custody.

Bias defect detection requires high-precision U-235 abundance analysis (±0.05 percent concentration RSU, ±0.10 percent abundance RSU)[11] and currently requires offsite mass spectrometer analysis. Safe radioactive material handling and transportation procedures are required since the 2926 sample bottle typically contains >500 mg of U-235 (10-20g total uranium) at low enrichment. The sample bottles are packaged and tamper-sealed in an approved shipping container such as a 3913A shipping drum, then stored onsite in an IAEA secure area until they are shipped to SAL. The current practice is expensive and resource-intensive, effectively limiting IAEA's ability to implement a comprehensive statistical sampling plan.

PNNL is proposing a new GCEP safeguards concept, called LAARS-DA, which addresses this bottleneck by conducting onsite UF_6 DA measurements to rapidly and accurately detect enrichment bias defects. UF_6 cylinder samples are collected using the current liquid sampling autoclave, but LAARS-DA sampling and analysis is distinguished by several important advantages. First LAARS-DA sampling acquires gaseous UF_6 samples instead of liquid. To accommodate sampling, a custom LAARS-DA sampling device, shown schematically in Figure 5, is attached to the manifold sample bottle connection. The same steps described above are used to collect a DA sample from the cylinder. The LAARS-DA sampler is positioned above the manifold liquid level. A chemisorption process in a thin film layer (e.g., NaF) collects UF_6 vapor in equilibrium with the liquid in the manifold. In this case, only a few micrograms of UF_6 is adsorbed and collected as a LAARS-DA sample. After the autoclave is cooled and the sample removed, the sampling device is attached to an onsite LAARS-DA instrument. Enrichment analysis is determined in a matter of minutes at sufficient accuracy to support reliable bias defect measurements, while greatly reducing DA sample volume, analysis time, and cost.

LAARS-DA feasibility measurements were conducted on samples that simulated adsorbed UF_6 collected by the LAARS-DA sampling concept. Natural (0.72 percent) and certified LEU (2.423(1) percent) uranium samples were dissolved in nitric acid and applied to a carbon planchet to form two dried side-by-side elongated residue regions. Each residue region contained approximately 2 µg of total uranium. The sample was spatially characterized using LAARS. At each LAARS residue measurement point, between 40 to 150 fg of U-235 is vaporized per ablation laser shot, depending on the sample enrichment. The LAARS measurement data is post-analyzed to produce a histogram of all U-235 abundance measurement points that exceed an absorbance discriminator value of 20 milli-absorbance. The U-235 relative

Figure 6. LAARS post-analysis showing the binned U-235 relative abundance data and the Lorenztian fit to the peaks

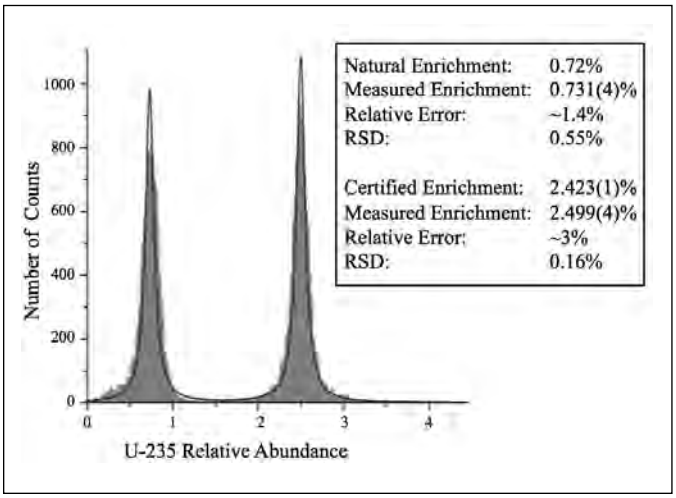

abundance distributions of both residues are shown in Figure 6. The solid lines are the Lorenztian fits to the peaks and the analysis results are tabulated in the boxed inset. The abundance uncertainty of the natural uranium was unknown, so the relative mean error (1.4 percent) is reported against the sample inventory value (0.72 percent). The natural uranium abundance distribution had a 0.55 percent relative standard deviation (RSD). Analysis of the certified LEU residue produced a larger relative mean error (3 percent), but a smaller RSD (0.16 percent). RSD should decrease as the enrichment increases to 50 percent, since more minor isotope atoms are interacting with the probe laser, resulting in a larger absorbance signal above the noise level.

The LAARS-DA study demonstrated the feasibility of this concept. The abundance uncertainty is within a factor of 1.6 of meeting the bias defect measurement requirement, and it is reasonable to project LAARS performance improvements that allow LAARS-DA to reach this target. We also plan to integrate a uranium calibration standard that is measured for each LAARS scan row to provide continuous calibration (to minimize the large relative mean error) of the unknown sample U-235 abundance value.

Conclusions

The PNNL-developed LAARS safeguards verification technology enables new methods for onsite GCEP misuse and bias defect detection. Feasibility studies have demonstrated LAARS-ES ability to detect and accurately assay rare uranium particles, generated during UF_6 emissions, entrained in predominately background nuisance dust and other materials. The LAARS rotating drum impactor represents an integrated solution to combine the unique particle analysis capabilities of LAARS with an onsite ES system that continuously acquires uranium aerosols when and where they are generated before loss or diffusion within the GCEP. The LAARS-DA concept was introduced as a viable option for bias defect detection. LAARS-DA sampling is conducted within the framework of existing sampling procedures familiar with the operator and sidesteps the cost and operational limitations associated with offsite analysis. LAARS-DA feasibility studies demonstrated enrichment measurements having ~0.16 percent relative precision on microgram quantities of uranium, which is within a factor of 1.6 of meeting the bias defect measurement accuracy requirement.

Current LAARS-ES uranium particle studies are underway, as well as the evaluation of the rotating drum impactor performance. LAARS-DA measurements on adsorbed UF_6 are also in progress, in conjunction with the design of a prototype LAARS-DA sampler. Planned future work includes design of an onsite LAARS-ES instrument, followed by field trials. The LAARS-DA sampler design will be characterized, calibration methods evaluated, and adsorbing films developed that provide efficient and stable UF_6 uptake.

Acknowledgements

Pacific Northwest National Laboratory is operated for the U.S. Department of Energy by Battelle Memorial Institute under Contract No. DE-AC05-76RL01830. This work was performed under a PNNL Laboratory Directed Research and Development Program and also supported by the Next Generation Safeguards Initiative (NGSI), Office of Nonproliferation and International Security, National Nuclear Security Administration. Thanks especially to PNNL staff Matthew O'Hara and Jennifer Carter for LAARS sample preparation.

References

1. Pietsch W., A. Petit, and A. Briand. 1998. Isotope ratio determination of uranium by Optical Emission Spectroscopy on a Laser-produced Plasma—Basic Investigations and Analytical Results, *Spectrochimica Acta Part B: Atomic Spectroscopy*, 53, no. 5, 29: 751-761.
2. Smith, C. A., et. al. 2002. Pu-239/Pu-240 Isotope Ratios Determined Using High Resolution Emission Spectroscopy in a Laser-induced Plasma, S*pectrochimica Acta Part B: Atomic Spectroscopy*, 57, no. 5: 929-937.
3. Bushaw, B. A., and N. C. Anheier. 2009. Isotope Ratio Analysis on Micron-Sized Particles in Complex Matrices by Laser Ablation – Absorption Ratio Spectrometry, *Spectrochimica Acta Part B: Atomic Spectroscopy*, 64, no. 11-12: 1259-1265.
4. Anheier, N. C. Jr, and B. A. Bushaw. 2009. Isotope Enrichment Detection by Laser Ablation—Dual Tunable Diode Laser Absorption Spectrometry, *Proceedings of the Institute of Nuclear Materials Management 50th Annual Meeting*

5. Anheier, N. C., and B. A. Bushaw. "Unattended Monitoring of HEU Production in Gaseous 2010. Centrifuge Enrichment Plants Using Automated Aerosol Collection and Laser-based Enrichment Assay, *Proceedings of the Institute of Nuclear Materials Management 51st Annual Meeting*.
6. Anheier , N. C., J. T. Munley, and L. M. Alexander. 2011. Design of an Unattended Environmental Aerosol Sampling and Analysis System for Gaseous Centrifuge Enrichment Plants, *Proceedings of the Institute of Nuclear Materials Management 52nd Annual Meeting*.
7. Bush W., et. al. 2001. IAEA Experience with Environmental Sampling at Gas Centrifuge Enrichment Plants in the European Union. IAEA-SM-367/10/04, *Proceedings of the Symposium on International Safeguards, Verification and Nuclear Material Security*.
8. Vanderpool, R. W., D. A. Lundgren, and P. E. Kerch. 1990. Design and Calibration of an In-Stack Low-Pressure Impactor, *Aerosol Science and Technology*, 12, no. 2: 215-224.
9. Bostick, W. D., W. H. McCulla, and P. W Pickrell. 1985. Sampling, characterization, and remote sensing of aerosols formed in the atmospheric hydrolysis of uranium hexafluoride, *Journal of Environmental Science and Health, Part A*, 20, no. 3, (1985): 369-393.
9. Bench, G., et. al. 2002. The Use of STIM and PESA to Measure Profiles of Aerosol Mass and Hydrogen Content Respectively, Across Mylar Rotating Drums Impactors Samples, *Aerosol Science and Technology*, 36: 642-651.
10. Aigner, H., et. al. 2002. International Target Values 2000 for Measurement Uncertainties in Safeguarding Nuclear Materials, *ESARDA Bulletin*, no. 31: 39-68.
11. Aigner, H., et al. 2002. International Target Value for Measurement Uncertainties in Safeguarding Nuclear Materials, *ESARDA Bulletin,* No. 31; 39-68

Development of Micro-fluidics Lab on Chip Concept for Verification of Pu in Aqueous Process

Adrián E. Méndez-Torres and Poh-Sang Lam
Savannah River National Laboratory, Aiken South Carolina USA

Abstract

A continuing challenge to the analytical community is the quantification of the concentrations of compounds, elements, and isotopes at ultra-trace levels in the presence of huge quantities of competing species. Nuclear material processing, waste remediation, and nuclear nonproliferation applications all need this capability. Recent progress in micro-fluidics, nanofabrication, and far field nanoscopic velocimetry[1] have provided the underlying science foundations for developing a high-fidelity nanoscale Lab-on-a-Chip[2,3] sensors for the detection of ions and radionuclides. Understanding the science and technology of nanofluidics and nanofabrication would provide for sensor devices with ultra-high sensitivity, selectivity, and low cost. Savannah River National Laboratory (SRNL) in collaboration with the University of South Carolina (USC) is developing a program for fluidic sensors with the objectives of applying novel concepts based on electrokinetics and electrophoresis principles to develop a high sensitive detection system based on nanofluidics. The fundamental of the science of micro-to-nano fluidics based measurement techniques provides an opportunity to precisely control experimental condition for fast assay with unprecedented experimental capability for exploration in sensor technology. Microfluidic systems enable parallel operation for multiple assays with small amounts of samples and can be employed for sample pre-concentration (up to 10^6-10^8 fold) allowing detection of trace quantities of ions or materials, such as verification of trace Pu in aqueous system. The proposed concept can be applied to the measurement of special nuclear materials (SNM) in aqueous solutions, for example, during advanced fuel-cycle reprocessing or mixed oxide fuel plutonium purification (aqueous polishing). The ability to verify the SNM content on aqueous processes will enhance material accountability and verification technology.

This paper is intended to identify and highlight the present state of research in the nanofluidics field and discusses possible direction of development with focus in safeguard needs. A description of nanofluidic field and example of applicability in areas of safeguards are highlighted.

Introduction

With invention and wide availability of many new technological tools like AFM, STM, and micro-to-nano probes both for the inspection and creation of nanostructures, the electron, x beam and ion beam lithography, and the development of new micro-machining techniques with bottom-up assembly methods have made the study and application of nanofluidics more accessible.[4] This technological advance allows a previously unknown measure of control down to the nanoscale. Microfluidics devices promise to allow a broad range of chemical analysis and macromolecule separation using small sample volumes in compact low cost, and easily manufacturing devices.[5-7] Due to its high sensitivity and selectivity, expectations of applicability in the area of verification and safeguards technology are high.

The increase in size and complexity of modern nuclear facilities, and the predicted increase of states that will pursue nuclear energy as an energy resource will increase the load and difficulty of verification of nuclear activities by international agencies such as International Atomic Energy Agency (IAEA). The IAEA has established international safeguards standards for fissionable material at spent fuel reprocessing plants to ensure that significant quantities of special nuclear material (SNM) are not diverted from these facilities. There are a total of 159 planned new nuclear reactors and there are at least fifty countries building, operating or considering nuclear power as part of their energy mix. About half of these countries are newcomers to nuclear. There are more than sixty nuclear plants under construction, mainly in China, Russia, India, and South Korea, as reported by the World Energy Council (WEC). This situation will exacerbate the increased accumulation of non-separated plutonium in used nuclear fuel. The verification of Pu in used fuel and its disposition will increase the need to strengthen verification activities at the back end of the nuclear fuel cycle.

Currently, methods to verify material control and accountancy (MC&A) at these facilities require time-consuming and resource-intensive destructive assay (DA). Traditional DA methods such as isotope dilution mass spectroscopy (IDMS) are being employed for the accountability measurements of nuclear materials in spent fuel reprocessing plants. However, this method involves tedious procedures and requires highly skilled operators to separate analyte from complicated matrices such as waste solutions. It is large in size and expensive. Advancing the safeguards state-of-the-art requires advanced instrumentation

and monitoring systems for existing and new modern facilities. Innovative sensor technology can provide rapid analysis of small samples, and verification of possible diversion methods. Some of the challenges for verification of SNM in aqueous processes such as the aqueous polishing process for Pu purification include the determination of Pu for safeguards and materials control and accountancy purpose and the assurance of no diversion of material.

Micro and Nanofluidics

Micro and nanofluidics encompasses science and technologies that involve a fluid flowing in a system with at least one dimension in the scale of 100μm to 1nm[8] and it is a multidisciplinary field comprised of physics, chemistry, engineering, and biotechnology. Micro and nanofluidics have been investigated for applications in drug delivery and its control, DNA and biomolecular sensing, protein manipulation, and the manufacture of laboratories on a microchip (lab-on-a-chip). In this paper possible applications to safeguards are highlighted. One of the many advantages of microfluidics devices is from its feasibility to be integrated with electronic circuitry. Using mature electronic manufacturing technology it is possible to design nanofluidics systems, such as LOC with digital integrated circuit in a single chip. Therefore, the control and manipulation of particles in the electrolyte can be achieved in almost real-time.[9] In addition, low cost rapid fabrication techniques using paper base-microfluidics[10] devices are promising as low cost disposable sensing device.

The development of microfluidic technology has been stimulated by an assortment of fundamental features that accompany system miniaturization. These features include the ability to process and handle small volumes of fluid, enhanced analytical performance when compared to macro scale systems, low unit cost, small device footprints, facile process integration and automation, and high analytical throughput. In a broad sense the field of nanofluidics exploit certain unusual physical, material science, and chemistry at the nano scale[11] that do not exist at larger length scales,[12] e.g., Debye length. The transition from laboratory-science to real-live applications demands a better understanding of micro/nano scale fluid flow and particle transport phenomena. As dimensions shrink, the effective driving and dominating forces change radically. Conventional forces resulting from pressure, inertia, viscosity or gravity that usually plays the dominant role in macroscopic flows may not be practical in micro/nanofluidic systems while forces at interfaces such as surface tension become more important due to the increasing ratio of interfacial area and volume.[13]

In the area of sensors micro fluidics devices, such as LOC, take advantage of physical phenomena at the micro-to-nano scale such as electrokinetics, electrophoresis, and electric double layer (EDL). Electrokinetic phenomena refer to electro osmosis, electrophoresis, streaming potential, and sedimentation potential,

Figure 1. Representative fluid and ion dynamic in a micro capillary channel. Insertion of electrodes upstream and downstream will induce bulk fluid motion. On application of a tangential electric field in a capillary channel with a charged surface, the excess counter-ions that are present in the diffuse layer migrate toward the cathode, thus producing an electrokinetic slip velocity at the slip plane, which, in turn drags the liquid in the bulk along with it to produce a flat liquid velocity profile.[14]

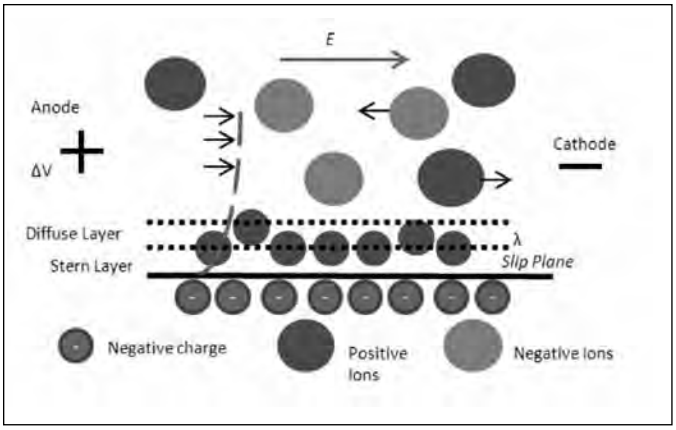

which are phenomena due to the interaction of the diffuse double layer and an applied electric field generally observed in porous medium or colloidal systems.[13] Electrokinetics plays a critical role for analyte separation as well as the manipulation and control of the fluid flow in micro/nanofluidic devices and is a convenient method to move materials, such as water, ions, and particles, in miniature systems for fast, high-resolution and low-cost analysis and synthesis. For example, a relatively low imposed electric field can generate significant volume flow rates which cannot be achieved using the conventional pressure-driven flow. Electrophoresis is defined as the relative motion of charged particles under an electric field and can involve the motion of ions of polar molecules. Streaming potential is the potential induced by the movement of the fluid. Sedimentation potential is the potential related to the motion of particle through a stationary liquid, also known as the *Dorn effect.* Under an electric field the flow near the wall will move under such a body force and thus generate a bulk fluid movement through the channel named electro osmotic flow (EOF) or electro osmosis. In immediate contact with the channel surface, there is a layer of cations strongly bound to the wall, called the Stern layer, as shown in figure 1. Outside the Stern layer, there is another layer where the cations are mobile called the diffuse layer. In these two layers, the surface potential significantly influences on the ion distribution and these two layers are usually termed the electric double layers (EDL). Away from the wall, the bulk of the solution remains electrically neutral. In the EDL a charged surface creates a concentration polarization as counter ions and co-ions in an electrolyte solution area attracted to or repelled away from it, respectively, thus resulting in a redistribution of ions near the surface. The redistribution creates a region adjacent to the surface

also known as the Debye layer. Under the EDL, the ions are assumed to be mobile; they can carry a current and can impart momentum on the water molecules to produce net flow. The bulk liquids flow that occurs when the diffuse part of the double layer slips over a charged surface in response to an applied electric field is the origin of all double layer electrokinetic phenomena. When electrodes are placed at the ends of a channel the cations are attracted to the cathode and the anions are attracted to the anode. In the bulk flow away from the walls, the concentration of cations and anions are the same and so the electric body force will balance. But in the EDLs, they are not the same and so there is a body force acting on the flow in the EDLs.

Multiphysics Modeling

Numerical analysis is used to determine the optimal micro/nano channel design and the experimental parameters such that the example ions (Pu) can be separated or pre-concentrated by utilizing the EDL characteristics. As an exploratory study, a two-dimensional finite element model of a channel with 10nm in diameter and 60nm was created. The finite element mesh must be highly refined near the channel wall and is capable of resolving the EDL effects. It was assumed that the Pu salt has been dissolved in water and filled through the channel. In this study, two types of fluid are used: 1) Case 1: [Pu+3]•[X-1]3, and 2) Case 2: [Pu+3]•[Y-3]. The channel wall is chemically treated and contains positive charges in order to create a negatively charged Stern layer and a mostly negative charged diffuse layer. As an electric potential is applied to the two ends of the channel, the mobile negative ions in the diffuse layer are attracted to the anode, resulting in a laminar flow of the bulk fluid moving in that direction.

This problem involved three physics, namely, 1) electrostatics (Gauss Law), 2) transport (Nernst-Plank equation), and 3) laminar flow (Navier-Stokes equation). These equations are highly nonlinear and are coupled. The multiphysics finite element program COMSOL[22] with Chemical Reaction Engineering Module and Microfluidics Module are used. Typical solutions are shown in Figures 2 and 3. All the preliminary calculations used the same finite element mesh and ion species, the electric surface charge density on the channel wall was fixed, and the initial concentrations and valences depend on the type of electrolyte. The effects being evaluated are the electric potential applied to the two ends of the channel. As Figures 2 and 3 show, the Pu ions are concentrated near the anodes as the applied voltage increases. This indicates that the separation of the ions can be achieved by varying the applied electric field if the channel size is limited due to fabrication difficulty or commercial availability.

Applications for Verification and Safeguards

In the area of used nuclear fuel, microfluidics system or LOCs have been employed for microscale solvent extraction intended for sample pretreatment or small-scale production purposes.[14-16] Microfluidic systems are especially suitable for solvent extraction studies with used nuclear fuel because the small volumes require minimizing exposure of laboratory personnel to radioactive solutions and reducing the high cost associated with handling and disposing of radioactive waste. Microfluidic devices have also been demonstrated for micro scale solvent extraction intended for sample pretreatment or small-scale production purposes.

As an example, the effect of the negative electric field generated by the EDL in the transverse direction on negatively charged ions and molecules within the fluid can be employed for sample preconcentration. This technique has been used successfully for preconcentration of proteins and peptides.[2] Such a preconcentration enables detection of extremely small analyte concentration in the sample that can be important for SNM verification in aqueous media. In negatively charged channels, the interactions between a negatively charged analyte and the channel walls can pinch the analyte in the transverse center region of the nanochannel. This effect gives rise to higher velocities for the negatively charged analyte due to a parabolic velocity distribution in the nanochannel, and may be exploited for new applications such as chiral separations and accelerated analyte preconcentration. Since the nanochannel itself can exert a physical constraint on single molecules and ions, the technique could prove viable for fast radionuclide detection at a low cost.

Selectivity of ions by speciation is also possible. The excess charges on the channel wall result in perm selectivity. The nanochannel rejects ions of the same charge (co-ions) while letting ions of the opposite charge (counter-ion) go through. This ions selective phenomenon can be used to integrate filtration or concentration functions (such as Pu ions). As the surface charge determines the ion transport in nanochannels, tailoring the surface chemistry allows for direct control of ionic transport characteristics. Monitoring the ion conductivity can be used as a method to detect adsorption of molecules on the walls of nanochannels. This can be employed as a simple method to confirm or deny the presence of an ion of interest in a solution. By exploring the recently discovered phenomenon—charge exclusion-based nanoseparation,[17] as demonstrated in previous simulations,[18-19] the protruding and overlapping electric double layers (EDL) can be employed to trap and concentrate the analytes at the entrance of a nanochannel array. The preconcentrated analyte can be used further for downstream electrophoreses separation for specificity detection. Since Pu liquid exists in ion form, and is positively charged, the surface of the nanochannel can be treated so that the surface charge of the channel array will be positive (as calculated in Figures 2 and 3). In this case, the nanochannel can preconcentrate Pu at the entrance of the nanochannel array.

In the area of detection, previously investigated optical spectroscopy with nanoscale spatial resolution can be employed. For example at the University of South Carolina a far-field

Figure 2. The applied voltage and the corresponding concentration profile for solution $[Pu^{+3}] \bullet [X^{-1}]_3$.

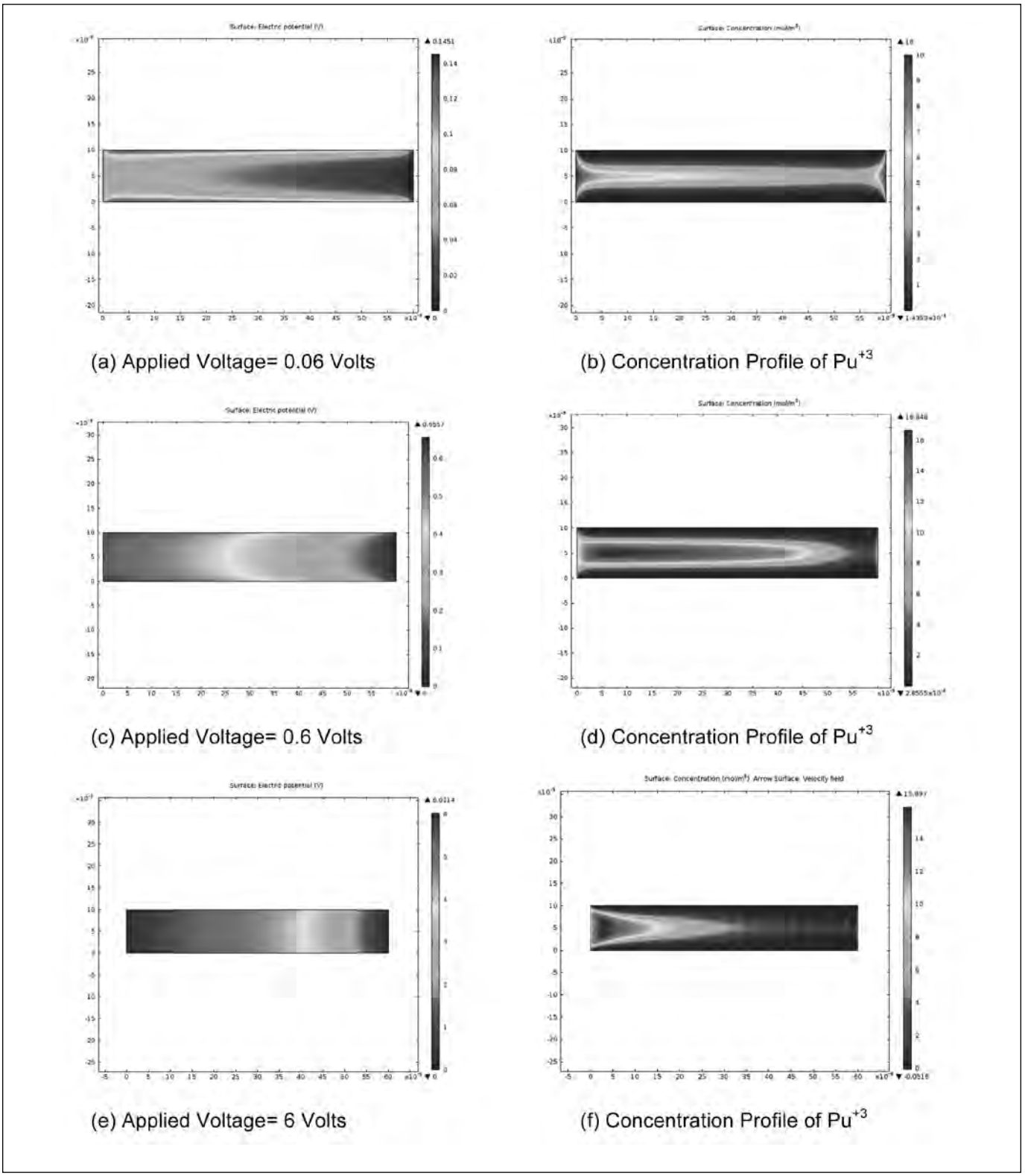

Figure 3. The applied voltage and the corresponding concentration profile for solution [Pu^{+3}] •[Y^{3}]

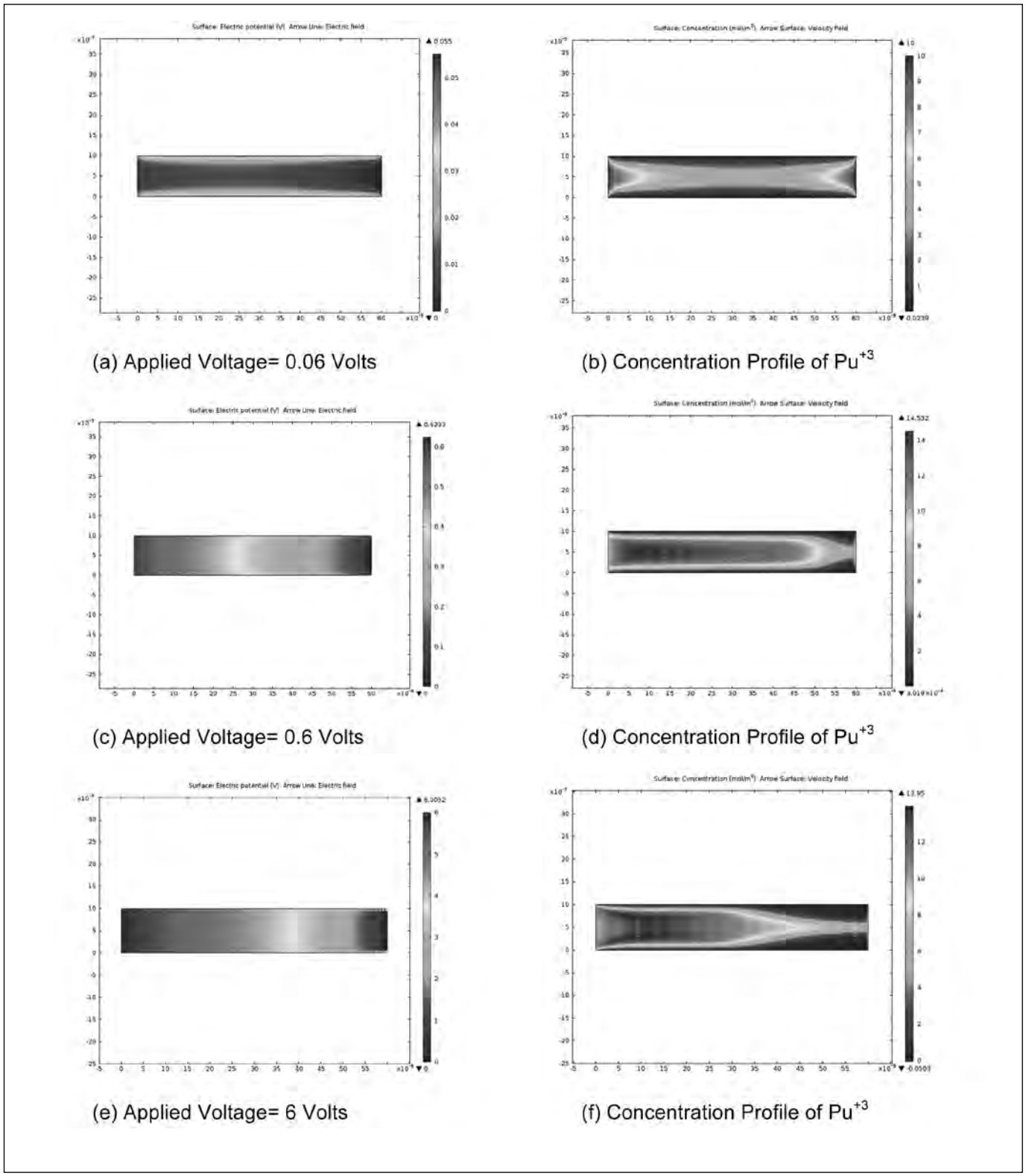

nanoscopic system based on stimulated emission depletion STED has been developed.[20,21] STED is a recent breakthrough technology in nanobiophotonics that enables a break in the diffraction limit barrier to achieve nanoscale spatial resolution.

Verification in Aqueous Polishing Processing

A key aspect for mixed oxide fabrication is the control and purification of impurities in the Pu content, a step achieved by aqueous polishing. The aqueous polishing process uses a conventional process-flow diagram of dissolution, ion exchange, oxalate precipitation, and calcination. Two main aqueous processes form the basis of the aqueous plutonium polishing process. The first is the mature plutonium purification process known as plutonium-uranium extraction, or PUREX. The second process applies ion exchange technology to separate the dissolved plutonium from the impurities. Both processes create an aqueous acidic waste solution with the various separated impurities such as gallium, americium, aluminum, fluorine, and other materials. Radiation detection methods in aqueous process such as plutonium aqueous polishing are limited due to elevated background level and the presence of several radioactive species in the liquid stream, making difficult the lower level detection and self-shielding and attenuation due to process configuration *pipes* volume distance, inhomogeneity in the fluid, turbulence and flow control. MCA and strengthened verification methods are critical during the purification phase. Key measurement points along the polishing process and waste streams can be implemented to verify the non-diversion of declared material. Emerging science in microfluidics may provide a timelier, cost effective, and resource efficient means for MC&A verification at such facilities.

Conclusion

State-of-the-art technologies based on fluidics with the characteristics of electrokinetics and electrophoresis are proposed to develop ultra-sensitive sensors capable of speciation of ion species and radionuclides in aqueous media. Microfluidic technology has been integrated into commercially available chips ("Lab on a Chip" or LOC) to provide chemical reactions, separations, and fluid control allowed by various channel arrangements. The technology offers many advantages for highly radioactive separations mainly due to small size and capabilities to control chemical concentrations in time and space. The small size allows much smaller footprints making it portable and less intrusive to operating facilities. Electrokinetics phenomena open a plethora of possibilities for ions speciation and manipulation. However, fluid flow and particle transport in microfluidic devices are difficult to control due to many complex factors such as surface composition and buffer characteristics. Understanding of fundamental fluid transport and particle transport is valuable for device design and optimization. Due to the difficulties of measuring fluid motion in such a small scale without disturbing the flow field, theoretical analysis and numerical simulation become essential tools.

Emerging science such as nanofluidics devices can contribute to the safeguard arena by developing tools that can alleviate the inspector work load by providing small sized, accurate, and low cost verification equipment. This measurement technique provides the opportunity not only to precisely control experimental condition for fast assay with high sensitivity and specificity at a low cost, but also to realize unprecedented experimental capability for exploration in sensor technology.

Reference

1. Kuang, C., and G. Wang. 2010. *Lab Chip* 2010, Vol. 10, 240-245.
2. Piruska, A. 2008. *Lab Chip l.* 1625-1631, 2008, Vol. 9.
3. Oh, Y. et al. 1609-1617, 2009, Vol. 9.
4. Eijkel, J. C., and A. van den Berg. 2005. *Microfluid Nanofluid, Vol. 1,* 249-267.
5. Ehrfeld, W., and V. Hessel, and H. Lowe. 2000. *Microreactors: New Technology for Modern Chemistry.*
6. Anderson, H., and A. van der Berg. 2003. *Sensors Actuators B, Vol. B*, 92, 315-325.
7. Han, J., and H. G. Craighead. 2000. *Science*, Vol. 288, 1026-1029.
8. Abgrall, P., and N.-T. Nguyen. 2009. *Nano Fluidics.*
9. Mijatovic, D., J. Eijkel, and A. van der Berg. 2005. *Lab Chip,* Vol. 5, 492-500.
10. Dungchai, W., O. Chailapakul, and C. Henry. 2011. *Royal Society of Chemistry, Analyst,* Vol. 136, 77-82.
11. Mukhopadhyay, R. 2006. What Does Nanofluidics Have to Offer? *Analytical Chemistry*, Vol. 78, 7379-7382.
12. Edel, J., and A. de Mello. 2012. *Nanofluidics, Nanoscience and Nanotechnology.*
13. Chang, H.-C., and L. Y. Yeo. 2010. *Electrokinetically Driven Microfluidics and Nanofluidics,* Cambridge University Press.
14. Nichols, K., et al. 2011. *Journal of the American Chemical Society*, Vol. 133, 15721-15729.
15. Kralj, L., M. Schmidt, and K. Jensen. 531-535, s.l. : Lab Chip, 2005, Vol. 5.
16. Silvestre, C. et al. 54-65, s.l. : *Analytica Chimica Acta*, 2009, Vol. 652.
17. Wang, Y.-C. A., Stevens, L., and J. Han, "Million-fold Preconcentration of Proteins and Peptides by Nanofluidic Filter," *Analytical Chemistry*, Vol. 77, No. 14, pp. 4293-4299, 2005.
18 Feng, J. J., Krishnamoorthy, S., Wang, G. R., and Sundaram, S. 2006. Simulation of Electrokinetic Flow and Analyte Transport in Nano Channels, presented at Nanotech 2006.

19. Wang, Y. Pant, K., Chen, Z., Wang, G., Diffey, W. F., Ashley, P., and Sundaram, S., *Microfluidics and Nanofluidics*, Vol. 7, No. 5, pp. 683-696, 2009.
20. Kuang, Cuifang and Wang, Guiren. 240-245, s.l. *Lab Chip,* 2010, Vol. 10.
21. Rittweger E., K. Y. Han, S. E. Irvine, C. Eggeling and S. W. Hell. 2009. *Nature Photonics,* 3,144-147
22. COMSOL Version 4.2a, 2012, COMSOL Inc., Burlington, Massachusetts, USA.

The Importance of Establishing and Maintaining Continuity of Knowledge During 21st Century Nuclear Fuel Cycle Activities

Chris A. Pickett, Nathan C. Rowe, James R. Younkin
Oak Ridge National Laboratory, Oak Ridge, Tennessee USA

Robert Bean
National Nuclear Security Agency, Office of Nonproliferation and Verification Research and Development, Washington, DC USA

Dianna Blair
Sandia National Laboratories, Albuquerque, New Mexico USA

Ray Lawson and George Weeks
Savannah River National Laboratory, Aiken, South Carolina USA

Keith Tolk
Milagro Consulting, Albuquerque, New Mexico USA

Abstract

During this century, the entire nuclear fuel cycle will expand and become increasingly more global, taxing both the resources and capabilities of the International Atomic Energy Agency (IAEA) to maintain an effective Continuity of Knowledge (CoK) and its ability to provide timely detection of diversion. Uranium that currently is mined and milled in one country will be converted, enriched, and fabricated into fuel for reactors in an expanding set of new countries. This expansion will make it harder to guarantee that regional activities stay regional and that diversion detection is timely unless new and sustainable tools are developed to improve inspector effectiveness. To deal with this emerging reality, the IAEA must increase its use of unattended monitoring and employ new tools and methods that enhance CoK during all phases of the fuel cycle. This approach will help provide useful information to aid in detecting undeclared activities and create opportunities for timely and appropriate responses to events well before they enter phases of greater concern (e.g., enrichment).

The systems that maintain CoK of safeguarded assets rely on containment and surveillance (C/S) technologies. The 21st century fuel cycle will require increased use of these technologies and systems, plus greater implementation of unattended systems that can securely collect data when inspectors are not present. This paper will describe the aspects and some of the capabilities that will be needed to address the expanding global fuel cycle to ensure that verifiable CoK of fuel cycle materials and activities can be established, maintained, and sustained.

Introduction

The international safeguards regime is a complicated environment that is increasing in complexity. The Treaty on the Nonproliferation of Nuclear Weapons (NPT) compels non-nuclear weapon state (NNWS) signatories to conclude safeguards agreements (SA) with the International Atomic Energy Agency (IAEA).[1,2] Implementation of safeguards agreements between the IAEA and member states allows the IAEA to perform verification activities to ensure the peaceful use of nuclear materials and activities. The IAEA employs nuclear material accountancy, the determination of the type, enrichment, and quantity of nuclear material, as the primary approach to verify comprehensive safeguards agreements (CSA). Containment and surveillance (C/S) are complementary measures that reduce the burden of repeatedly performing accountancy measurements on the declared nuclear material and activities to provide a means for ensuring Continuity of Knowledge (CoK) of the material and the declared activities. Without effective CoK, the costs for safeguards implementation to both the IAEA and operators would increase multi-fold.[3]

Recognizing that the worldwide demand for energy will continue to increase, there is an expectation of an expanded commercial nuclear power industry, which will increase the safeguards burden on the IAEA. It is projected that by the year 2030 the number of operating nuclear reactors producing electricity worldwide will be between 523 and 783, with a generating capacity between 501 GW_e and 746 GW_e.[4] To support this expansion, the infrastructure of the nuclear fuel cycle will also expand to new regions of the world. Mines, conversion and enrichment facilities, fuel fabrication plants, and storage or

Table 1 – Snapshot in Time of the World Nuclear Fuel Cycle

Status (as of 2/8/12)	Mining and Milling	Conversion	Enrichment	U Fuel Fabrication	Reactors	Spent Fuel Storage	Reprocessing/ Recycling	Spent Fuel Conditioning	Related Activities
Shutdown	53	10	4	8		2	12	0	9
Decommissioning	8	3	3	6		4	27	0	1
Decommissioned	65	7	8	22	63[1]	1	18	0	6
Stand-By	15	1	1	2		1	3	2	1
In Operation	56	22	19	54	435[2]	113	19	0	32
Under Study - Assessment	4	1	0	0		0	0	0	0
Planned	6	0	2	1	16[3]	5	2	0	0
Siting - Design	0	0	0	0		0	0	0	0
Under Construction	14	3	2	0	63[3]	4	1	0	1
Commissioning	1	0	2	0		0	2	0	1
Cancelled	1	0	0	1		1	3	0	1
Deferred	7	0	2	1		1	3	0	1
Total (past)	141	21	16	38	63	8	60	2	17
Total (present)	56	22	19	54	435	113	19	0	32
Total (future)	25	4	6	1	79	9	5	0	2
Total (other)	8	0	2	2	0	2	6	0	2
Total (all)	230	47	43	95	577	132	90	2	53

1 – denotes data obtained from http://en.wikipedia.org/wiki/Nuclear_decommissioning
2 – denotes data obtained from http://www.euronuclear.org/info/encyclopedia/n/nuclear-power-plant-world-wide.htm
3 – denotes data obtained from http://www.world-nuclear.org/info/inf17.html
All other data obtained from http://infcis.iaea.org/NFCIS/NFCISMain.asp?Order=1&RPage=1&Page=1&RightP=List

processing sites are all in various stages of planning, construction, or expansion. Table 1, Snapshot in Time of the World Nuclear Fuel Cycle, highlights the current dynamic nature of the enterprise, with facilities exiting the enterprise as new ones come onboard. In addition, the introduction of new nuclear activities to the global enterprise, such as laser enrichment and pyro-processing, underscores both the expanded and complex environment in which the IAEA must operate.

Implementation of the Additional Protocol, where the IAEA must verify not only the accuracy but the completeness of a state's declaration, moves the IAEA past a pure material accountancy model for ensuring a state's compliance and into the search for undeclared activities. This places additional strain on the IAEA's budget that has been essentially flat for the past thirty-five years, potentially impacting operations as well as research and development.

The IAEA is responsible for generating safeguards conclusions in this evolving environment. With what can be seen as vertical (number of facilities) and horizontal (types of facilities and activities) expansion of safeguards, exemplified in the enterprise scale and expanded scope, the IAEA must look at deploying technologies more extensively to manage costs, improve detection, and reduce risks. The judicious use of existing and new C/S techniques to maintain CoK on materials, facilities, and activities could significantly help improve the IAEA's ability to validate safeguards conclusions.

Continuity-of-Knowledge in Safeguards

The nuclear fuel cycle consists of nine key operations: mining, milling, conversion, enrichment, fuel fabrication, reactor operations, spent fuel storage, reprocessing, and long-term storage (Figure 1). Safeguards currently begins "when any nuclear material of composition and purity suitable for fuel fabrication or for being

Figure 1. Nuclear fuel cycle[5]

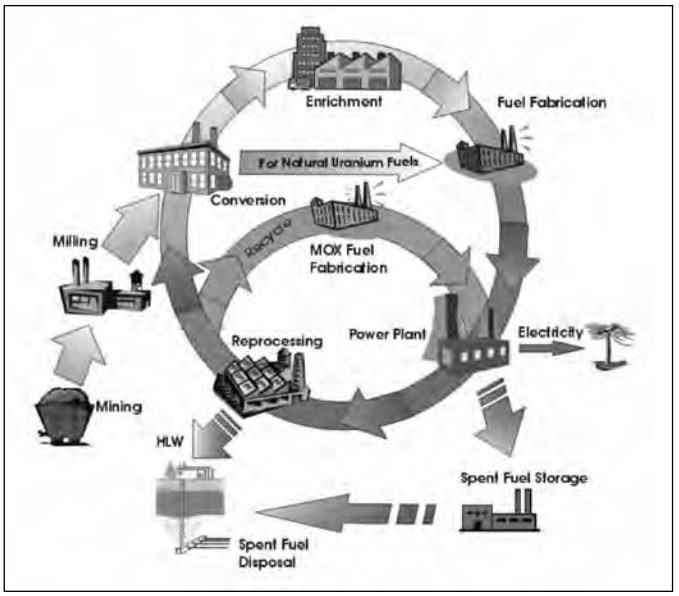

isotopically enriched leaves the plant or process stage in which it has been produced" and terminates when "it has been consumed, or has been diluted in such a way that it is no longer usable…or has become practicably irrecoverable."[2] In general, C/S measures to ensure CoK occur throughout this safeguards portion of the nuclear fuel cycle in applications where bulk material is static, such as inventory storage, or when declared material is moved in the absence of an inspector, such as some refueling activities. Some C/S measures, such as cameras, monitor broad areas and multiple assets, while others, such as tamper-indicating devices (TIDs), also known as seals, monitor discrete items.

Currently the IAEA annually uses more than 20,000 metal cup seals (Figure 2) as part of its verification activities to ensure CoK of material and equipment. Just as images from the surveillance cameras must be reviewed by an inspector or analyst, every seal must be returned to IAEA headquarters for postmortem verification of its integrity and authenticity.

In recent years, the IAEA has begun a shift toward greater reliance on CoK systems, particularly unattended and remote-monitoring systems. This shift is due in part to the expanding number of facilities under safeguards that stretch limited inspection resources and the consistent need for timely detection. CoK systems, particularly remotely monitored systems, are able to provide improved timeliness of detection for both the verification of declared activities and the detection of events by continuous monitoring. This increases inspection efficiency and reduces inspector workload.[3]

As stated in Table 1, there are a number of facilities in the safeguards portion of the nuclear fuel cycle that are in a shutdown, decommissioning, or decommissioned state. To ensure their status remains as declared, and to minimize the burden on the IAEA,

Figure 2. Type-E metal cup seal[6]

new C/S approaches and technologies will need to be identified to ensure CoK of the status of the facility. Moving C/S outside facilities is a new problem space. C/S, traditionally applied as a complementary measure for nuclear materials accountancy, will become a complementary measure for inspector determinations. A further extension of this problem is the need for new approaches and technologies for providing CoK for declared material in long-term storage, such as geo-repositories where safeguards approaches are still being developed.

Increased globalization of the fuel cycle will increase the quantities and types of materials transported both within states and internationally. To minimize the impact on IAEA resources, CoK of this material as it is handled and moved will require approaches that include application and removal by operations and global tracking.

It should also be recognized that any expansion of the safeguards portion of the nuclear fuel cycle (horizontal expansion) to earlier stages than is stated in INFCIRC/153[2] could require new C/S approaches and possibly new technologies to reduce inspector presence while collecting verification information. It would become prohibitively expensive for the IAEA, and current approaches, such as single-use, laboratory-verified seals and surveillance cameras that require labor-intensive review, would be challenging with a zero growth budget for the IAEA.

Continued investment in C/S technologies to meet the growing safeguards need has been recognized in expert forums such as the 2010 INMM International Containment and Surveillance Workshop Focused on Concepts for the 21st Century and a recent November 2011 IAEA Workshop on Sealing, Containment, and Authentication Technologies that identified needs for improved tools for enhancing current CoK measures.[7,8] Both workshops recognized an increased need to improve the tracking and monitoring of nuclear materials and activities throughout the fuel cycle. It was observed that the ability to establish and maintain effective CoK is rapidly becoming paramount to detecting diversion and undeclared activities occurring in a state or region.

These workshops also recognized the need for the IAEA to have additional C/S tools that are designed for application-specific needs and to provide a pipeline of new technologies/tools that are resistant to new and evolving threats (i.e., cyber attacks).

Twenty-first century CoK should include improved review techniques for surveillance images, exploration of extended wavelength range imagers, cost-effective camera configurations, and a systems-level decrease in the life-cycle cost of these seals by allowing in-field verification and extended lifetime. Other tamper-indication technologies, such as new tamper-indicating materials and enclosures, could also benefit the community.

The above specific C/S technologies are not meant to be a complete list of the problems facing the safeguards community in the future nor are the technologies discussed intended as a complete roadmap of solutions. The intent is to illustrate some of the evolving challenges and how continued research is needed to improve existing approaches and maintain systems that are effective against evolving threats.

Fundamental Elements of Continuity-of-Knowledge

Although the applications for CoK will expand in the 21st century and new technologies will be developed to accomplish this, the basic philosophy of what the technology must provide remains unchanged. To maintain CoK of a nuclear material inventory or status of a monitored facility, the IAEA needs a complete set of data that accurately reflects conditions at the facility. These data will generally come from a wide range of sources and systems and equipment, including seals, surveillance cameras, radiation-monitoring equipment, material-tracking systems, and weighing systems. To maintain a credible CoK, data must satisfy three important criteria – trust, completeness, and timeliness.

Trust

The monitoring agency must be confident that the data being reported by the monitoring system accurately reflects the conditions at the facility and has not been defeated. The process required for obtaining this trust in the data and the equipment that is generating it is called *authentication.* Generally, the equipment for generating, collecting, and transmitting the data must be designed with authentication in mind. Adding authentication after the system has been developed can be very expensive and perhaps even impossible. Several papers on equipment and data authentication have been published previously,[9–13] so the processes will not be discussed further here.

Completeness

The data set must not contain gaps that would allow an adversary to divert material or perform other prohibited acts without detection. Such gaps will be system specific. Note that this does not mean that gaps are not allowed but that the monitoring system must be designed based on objectives to be accomplished and assumed threats. For example, an electronic seal might go for days without reporting, provided there is adequate assurance built into the sealing system that any attempt to open the seal would be reported. However, gaps in surveillance data longer than the time required to carry out a prohibited act cannot be tolerated, since the inspector would have no information as to what happened in the facility during the information gap.

Timeliness

The time frequency within which the monitoring agency must have information to detect material diversion or other prohibited acts is defined by their timeliness criteria. For many data streams, existing remote-monitoring systems at current facilities with current criteria satisfy this requirement. However, with longer intervals between inspector visits, current passive seals and tamper-indicating enclosures (TIEs) may no longer be acceptable. This will become a larger issue when new types of facilities are put under safeguards. If an inspector shows up at a facility several months after the previous inspector visit and finds a damaged (or open) passive seal or TIE, there may not be an effective way to recover CoK, since the material in question may no longer be available for measurements and the facility status during that time will be unknown. The result would be the inability to claim timely detection of a possible material diversion or activity.

Other Considerations

Remote-monitoring systems are a growing area for C/S. All systems must be designed and evaluated for the remote-monitoring scenario in which they will be used. These scenarios are different from existing monitoring scenarios and may require considerable changes to equipment, procedures, and policies.

The facility operator may be called upon to perform more hands-on safeguards activities, since the inspectors will not be present, and equipment and procedures must be developed to accommodate this. An obvious example is sealing material containers in a processing facility. Currently operators cannot apply or remove IAEA seals. This role may be expanded in future systems, requiring new methods for ensuring that the operator cannot tamper with the seal before it is applied or after it is removed to hide surreptitious opening and closing events and to ensure that the seal has been applied properly. Continuity of Knowledge equipment that would not require inspector presence for application or removal and that is integrated into a remote monitoring system could be a game changer for safeguards activities. However, the reliability of such a sealing system would require a robust design and extensive vulnerability assessments.

Sustainability

A sustainable system can be viewed as one that meets the needs of today without compromising the ability to satisfy all perfor-

mance and prescriptive requirements in the future. For technology-intensive applications, it is challenging to keep pace with technological changes and it is extremely difficult to plan for them.[14] However, there are sustainability programs that are recommended for state physical protection regimes that could be considered for safeguards systems.[15] These programs encompass operating instructions, human resource management and training, equipment updating, maintenance, repair, and calibration, performance testing and operational monitoring, and configuration management.

Ensuring that equipment is not obsolete, a condition in which it is no longer possible to maintain the equipment due to lack of expertise or replacement parts, when first deployed requires a rapid approval and procurement system, which is discussed further in the policy section of this paper. Determining when equipment is obsolete can be relatively straightforward in terms of maintenance, but recognizing when C/S equipment is becoming obsolete can be more challenging. Obsolescence can be viewed as a complex calculation of equipment reliability and performance when compared to newer versions or concepts.

The surreptitious defeat of a security device by an adversary creates an environment in which the information that the IAEA is relying upon to draw its conclusions is faulty and makes the equipment obsolete, possibly without the IAEA even being aware. Therefore, for safeguards, and other security applications, it is important to have a robust system in which research, technology evaluation, and vulnerability assessments are routinely utilized to allow proper response to the evolving threat environment. The good news is that many of these threats can be addressed with relatively straightforward changes in software and operational procedures, but the ability to apply these fixes to systems that are deployed around the world quickly and efficiently must be included in the system design early in the development process. Processes for evaluating and controlling changes to the systems must also be developed.

Recognizing that taking advantage of future technological developments will enable the IAEA to respond to the evolving threat matrix, the utilization of standards for interface, communications, and security protocols would provide for forward compatibility of various system elements. The standards should be adopted from the many international standards available. Determining which standards to employ is a difficult policy decision, however.

Also, integrated systems should be developed with modular architecture so that elements can be updated as new technologies become available.

Policy and Best Practice Recommendations

As safeguards continue to develop and identify technologies for areas such as remote-monitoring applications, the need may grow for operators and state authorities to access areas and items under safeguards. This will require access beyond the IAEA control boundary and the TIDs and TIEs designed to indicate penetration. Though possibly exercised under special conditions, it is recommended that a policy be established that outlines requirements and limitations regarding access to and the removal and attachment of IAEA seals by non-IAEA individuals.

Recognizing that the integrity of tools and equipment can be compromised at any point throughout its manufacturing cycle, we recommend establishing a performance-based procurement policy to ensure that no undocumented features are embedded in any of devices and that the equipment performs, and continues to perform, as advertised. An additional benefit would be that this performance-based system would allow for new equipment to be introduced into the safeguards toolbox in a timely manner.

Due to changes that vendors can introduce in the manufacturing process of inspector tools, vulnerability assessments should be repeatedly performed at various time intervals on authorized equipment to ensure that it continues to perform as required and that no new vulnerabilities have been introduced.

Summary and Next Steps

CoK systems have been in use since the IAEA first began using seals and cameras to verify containment and surveillance. These systems have evolved, but many of the basic ideas and methods have survived as the systems have been continually adapted and reinvented to meet changing needs. New systems have been introduced, but it is important to keep in mind that CoK systems and their components need to periodically be assessed and updated to counter new threats. The IAEA will increasingly rely on more unattended systems and remote methods of verifying safeguards declarations in the 21st century to achieve greater efficiencies. Improving both the frequency and quality of communication between the IAEA and R&D program managers, technology providers, and facility operators can help ensure that needs are effectively identified, proper technologies are introduced, and the evolving adversary threat is addressed. Mechanisms to improve the communication of both needs and emerging technology must be developed and sustained if the increasing CoK needs of the IAEA are to be met. Workshops that focus on specific technology areas or needs are useful because they provide a forum for active exchange of ideas. Recognizing the financial limitations of the IAEA, increased R&D focus by support programs on these needs is critical to ensuring a supply of tools and methods are available for IAEA consideration.

Informal discussions, technology exchanges, laboratory visits, and distribution of reports articulating recent developments and needs would help fill a communication void as well.

Also, sustainability in the context of the IAEA's acceptance process must be evaluated. Further, moving towards a performance-based acceptance process or development of replacement systems

immediately after, or even before, the deployment of the current systems should be considered. It needs to be recognized that new tools are needed for the 21st century safeguards challenge, and this requires sustainable long-term research and development efforts.

This manuscript has been authored by UT-Battelle LLC under Contract No. DE-AC05-00OR22725 with the U.S. Department of Energy. The United States government retains and the publisher, by accepting the article for publication, acknowledges that the United States government retains a non-exclusive, paid-up, irrevocable, world-wide license to publish or reproduce the published form of this manuscript, or allow others to do so, for United States government purposes.

Sandia National Laboratories is a multi-program laboratory managed and operated by Sandia Corporation, a wholly owned subsidiary of Lockheed Martin Corporation, for the U.S. Department of Energy's National Nuclear Security Administration under contract DE-AC04-94AL85000.

References

1. IAEA. Treaty on the Nonproliferation of Nuclear Weapons, INFCIRC/140.
2. IAEA. 1972. The Structure and Content of Agreements Between the Agency and States Required in Connection with the Treaty on the Nonproliferation of Nuclear Weapons, INFCIRC/153 (corrected), Vienna, Austria.
3. Crawford, D., and O. Johnson. 1998. Role of Containment and Surveillance Strategies in the U.S. National Safeguards Program, *ESARDA Bulletin* No.28, January 1998.
4 http://www.iaea.org/newscenter/news/2011/nuclgrowth.html, IAEA Projects Slower Nuclear Growth after Fukushima, IAEA General Conference.
5. http://infcis.iaea.org/NFCIS/Background.cshtml?page=background&RightP=Background, International Atomic Energy Agency (IAEA), NFCIS Nuclear Fuel Cycle Information System Web site.
6. Zendel, M., and M. Moeslinger. 2007. IAEA Safeguards Equipment, *Advanced Sensors for Safeguards*, Santa Fe, New Mexico USA. http://www.bnl.gov/ISPO/BNLWorkshop07/Presentations/Zendel_Moeslinger.pdf.
7. Pickett, C. A., K. M. Tolk, F. Keel, and S. LaMontagne. 2010. *Results from the 2010 INMM International Containment and Surveillance Workshop Focused on Concepts for the 21st Century,* IAEA Safeguards Symposium.
8. http://www-pub.iaea.org/mtcd/meetings/pdfPlus/2011/43123/43123_Leaflet.pdf.
9. Tolk, K., M. Aparo, C. Liguori, and A. Capel. 2006. Design of Safeguards Equipment for Authentication, presented at *Symposium on International Safeguards – Addressing Verification Challenges*, Vienna, Austria.
10. Kouses, R., L. Bratcher, T. Gosnell, D. Langner, D. MacArthur, J. Mihalczo, C. Pura, A. Ready, P. Rexroth, M. Scott, and J. Spingarn. 2001. Authentication Procedures, *Proceedings of the Institute of Nuclear Materials Management 42nd Annual Meeting*.
11. Tolk, K. M., and R. K. Rembold. 1997. Verification of Operating Software for Cooperative Monitoring Applications, *Proceedings of the Institute of Nuclear Materials Management 38th Annual INMM Meeting*, Phoenix, Arizona, 1997.
12. Mayo, D., L. R. Avens, J. Spingarn, K. Tolk, K. Pitts, J. Tanner, S. J. Luke, D. Lee, and T. Dunham. 2001. Authentication Task Force – Hardware Task Group, *Proceedings of the Institute of Nuclear Materials Management 42nd Annual Meeting*.
13. Tolk, K. 2010. Hardware Authentication, *Proceedings of the Institute of Nuclear Materials Management 51st Annual Meeting*.
14. Kurzweil, R. 2001. The Law of Accelerating Returns, March 7, 2001, http://www.kurzweilai.net/the-law-of-accelerating-returns.
15. Physical Protection of Nuclear Material and Nuclear Facilities, INFCIRC/225/Revision 5.

Enhanced Safeguards: The Role of Smart Functional Coatings for Tamper Indication

A. E. Méndez Torres, M. J. Martínez-Rodríguez, K. Brinkman, and D. Krementz
Savannah River National Laboratory, Aiken, South Carolina USA

Abstract

This work investigates the synthesis of smart functional coatings (SFC) using chemical solution deposition methods. Chemical solution deposition methods have recently received attention in the materials research community due to several unique advantages that include low temperature processing, high homogeneity of final products, the ability to fabricate materials with controlled surface properties and pore structures, and the ease of dopant incorporation in controlled concentrations. The optical properties of thin films were investigated using UV-Vis spectroscopy, Raman, SEM, and EDS, with the aim of developing a protective transparent coating for a ceramic surface as a first line of defense for tamper indication. The signature produced by the addition of rare earth dopants will be employed as an additional tamper indicating feature. The integration of SFCs as part of a broader verification system such as an electronic seals can provide additional functionality and defense in depth. SFCs can improve the timeliness of detection by providing a robust, in-situ verifiable tamper indication framework.

Introduction

The International Atomic Energy Agency (IAEA) has recognized the need for the development and implementation of advanced authentication, verification, unique identification (UID), and tamper indications schemes for international safeguards applications.[1] New materials, including coatings and heterostructures open up the possibility of low-cost fabrication of in-field verifiable coatings that can provide protective features and optical responses as a verifiable tool with applicability to tamper indication systems such as seals.

In order to strengthen verification schemes, the IAEA has anticipated the authorization of laser surface authentication (LSA[2]) for the verification of existing metal seals.[3] In addition, they have recommended the development of an easy to use and inexpensive active-electronic seal, along with the establishment of an effective capability to assess the seal system vulnerabilities. LSA utilizes the random speckle patterns, which are formed by shining a laser on the surface of an object. It can read the unique *fingerprint* inherent in certain manufactured items by mapping microscopic variations across the surface of a range of materials, including paper, plastic, metal, and ceramics. It is therefore imperative that the material, surface preparations, and potential coatings that are being developed are compatible with this technique. Compatible transparent coatings can be employed to protect the surface features and include additional functionality such as tamper indication. Smart functional coatings (SFC) will serve as a first layer of protection for authentication and would allow in-situ verification of the item.

Researchers at the Savannah River National Laboratory (SRNL) are investigating the science of SFC as a versatile tamper-indication technique that may be applied to a variety of materials, containers, and equipment. All of these are vulnerable to tampering when fielded. It is envisioned that a SFC applied to the material or system (i.e., UF_6 cylinder, camera housing, or seal) can allow an IAEA inspector to verify the authenticity of the item in-situ and extract information that can indicate whether tampering has occurred.

Smart Functional Coatings (SFC)

A SFC is a system that can perform as a sensor or actuator by its capability to respond to physical, chemical, or mechanical stimuli. Changes in properties and structure can then be verified by a readable signal. The integration of functional materials such as rare earth dopants, inorganic, and polymeric coatings is being investigated to produce smart materials that combine photon stimulation with other properties that may respond to external conditions. SFC can act in a passive or active mode. In an active mode, it may be integrated into various elements including sensors, actuators, control algorithms, control hardware, and structural members that make up a complete smart system. Some of the benefits of smart coatings include the capability to respond to physical, chemical or mechanical stimuli by developing readable signals, and changes in properties and structure, in response to a change in environmental conditions. The use of rare earth dopants when combined with chemical solution deposition techniques provides a visual, identifiable detection method by a stimulus-response mechanism or photo-stimulation. The response is the emission of a characteristic wavelength associated with the state of the system. For sensors based on *color* response, the response may be visible color change, fluorescence, or phosphorescence as a result of a variety of stimuli. This simple, in-situ method of detection can provide to the inspector information for verification of the state of the system. Examples of such systems are summarized in Table 1.

Table 1. Smart Polymeric coatings containing functional colorants (adapted from Reference 6).

Sensor type	Sensing Mechanism	Stimulus	Response
pH indicator	Ionic form of different color	pH change	Color
Fluorescence probe	Change in fluorescence intensity	Sorption, diffusion	Fluoresnce
Colorimetric dye	Colored metal complex	Heavy metal, radioactive contamination	Color change
Fluorescent polymer fiber, reactive sensor	TNT binds to receptor on chromophores, reducing signal, nerve gas reacting with sensor	TNT, nerve gas presence	Quenching fluoresnce
Conducting polymer	Switch between charged and neutral state. Change in surface conductivity or impedance	Oxide layer formation	Optical Absorbance, change in conductivity or electrical properties

One of the largest advantages of coating deposition by solution methods is the independence from the geometry of the substrate. Solutions can be deposited onto a variety of substrates such as ceramics, plastics, or metal by well-known methods including spin coating and dip coating. Solutions can be cast into a mold, and with further drying and heat-treatment, dense ceramic or glass articles with desired properties can be formed.[4,5] For example the reduction of the particle size well below the wavelength of visible light (~ 0.5 μm or 500 nm) eliminates much of the light scattering, allowing fabrication of a translucent material—a key factor for LSA compatibility.

Application to Safeguards

Containment verification is a high priority for the international safeguards community. Nuclear material containers, equipment cabinets, camera housing, and detector cable conduits are all vulnerable to tampering or counterfeiting when fielded. In many cases, it is very difficult to distinguish counterfeit items from genuine products. SFCs applied to genuine materials surfaces allow the inspector to identify the item in-situ and extract information that can be used for continuity-of-knowledge. Additional advantages of smart coatings include: i) incorporation onto almost any surface, ii) the potential to incorporate active dopants for enhanced safeguards, verification and monitoring, iii) non-intrusive methodology for UID, iv) easily tailored for process or facility specific applications.

Experimental

Material Selection

Transparent films prepared by chemical solution deposition methods based on alumina and silica were selected due to the ease of preparation, optical properties, ease of incorporation of dopants such as rare earth elements or nanoparticles, nontoxicity, scalable processes that do not depend on the object geometry, and the compatibility with ceramic materials of interest for the seal body.

Silica gel is the most common type of gel and the most extensively studied and used.[4,7] It is a granular, vitreous, porous form of silicon dioxide made synthetically from sodium silicate. Despite its name, silica gel is a solid. It is a naturally occurring mineral that is purified and processed into either granular or beaded form. It allows the construction of materials that let light into buildings but trap heat for solar heating. It has remarkable thermal insulative properties, having an extremely low thermal conductivity.

Alumina gels can be synthesized using aluminum oxide,[8] chlorides, or nitrates. These gels are used typically as catalysts, especially when "metal-doped." Nickel-alumina gel is the most common combination. Alumina are also being considered by NASA for capturing of hypervelocity particles; a formulation doped with gadolinium and terbium could fluoresce at the particle impact site, with amount of fluorescence dependent on impact energy. By controlling synthesis conditions carefully, the sol morphology can be directed toward weakly branched polymeric systems or to particulate systems.[9] Important process parameters are water content, the solvent, the catalyst used and its concentration, and type of alkoxide used.[4,10]

Selection of Optical Centers

Terbium (Tb^{3+}) and Erbium (Er^{3+}) were chosen as dopant due to the capability of dual excitation (UV and visible region) and compatibility with both alumina and silica matrix materials envisioned for film deposition.[11] Figure 1 shows the fluorescence spectra for 0.03 mol/L dopant concentration of (Tb^{3+}) and Erbium (Er^{3+}) in ethanol when excited with 375 nm UV light. Tb^{3+} is of particular interest due to the high intensity of emission (peak at 550 nm). Er^{3+} is known to have a strong emission in the visible and infrared region at 1540 nm that can serve as a hidden signal.

Mixture of dopants can also be employed as method to increase the complexity of the coating. Mixtures of dopants in ethanol with a 50/50 ratio of Er^{3+}/Tb^{3+} display spectral features shown in Figure 1. The intense Tb^{3+} peak at 555 nm and 493 nm serves to mask the Er^{3+} emissions at 426 and 575 nm. A casual observer examining the fluorescence of Tb^{3+} and Er^{3+} mixtures in the visible region may conclude that only Tb^{3+} is present. If tampering is thought to have occurred, an examination of the broad range optical response of the seal can indicate if a counterfeit fluorescent coating was applied. Excitation and emission lines of selected dopant are summarized in Table 2.

Figure 1. Comparison emission spectra of Er^{3+} and Tb^{3+} in ethanol[12]

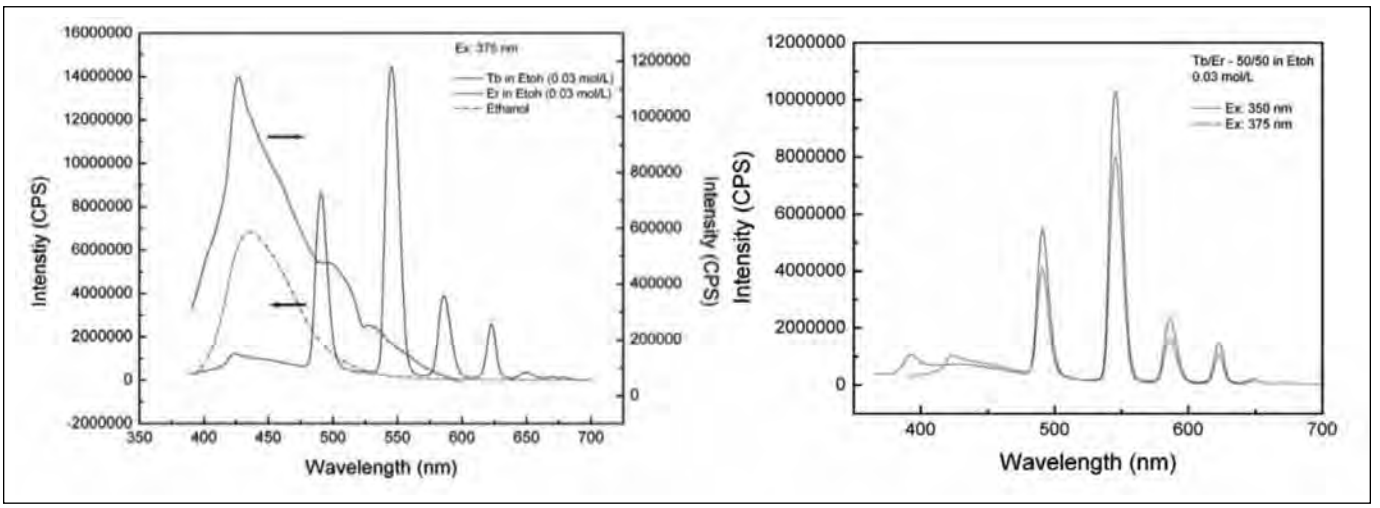

Table 2. List of selected: their excitation and emission lines

PSL precursor	Absorbs in	Emits in	λ_{ex} (nm)	λ_{em} (nm)
Erbium [13]	UV, Visible, IR	UV, Visible	377	426
			488	575
			520	617
Terbium [11]	UV	Visible	350	493, 539, 555, 585, 623

Method of Preparation

Amongst the different techniques available, the sol-gel method seems to be the most attractive one due to coating on the desired shape and area, easy to control of doping level, solution concentration, and homogeneity without using expensive and complicated equipment when compared with other methods.

Undoped and Er^{3+}-doped alumina and silica were prepared by sol-gel method. All reagents were obtained from Sigma Aldrich. Alumina sol was obtained from aluminum sec-butoxide (ASB) in excess of water and by implementing the Yoldas process.[14,15] HNO_3 was used for peptization. The molar ratios of ASB:H_2O:HNO_3 used were 1:110:0.07. The silica sol was prepared by reacting tetraethoxysilane (TEOS) and water in ethanol (EtOH) as a mutual solvent following the procedure of Lenza and Vasconcelos.[16] HNO_3 was used as catalyst. The molar ratios of TEOS:H_2O:EtOH:HNO_3 used were 1:6:10.085. The Er^{3+}-doped sol were obtained by adding a solution of $Er(NO_3)_3$ in EtOH in sufficient amount to give a molar ratio of 0.1 as metal ion per alumina or silica. Undoped and Er^{3+}-doped sol samples were removed by pipette and deposited into quartz slides to form a thick film or by spin coating (200 – 800 rpm, 15 s) to form thinner films. The coated quartz slides were allowed to cool to room temperature and left to dry, at least 24 hours.

Analysis

Raman Spectroscopy

Raman spectroscopy is a useful technique for the identification of a wide range of substances—solids, liquids, and gases. It is a straightforward, non-destructive technique requiring no sample preparation. Raman spectroscopy involves illuminating a sample with monochromatic light and using a spectrometer to examine light scattered by the sample. Raman spectrum can be further utilized to map the distribution of dopants or additive to the gel, and can be employed as a method for material authentication. Raman scattering investigation was carried out in alumina and silica sol-gel, synthesized by Yoldas process, as function of rare earth concentration in the gel. Raman spectra were obtained at room temperature using a JASCO NRS5100 micro Raman spectrometer. An argon laser operating at 532 nm was the excitation source. The laser power at the sample was approximately 8 mW. We used an instrumental bandwidth of 2.1cm cm^1 focusing in the surface of the gel as deposited in a corning glass and air dried (>24 hrs) in a single point using a 20X optical objective. Each sample was scanned for a total of 30 seconds.

Alumina-Gel

The Raman spectra of alumina samples doped with 0.1 mol Tb^{3+} after < 48hrs curing at room temperature are given in Figure 2 and Figure 3. Spectral bands associated to crystalline boehmite (AL-OH),1[7,18], at 751, 681, 497, 369, 272, and 238 cm^{-1} were identified. Similar to the Si-gels spectrum an intense and sharp band at 1049 cm^{-1} is observed and is assigned to NO^{3-} vibration.[19] An unidentified sharp peak in the region of 1195cm^{-1} was identified in the alumina samples doped with Tb and is preliminarily assigned to the C-O- stretching band. It is known that carboxylic salt (C-O-C) have very strong characteristic bands in that region[20] and they double ~1050 cm,[1] a band that is also pres-

Figure 2. Raman spectra of silica and alumina sol-gel doped with Tb^{3+} (left) and Raman spectra of silica and corning glass (right)

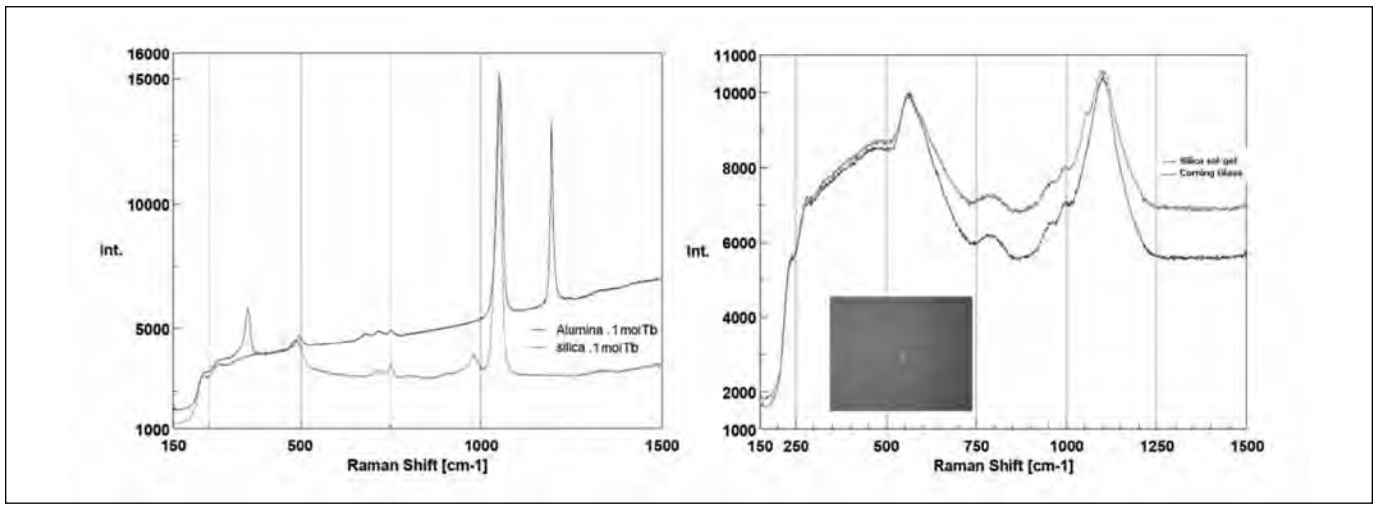

ent in the Raman spectrum. A further evaluation of this region including IR spectroscopy will be needed to confirm the origin of this peak.

Silica Gel

In order to facilitate the analysis of the experimental data of the Raman spectrum of corning glass and the sol-gel silica are shown in Figure 2. Raman spectra of Tb^{3+} (0.1 mol) doped alumina and silica are shown in same figure. The spectra of the silica gel show characteristic Raman bands at ~1180, ~1080, ~800, ~430 cm^{-1} of fused quartz.[21]. The spectrum of the sample [< 48hrs h] shows a broad band ranging from 250 to 500 cm^{-1} that is assigned to the SiO_4 tetrahedral deformation vibrational mode. Characteristic band related to OH stretching vibration of Silanol groups at about 980 cm^{-1} due to the Si-O stretching vibration were also identified. The intense and sharp band at 1050 cm^{-1} is assigned to the C-O stretching vibration and is due to the presence of Si-O-CH_3 groups, originating from TEOS and to the presence of ethanol.[22] The broad band ranging from 250 to 500cm^{-1} is assigned to SiO_4 tetrahedral deformation vibrations.[23] The sharp band at 490cm^{-1} is due to the vibration of a O_3Si-OH tetrahedral.[24] Some weak bands appear between frequencies of 500 and 700 cm^{-1} indicating the presence of a small amount of partially hydrolyzed TEOS. A broad band centered at 800cm^{-1}, is assigned to Si-O-Si network vibration. Peaks at 980 cm^{-1} attributed to Si-OH stretching modes were also detected.[25] The spectrum obtained in the Tb and Er doped silica is similar to those obtained for undoped silica gels prepared under acidic conditions.[26] The Raman spectra of both silica and alumina gel have a luminescence background often observed in xerogels.

Figure 4 shows a Z (depth profile) map of silica film deposited by spin coated methods (400 rpm, 15 s) using as reference the 500-700 cm^{-1} region of associated with Si-O-CH_3 groups that are well known in the literature.[27] The estimated silica films ~5 microns.

Figure 3. Raman map of alumina left and optical image of area scanned (40 x 40 µm) film deposited by spin coating (400rpm, 15 sec) in corning glass substrate. Color charge showing slightly variation (4%) in counts in the intensity Raman band. Figure Z map of alumina film deposited by spin coating (400rpm, 15sec).

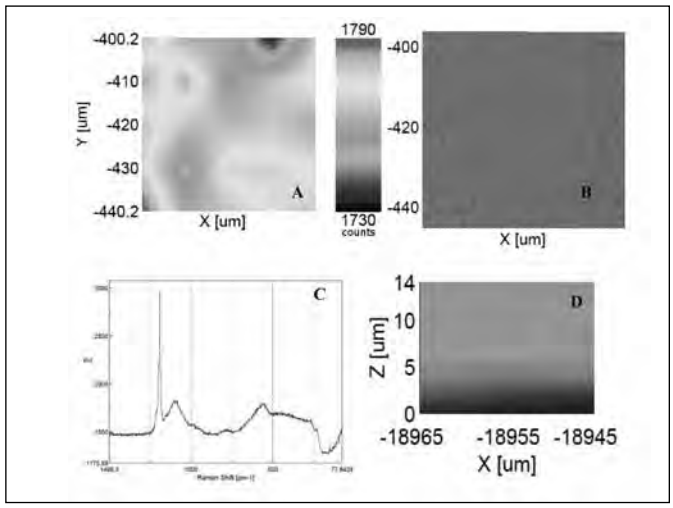

Scanning Electron Microscope and Energy Dispersive X-Ray

Electron microscopy forms the most widely used surface characterization methods. Scanning electron microscopy (SEM) provides information on the appearance, morphology, and topography of the sample surface and near surface. SEM when combined with Energy Dispersive X-Ray spectroscopy (EDS) can be a powerful tool for elemental identification and elemental surface mapping. Advances in technology and miniaturization have made SEM available in small portable units that may allow field verification and analysis of samples.

Figure 4. Raman Z map of deposited silica gel in quartz substrate by spin coating method (400 rpm, 15 s)

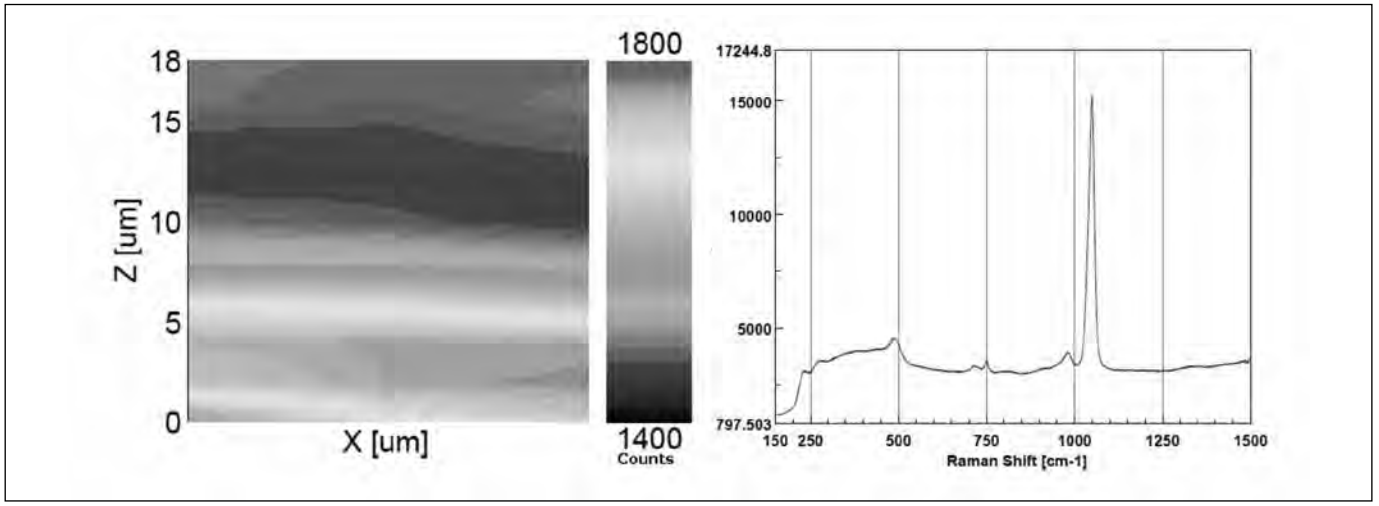

Figure 5. SEM micrograph (topography mode acc V-15 keV wd-7.9) of synthesized alumina gel deposited in corning glass surface by spin coating methods (400 rpm, 15 sec). Magnification from left to right 180X, 400X and 1000X.

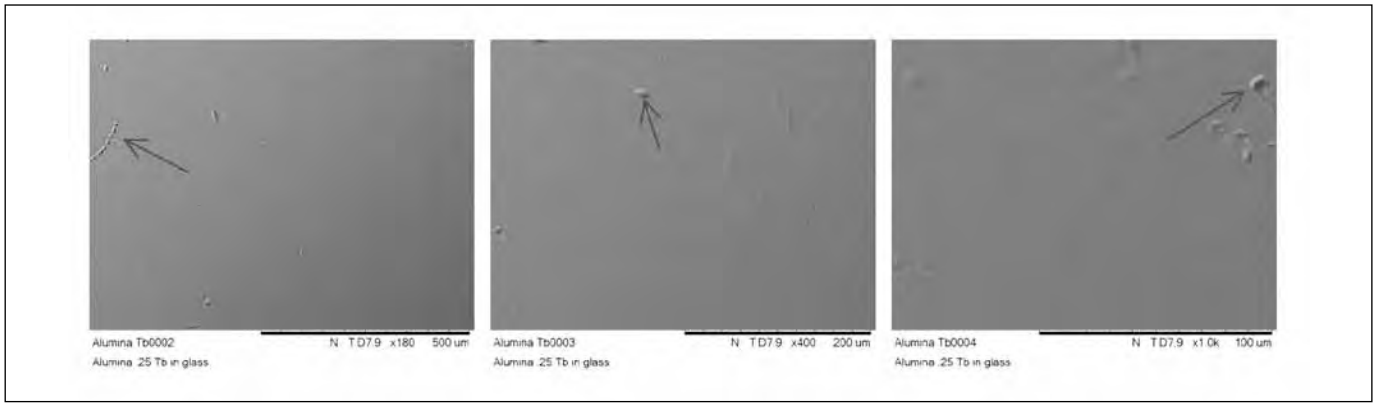

Scanning electron microscopy (SEM) compositional (BSE) and topological analysis was employed to determine homogeneity and surface features of the sol-gel. BSE imaging is highly dependent on the atomic number Z and provides visual identification based on contrast of phases within the material. The higher the atomic number Z the brighter the resulting image, thus, the contrast is essentially a *chemical* contrast dependent on the atomic number Z and relative difference in densities of phases formed in sol-gel. SEM – BSE imaging was accompanied by the use of energy dispersive spectroscopy (EDS) for elemental identification and elemental composition mapping. The SEM used was a Hitachi TM-3000 (bench top scanning electron microscope) equipped with an energy dispersive spectroscopy (EDS) Bruker Quantax-70. EDS mapping creates an elemental image of the SEM image. This creates a distribution of the main elements and phases. The EDS system enabled the acquisition of X-ray data to confirm the elemental composition and provide qualitative/quantitative information of element distribution and atomic weight percentage on the region of interest. The combination of the data from these two techniques was used for elemental qualitative/quantitative analysis. While EDS combined with SEM is a powerful tool to characterize the samples, this method alone does not provide crystallographic orientation of the phases or oxidation states of the phases' constituents. Regardless, it provides qualitative and quantitative analysis that can be used to determine the stoichiometry (or ratio) of elements present in an area of interest or phase. The examined samples were prepared by spin coating of the sol-gel (400 rpm, 15 sec) on a corning glass microscope slide. Figure 5 shown typical results of air dried (>24 hrs) sol-gel. Homogenous, crack free films were observed in samples at magnification from 180 – 1000X. Small features ~10 micron size were identified and possibly related to impurities or dust at the surface of the glass during spin coating.

EDS elemental analysis (Figure 6) and EDS mapping were used to determine the elemental composition of the sol-gel and

Figure 6. Energy dispersive spectrum of synthesis alumina Sol-Gels doped with Er^3 and Tb^3

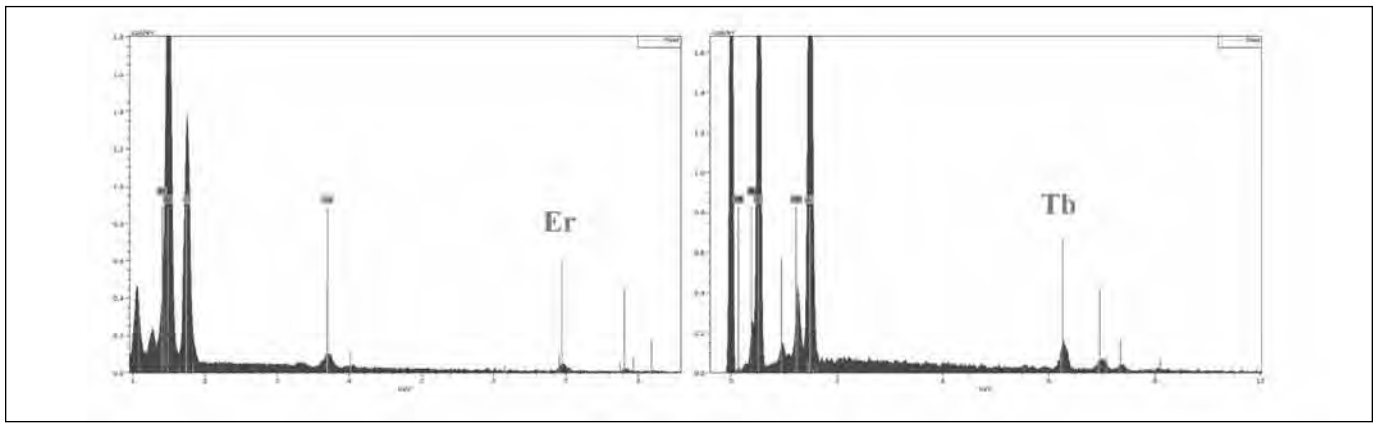

Figure 7. Optical transmission spectra 1- silica sol-gel and 2- alumina sol-gel deposited in corning glass slide by spin coating methods (400 rpm, 15 sec). Feature observed at 450 nm is related to transition of excitation source (deuterium-to-tungsten).

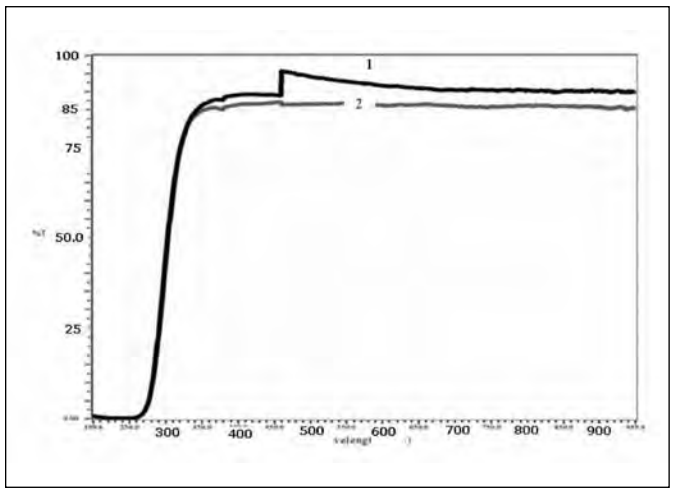

the identification of dopants. Elements in the sol-gel Al, Si, O, N, were identified by EDS. Rare earth dopants Er and Tb were also identified in the sol-gel. Based on the SEM and EDS examination, the dopants were homogenously distributed in the bulk specimen.

UV-Vis

Ultraviolet and visible (UV-Vis) absorption spectroscopy is the measurement of the attenuation of a beam of light after it passes through a sample or after reflection from a sample surface. Absorption measurements can be at a single wavelength or over an extended spectral range. Ultraviolet and visible light are energetic enough to promote outer electrons to higher energy levels. Since the UV-Vis range spans the range of human visual acuity of approximately 400 - 750 nm, UV-Vis spectroscopy is useful to characterize the absorption, transmission, and reflectivity of a variety of technologically important materials, such as pigments, coatings, windows, and filters. Due to the compact size and easiness of operation, handheld UV-Vis systems have been employed in a variety of applications including food, drug and coating inspection.

UV-Vis absorbance and percentage of transmission measurements were conducted on silica and alumina doped films spin coated in glass slides. A spectrophotometer with CCD array detector (Si Photonics 440), housing a deuterium and tungsten source for both ultraviolet (300 - 450nm) and visible (450 nm - 950 nm) excitation, was used. Examination of the optical transmittance of the films is show in Figure 7. Both films exhibit high level of transparency (< 85 percent) over the visible range (400 nm - 950 nm). Information concerning optical transmittance is important in evaluating the optical performance of the deposited sol-gel. A high transparency in the visible region will be required in applications where LSA will be utilized to read the surface features of the underlying coating.

Because the absorbance of a sample will be proportional to the number of absorbing molecules in the spectrometer light beam (e.g., their molar concentration in the sample tube), dope silica, and alumina sol-gel were prepared using the same dopants and dopants concentration.

Optical absorbance of silica and alumina gel as deposited in glass substrate is shown in Figure 8. Optical absorption bands related to Er^{3+} (377, 488, 520, 655 nm) were observed both in synthesized alumina and silica sol-gels for Er^{3+} concentrations of 0.1 mol and 0.25 mol. Absorption spectra appear to be more pronounced for the same Er^{3+} concentration in silica gel than in alumina gel.

Conclusions

This paper highlights the research activities that have been conducted by SRNL in the areas of SFC, specifically materials selec-

Figure 8. Optical absorption spectra of erbium doped silica and alumina sol-gel deposited in corning glass slide by spin coating methods (400 rpm, 15 sec). Absorption bands characteristics of Er^{3+} (377, 488, 520, 655 nm) were observed on the synthesized sol-gel. The insert figure corresponds to free standing silica sol-gel doped with Er^{3+}.

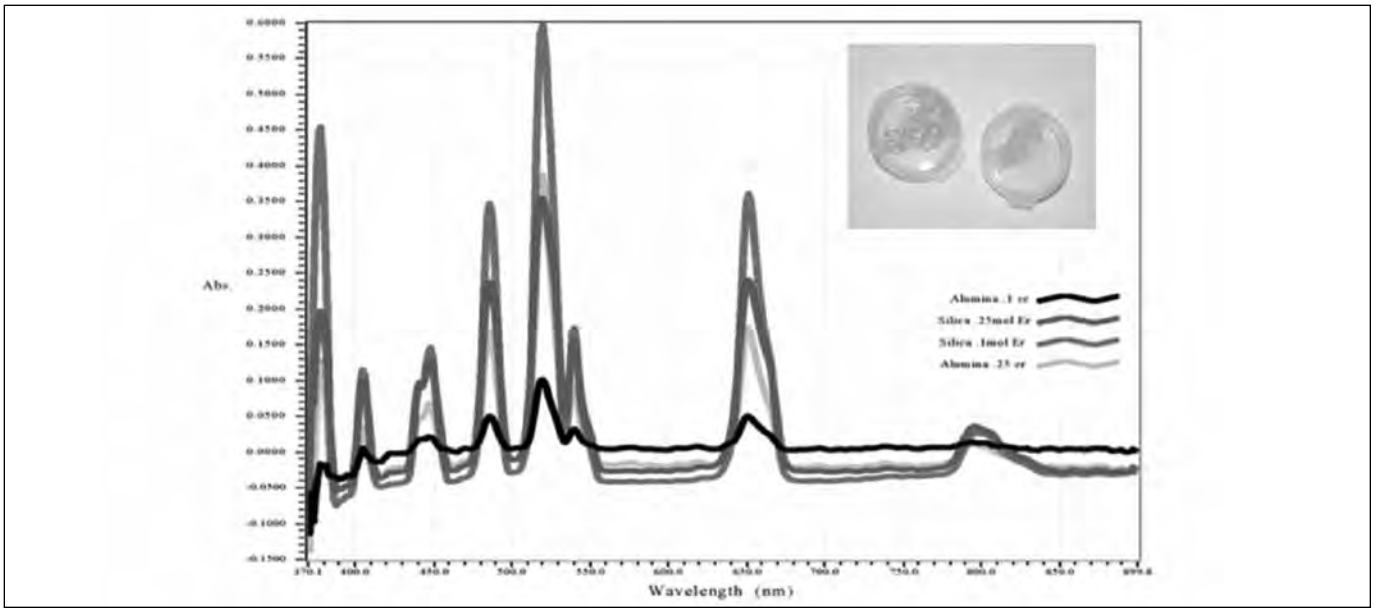

tion and the development of SFC for use in a new generation of intrinsically tamper-indicating ceramic seals (ITICS)[12] that may replace the current metal cup seal used by the international safeguard community. Synthesis of transparent coatings by chemical solution deposition methods including alumina and silica has been performed and deposited in quartz substrates. In addition, rare earth dopants that exhibit fluorescence have been successfully incorporated in the gel matrix and the optical properties have been characterized. Erbium (Er^{3+}) and Terbium (Tb^{3+}) have been identified as possible candidates for optically active dopants due to their optical response (UV excitation with visible emission), and in the case of Er^{3+} additional emissions band in the infrared region. Films fabricated from Er^{3+} and Tb^{3+} doped alumina and silica gels have been analyzed by visible absorption spectroscopy and have demonstrated a high degree of transparency in the visible range indicating potential compatibility with LSA. Alumina and silica based coatings were fabricated by chemical solution deposition by hydrolysis and condensation reactions starting from a metal-alkoxide such as tetraethylorthosilicate (TEOS) and alumina sec butoxide. For solutions and coatings with an optical response it is of importance to understand the effect of dopants such as Er^{3+} and Tb^{3+}, their concentration, and their effects on the mechanical properties of the final film. The effects of additional parameters such as mechanical and chemical resistance need to be well understood in order to make solution methods a reliable and practical technology for safeguards applications. Future work will include the study of dopant mixtures and sensitizer incorporated into the material that may enhance the optical response and increase the complexity of the final gel. Other optical centers including transition metals, can be also incorporated into the film processing.

Techniques for the deposition of the Er^{3+} and Tb^{3+} doped alumina gels on alumina ceramics with tailored thickness in the micron range including dip coating and spin coating are currently being developed. The transparent nature of doped alumina gels indicate that fluorescent coatings may potentially serve dual roles of tamper indication through fluorescence as well as a protective surface layer compatible with LSA techniques. Fluorescent coatings applied to the seal body could provide the inspector with a quick and easy method to inspect seal integrity. The surface could potentially be inspected using a UV flashlight to check for defects in a continuous coating which could indicate cutting, drilling or other methods of seal penetration that would trigger in-depth seal verification. The science of SFC combines a low cost, easy to use and scalable technique that merges existing technology with new features that include multilayered protection with overt, covert and forensic-level security features.

Applications on Seals

Seals are used in nuclear verification regimes to determine that material is neither introduced nor removed from a tamper-indicating container or that unattended monitoring equipment is not tampered with. Additionally, seals provide a unique identity (a tag) for the sealed container or item. Seal criteria include reliability, tamper-indication, *in situ* verification to reduce inspection effort, ease of evaluation of results, and ease of conclusiveness. These requirements are met by incorporating various layers of authentication and tamper indication, such as specially designed

coatings. The IAEA in particular is interested in exploring new coating materials and techniques that would allow for quick and reliable verification of seal authenticity and integrity through characteristic optical measurements unique to the coating. Such innovations could serve the safeguards community by improving the timeliness of detections and confidence in verification.

References

1. IAEA Department of Safeguards. 2010-2011. R&D Program.
2. *LSA Technology*. Ingenia Technology accessed Feb. 23 2012. Available from http://www.ingeniatechnology.com/the-lsa-technology/.
3. LaMontagne, S. 2010. Overview of Containment/Surveillance for International Safeguards, in NNSA Office of Safeguards at the INMM International Workshop on Containment and Surveillance: Concepts for the 21st Century, June 7-11, at Oak Ridge, Tennessee USA.
4. Brinker, C. J., and G. W. Scherer. 1990. *Sol-Gel Science: The Physics and Chemistry of Sol-Gel Processing*. San Diego, CA: Academic Press, Inc.
5. Schwartz, R. W., T. Schneller, and R. Waser. 2004. Chemical Solution Deposition of Electronic Oxide Films, *Comptes Rendus Chimie* 7 (5):433-461.
6. Feng, W., S. H. Patel, M. Y. Young, J. L. Zunino, and M. Xanthos. 2007. Smart Polymeric Coatings—Recent Advances, *Advances in Polymer Technology* 26 (1):1-13.
7. Hench, L. L., and J. K. West. 1990. The Sol-Gel Process, *Chemical Reviews* 90 (1):33-72.
8. Lichtenberger, R., and U. Schubert. 2010. Chemical Modification of Aluminium Alkoxides for Sol-gel Processing, *Journal of Materials Chemistry* 20 (42):9287-9296.
9. de Lange, R. S. A., J. H. A. Hekkink, K. Keizer, and A. J. Burggraaf. 1995. Polymeric-silica-based Sols for Membrane Modification Applications: Sol-gel Synthesis and Characterization with SAXS, *Journal of Non-Crystalline Solids* 191 (1-2):1-16.
10. Lenza, R. F. S., and W. L. Vasconcelos. 2001. Preparation of Silica by Sol-Gel Method Using Formamide, *Materials Research* 4 (3):189-194.
11. Ishizaka, T., R. Nozaki, and Y. Kurokawa. 2002. Luminescence Properties of Tb(3+) and Eu(3+)-doped Alumina Films Prepared by Sol-gel Method Under Various Conditions and Sensitized Luminescence, *Journal of Physics and Chemistry of Solids* 63 (4):613-617.
12. Mendez-Torres, A., D. Krementz, G. Weeks, K. S. Brinkman, J. E. Walker, D. L. Zamora, J. A. Romero, T. M. Weber, H. A. Smartt, and B. Schoeneman. 2011. Intrinsically Tamper Indicating Ceramic Seal (ITICS), *Proceedings of the Institute of Nuclear Materials Management 52nd Annual Meeting*.
13. Cabello, G., L. Lillo, C. Caro, G. E. Buono-Core, B. Chornik, and M. A. Soto. 2008. Structure and Optical Characterization of Photochemically Prepared ZrO2 Thin Films Doped with Erbium and Europium, *Journal of Non-Crystalline Solids* 354 (33):3919-3928.
14. Yoldas, B. E. 1975. A Transparent Porous Alumina, *Ceramic Bulletin* 54 (3):286-288.
15. Yoldas, B. E. 1975. Alumina Sol Preparation from Alkoxides, *Ceramic Bulletin* 54 (3):289-290.
16. Lenza, R. F. S., and W. L. Vasconcelos. 2001. Structural Evolution of Silica Sols Modified with Formamide, *Materials Research* 4 (3):175-179.
17. Roy, A., and A. K. Sood. 1995. Phonons and Fractons in Sol-gel Alumina: Raman Study, *Pramana-Journal of Physics* 44 (3):201-209.
18. Krishnan, R. S. 1947. Raman Spectrum of Alumina and the Luminescence of Ruby, *Proceedings of the Indian Academy of Sciences, Section A* 26:450-459.
19. Doss, C. J., and R. Zallen. 1993. Raman Studies of Sol-gel Alumina: Finite-size Effects in Nanocrystalline AlO(OH), *Physical Review B* 48 (21):15626-15637.
20. Socrates, G. 2001. *Inrfrared and Raman Characteristics Group Frequencies: Tables and Charts*. 3rd ed. West Sussex, England: John Wiley and Sons.
21. Bertoluzza, A., C. Fagnano, M. A. Morelli, V. Gottardi, and M. Guglielmi. 1982. Raman and Infrared Spectra on Silica Gel Evolving Toward Glass, *Journal of Non-Crystalline Solids* 48 (1):117-128.
22. Pucker, G., S. Parolin, E. Moser, M. Montagna, M. Ferrari, and L. Del Longo. 1998. Raman and Luminescence Studies of Tb3+ Doped Monolithic Silica Xerogels, *Spectrochimica Acta Part a-Molecular and Biomolecular Spectroscopy* 54 (13):2133-2142.
23. Galeener, F. L. 1985. Raman and ESR Studies of the Thermal History of Amorphous SiO_2, *Journal of Non-Crystalline Solids* 71 (1-3):373-386.
24. Riegel, B., I. Hartmann, W. Kiefer, J. Gross, and J. Fricke. 1997. Raman Spectroscopy on Silica Aerogels, *Journal of Non-Crystalline Solids* 211 (3):294-298.
25. Murray, C. A., and T. J. Greytak. 1979. Intrinsic Surface Phonons in Amorphous Silica, *Physical Review B* 20 (8):3368-3387.
26. Gottardi, V., M. Guglielmi, A. Bertoluzza, C. Fagnano, and M. A. Morelli. 1984. Further Investigations on Raman Spectra of Silica Gel Evolving Toward Glass, *Journal of Non-Crystalline Solids* 63 (1-2):71-80.
27. Lippert, J. L., S. B. Melpolder, and L. M. Kelts. 1988. Raman Spectroscopic Determination of the pH Dependence of Intermediates in Sol-gel Silicate Formation, *Journal of Non-Crystalline Solids* 104 (1):139-147.

Object-based Image Analysis Using Very High-resolution Satellite Data

Irmgard Niemeyer and Clemens Listner
Forschungszentrum Jülich, Institute of Energy and Climate Research, IEK-6: Nuclear Waste Management and Nuclear Safety, Jülich, Germany

Sven Nussbaum
University of Bonn, Center for Remote Sensing of Land Surfaces, Bonn, Germany

Abstract

Under the Additional Protocol of the Nonproliferation Treaty (NPT), complementing the safeguards agreements between states and the International Atomic Energy Agency (IAEA), commercial satellite imagery is an important source of information within the "information-driven safeguards" approach of the IAEA. The IAEA faces the challenge of a steadily increasing number of nuclear facilities worldwide and therefore (semi-) automated and computer-driven methodologies can add a big value in the verification process. With regard to satellite imagery, a large number of new commercial optical and SAR sensors with higher resolution, shorter revisiting time, more spectral bands, multiple polarizations, etc., have become available. Another challenge of the IAEA is to stay on top of these new technologies and to use them effectively and efficiently for nuclear verification.

With the advances in satellite sensor technologies as to spatial resolution, the concept of object-based image analysis (OBIA) has been become widely used in different remote sensing applications. By presenting some developments of OBIA algorithms and procedures, our paper aims to highlight the advantages of applying OBIA approaches for nuclear verification. In detail, procedures for object-based change detection, object-based classification, and geoinformation system (GIS) integration are demonstrated.

Introduction

Since the discovery of the Iraqi nuclear weapons program in 1990, satellite imagery has become a powerful and intensely used tool for verifying the states' compliance with their Nonproliferation Treaty (NPT) safeguards agreements. Satellite imagery can assist in the evaluation of site declarations, the detection of undeclared nuclear facilities, and the preparation of inspections or other visits. For analyzing and assessing the development of sites under construction (whether declared or not) and for monitoring clandestine facilities, multitemporal satellite imagery acquired over the same area at different times is needed. In remote sensing processing, the comparison of two or more images acquired at different times in order to identify significant changes of or at the earth's surface is known as change detection.

Change detection has always been an important application for remote sensing data. Change detection techniques are being used in a variety of fields, such as disaster management, forestry monitoring, water level monitoring, infrastructure planning, and many more. According to the broad range of change detection applications using remote sensing data, also a huge number of data processing methods were proposed,[1-4] methods analyzing difference images, classification-based approaches, and kernel-based methods such as principal component analysis or multivariate alteration detection, to name just a few examples. All these approaches have in common that they compare corresponding image pixels of different acquisition times.

However, the results of the pixel-based change detection and classification approaches are often limited when used with very high spatial (VHR) imagery. Due to the increased information density of the VHR image data, too many changes or small scale pixel value varieties are detected that may not be of interest for the particular application. This problem is also known as the "salt and pepper" effect when applying pixel-based classifiers to VHR imagery.

For processing VHR imagery, the aggregation of similar neighboring pixels into homogeneous objects, also referred to as segmentation, has therefore become more and more popular in the last ten years. By segmenting the image pixels into meaningful segments (or objects) based on different criteria, the images can then be analyzed based on the image objects and their object features such as shape, relations, and texture. This paradigm is called object-based image analysis (OBIA). Both object-based change detection and classification methods show benefits compared to pixel-based approaches when applied to VHR imagery, as shown in a number of studies.[5] Besides the advantage of extracting and managing image information more effectively and efficiently, OBIA is also promising in terms of automating the operational imagery analysis task.

Given these advantages, OBIA approaches can also support and enhance the satellite imagery analysis within nuclear

safeguards applications, in which VHR imagery is the most commonly used type of remote sensing data. Our paper aims to highlight the advantages of applying OBIA approaches for nuclear verification. In detail, procedures for object-based change detection, object-based classification and GIS integration are demonstrated.

First, we will present an object-based change detection procedure for nuclear verification applications, consisting of a segmentation method adapted for change detection.

Second, we will focus on object-based techniques for change detection. We will present the idea of the regularized iteratively reweighted multivariate alteration detection (MAD) method and show which modifications are necessary to obtain a stable behavior of the algorithm. We briefly review the use of class-based feed-forward networks for classifying the objects' changes and show the change detection workflow including generating the object correspondence.

Third, we will demonstrate how to use the results from object-based change detection and object-based classification in geoinformation systems (GIS), such as geo-mapping tools, geo-browsers, or more advanced geospatial databases. As the segmentation of the image prior to change detection or classification means provides GIS ready entities in the form of objects, results from object-based image analysis can easily be integrated and utilized in GIS.

Investigations on the suggested segmentation procedure are presented. Starting with three experiments using three different change detection approaches, case studies on real data will be shown. Then we give some general conclusions.

Image Segmentation Adapted for Object-based Change Detection

Introduction

Earlier studies[6,7] turned out that segmentation is the crucial step in object-based change detection. For image data taken over the same area at two different acquisition times, the image segmentation could be generally performed in three different ways:

a) on the basis of the bi-temporal data set, i.e., using a data stack consisting of both scenes;
b) based on the image data of one acquisition time, the generated object boundaries are then simply assigned to the image data of the second acquisition;
c) separately for the two times, i.e., the two data sets are segmented independently.

When using a segmentation as suggested in (a) or (b), the resulting image objects have the same geometric properties at the two times, i.e., time-invariant shape features. Change detection can only be applied to a limited number of time-variant object features, such as layer values, texture etc. Provided independent segmentation of the two scenes (c), also the image object geometry varies in time. In this case, all available object features could be used for object-based change detection. However, the issue of linking objects has not been solved satisfactorily yet. In summary, each of the three approaches has severe drawbacks concerning the use of shape features, segmentation robustness and quality, or the problem of linking corresponding objects of different acquisition times. See Reference 6 for a more detailed discussion.

Therefore, we will present a new segmentation approach for object-based change detection.[8] The method is based on the idea of multiresolution segmentation,[9] which is a core component of the eCognition software.[10] Given a bi-temporal dataset acquired over the same area, the adapted procedure aims to provide almost identical segments for image regions where no temporal changes occurred and different segments for temporally changed image regions.

Multiresolution Segmentation Adapted for Object-based Change Detection

The general idea of our work is to create segmentations of the two images I_1 and I_2, acquired at different times over the same area, that only differ in image regions where actual changes took place. For this purpose we adapted a region-growing segmentation algorithm called multiresolution segmentation,[9] which is available in the eCognition software for object-based image analysis.[10] The multiresolution segmentation starts with pixels as initial segments and iteratively aggregates neighbouring segments to bigger segments according to predefined heterogeneity criteria.

However, object-based change detection requires a segmentation technique that similarly extracts objects that have not changed their shape and size between the two acquisition times. The multiresolution segmentation implemented in the eCognition software uses homogeneity criteria based on color and shape, and a scale parameter in combination with local and global optimization techniques. Thus, applying the same segmentation parameters to both scenes does hardly produce similar objects in image regions with no or negligible changes, if other parts of the image have slightly changed.

In our procedure, the multiresolution segmentation is used to generate a segmentation of I_2. After that, the segmentation is also applied to I_2 and tested for its consistency. If a segment is found to be inconsistent with I_2, it will be split up. But let us start with describing the multiresolution segmentation in more detail, before introducing the adaption for change detection.

Multiresolution segmentation is a region-based approach. In this approach, segments can be considered as binary trees in which the leaf nodes correspond to single pixels and every merge step can be represented by a non-leaf node. According to this model, we will use the terms segment and node synonymously throughout this paper.

The multiresolution segmentation starts with an initial chessboard segmentation that identifies each pixel as an individual segment. Then, segments grow in multiple cycles. In each cycle a random seed S_1 of minimal tree depth is selected iteratively in

order to check if one of its neighbors S_2 can be merged with S_1 to a new segment S_{new}. The degree of fitting is modeled by the measure of heterogeneity h that has to fulfill

$$h(S_{new}) < T, \quad (1)$$

T being a given threshold.

The aim is to minimize h in the neighborhood of S_1 when being merged with S_2. Furthermore, S_1 has also to minimize h in the neighborhood of S_2. Otherwise, S_2 is set to be the next seed. This strategy, called *local mutual best fitting* (see Figure 1), results in a path of descending values for h leading to a local minimum. Hence, it is impossible to run into an infinite loop. Moreover, this strategy causes a regular growth of the segments. For specific formulas on the heterogeneity measure, see Reference 11.

If no local mutual best fitting neighbor has been found given seed S_1, it is marked as final. Final segments can no longer be merged with other segments until the end of a segmentation cycle or a merge of neighboring segments. If all segments have been marked as final, the algorithm continues with the next cycle by resetting all segments from final. The algorithm ends if none of the present segments has been merged with another segment during a cycle.

In case a single image is being segmented, the information about the child segments has no further relevance after merging them. However, as we intend to test the segmentation of one acquisition time for consistency with an image of another acquisition time, the information on the segment history, i.e., the segment hierarchy, needs to be saved within the process. Depending on the applied consistency tests, also information on the neighborhood existing at the time a segment was created could be necessary.[11]

Following the insight into the multiresolution segmentation algorithm, we now focus on adapting this algorithm to the problem of segmenting two images of the same area acquired at different times. We therefore propose the following approach:

1. Segment image I_1 using the multiresolution segmentation algorithm.
2. Apply this segmentation to image I_2 and recalculate the heterogeneity of each segment based on the data of I_2.
3. Check every merge, i.e., every segment that consists of more than one pixel, for consistency by applying a test criterion. Not only the top-level segments, i.e., the nodes without parents, need to be examined but all nodes in each segment tree except for the leaf nodes.
4. Remove all inconsistent nodes using a segment removal strategy.
5. Rerun the multiresolution segmentation to obtain a final segmentation of the second image.

These steps present a general process which has to be specified in two aspects. First, how can segments of image I_1 be checked for consistency with image I_2 and second, how can inconsistent segments be removed?

Figure 1. Local mutual best fitting strategy

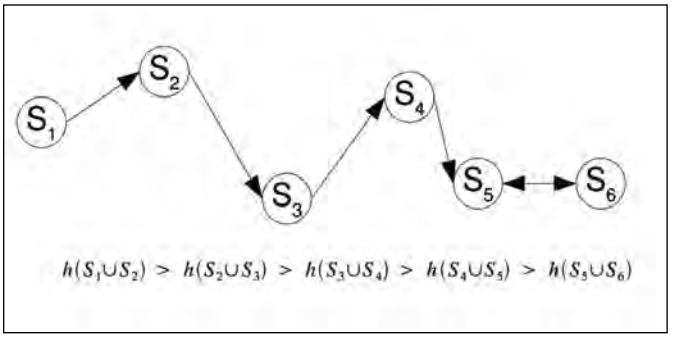

With regard to the consistency tests we propose three different criteria. The first one, named *threshold test*, examines whether a given segment S fulfills the condition

$$h(S) < T_{check}. \quad (2)$$

Otherwise the segment S is marked as inconsistent. The threshold test is the weakest test with respect to changes between the two images.

The second test, called *local best fitting test*, tries to repeat the merge procedure with the data of image I_2. Given an exemplary segment structure with parent segment S_3 and its children S_1 and S_2, the test assumes S_1 to be a seed and searches for locally best fitting neighbors from the list of merge candidates that has been stored during the segmentation of image I_1. If the best fitting neighbor is S_2, the test is passed, otherwise it is failed. Besides, also the condition given in Equation 2 needs to be fulfilled. Obviously, this test is very sensitive even to small changes or noise in the imagery. In order to reduce the sensitivity of the test, a parameter $T_{checktolerance}$ is introduced. The idea of this additional parameter is that a merge may not be the locally best fitting one but could belong e.g., to the 10 percent best fitting ones. Therefore the test checks how many merge candidates perform better (n_{better}), equally well (n_{equal}) and worse (n_{worse}) than the segment that has been merged to the seed. If the condition

$$\frac{n_{better}}{n_{better} + n_{equal} + n_{worse}} < T_{checktolerance} \quad (3)$$

holds, the consistency test is considered to be passed.

Finally, the third test is named *local mutual best fitting test*. It also tests if S_2 is the best fitting neighbor for seed S_1 in the list of merge candidates but checks additionally if S_1 is the best fitting neighbor for S_2. This test's principle is derived from the idea of local mutual best fitting presented before. Compared to the local best fitting test, this test is more sensitive; however, applying Equation 3 could also reduce the sensitivity of this test. In general, splitting-up segments could be avoided by increasing

Figure 2. Universal segment removal strategy

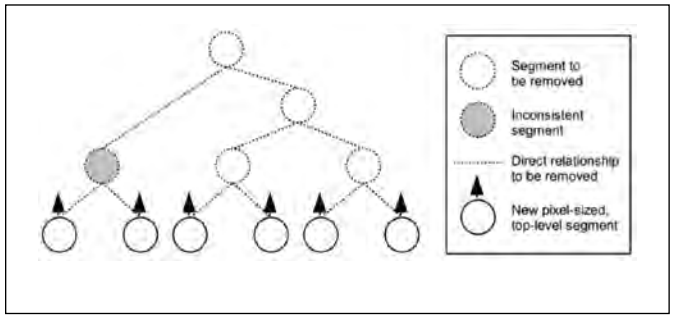

threshold T_{check}. Then, not all changes between I_1 and I_2 may result in changes of the segmentation.

After testing all given segments for consistency with the image I_2, those segments that did not pass the test have to be handled. We therefore introduce three strategies to remove these segments. The first strategy is named *universal segment removal strategy*. The principal idea of this strategy is illustrated in Figure 2. It searches for the top-level segment of an inconsistent segment and splits it into its elements. As a result, only pixel segments will remain. Obviously, this strategy affects the segmentation intensively and could therefore create changes in the final segmentation in areas where no actual changes can be observed.

The second strategy for removing inconsistent segments is the *global segment removal strategy*. Its basic principle, as illustrated in Figure 3, is to remove the inconsistent segment and all its ancestors from the segment tree. During this process all remaining segments are considered to be new top-level segments. In this way, the impact on the segment tree is reduced. However, this strategy is very adaptive in creating changes only in parts of the segment tree in which changes can be detected and leaves the rest as it is.

The third and most complex segment removal algorithm is called *local segment removal strategy*. It is developed due to the fact that the global segment removal strategy affects parts of the segment tree which do not necessarily change between different acquisition times. Consider for example a big object in image I_1 that is segmented correctly. If only a small part of this object changes from one acquisition time to another, it may be a better to extract this small part instead of splitting up the whole object.

Therefore we propose an additional method for removing inconsistent segments: Assume I to be an inconsistent node. Then remove I and its parent P from the segment tree. Set I's children C_1 and C_2 as top-level segments and put I's sibling S as child of I's grandparent G. This method is illustrated in Figure 4. It has turned out that the local segment removal strategy cannot be applied directly in all possible constellations. See Reference 11 for a more detailed discussion of this issue.

In this section we have shown some ideas for addressing the problem of segmentation for object-based change detection. These ideas were implemented using the C++ programming language including STL[12] and GDAL.[13]

Figure 3. Global segment removal strategy

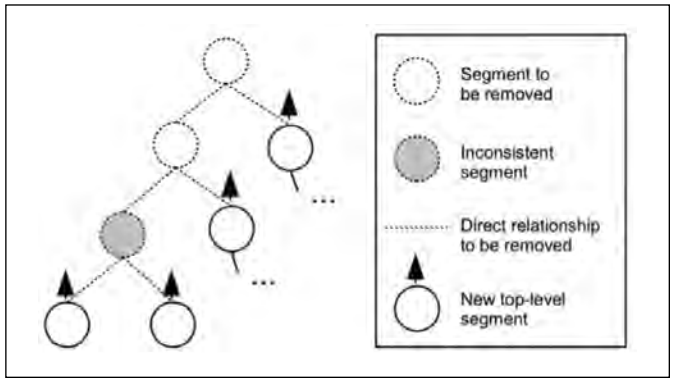

Figure 4. Local segment removal strategy

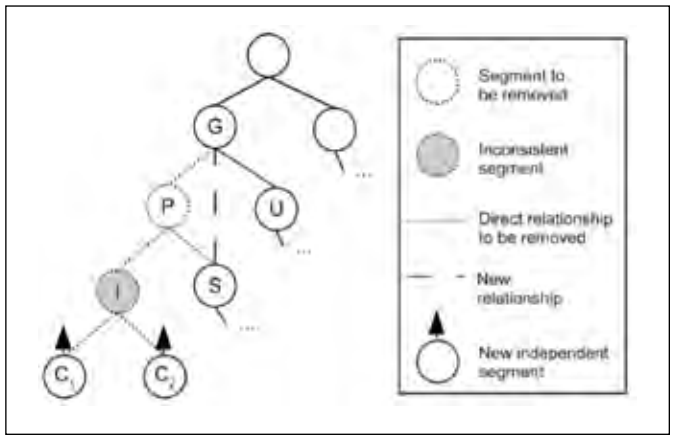

Object-based Techniques for Change Detection

Introduction

Interesting object-based approaches have been introduced in the last years. Some authors presented object-based classifications for change detection studies.[14-18] Other authors proposed change detection combining object-based classification and geo-information systems (GIS).[19-21] Some other authors developed object-based change detection techniques employing the differences of spectral and textural object features existing at the considered acquisition times.[22-25] See Reference 8 for a comprehensive discussions of the cited publications on object-based change detection.

Besides object class membership, spectral, and textural differences, also the temporal modification of other object features could be utilized for statistical change detection. Additional layer features, like ratio, standard deviation, and others, as well as relational and shape features could help to address thematic, geometric and topologic object changes between two acquisition times. In References 6 and 7, the so-called regularized iteratively reweighted multivariate alteration detection (IR-MAD)[26] was

applied for analyzing changes of image objects based on their features. The MAD transformation[27] was originally developed for pixel-based change detection. It is based on a classical statistical transformation of the multispectral feature space referred to as canonical correlation analysis to enhance the change information in the difference images. When applying the IR-MAD transformation to a feature space with only small correlations between the dimensions, normally no numerical issues occur. However, in datasets with high correlation between the dimensions, as it can be found in hyperspectral data or object-based processing using many features, the algorithm results in near-singular covariance matrices which cannot be inverted in a straightforward way. In this context, it was proposed in Reference 26 to reduce the dataset dimensionality and hence to decrease the correlation between the dimensions. We therefore implemented a principal component analysis (PCA) transformation into the object-based change detection process for reducing the feature space dimensions before applying the IR-MAD method.

IR-MAD Adapted for Object-Based Change Detection

The IR-MAD method is a linear transformation of the feature space aimed at enhancing the change information in the difference image. It models an object's feature vector as random vectors F and G of length N with F representing the information from the first and G from the second image. It then uses the corresponding covariance matrices Σ_{FF}, Σ_{FG} and Σ_{GG} to calculate the transformation vectors a and b as the solution of the generalized coupled eigenvalue problem

$$\begin{aligned}\Sigma_{FG}\Sigma_{GG}^{-1}\Sigma_{FG}^{T}a &= \rho^{2}\Sigma_{FF}a,\\ \Sigma_{FG}\Sigma_{FF}^{-1}\Sigma_{FG}^{T}b &= \rho^{2}\Sigma_{GG}b.\end{aligned} \tag{4}$$

Solving this problem yields N solutions with eigenvectors a_i and b_i and corresponding eigenvalues ρ_i sorted in ascending order. Using this result, the transformed difference images M_i is calculated as

$$M_i = U_i - V_i = a_i^T F - b_i^T G. \tag{5}$$

It can be shown that M_1 has maximum variance and thus U_1 and V_1 minimum correlation under the constraint that $Var(U)=Var(V)=1$. The transformed imagery emphasizes the differences between the two acquisition times. Moreover, the M_i's, referred to as MAD components, are mutually uncorrelated which has the effect that different components show different types of changes. The sum of squares of standardized variates is approximately chi-square distributed with N degrees of freedom. Supposing that no-change pixels have a chi-square distribution with N degrees of freedom, N being the number of MAD components, the change-probability can be derived for each pixel or object. See References 26 and 4 for a more comprehensive explanation of the IR-MAD method.

As the covariance matrices have to be estimated from the imagery, they may not always be invertible.[26] However, Equation 4 requires the inversion of Σ_{FF} and Σ_{GG}. Therefore, we propose to reduce the dimensionality of the data using the principal component analysis (PCA). Principal component analysis is a linear transformation like the IR-MAD method. The difference to IR-MAD is that PCA operates on a single dataset which is modeled by a random vector F. Based on this vector's covariance matrix Σ_F, the eigenvalue problem

$$\Sigma_F a = \rho a \tag{6}$$

is solved. This yields N pairs of eigenvalues a_i and corresponding eigenvectors ρ_i sorted in descending order, that are then used to carry out the transformation

$$U_i = a_i^T F. \tag{7}$$

It can be shown that the variance is maximized for U_i under the constraint that $|a_i|=1$ and that U_i is not correlated to any component U_j with $j<i$. The variance of the single components is given by

$$Var(U_i) = \rho_i . \tag{8}$$

For more information on PCA see Reference 4. Hence, only those components containing a significant high variance are used for further analysis, the remaining features are ignored.

In practice, we estimate the covariance matrix Σ_F by using both images. Then the imagery is transformed and the features $U_1,\ldots,U_M$ are selected if they describe at least 95 percent of the total variance, i.e.,

$$\sum_{i=1}^{M} Var(U_i) \Big/ \sum_{i=1}^{N} Var(U_i) \geq 0.95. \tag{9}$$

Both IR-MAD and PCA transformation were programmed using the Newmat C ++ matrix library and Numerical Recipes Software and implemented as eCognition Developer plug-in using the eCognition Software Development Kit (SDK).

Classification of Object Changes Using Neural Networks

In earlier studies,[30,7] two different two-layered feed forward network topologies were tested for object-based classification: Standard feed forward network (FFN) and the so-called class-based feed forward network (CBFFN). The new architecture of CBFFN was developed using the feed forward neural networks to especially facilitate the handling of the huge feature space within the object-based image analysis and to automatically extract the relevant object features. This architecture is named class-based as the output of the individual class-related FFNs defined in the architecture only use the characteristic features of the particular classes and make a final decision in the end. The proposed ar-

Figure 5. Object correspondence: a) Directed, b) via intersection

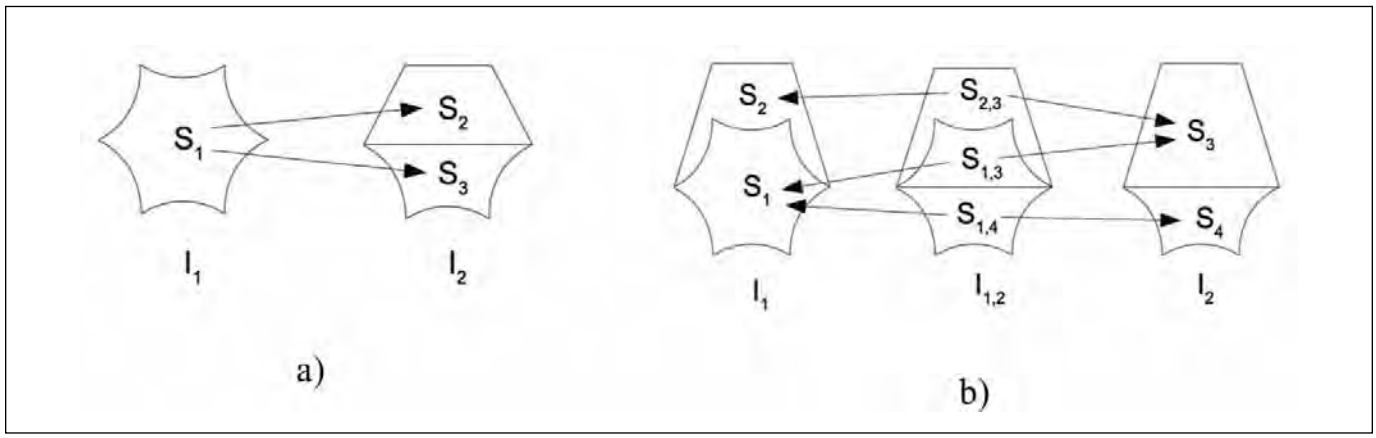

chitecture consists of two layers of neural networks. In the first layer there are exactly K networks NN_k representing K classes. The network representing class k is only fed with the characteristic features of that class. The output of each network represents a fuzzy value of each class which are then fed as input to the second layer network. The second layer network finally gives a class membership probability for every class. Three learning algorithms and two combinations for a two-layered feed forward network (FFN) were used: back propagation, Kalman filter training, scaled gradient conjugated (SCG), Kalman filter and back propagation, Kalman filter and SCG. The two network topologies with the five learning algorithms were programmed and implemented as eCognition Developer plug-in using the eCognition Software Development Kit (SDK) and IT++ library. For more detailed information, see References 30 and 7.

Object-based Change Detection Workflow

Using the segmentation as described above, it is possible to retrieve a segmentation of the imagery with at least three advantages: Firstly, we are now able to integrate shape features into the change analysis. Secondly, the presented segmentation algorithm is robust as it only leads to a different segmentation of image I_2 in areas where using the segmentation of I_1 would not be consistent with the data of I_2. Thirdly, the segmentation results have a high quality because it is not necessary to produce a single segmentation taking both images I_1 and I_2 into account. However, we still receives separate object layers for either acquisition time, which have to be connected in order to obtain a correspondence between the image objects. Corresponding objects are required for applying the IR-MAD transformation, since the IR-MAD algorithm models the objects from I_1 and I_2 as realisation of random feature vectors F and G respectively. Hence, we need to estimate the parameters using corresponding realisations of F and G. For that reason we will propose two procedures on how to establish a one-to-one relationship between the segmentations of image I_1 and I_2.

The first procedure, named *directed object correspondence*, associates each segment S_i in I_1 with all segments $T_1,\ldots,T_n$ in I_2 that are overlapping S_1. Since this would not establish a one-to-one relationship, we set the realisations of X and Y to

$$x_i = f_x(S_i),$$
$$y_i = \frac{1}{n}\sum_{k=1}^{n} f_y(T_k), \tag{10}$$

where f_x and f_y are functions returning the feature vectors of a given segment in the image I_1 and I_2 respectively. Thus, a pair of values (x_i,y_i) is available for every segment S_i in image I_1. This result can now be used to estimate the probability distribution's parameters. An example for a specific object constellation illustrating the method is given in Figure 5a.

The second procedure for establishing an object-to-object relationship between the segmentations of image I_1 and I_2 is called *correspondence via intersection*. The main idea of this method is to construct a third segmentation by intersecting segments from the segmentations of I_1 and I_2. Given the segments S_1 from the segmentation of I_1 and S_2 from the segmentation of I_2, a segment $S_{1,2}$ is constructed by

$$S_{1,2} = S_1 \cap S_2 \tag{11}$$

This automatically involves a unique correspondence of $S_{1,2}$ in the images I_1 and I_2. Hence, the realisations of X and Y can be calculated straightforwardly for each segment $S_{1,2}$ by

$$x_i = f_x(S_1),$$
$$y_i = f_y(S_2). \tag{12}$$

An example for the application of the method for *object correspondence via intersection* is given in Figure 5b.

Information Management by using Geographic Information Systems (GIS) and Geodatabase Systems

Introduction

In the procedure of implementing the so-called "information-driven safeguards" the IAEA faces the challenge not to drift into "information-overloaded safeguards." The IAEA has a very large amount of data stored in different locations, in different formats like paper or digital and in multiple formats. The data is available in form of structured and non-structured data. One way of organizing the vast amount of information is based on location using Geographic Information Systems (GIS) and Geodatabase Systems (GDBS). The IAEA has a lot of information that is bound to a location, e.g., information about a nuclear site, a facility, a material balance area or even an environmental sample location. Organizing the data in a geographic way based on location is therefore one natural step in the process of information driven safeguards.

Using GIS or GBDS will not only be beneficial for organizing and visualizing the data. It will also increase the analytical capabilities by introducing new tools, methods and services and it allows the perform analysis in the area of geospatial analysis.

Object-based Geospatial Analysis — A Useful Tools for Safeguards

According to Tobler's first law of geography, "Everything is related to everything else, but near things are more related than distant things." This is also true for safeguard relevant information, meaning that the location of things matter. Examples are general facts like the following: nuclear power plants need water for cooling, so they are generally near to water, mining and milling facilities are often close together because of transportation issues and cost. Taking site-specific features into account, visualization of the data by location might reveal relationships which were not visible before. Having location information allows also the implementation of spatial queries to the data. This could be for example, "Is there any big water supply within a radius of 10 km of that facility?"or "Are there any buildings within a radius of 50m of the reactor that deal with waste processing?"

Having data organized in a GIS and therefore having spatial information available also opens the door to the field of more complex spatial analysis. These tools and algorithms should be considered in the verification process and the IAEA might integrate these more often in its methodology portfolio.

One example that might be of interest are the so-called visibility tools, like view shed or line of sight (LoS). These are available in the ESRI ArcMAP software suite (www.ESRI.com). The LoS determines whether a given target is visible from a point of observation.[29] This tool is important so inspectors can plan their inspection routes through the facilities from the headquarters and are aware of which buildings and structures they see on the route and which they will not. If the inspectors is interested in a special area or building he can find out beforehand where he needs to be at that facility to see that special feature. A requirement for an efficient use of that tool is the existence of a good model of the site and capable of 3D information. A model of a nuclear site can be derived by using the previously introduced segmentation techniques or a manual digitizing of the objects of interest. The height of the single buildings might be provided using Digital Surfaces Models (DSM) from high-resolution satellites,[30] or specialized software or from a single satellite scene using shadow measurements of buildings.

Once 3D information exists other analysis can be performed. There are many examples from civil engineering which could be also applied to the area of safeguards. ESRI asked on its homepage (www.esri.com) "Who Benefits from 3D GIS?" and gives some example answers like: "Mining and geoscientists can examine subsurface structures and calculate volumes." That is interesting for

Figure 6 shows an example from the ESRI webpage, using ESRI City-engine to model a site and then perform a LoS analysis. The orange square is the position of the observer (like the inspector) and the green lines are her/his visible field. The red lines cannot be seen from the position of the inspector.

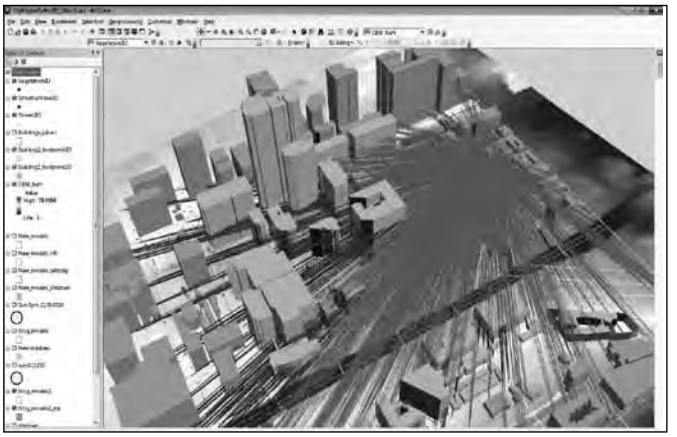

Figure 6. A visibility analysis performed on a 3D model, © by ESRI.com

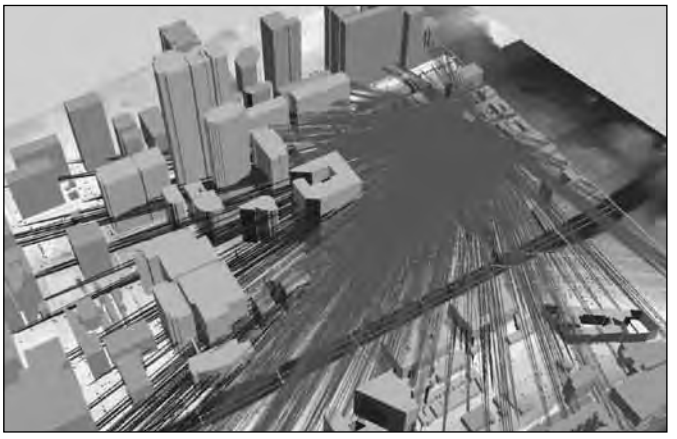

Figure 7. Results of the experiment. Left: Segmentation of the bi-temporal imagery using the threshold test (top) and the universal segment removal strategy (bottom). Middle: Directed change detection. Changes from time 1 to time 2 (top) and from time 2 to time 1 (bottom). Right: Change detection using intersected objects (top) and using MAD objects.

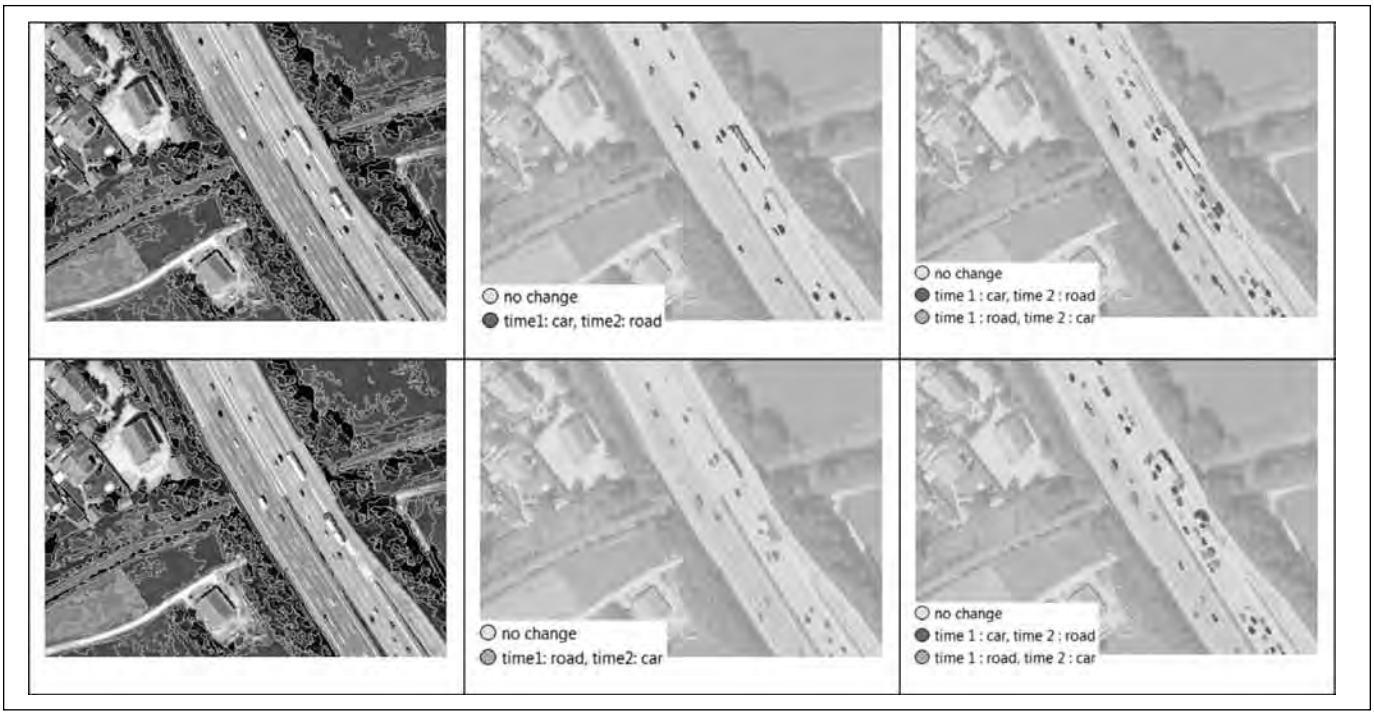

the IAEA and the area of safeguards too. Could geospatial analysis be used to calculate the volume of mining spoils from a uranium mine and then give conclusions about the amount of material possible mined? Geospatial analysis can also be used to monitor the earth spoils from an underground facility under construction. An example is given in Reference 31; here the amount of spoils over time gives a hint about how much activity is taken out at that site.

Investigations

Experiments

Some experiments were carried out using bi-temporal RGB aerial imagery, acquired over a German motorway with a time difference of 0.7s. This particular dataset was selected to focus on the specific changes (vehicles movement) and to limit false alarms due to illumination and/or seasonal changes at the two acquisition times. However, some false alarms may result from sensor noise, different acquisition angles and registration inaccuracy.

For segmentation, the threshhold test and the universal segment removal strategy and turned out to provide the best results. The procedure similarly extracted objects that have not changed their shape and size on both sides of the motorway and provided different results for the motorway.

The change detection procedure was tested using the eCognition Developer software with three different configurations. In the first experiment, hereinafter referred to as *directed change detection* the changes were estimated in either directions, i.e., from time 1 to time 2 and from time 2 to time 1. The second experiment applied the object correspondence via intersection and was named *Change detection using intersected objects* in the following. The third experiment, titled *Change Detection Using MAD Objects,* conducted the IR-MAD on the image pixels and continued with an object-based classification using neural networks (Figure 7).

The accuracy assessment of the three experiments gave high overall accuracy (0.98-0.99) and promising kappa coefficients (0.75-0.82) for either approach. However, the user's and producer's accuracy varied for the three approaches and for the change classes. For more information on the experiment and the accuracy assessment, see Reference 8.

Case Studies

Finally, we tried to apply our methodology to real satellite imagery. Therefore, we used two images acquired in June 2005 and July 2006 over the Olkiluoto site in Finland, with two reactors in operation and the third under construction. As these images were taken almost at the same time of the year, it was expected to reduce influences of different shadows and changes in vegetation which normally cause false alarms. After co-registering the imagery, we applied radiometric normalization and segmentation using the methodology introduced before with the universal segment removal and the threshold test. This was followed by

Figure 8. Change analysis of the Olkiluoto site, from upper-left to lower-right: image acquired in June 2005, image acquired in July 2006, χ^2-values, change classification.

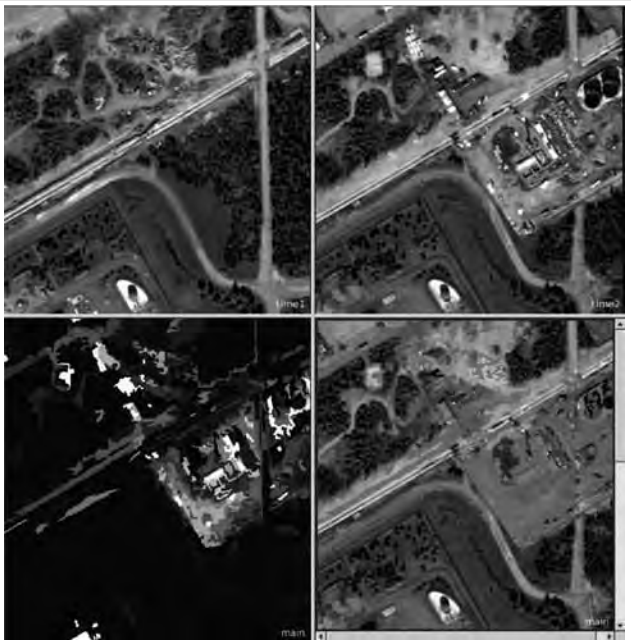

establishing the object links using change detection using intersectional objects (CDIO). Using this segmentation as a basis, we carried out a dimensionality reduction using PCA using mean, standard deviation, shape index and compactness as input object features. After that, the IR-MAD was applied on the principal components. Finally, we classified the relevant changes using a threshold on the χ^2-value. The result of this process is displayed in Figure 8. It can be seen that still some false alarms occur in the resulting change map. However, the most relevant changes in the imagery have been detected using the proposed method.

Conclusion

We presented some new ideas for object-based change detection using remote sensing imagery. An enhanced procedure for segmentation was introduced and implemented into the change detection workflow. Moreover, numerically issues in the IR-MAD method were addressed. The proposed methods showed good results in three experiments using aerial imagery.

Nevertheless, further developments are needed such as new consistency tests and segment removal strategies. Moreover, methods for enabling the user to easily select the segmentation parameters, e.g., by using training samples, would be helpful. Finally, the adapted multiresolution segmentation needs to be implemented as eCognition plugin for allowing its direct use in the proposed change detection workflow.

The presented OBIA tools are available for download at http://www.treatymonitoring.de/tools/.

In general a GIS is a good tool for organizing, visualizing, and analysing safeguard relevant information and geospatial analysis is a valuable add-on to consider in the analysis portfolio of the IAEA analysts. But of course not all the information the IAEA has is location based. GIS systems and spatial analysis can only be one tool within many, but in the mind of the authors there should be part of the agency' information driven safeguards.

References

1. Singh, A., 1989. Review Article Digital Change Detection Techniques Using Remotely-Sensed Data, *International Journal of Remote Sensing* 10 (6), 989–1003.
2. Lu D., P. Mausel, E. Brondizio and E. Moran. 2004. Change Detection Techniques. *International Journal of Remote Sensing,* 25(12), 2365–2407.
3. Radke, R., Andra, S. & Al-Kofahi, O., 2005. Image Change Detection Algorithms: A Systematic Survey. *IEEE Transactions on Image Processing* 14 (3), 294–307.
4. Canty, M.J., 2009. *Image Analysis, Classification, and Change Detection In Remote Sensing: With Algorithms For ENVI/IDL.*
5. Blaschke, T., S. Lang, and G. Hay, (Eds.), 2008. Object-based Image Analysis Spatial Concepts for Knowledge-Driven Remote Sensing Applications. Series: Lecture Notes in Geoinformation and Cartography. Springer, Berlin.
6. Niemeyer, I., P. R. Marpu, and S. Nussbaum, 2008. Change Detection Using Object Features. In: Blaschke, T., Lang, S. & Hay, G. (Eds.), 2008: *Object-Based Image Analysis Spatial Concepts for Knowledge-Driven Remote Sensing Applications.* Series: Lecture Notes in Geoinformation and Cartography. Springer, Berlin, 185-201.
7. Niemeyer, I., F. Bachmann, A. John, C. Listner, and P. R. Marpu, 2009. Object-based Change Detection and Classification. *Processing SPIE Europe Remote Sensing* 09, Vol. 7477A, Image and Signal Processing for Remote Sensing, Berlin.
8. Listner, C. & Niemeyer, I., 2011: Object-based Change Detection, In *Photogrammetrie, Fernerkundung, Geoinformation* (PFG), Vol. 4 (2011), 233-245.
9. Baatz, M. and A. Schäpe, 2000. Multiresolution Segmentation: An Optimization Approach For High Quality Multi-scale Image Segmentation. Strobl, J., Blaschke, T. & Greisebener, M. (Eds.), 2000. *Angewandte Geographische Informationsverarbeitung XI.* Beiträge zum AGIT-Symposium 1999, Salzburg, Austria, 12 23.
10. Definiens Imaging, 2009: Definiens eCognition Developer 8 User Guide. Munich.

11. Listner, C. and I. Niemeyer. 2010. Multiresolution segmentation adapted for object-based change detection. *Process of the SPIE Europe Remote Sensing* 10, Vol. 7477A, Image and Signal Processing for Remote Sensing.
12. Musser, D.R. and A. Saini, 1995. The STL Tutorial and Reference Guide: C++ Programming with the Standard Template Library.
13. GDAL Development Team, 2010. GDAL - Geospatial Data Abstraction Library, Version 1.6.0. Open Source. Geospatial Foundation.
14. Zhou, W., A. Troy, and M. Grove, 2008. Object-based Land Cover Classification and Change Analysis in the Baltimore Metropolitan Area Using Multitemporal High Resolution Remote Sensing Data. *Sensors* (8), 1613–1636.
15. Hese, S. and Schmullius, C., 2006. Object Context Classification for Advanced Forest Change Classification Strategies, *International Archive of Photogrammetry and Remote Sensing XXXVI* (4/C42), Salzburg, Austria.565–569.
16. Concheddaa, G., Durieux, L. and Mayaux, P., 2008. An object-based method for mapping and change analysis in mangrove ecosystems. *ISPRS Journal of Photogrammetry and Remote Sensing* 63, 578–589.
17. Im, R., J.R. JenSen, and J.A. Tullis, 2008. Object-based change detection using correlation image analysis and image segmentation, *International Journal of Remote Sensing* 29 (2): 399–423.
18. Niemeyer I. and S. Nussbaum, 2006. Change Detection - The Potential For Nuclear Safeguards, In: Avenhaus R., Kyriakopoulos, N., Richard M. and Stein G. (Eds.), 2006. *Verifying Treaty Compliance. Limiting Weapons of Mass Destruction and Monitoring Kyoto Protocol Provisions,* Springer, Berlin, 335–348.
19. Walter, V., 2004. Object-based Classification of Remote Sensing Data for Change Detection, *ISPRS Journal of Photogrammetry & Remote Sensing* 58, 225–238.
20. Hofmann, P., P. Lohmann, and S. Müller, 2008. Concepts of an Object-based Change Detection Process Chain for GIS update, *International Archive of Photogrammetry and Remote Sensing* XXXVII (B4), Beijing, China, 305–312.
21. Changhui, Y., S. Shaohong , H. Jun, and Y. Yaohua, 2010. An Object-based Change Detection Approach Using High-Resolution Remote Sensing Image and GIS Data. *Proccess IEEE International Conference on Image Analysis and Signal Processing* (IASP10), Zhejiang, China,
22. Desclée, B., P. Bogaert, and P. Defourny, 2006. Forest Change Detection by Statistical Object-based Method, *Remote Sensing of Environment* 102, 1–11.
23. Lefebvre, A., T. Corpetti, and L. Hubert-Moy, 2008. Object-oriented Approach and Texture Analysis for Change Detection in Very High Resolution Images. *Proccess International Geoscience and Remote Sensing Symposium* (IGARSS 08), Boston, USA (CD-Rom).
24. Huo, C, K. Z. Chen, H. Lu Zhou, and J. Chenga, 2008. Robust Change Detection by Integrating Object-specific Features, *International Archives of Photogrammetry and Remote Sensing,* XXXVII (B7), Beijing, China, 797–802.
25. Huang, L., G. Zhang, and Y. Li, 2010. An Object-based Change Detection Approach by Integrating Intensity and Texture Differences. *Proccess IEEE 2nd International Asia Conference on Informatics in Control, Automation and Robotics* (CAR 10), 258–261.
26. Nielsen, A.A., 2007. The Regularized Iteratively Reweighted MAD Method for Change Detection in Multi-and Hyperspectral Data. *IEEE Transactions on Image Processing* 16 (2), 463-478.
27. Nielsen, A.A., K. Conradsen, and J. J. Simpson, 1998. Multivariate Alteration Detection (MAD) and MAF Processing in Multispectral, Bitemporal Image Data: New Approaches to Change Detection Studies. *Remote Sensing of Environment* 64, 1–19.
28. Marpu, P. R., 2009. Geographic Object-based Image Analysis. PhD Thesis, Institute of Mine-Surveying and Geodesy, TU Bergakademie Freiberg.
29. ESRI, 1998. ArcView 3D Analyst Features, ESRI Whitepaper.
30. Digital Globe, Advanced Elevation Series, http://www.digitalglobe.com/downloads/Advanced-Elev-Series-DS-AES-Web.pdf
31. Brannan, P., 2009. New Satellite Image Further Narrows Fordow Construction Start Date, ISIS Reports, November 18, 2009, http://isis-online.org/uploads/isis-reports/documents/ISIS_Analysis _of_Imagery_18Nobember2009.pdf.

Scintillating ^{99}Tc Selective Ion Exchange Resins

Mitchell Greenhalgh, Richard Tillotson, and Troy Tranter
Aqueous Separations and Radiochemistry Department, Idaho National Laboratory, Idaho Falls, Idaho USA

Abstract

Scintillating technetium (^{99}Tc) selective ion exchange resins have been developed and evaluated for equilibrium capacities and detection efficiencies. These resins can be utilized for the in-situ concentration and detection of low levels of pertechnetate anions ($^{99}TcO_4^-$) in natural waters. Three different polystyrene-type resin support materials were impregnated with varying amounts of tricaprylmethylammonium chloride (Aliquat 336) extractant, several different scintillating fluors and wavelength shifters. The prepared resins were contacted batch-wise to equilibrium over a wide range of $^{99}TcO_4^-$ concentrations in natural water. The measured capacities were used to develop Langmuir adsorption isotherms for each resin. ^{99}Tc detection efficiencies were determined and up to 71.4 ± 2.6 percent was achieved with some resins. The results demonstrate that a low level detection limit for $^{99}TcO_4^-$ in natural waters can be realized.

Introduction

The main sources for ^{99}Tc in the environment are from nuclear weapons detonation and nuclear fuel reprocessing. ^{99}Tc, with a half life of 2.13×10^5 years, exists in natural waters mainly as the pertechnetate anion species ($^{99}TcO_4^-$). The anion is extremely mobile in the environment and is not easily exchanged onto sediment or geological surfaces.[1] This high mobility makes it possible to detect ^{99}Tc up to hundreds of kilometers from the source,[2] enabling monitoring of natural waters for ^{99}Tc in a variety of locations. A Savannah River Site (SRS) study reported that the ^{99}Tc concentrations in the water surrounding the site to be in the range of 0.59 to 5.9 pg/L.[3]

Typical monitoring efforts consist of acquiring samples, transferring to analytical laboratories for concentration of ^{99}Tc with anion exchange resins and analysis via liquid scintillation counting. The analysis is labor-intensive, time-consuming, and not well-suited for onsite or remote analysis. A large amount of work has been done with extractive scintillating resins that can be utilized in-situ for ^{99}Tc monitoring.[4] Previous research has demonstrated that these specialized resins can be used but suffer from regeneration effects and have mostly focused on relatively high concentrations of ^{99}Tc. The materials prepared in the current studies have been evaluated for equilibrium capacities and detection efficiencies at very low concentrations of ^{99}Tc in natural water. In an equilibration type mode, the amount of activity on a resin changes in proportion to the concentration change of ^{99}Tc in the surrounding environment.[5] Two candidate scintillating resins have been identified that could be incorporated into an in-situ detector system operating in an equilibration type mode for the continuous monitoring of ^{99}Tc in natural waters thus negating the need for resin regeneration.

Experimental

Materials and Chemicals. Polymeric resin beads Amberchrom® CG161 (75 micron), Amberchrom® CG300 (75 micron), Amberchrom® CG71 (75 micron), organic fluor 2,5-Diphenyloxazole(PPO), wavelength shifter 1,4-Bis(2-methylstyryl)benzene(Bis-MSB), methanol (anhydrous 99.8 percent), 2-Propanol (anhydrous 99.5 percent) and benzene (anhydrous 99.8 percent) were obtained from Sigma Aldrich (St. Louis, Missouri USA). Extractant, tricaprylmethylammonium chloride (Aliquat 336) was obtained from General Mills Chemicals (Minneapolis, Minnesota USA). Organic fluor 2-(1-naphthyl)-5-phenyloxazole (α-NPO) and wavelength shifter 1,4-Bis(4-methyl-5-phenyloxazol-2-yl) benzene (dm-POPOP) were from Alpha Aesar (Ward Hill, Massachusetts USA). $^{99}TcO_4^-$ was from Isotope Products Laboratories (Valencia, California USA). $^{99m}TcO_4^-$ was from Advanced Isotopes of Idaho (Pocatello, ID). Natural water was obtained from an untreated well (Idaho Falls, Idaho USA). All chemicals were used as received.

Preparation of Resins. Non-scintillating extractive resins were prepared with all three support materials and Aliquat-336 loadings ranging from 0.1 to 40 wt percent following a modified published procedure.[6] These resins were utilized to evaluate the effects of extractant loadings and various support materials on the Tc uptake capacities. Two grams of air-dried support material was placed into a 100 mL round bottom flask. Twenty mL of methanol was added to the flask and placed on a Buchi rotary evaporator. The mixture was rotated at 150 rpm for thirty minutes. The flask was then lowered into a 45°C water bath under vacuum and the methanol evaporated to near dryness. The flask was removed from the evaporator and a 20 mL solution of methanol containing the appropriate mass of Aliquat-336 was added to the flask containing the resin and then returned to the evaporator. This slurry was rotated at 150 rpm at room temperature for two hours to ensure homogeneity. The flask was lowered into the 45°C water bath under vacuum and the methanol was slowly evaporated to dryness typically over a period

of six to eight hours. The dry resin was slurried in a 20 percent 2-Propanol/water solution and transferred to a glass column. This slurry was allowed to stand for two or more hours until all resin particles had become wetted. The resin was then rinsed with 400 mL of Nanopure water (18 Mohm-cm^{-1}). The prepared resin was stored in this manner until use.

Scintillating extractive resins were prepared in the same manner as above except benzene was used as the solvent, appropriate amounts of scintillating fluors and wavelength shifters were added with the extractant and the water bath temperature was increased to 50°C.

Equilibrium Tc Uptake. One hundred milligrams of prepared resin was transferred into a 20-mL glass tube and contacted for more than three hours on a mechanical shaker with 20mL of ^{99}Tc or ^{99m}Tc spiked well water in the concentration range of approximately 3.0 to 5.9x10^{9} pg Tc/L. All resin batch contacts were performed in triplicate. Samples of the remaining aqueous phase after equilibration were filtered through a 0.2 µm PTFE syringe filter and 1mL of this solution was analyzed for Tc either by a Perkin Elmer Tri-Carb 3100TR liquid scintillation counter (LSC) for ^{99}Tc, or an Ortec gamma spectrometer for ^{99m}Tc. Distribution coefficients (K_d) with the units of mL/g resin for each contact were calculated according to the formula $K_d = ((A_0–A_S)/W)/(A_S/V)$, where A_0 is the activity of the feed solution, A_S is the activity of the test solution after equilibration with the resin, W is the weight of the resin (g), and V is the volume of the contact solution (mL). Tc equilibrium adsorption isotherms were plotted as amount Tc adsorbed (pg/g resin) vs. equilibrium Tc (pg/L) remaining in the aqueous phase. A Langmuir regression was performed on the collected data to obtain the Langmuir constants and the data was fit to a Langmuir equation.

Efficiency Evaluation. Twenty-nine milligrams of scintillating extractive resin was transferred into a 3-mm ID glass tube that had been glued into the bottom of a 20mL glass scintillation vial. An example of the experimental vial can be seen in Figure 1. Two hundred microliters (µL) of a 300Bq/mL ^{99}Tc spiked solution was added to the inner tube containing the resin and the scintillation vial was filled with Nanopure water to maintain optical continuity. The resin was the only scintillating material introduced into the vials.

The samples were counted on an LSC over a range of time from 1 to 300 hours. The efficiency determinations were all performed in triplicate and were calculated as a percent of observed count rate divided by the disintegration rate of 200 µL of the spiked solution in 15 mL of Ultima Gold Scintillation cocktail.

Results and Discussion

Non-Scintillating Resins: Distribution coefficients (K_d) were obtained for each of the Amberchrom CG support materials 161, 300, and 71 with reported surface areas of 900, 750, and 500 m^2/g respectively. Initial tests indicated that equilibrium was attained after three hours and all resins were allowed to contact the Tc spiked water for at least three hours prior to sampling and analysis. The K_d was calculated for each resin and then plotted as K_d vs. the wt percent loading. The results can be seen in Figure 2.

It is apparent from these data there are significant differences in the K_d for the support materials at the 0.1 and 1.0 wt percent loading. However, at loadings of 5.0 wt percent or higher these differences are no longer as pronounced and they do not change significantly above the 10 wt percent extractant loading.

Equilibrium Tc adsorption isotherms were obtained for resins with 10 wt percent extractant loading over a range of Tc concentrations. ^{99m}Tc was utilized at the lower concentration

Figure 1. Experimental efficiency vial

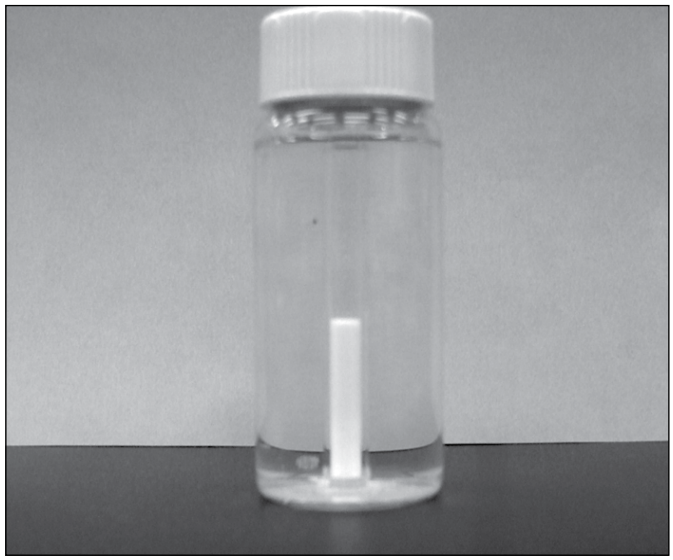

Figure 2. Non-scintillating resin K_d vs. loading

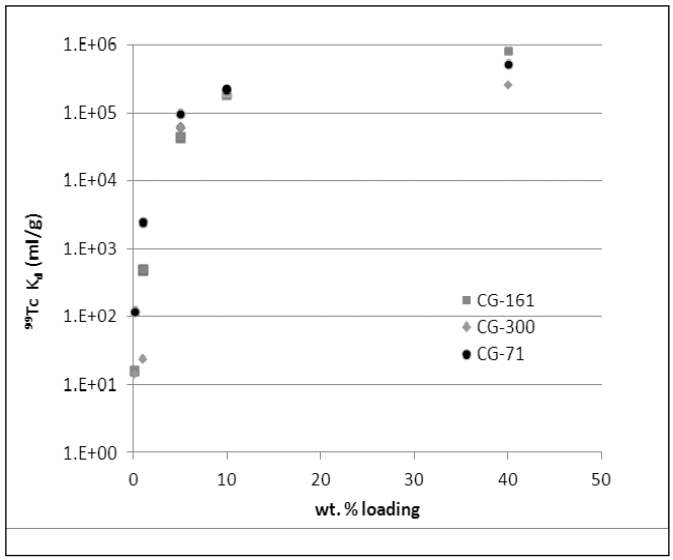

Figure 3. Example Tc Adsorption Isotherm

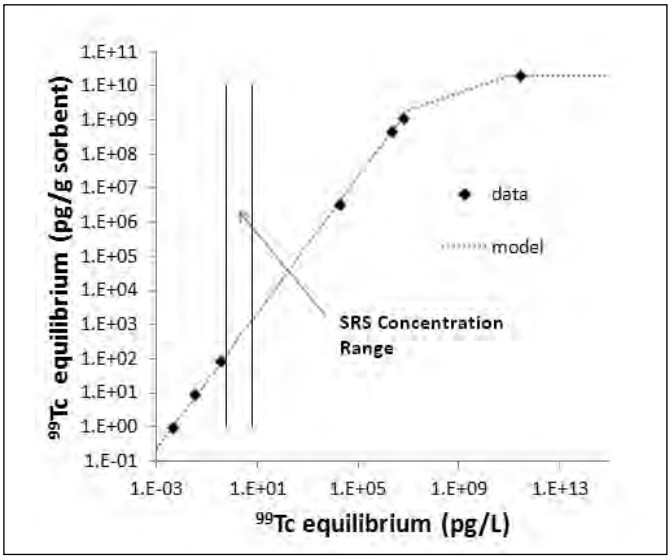

Figure 4. Efficiency of scintillating resins vs. time

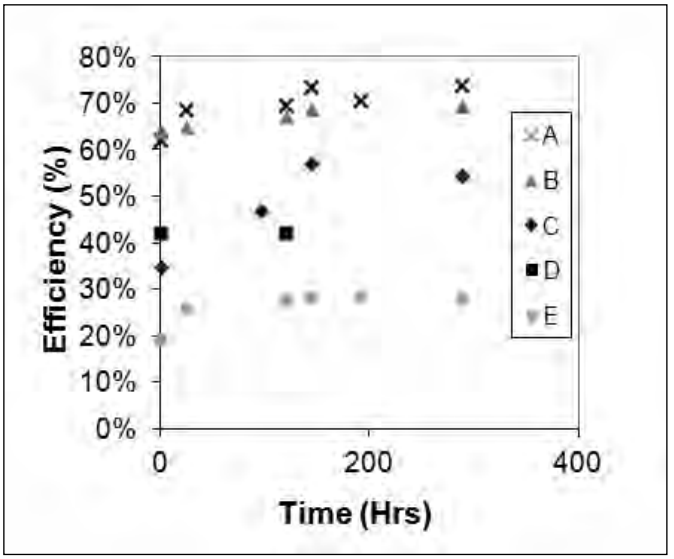

range due to its much higher specific activity compared to that of ^{99}Tc. The data was fit to a Langmuir equation and those followed the equation prediction quite well. An example of a Tc adsorption isotherm with CG-161 loaded to 10 wt percent with Aliquat-336 can be seen in Figure 3. The solid lines indicate the concentration levels reported in the water surrounding the SRS site and the broken line indicates the Langmuir prediction. These initial results provide valuable information for a starting point to begin the development of the optimum extractive scintillating resins that can achieve a maximum K_d. This high level of concentration would be required in order to detect ^{99}Tc at the SRS reported levels.

Scintillating Resins: Extractive scintillating resins were prepared with greater than 10 wt percent Aliquat-336, various fluors and wavelength shifters. The detection efficiency was evaluated utilizing the experimental vials described previously, with ^{99}Tc spiked well water at 300 Bq/mL. Figure 4 shows the results of the measured efficiencies of five scintillating resins; A) CG-161 with 10 percent Aliquat-336, 10 percent α-NPO, and 2 percent Bis-MSB, B) CG-161 with 20 percent Aliquat-336, 20 percent PPO and 2 percent Bis-MSB, C) CG-71 with 10 percent Aliquat-336, 20 percent PPO, and 2 percent Bis-MSB, D) CG-71 with 10 percent Aliquat-336, 20 percent PPO, and 2 percent dm-POPOP and E) CG-71 with 10 percent Aliquat-336, 20 percent α-NPO, and 2 percent Bis-MSB. The efficiencies were obtained over a period of up to 300 hours to ensure that the ^{99}Tc had come to equilibrium with the resins. The results indicate that the CG-161 resins had higher detection efficiencies than the CG-71 resins regardless of the scintillating fluor, wavelength shifter, or extractant loading used.

Based on the efficiency results, the CG-161 support material was selected as the superior support and two *candidate* resins were prepared; 1) with 20 percent Aliquat-336, 10 percent α-NPO and 2 percent Bis-MSB and 2) with 15 percent Aliquat-336, 20 percent PPO and 2 percent Bis-MSB for a full evaluation of extractive capacities and efficiencies. Figure 5 is an adsorption isotherm of both candidate resins with resin 1 being fit to a Langmuir equation. The solid vertical lines indicate the ^{99}Tc concentration range surrounding the SRS.

The K_d obtained for resins 1 and 2 at a ^{99m}Tc feed concentration of 3.0 pg/L were 1.38×10^5(mL/g) ± 7.87 percent and 5.01×10^4(mL/g) ± 4.11 percent respectively. This feed concentration is within the range reported to be in the surrounding water at SRS and these capacities are what would be expected at equilibrium. Efficiencies for resins 1 and 2 were 71.4 ± 2.6 percent and 68.0 ± 4.9 percent respectively.

Utilizing the acquired data, a Minimum Detectable Activity (MDA) for a resin can be calculated from Equation 1:

$$MDA = \frac{2.71 + 4.65\sqrt{Cbt}}{t\,E} \qquad (1)$$

Where:
Cb = background count rate (cps)
t = count time (seconds)
E = detector efficiency

Assuming a detection efficiency of 70 percent, a background count rate of 0.16 cps and a count time of seven hours, the MDA for 1 gram of scintillating resin would be 0.017 disintegrations per second (dps) or 26.81 pg of ^{99}Tc.

The amount of ^{99}Tc that will be adsorbed on 1 gram of resin at equilibrium at the low level SRS concentration range can be calculated from the Langmuir equation after the Langmuir constants have been determined by a Langmuir regression of

Figure 5. Tc Adsorption Isotherm for candidate resins

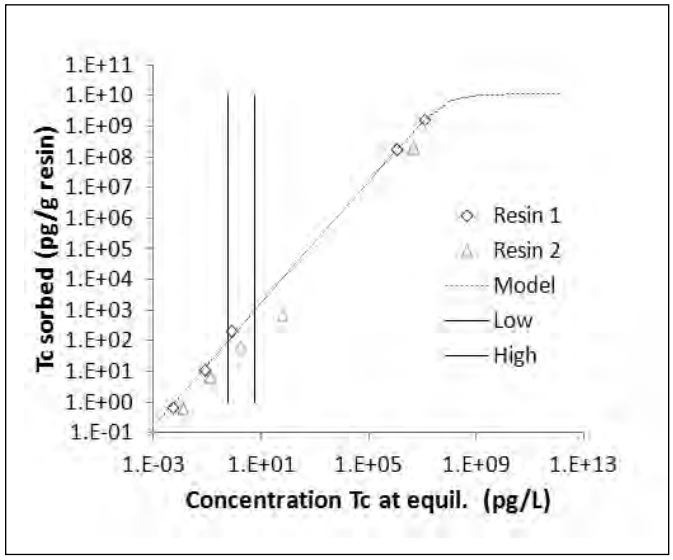

experimental data. Based on the parameters obtained for resin 1, one gram of resin in complete equilibrium with 0.59 pg ^{99}Tc/L water, the Langmuir equation predicts that 96.67 ± 10.20 pg ^{99}Tc, or 0.061 dps activity will be retained on the resin. This is more than three times the calculated MDA for the resin.

Conclusions

Two candidate extractive scintillating resins have been optimized and prepared based on the obtained experimental results. The resins were evaluated for very low level detection of ^{99}Tc in natural waters. These resins could be incorporated into a portable in-situ detector system that could be used for the remote continuous concentration and detection of ^{99}Tc in natural waters in an equilibration type mode.

Mitchell Greenhalgh has twelve years of experience in radiochemical separations and nuclear measurements using a variety of radiation detection systems including high-purity germanium, sodium iodide, liquid scintillation, alpha, and gas-flow proportional detectors. He is a senior staff scientist for the Fuel Cycle Science and Technology Division of Idaho National Laboratory. He is currently responsible for supporting research and development in advanced separation technologies related to the nuclear fuel cycle, and specifically nuclear fuel reprocessing including offgas separations. Greenhalgh holds a B.S. degree in chemistry (1995) from Utah State University.

Richard Tillotson is a staff scientist for the Fuel Cycle Science and Technology Division of Idaho National Laboratory. He has twenty-four years of experience in spent nuclear fuel reprocessing operations, fuel cycle separations, and waste treatment research. He specializes in solvent extraction and ion exchange separation technologies and is experienced using high purity germanium detectors and liquid scintillation detectors. He is experienced in remote handling and operations systems for spent fuel reprocessing and proof of principle separations research.

Troy Tranter, Idaho National Laboratory (deceased), held Ph.D. and M.S. degrees in chemical engineering and had twenty-four years experience in nuclear fuel reprocessing, uranium enrichment, and nuclear reactor technologies and operations. He was recognized within the U.S. Department of Energy (DOE), industry, and international communities for expertise in the fields of radiochemistry and radionuclide separations. He was employed at the INL for more than sixteen years and was a member of the Fuel Cycle Science and Technology Division. He was responsible for leading research and development in advanced separation technologies applicable to fissile/fertile isotopes, fission products, and other radionuclides related to the nuclear fuel cycle, and specifically nuclear fuel reprocessing. He was also the principal investigator (PI) on several national security programs. He formerly worked at ^{235}U enrichment and commercial nuclear reactor facilities and had extensive experience with various alpha, beta, and gamma measurement techniques, including high-purity germanium, sodium iodide, silicon surface barrier, plastic scintillator, liquid scintillation, and gas-flow proportional detectors. Dr. Tranter published more than eighty journal articles, conference proceedings, and technical reports in the fields of chemical separations and radiochemistry. He was awarded twelve patents (nine U.S., and three Russian), with ten additional patents pending, all relating to radionuclide separation or stabilization technologies. Much of his recent work involved the synthesis of selective polymer composites with engineered specificity for adsorbing key radionuclides and hazardous elements. He received the R&D 100 award, NASA Nanotech Briefs Nano50 award, Federal Laboratory Consortium Outstanding Technology Development award, Stoel Rives Idaho innovation award, and was chosen Outstanding Engineer for the Idaho National Laboratory in 2006. He was recognized in Chemical &Engineering News *for developing an engineered nano-composite material capable of effecting highly selective chemical separations, and served on the Editorial Advisory Board for NASA Nanotech Briefs.*

Acknowledgements

This work was supported by the United States Department of Energy and the Laboratory Directed Research and Development (LDRD) program at the Idaho National Laboratory (INL) through contract DE-AC07-05ID14517.

References

1. Turcotte, M. D. S. 1982. *Environmental Behavior of Technetium-99,* DP-1644, E.I. Du Pont de Nemours and Co., Savannah River Laboratory.

2. Barci-Funel, G., S. Ballestra, E. Holm, J. J. Lopez, and G. Ardisson. 1991. Technetium-99 in the Rhone River Water, *Journal of Radioanalytic and Nuclear Chemistry, Letters* 153(6) 431-38.
3. Carlton, W. H., M. Denham, and A. G. Evans. 1993. *Assessment of Technetium in the Savannah River Site Environment,* WSRC-TR-217.
4. Grate, J. W., O. B. Egorov, M. J. O'Hara, and T. A. DeVol. 2008. Radionuclide Sensors for Environmental Monitoring: From Flow Injection Solid Phase Absorptiometry to Equilibration-Based Preconcentrating Minicolumn Sensors with Radiometric Detection, *Chemical Reviews* 108, 543-62.
5. Egorov, O. B., M. J. O'Hara, J. W. Grate, M. Knopf, G. Anderson, and J. Hartman. 2005. Radiochemical Sensor System for the Analysis of ^{99}Tc(VII) in Groundwater, *Journal Radioanalytic Nuclear Chemistry* 264, No. 2, 495-500.
6. Egorov, O. B., S. K. Fiskum, M. J. O'Hara, and J. W. Grate. 1999. Radionuclide Sensors Based on Chemically Selective Scintillating Microspheres: Renewable Column Sensor for Analysis of Tc in Water, *Analytical Chemistry* 71, 5420-29.

Strengthened Nuclear Safeguards: A Statistical View in the Context of Combining Process Monitoring and Nuclear Material Accounting Data

Tom Burr, Kory Budlong-Sylvester, Michael S. Hamada, Claire Longo, and Brian Weaver
Los Alamos National Laboratory, Los Alamos, New Mexico USA

John Howell
University of Glasgow, Glasgow, Scotland UK

Mitsutoshi Suzuki
Japan Atomic Energy Agency, Ibaraki, Japan

Abstract

"Integrated/strengthened safeguards" is the International Atomic Energy Agency (IAEA) concept that effective safeguards must be maintained at monitored nuclear facilities, the mission of monitoring for undeclared facilities must be added, and the safeguards budget must remain approximately constant.

In traditional safeguards, periodic nuclear materials accounting (NMA) measurements confirm the presence of special nuclear material (SNM) in accountability units to within relatively small measurement error. Process monitoring (PM) is used to confirm the absence of undeclared flows that could divert SNM for illicit use. Despite occasional attempts to quantify the diversion detection capability of PM, nearly all quantified statements regarding safeguards effectiveness involve NMA, with PM used as a qualitative added measure. To assess the extent to which PM can provide quantitative assessment in effectiveness evaluation is one of ten recognized technical challenges (discussed during the IAEA's "Consultancy Meeting on Proliferation Resistance Aspects of Process Management and Process Monitoring/Operating Data" held in Vienna, September 28-30, 2011) in the anticipated increased use of PM data.

Effective resource allocation requires effective safeguards system evaluation. This paper reviews safeguards system evaluation methods based on statistical and decision theory, proposes a new evaluation method that quantifies an overall system consisting of both PM and NMA via detection probabilities for specified scenarios that are prioritized using diversion path analysis, and gives three examples at a hypothetical aqueous reprocessing facility.

Introduction

Since the discovery of undeclared nuclear material and facilities in Iraq in 1992, the International Atomic Energy Agency (IAEA) has expanded its mission via an "additional protocol" to include monitoring for undeclared activities within countries ("member states") that sign the Nonproliferation Treaty. While traditional safeguards at declared facilities continues, "strengthened safeguards" involves expanding to state-wide surveillance. "Integrated safeguards" is the concept that effective safeguards must be maintained at declared facilities, the new mission of monitoring for undeclared facilities must be added, and the safeguards budget must remain approximately constant.[1] One component of integrated safeguards is to improve safeguards at declared facilities by making use of more data, which is our focus.

In this special issue devoted to science for verification, this paper reviews the current safeguards approach in the context of statistical and decision theory, proposes an expanded evaluation method, and describes challenges in maintaining effective safeguards at declared facilities.

Background

Statistical hypothesis testing receives considerable attention in nuclear safeguards because of the appeal of quantified, objective testing.[2] In the safeguards context, the question "does this data indicate a safeguards-related event?" is repeatedly asked, so sequential testing or change-detection methods are used.

One IAEA goal is for a statistical test to alarm with high probability (0.95 or higher) if a protracted diversion of one significant quantity (SQ) or more of Pu occurs over a one-year time frame. This detection probability (DP) goal is unachievable in high-throughput facilities because one SQ is only approximately 0.1 percent or less of the annual throughput. Because this is a goal, not a requirement, the IAEA must then negotiate with the facility operator regarding additional measures used to make qualitative judgments. In addition, the IAEA must "trust, but verify," by making random confirmatory re-measurements of the operator's declared measurements, so the IAEA's measurement

error is even larger than the operator's measurement error, making the quantified portions of the safeguards conclusions even less capable.

Many believe that large-throughput facilities can be effectively safeguarded even in those cases having low DP on the basis of sequential statistical testing to alarm in the event of a protracted loss of one or more SQ acquired over a long time period, such as one year. Such optimistic beliefs are based on qualitative assessments that rely on some combination of process monitoring (PM), containment and surveillance (C/S), and quantitative nuclear materials accounting (NMA).

For small or large throughput facilities, we advocate using diversion path analysis quantitatively combined with NMA and PM (and possibly C/S) to allocate resources so that effective safeguards can be achieved for domestic or international safeguards.

Nuclear Material Accounting

NMA involves measuring facility inputs, outputs, and inventory to compute a material balance (MB). The MB at time t is $MB_t = BI_t + T_{in t} - EI_t - T_{out t}$, where BI is beginning inventory, T_{in} is transfers in, EI is ending inventory, and T_{out} is transfers out. The MB is measured periodically, its measurement error standard deviation, σ_{MB}, is estimated, and the null hypothesis, H_0: $MB_{true} = 0$ versus the alternative H_A: $MB_{true} > 1$ SQ, is tested. For testing a sequence of n MBs, the n-by-n covariance matrix Σ_{MB}, with σ_{MB} at each period on the diagonal, and covariances between balance periods on the off-diagonals determines loss DPs. One statistical issue is that the loss pattern for which a given sequential test is optimal depends on Σ_{MB}. Speed and Culpin[2] have more details regarding sequential testing.

Near-real-time accounting (NRTA) is a blend between PM and NMA that has existed for decades.[2-12] NRTA requires that MBs are computed frequently, approximately once per ten to thirty days. With such frequent balance closure, full NMA with Pu assays in each inventory and holdup location is not feasible, so PM can be used to help estimate in-process Pu inventory.[8] The motive for such frequent "balance closure" is to meet the IAEA DP goals for abrupt (over one month or less) diversion without much harm to protracted (over 1 year) diversion detection. These goals require that σ_{MB}, satisfy $\sigma_{MB} \leq 8$ kg/3.3 = 2.4 kg. This test is based on a significant quantity of 8 kg; the factor of 3.3 is chosen to give a 0.95 DP with a false alarm probability of 0.05, assuming that the measured MB has a normal distribution with zero mean. This is a reasonable assumption because measurements are summed to compute a MB; therefore, the central limit effect suggests that MBs have approximately a normal distribution. However, because σ_{MB} changes each month, it is important to thoroughly characterize each key error source in the MB calculation so that σ_{MB} can be well estimated each period.

For a large commercial plant (>8,000 kg per year Pu throughput) like that in Rokkasho, Japan, these DP goals imply that the monthly σ_{MB}has to be 0.36 percent or less of monthly throughput, and for protracted diversion detection, the yearly σ_{MB} has to be 0.03 percent or less of the yearly throughput. The monthly detection goal is marginally achievable with good measurements and the yearly goal is not achievable with any conceivable measurements. We emphasize two points. First, these DP goals are goals, not requirements; if they cannot be met, the burden is on the IAEA and the plant operator to convince themselves and others that an undetected diversion of 8 kg or more is unlikely. Second, whether a quantitative estimate of the probability of detecting an 8 kg loss using all available information (C/S, NRTA, operator data, expert opinion, diversion path analysis, etc.) is an effective goal is an open question. Meanwhile, we anticipate strong interest in making the most effective use of all available operator data in order to draw safeguards conclusions.

Large throughput bulk-handling facilities often try to keep σ_{MB}small as a percent of throughput (perhaps $\sigma_{MB} < 1$ percent of throughput) but cannot achieve $\sigma_{MB} \leq$ SQ/3.3. They must then negotiate what level of increased C/S will be required to compensate for failure to meet the DP.[9,10] One reasonable approach is to evaluate the cost of reducing σ_{MB}. Statistical evaluation is a key tool to estimate σ_{MB} as a function of measurement type(s) and translate the result to a relation between $\sigma_{MB}$and cost. We would then choose the cost where the relation flattens (diminishing returns) and accept the resulting σ_{MB}. There is virtually no disagreement that the resulting σ_{MB} will be too large to meet the IAEA goal over one year, but there is reasonable hope that the goal can be met over perhaps ten days or less. An important practical issue in ten-day balance closures is that significant in-process Pu will not be well measured.

Containment and Surveillance

The IAEA uses NMA and C/S plus some level of inspector presence to perform its verification responsibilities. C/S includes cameras, radiation monitors, tamper indicating devices, and other measures, some of which overlap with NMA and PM measures.

Although there have been efforts to quantify the vulnerability of, for example, tamper-indicating seals,[13] currently, there is no accepted approach for giving credit for C/S that is analogous to the NMA approach. However, the NMA approach for a sealed and static inventory item is usually different from the NMA approach for an unsealed item. The IAEA guards against instrument, data, and materials tampering. C/S measures can support NMA for example by helping to ensure that a sample for chemical analysis is authentic and to guard against materials tampering or falsification.[9] C/S also supports design verification, which can be a daunting task; for example, in the head end alone (where receipt and dissolution of spent fuel assemblies occurs) of a large reprocessing plant, there can be more than 300 penetrations including pipes, doors, and hatches, any of which could provide a diversion route.[14]

Facilities that cannot meet the IAEA DP goal using NMA

are required to have negotiated levels of additional C/S measures. For example, the Rokkasho reprocessing facility in Japan includes solution monitoring (SM, which has PM, NMA, and C/S features) as a separate, additional safeguards measure offered to the IAEA.[9,10] Qualitative arguments regarding the benefits of SM are reasonably strong,[15] and there are current efforts to better quantify DPs of various diversion scenarios using SM data.[15,16] However, the cost/benefit of purported improvements to SM systems (such as including in-line Pu concentration if safety concerns can be addressed, or including all key flow rates) cannot yet be quantitatively evaluated.

Designing an effective safeguards system that is "good enough" without being too costly is challenging. Here "good enough" can mean that the system meets IAEA DP goals using NMA and/or has adequate additional C/S and PM measures. At least two major obstacles have prevented developing a safeguards evaluation methodology for C/S. First, most agree that C/S measures add value, but there is no consensus regarding how to take quantitative credit (for example, through improved DPs) for C/S in the same manner that improved NMA measurements are given credit (through reduction in σ_{MB}). Second, there is no consensus regarding the utility of enumerating and characterizing the most likely diversion routes and scenarios. It is assumed that no system can detect all types of diversion;[17] however, an evaluation of proliferation risk could identify vulnerable diversion routes and prioritize additional C/S measures. Without such evaluation, there will be arbitrary but perhaps reasonable decisions made regarding diversion scenarios the system should detect and therefore what C/S measures will be used.

Current Safeguards Practice: NMA + Additional Measures

Complications of NMA include: (1) poorly understood measurement errors for some of the material; (2) unmeasured or poorly measured inventory (holdup) in process pipes and other equipment, and (3) the use of short-cut assays that do not directly measure the SNM of interest. Regarding (1), for example, results on physical standards are often not representative of results on facility material for some flow streams or items, especially for waste streams. One statistical approach for addressing this "item-specific" bias has been presented, but it requires having a gold-standard assay method for a small subset of items that is less dependent on physical attributes of the items.[18] International target values for uncertainty (including random and systematic errors) are fairly well established on the basis of multiple years of operator and inspector data using different instruments on the same items.[19] Regarding (2), if there were no measurement error in the transfers and inventory, then the MB would equal the change in holdup plus the true loss. The presence of measurement error complicates MB evaluation, and the presence of nonnegligible holdup together with measurement error further complicates MB evaluation. Regarding (3), for example, if it is believed that Pu cannot be separated from Cm, then a neutron counter designed to detect neutrons for Cm can provide partial assurance that Pu has not been diverted,[9,10] and might provide the basis for a pseudo-balance closure on the basis of assuming no diversion.

Despite these complications in NMA, provided σ_{MB} is well estimated, it is understood what it implies about DP. Adequate estimation of σ_{MB} is not a scientific challenge, but is often an engineering challenge constrained by limited time and budget. Regardless whether a facility has a sufficiently small σ_{MB} to meet DP goals, the IAEA technical objectives[2] include the statement that C/S and PM are important complementary measures. In the spirit of "strengthened safeguards,"[1] it becomes important to quantify the value of additional C/S and PM measures.

Near-real-time Accounting (NRTA)

NRTA is typically described as frequent balance closures based mostly on measurements of the shipments and receipts, with varying capability to measure or estimate in-process inventory. In practice, *frequent* is typically daily or weekly (however, process-monitoring-based balance closures are common on a per-batch basis that could be daily or multiple times per day). Close inspection of facilities that claim to close balances very frequently, such as daily or after each batch transfer, usually reveals that various shortcuts or partial measurements are in effect. For example, it is rare to equip each processing unit with in-line holdup or in-process inventory monitors. Therefore, either engineering estimates, or historical by-difference estimates are used for negotiated portions of the in-process inventory measurement.[7,8,20]

Also, in aqueous reprocessing facilities, in-line dip tubes measure vessel volume every few seconds, but there is rarely the budget to measure the Pu concentration in-line. In-line dip tubes estimate solution density, so empirical relations together with the density estimate can infer (but not directly measure) the Pu concentration. An NRTA system that measures all material is obviously preferred, but even the best system will typically rely on partial measurements and/or engineering estimates for a least part of the in-process material.

A sequence of MBs must be statistically evaluated using sequential testing. One main challenge is to estimate Σ_{MB}, the covariance matrix of a sequence of MBs. Sequential tests are in use, including the basic two: MUF (material unaccounted for, the same as the MB, which is good for a one-time abrupt loss) and CUMUF (cumulative MUF, which is good for a long-term loss). Another good choice is Page's test, which is defined at period t as P_t = maximum(P_{t-1} + SITMUF$_t$ – k, 0), where SITMUF is the standardized, independently transformed MUF (should have zero mean, unit variance, and be uncorrelated with all previous SITMUF values), k is a control parameter usually defined to be one half of the mean shift to be detected.[2,3] Burr, Jones, Wangen[21] also evaluated a multivariate version of Page's test (Crosiers' Cusum) in the setting of monitoring multiple vessels frequently.

One issue in sequential testing is that the test should have good DP for either abrupt or various types of protracted diversion. The best sequential test depends on the type of loss so no test can be uniformly more powerful for all loss types. The CUMUF test is good if diversion begins on the first balance period and continues at the same rate for all subsequent periods. Page's test is optimal if the diversion begins in an arbitrary period, persists at the same level for an arbitrary period, and then returns to zero. Slight complications arise due to the transformation required (that uses σ_{MB}) to convert a MUF sequence into a SITMUF sequence, but Page's test applied to the SITMUF sequence has been shown to be among the most versatile tests, and is arguably the most versatile. Advantages[12,14,22] of NRTA include improved abrupt loss DP, timeliness, improved alarm resolution, and refinement of error models.

Process Monitoring

PM data can be dedicated for safeguards use but can also include process control measurements such as those used by the operator to control the chemical processes.[6] Example process control measurements in an aqueous reprocessing plant include: mass and density measurements in tanks, inline flow meters, concentration measurement of non-nuclear material reagents, and process temperatures. As a rough comparison to NMA, PM data is typically collected frequently (multiple times per hour) while MBs are computed less frequently (perhaps every ten days at large aqueous reprocessing plants, with PM used to help estimate in-process inventory), and PM data often tracks bulk attributes such as mass rather than SNM mass. As examples of PM, radiation detectors can monitor either declared SNM transactions or can monitor for undeclared transactions (such as portal monitors do). Smart cameras can save and archive scenes involving declared transactions (an item was shipped from A to B so the detector should confirm this using detected radiation), watch for undeclared transactions, and alert an inspector to sections in the archive that require human review.

Solution monitoring (SM) is a type of PM that includes level (L), density (D), and temperature (T) measurements of solution in tanks.[20] Unless there is an in-line Pu concentration measurement, then empirical relations linking Pu concentration to D and T for a given nitric acid concentration are required to estimate the Pu concentration.[20] Together with a volume estimate using the calibrated relation $V = f(L)$ + error, an estimate of Pu mass is available. This is a pseudo-measurement because Pu is not actually measured, but it might qualify as NRTA. A second example is Cm accounting where it is assumed that the Pu cannot be separated from the Cm; therefore, tracking Cm by neutron counting ensures that all the Pu remains in the declared stream.[9,10]

Related Work and Literature Review

Classical statistical hypothesis testing as used in NMA has been criticized.[2,23] For example, Bayesians believe it is misguided to operate as if misclassification costs (the costs of false negatives and false positives) cannot be agreed upon. Similarly, game theorists believe assumptions should be made clear regarding the penalty to the state for a detected diversion attempt, the reward to the state for a successful diversion attempt, and penalties and rewards to the inspector for the various outcomes (cost of false alarms and non-detections). This line of reasoning leads to a debate regarding whether the DP goal is a suitable goal. However, in all methods, there is still the need to calculate the DP under the assumptions that diversion has occurred. Therefore, much of the debate reduces to how large the DP needs to be in the event that diversion occurs in order for safeguards to be effective in the presence of specified costs or cost ratios.

Bayesian Perspective

The Bayesian expected cost of misclassification adds valuable insight. Let D denote the event "diversion attempted," and A denote the event "anomaly indicated" (for example, A could be the event $MB > 2\ \sigma_{MB}$). Then by straightforward application[2] of Bayes' rule,

$$P(D|A) = 1/(1+ (1-\pi)\alpha /(\pi\ (1-\beta)), \quad (1)$$

where π is the *prior* probability of attempted diversion, $\pi = P(D)$, α is the false alarm probability, and $1-\beta$ is the detection probability. Equation 1 implies[24] that if π is small, then most alarms will be false. For example, with $\alpha = \beta = 0.05$, and $\pi = 0.001$, $P(D|A) = 0.02$. If $\pi = 0.5$, then $P(D|A) = 0.95$ and if $p = 0.9$, then $P(D|A) = 0.99$.

Having to specify the prior and sensitivity of conclusions to misspecifying the prior is one objection to Bayesian analysis. However, the Bayesian view is that the Bayesian expected misclassification cost (involving the probability of false alarm or of failure to detect diversion), and the *costs* of those two undesired events is the logic behind any procedure. For example, let f = false alarm cost, and d = undetected diversion cost, then the expected cost is

$$E(\text{Cost}) = \pi\beta d + (1-\pi)\alpha f \quad (2)$$

Many believe that π is small. In fact, inspectors have usually developed effective procedures to assess and resolve alarms (often including the possibility that σ_{MB} has been underestimated) because they assume that most alarms will be false. A difficult question is how to ensure that π continues to be small when inspection resources at declared, safeguarded facilities are reallocated to monitor for undeclared facilities. Equation 2 forces

us to realize that when we *arbitrarily* opt for specific small values of α and β, we are implicitly assuming something about π, d, and f (so we are all at least "hidden Bayesians") because it is generally accepted that at least subconsciously, we seek to minimize E(cost).

Game/Decision Theory in Safeguards

Two classes of member states have signed the NPT:

1. states that want to cooperate with inspectors to prove that safeguards is effective and that state is compliant with NPT; and
2. states that want to violate the NPT and divert material.

The IAEA's safeguards goal for class 1 states might be to have extremely small σ_{MB} at low cost. The state's goal for class 1 states is to divert from either declared or undeclared facilities. We see no strategic advantage of diverting via a declared facility rather than via an undeclared facility. There are advantages in diverting from a declared facility simply because it exists and/or it is more convenient. To date, the decision theory literature[2,25] has considered only class 2 states. There is an assumed positive payoff to the state for undetected diversion, negative payoff for detected diversion, and zero payoff for legal behavior. Similar payoffs exist for the inspector. In this case, it has been shown[25] that we need either a strong penalty for detected diversion or very high DP.

Regarding how much inspection effort is appropriate at a declared facility, in Reference 25 the authors state, "The obvious and only answer is that the inspector should invest that amount of verification effort which will deter the facility operator, through the risk of timely detection, from illegally breaking a seal, no more and no less." Suppose that n items will be inspected in a storage facility with N sealed items, each containing at least 1 SQ of SNM so that it is important to ensure that 100 percent of the N items are intact. How large should n be? Assume the time to inspect each item is t hours, then the DP = $1 - \beta = n/N = T/(Nt)$ for a total effort of T hours. Assume the operator will gain advantage d for undetected illegal behavior, advantage 0 for legal behavior, and advantage $-b$ for detected illegal behavior. Then the operator's expected advantage (*utility U* in game theory) if he behaves illegally is $U = -b(1-\beta) + d\beta$, and if $U < 0$, then the operator will be inclined toward legal behavior. We could then choose $T > Nt/(1 + b/d)$ to strongly discourage illegal behavior, which implies that for large b/d values, a small effort T is suitable for deterrence.

We do not address the delicate issue that it is possible for a state to gain some advantage by detected illegal behavior because this is an issue that is normally decided at very high political levels. We concur with Avenhaus and Canty[25] that for the goal of deterring illegal behavior, we implicitly assume a b/d value when we design inspection efforts targeted for class 2 states. Athough b/d is rarely if ever stated explicitly, it provides the only rational basis for choosing inspection effort. Avenhaus and Canty[25] have also considered N locations within a state, having subjective and technical parameters (d_i, b_i, $1\text{-}b_i$), diversion probabilities q_i, and inspection probabilities p_i for i = 1, 2, …., N. The Nash criteria for rational behavior in a noncooperative (class 2 states) situation determines both the inspector behavior (p_i) and the state behavior (q_i). An interesting extension would include $1 - b_i$ as part of the "inspector behavior" because it is a function of the safeguards and inspection resources.

Despite the merits of Bayesian decision theory, we believe non-Bayesian statistical hypothesis testing has more relevance to our problem and is recommended by virtue of its simplicity. For example, if $\sigma_{MB} < SQ/3.3$ then the claim that safeguards is effective can be quantitatively defended. If $\sigma_{MB} > SQ/3.3$, then the operator must negotiate what additional measures will be required to ensure adequate safeguards. Nevertheless, it is useful to consider decision theoretic notions of costs and payoffs to understand the hidden assumptions of our subjective but reasonable DP goals. This would be relevant for class 1 states.

Technical Objectives of the IAEA

The technical objectives[1,2] of IAEA safeguards are described in information circular INFCIRC/153. The agreement provides that safeguards objectives include timely detection of diversion of significant quantities of SNM from peaceful nuclear activities, and deterrence of diversion by the risk of early detection. Material accountancy is the fundamental measure, with C/S and PM as important complementary measures.[2]

INFCIRC/540 has been added to the agreements as a model protocol intended for strengthened safeguards to monitor for undeclared nuclear activities within a country. This agreement provides the means for the IAEA to monitor much more information about a country's nuclear activities, broadening the IAEA's mission from facility-based to country-based. Additional protocols are described in Cooley.[1]

Speed and Culpin[2] argue that facility-based safeguards covered for example by INFCIRC/153 should explicitly quantify the costs (as in Section 4) so that inspection resources can be optimally allocated, using a decision theory framework. To date, this has not been done, and the suggestion met considerable opposition in the rejoinder section of the paper. The opposition largely involves the inability to specify the costs of false negatives. Nevertheless, currently it is assumed or hoped that declared facilities can be effectively safeguarded using a reduced budget so that the overall safeguards budget can remain approximately constant while expanding the mission to country-wide surveillance.

Also, Avenhaus and Jaech[23] is a landmark safeguards paper that points out that frequent NMA balance closure is not a panacea; in fact, less frequent balance closure has higher DP against worst-case protracted diversion. Avenhaus and Jaech[23] did not adopt a true sequential testing approach but instead assumed safeguards conclusions would be made at the end of each calendar year (or whenever the facility is shut down and cleaned out). Therefore,

diversions over multiple years were not considered. Differences between such "period driven" decision making and "data driven" sequential testing that allows for the possibility of SNM loss over multiple years are being investigated. Here, we point out two important facts: (1) Abrupt loss should be easily detectable in any system using PM, NMA, or both, and (2) Protracted loss over a period such as one year for which facility throughout is one thousand or more SQs will be difficult to detect using any combination of PM and NMA, except for those scenarios that are amenable to the new "model-based predicted value" concept.

Alternative Evaluation Method to Combine PM with NMA

The difficulty in integrating PM and/or C/S measures with NMA to measure effectiveness has long been recognized.[26] However, ignoring the problem only buries hidden assumptions in effect when PM and C/S systems are evaluated. In practice, we either implicitly or explicitly assume that PM and C/S measures are sufficient, and perhaps also that they are efficient.

What is a defensible way to integrate the disparate data to provide reliable diversion detection? Or more generally, how can we provide good classification performance in the context of making sequential decisions regarding whether all the SNM is in the declared locations? Here we evaluate the feasibility of quantifying PM, combining its DPs with NMA, and using the overall DP as the performance metric.

We avoid a Bayesian approach to evaluate Prob(diversion), opting instead to evaluate DP = Prob(alarm). This avoids the thorny issue of the prior probability (prior to observing any sensor or measurement data) of diversion. The proposed concept is to consider the probability of an alarm given true states of nature x_1, x_2, …, x_M, P(alarm | x_1, x_2, …, x_M), where the vertical line denotes conditional probability. The terms x_1, x_2, ,,,, x_M include the most recent true (true, not measured) MB values, plus all relevant states of nature such as flows along pipes (relevant if observable by the PM system). Similar conditional probability methodology has been developed in event tree and fault trees in probabilistic safety analysis. But a unique feature here is the sequential decision making as discussed later in this paper.

The following subsections describe: previous efforts to quantify the benefits of PM; a proposal to estimate P(alarm | diversion path *i*) so P(alarm | x_1, x_2, …, x_M) can be evaluated, and a discussion comparing the proposed strategy to the present-day safeguards evaluation methods.

Previous Efforts to Quantify the Benefits of PM

SM is an example of PM that contributes to NMA by helping to validate volume measurement error models and to validate shipments and receipts for the MBA.

There have been several attempts to take credit for SM in a quantitative way. For example, Reference 15 showed that abrupt loss detection probability can be greatly improved using SM, with a trivial reduction in protracted loss detection. This is not necessarily true in general because it will depend on the number of tanks being monitored. Howell and Scothern[27,28] have used SM for anomaly resolution. Facilities often offer process monitoring data to the inspector as a cost-effective measure, arguing that the cost to the safeguards budget is low because the data is being collected for other purposes. Of course, until the inspector decides how to use process monitoring data, the main result could be data indigestion.

There have also been a few efforts to quantify the effectiveness of container tamper indicating devices (TIDs) and seals.[13] Here the diversion path analysis could be more complicated than one might think at first, and the international perspective is very different from the domestic perspective, where, for example, two-person rules make it difficult for an individual to tamper with a sealed item that contains SNM. However, two-person rules are meaningless in international safeguards. Johnston[13] emphasizes that defeating a seal implies that the seal was removed and replaced without detection. Certainly this can be tested by designing experiments that repeatedly remove and attack the type of seal being assessed, perhaps initially by assuming the best possible resources and least possible constraints for the adversary. If a seal is defeated, the full diversion path analysis must then consider how the adversary will remove the SNM from the facility. Because there are many options for seal defeat and subsequent SNM removal, the full diversion path analysis might seem like a daunting task.

Proposal for Integrating PM with NMA

We propose an integrated data analysis that combines PM with NMA using these steps:

(a) Describe diversion scenarios to inform how data should be evaluated to provide a means of event detection;
(b) Extend anomaly resolution work that has focused on identifying, categorizing, and resolving false alarms[27,28] to the case of recognizing diversion signatures and examine a variety of pattern recognition/fault detection and diagnosis approaches[27,28], and
(c) Evaluate P(alarm | x_1, x_2, ,,,, x_M) for given true states of nature x_1, x_2, ,,,, x_M. The terms x_1, x_2, ,,,, x_M include the most recent true (true, not measured) MB values, plus all relevant states of nature such as flows along pipes (relevant if observable by the PM system). Some subset of x_i could perhaps be dichotomized into "alarm" or "no alarm."

Jointly, these steps can provide a platform for integrating PM measures with NMA for evaluation of effectiveness. Two key elements of our approach are to define and parameterize acquisition paths in terms of observables using PM and integrated data analysis such as in Example 3 later in this paper.

Step A: Acquisition/Diversion Path Analysis

Lyman[17] points out that "... any system will have diversion pathways that can defeat containment and surveillance. There is no substitute for material accountancy…" We agree, but believe diversion path analysis[29] can guide the choice of safeguards measures. The expert elicitation divides the experts into teams and the teams do not communicate during various phases of exercise. Division into teams helps to address how ambigious the possible diversion paths are, as well as the completeness and adequacy of the final list of most likely diversions.

Steps B and C: Advanced Process Monitoring/Data Analysis

We assume that paths identify new signatures such as PM observables and that these signatures can generate residuals or *scores* to be monitored. Adding them to NMA data could enable pattern recognition and we envision two options.

Option 1 uses a subset of subsystems as "first alarmers" and another subset of subsystems to either resolve the master alarm or to lead to a system alarm. For example, monitor PM data for alarms and alarming periods are evaluated using other data. Use a filter to reconcile alarms,[27,28] perhaps reducing the alarm threshold to correspond to less than 1 SQ (perhaps 1 kg instead of 8 kg). Extend the alarm reconciliation approach in Reference 28 to facilitate better decisions. In one example, in Reference 28, the shipper tank's level over time was compared to the receiver tank's level over time. There were some small dips and rises even during "no tank-to-tank transfer" modes due to evaporation, sparging, dip tube plugging, sampling, recirculation, and recovery from pumps. If such patterns in L measurements are explainable under H_0 using knowledge of the system (historical and/or first principles modeling), then conclude H_0.

In option 2 all observables are on the same footing. Burr et al.[6] give examples of option 2, putting PM on the same statistical footing as NMA without distinguishing first alarmers. A new feature in the quantitative roles for PM in Burr et al.[6] is the notion of a model-based predicted value and resulting residuals that can be monitored on equal footing with residuals (MBs) from NMA.

New aspects of this approach of combining systems that each have alarm probabilities using either option 1 or 2 include parameterizing the diversion space and using expert elicitation to assess completeness of the diversion path list. Analysis details would be different for the two options. Furthermore, either option could dichotomize the measurements as *alarm* or *no alarm*, or accept the raw measurements as input. Again, analysis details would be different depending on whether observations were dichotomized. In addition, we could consider including investigation steps taken during the alarm resolution stage. One or more alarms from the first-alarmers subset would trigger an investigation where all data is analyzed to determine whether diversion is the most likely explanation. A notional example of this using SM data is illustrated by Bevan et al.[30]

Both option 1 and option 2 are likely to need a "coincidence window" where multiple subsystem alarms within a to-be-determined time frame raise the system alarm probability significantly.[31] Therefore, important variations of alarm rules motivated by path analysis would include using novel pattern recognition methods to identify effective *triggering* subsystems that open coincident time windows within which alarms in other systems significantly raise the alarm probability. Realistically, if the path list and alarm rules become long and unwieldy, this approach will not be sustainable.

In data-driven monitoring, we assume that the operating hypothesis H_0 is that all SNM is in declared locations, while the alternate hypothesis H_A is that some SNM is outside declared locations either at the time the decision is to be made or during the time period since the last decision was made. The goal is to frequently assess whether H_0 or H_A is the correct state of nature, in the presence of complicating factors such as the possibility of data falsification, the need for the inspector to rely on small samples from the operator's data, and fluctuating in-process inventory (*holdup*).

A challenge will be to calculate P(alarm at any time 1, 2, …, $t|x_1, x_2, \ldots, x_M$), For example, using only NMA data, so that $x_1, x_2, \ldots, x_M$ are the true MB values, P(alarm at any time 1, 2, …, $t|MB_1, MB_2, \ldots, MB_t$), is a complicated function of the alarm rule, sequential test used, the values $MB_1, MB_2, \ldots, MB_t$, and σ_{MB}. Therefore, simulation is used to estimate such alarm probabilities. When $x_1, x_2, \ldots, x_M$ are extended to include PM data, simulation will again be needed, but also to model the signals and measurements from specified diversions. Therefore, we must rely on "modern facility simulation" (not currently available) to assess needed probabilities. The calculation P(alarm at any time 1, 2, …, $t|x_1, x_2, \ldots, x_M$) is much simpler in period-driven testing, where a time window such as one month or year is specified, limiting the $x_1, x_2, \ldots, x_M$ vector to manageable size (Figure 2).

Key open issues include: (a) the completeness of diversion path list, (b) the ability to parameterize diversions, (c) the ability to combine probabilities from multiple sensors, and (d) the feasibility of developing a "modern simulation capability" to assess needed probabilities. Regarding (a), it could simply be assumed that the path list is *complete* for purposes of sensor selection. Alternatively, this can be addressed by the expert elicitation, and it would be useful to assess how subjective the list was so that if separate set of experts made the list, the result would be a different resource allocation among sensors. Regarding (b), a key question is whether assumptions would need to be too strong to be defensible in order to calculate P(alarm of given sensor for given SNM flow rate along diversion path). Regarding (c), the ability to combine probabilities from multiple sensors depends on the independence or nonindependence of subsystems and issues similar to those in evaluating physical protection systems where the issue is that the events that happen in what order must be clearly specified in the path analysis. Regarding (d), we would

need a virtual facility with realistic SNM flows and PM system included in the simulation.

Here we also list other open questions mentioned previously: (a) an ambitious strategy would be to model the alarm-investigation process as a second analysis that has its own false fail and false pass rates. An open question involves the issue that our analysis ends prior to the "human-interaction" stage where experts assess system alarms. However, it is not unrealistic to at least consider modeling the human-interaction as another data source impacted by true states of nature, just as we propose for NMA and PM); (b) realistically, if the path list and alarm rules become long and unwieldy, this approach will not be sustainable (open question), and (c) a good first step is to think in terms of sensors alarming (exceeding thresholds) but the analysis should investigate the use of actual sensor readings as input to a pattern recognition algorithm.

Although we value having a system with known performance against recognized diversion possibilities, we have tried to convey that the present system is arbitrary, reasonable, and considerably *cheaper* than this proposed system. The present system uses informal expert elicitation and tension between the operator and inspector to decide what PM measures will be in place. Also some arbitrary decisions are made regarding the *completeness* of NMA system. We also note here that it would be valuable to estimate the AP of PM measures for specified diversion scenarios even in facilities that do meet the current IAEA AP goal.

Finally, although it is acceptable to tune to a few loss scenarios, a catch-all anomaly detection option is needed for residuals or scores that are unlike anything seen in training data. The *training* phase for a combined NMA/PM system allows alarm rules to be developed (pattern recognition methods are trained) on data that is assumed to contain no diversions. The trained methods are then tested on new (testing) data. Most current work related to training a combined NMA/PM system has been applied to simulated training data. There are ongoing efforts to improve the simulation fidelity so that simulated data has adequate quality to mimic key features in real NMA/PM data.

Cost/Benefit Discussion of Proposed Integrated Data Evaluation

In trying to meet resource allocation goals we are suggesting some relatively costly analyses in order to evaluate the cost/benefit of candidate safeguards measures. It is therefore reasonable to consider whether such a cost/benefit analysis is feasible. The benefit involves potentially improving the current reasonable but ad hoc approach to resource allocation by using formal expert elicitation to choose the most likely diversion paths for which the safeguards system will be designed. Even if that is done, some subjectiveness will remain, but objective decisions would follow from the up-front subjective ranking of diversion scenarios. There is some appeal in knowing what a system is designed explicitly to detect.

Examples

Two-tank Problem

Consider a simple two-tank system where tank 1 ships Pu solution to tank 2 with zero waste generation. Flow rates along connecting pipes are measured every six minutes, and in-tank measurements of L, D, and T are every six minutes. Simple flow models and measurements lead to residuals that can be monitored. For example, measured flow rates allow prediction of receiver volume rise which leads to two ways to estimate receiver tank volume at each time step. Having two estimates of receiver tank volume leads to smaller measurement errors than having one estimate based solely on in-tank measurements; however, we do not anticipate that can improve much beyond 0.3 percent total measurement error standard deviation. Alternatively, each tank can be monitored during "wait" modes and transfer modes, without evaluating the residuals every six minutes. All examples below use this second option, which involves marking the start and stop times for each tank event.[32,33]

Consider testing the null hypothesis, H_0: no diversion versus the alternate hypothesis, H_A: diversion of 1SQ or more, in the two-tank system with no waste generation. Assume the throughput is 50 kg of Pu per day, 160 operating days per year, corresponding to 8,000 kg Pu per year. Assuming 0.3 percent measurement error relative standard deviation, this implies σ_{MB} = 24 per year, or 0.15 kg per day. Diversion could occur during transfer or during wait mode.[32,33] Loss detection is higher during wait mode than during transfer mode because the ability to detect change in one tank is not very sensitive to systematic/calibration errors.

In this example, in the expression P(alarm at any time 1, 2, …, $t|x_1, x_2, \ldots, x_M$), $x_1, x_2, \ldots, x_M$ are the true volume and mass transfer differences (TDs) between the two tanks over a specified time in the period-driven approach, where an analysis time window such as one month or one year is specified. A good sequential test such as Page's test could be applied to the sequence of TDs. Also, to improve detection of protracted loss over many transfers, we might consider either:

(1) Using the measured flow rates in all declared pipes — This turns out to be inadequate; however, because this leads to a second way to estimate receiver volume as mentioned above, this options does reduce σ_{MB} by the averaging two volume estimates in each tank, or

(2) Capitalize on monitoring and observing no solutions flowing except along the single monitored pipe connecting the two tanks during the tank-to-tank transfer—That is, the safeguards concept is to monitor all pipes for absence of undeclared flow. Monitoring for the absence of undeclared flow is in some ways easier than monitoring the declared flows; however, such monitoring covers only very specific diversion routes along particular pipes. Such an approach would require strong confidence in facility design verification.

Figure 1. Simulated data from tanks 0 to 6. The holdup in subplot (h) is in the holdup in the pulsed column between the feed and receipt tank.

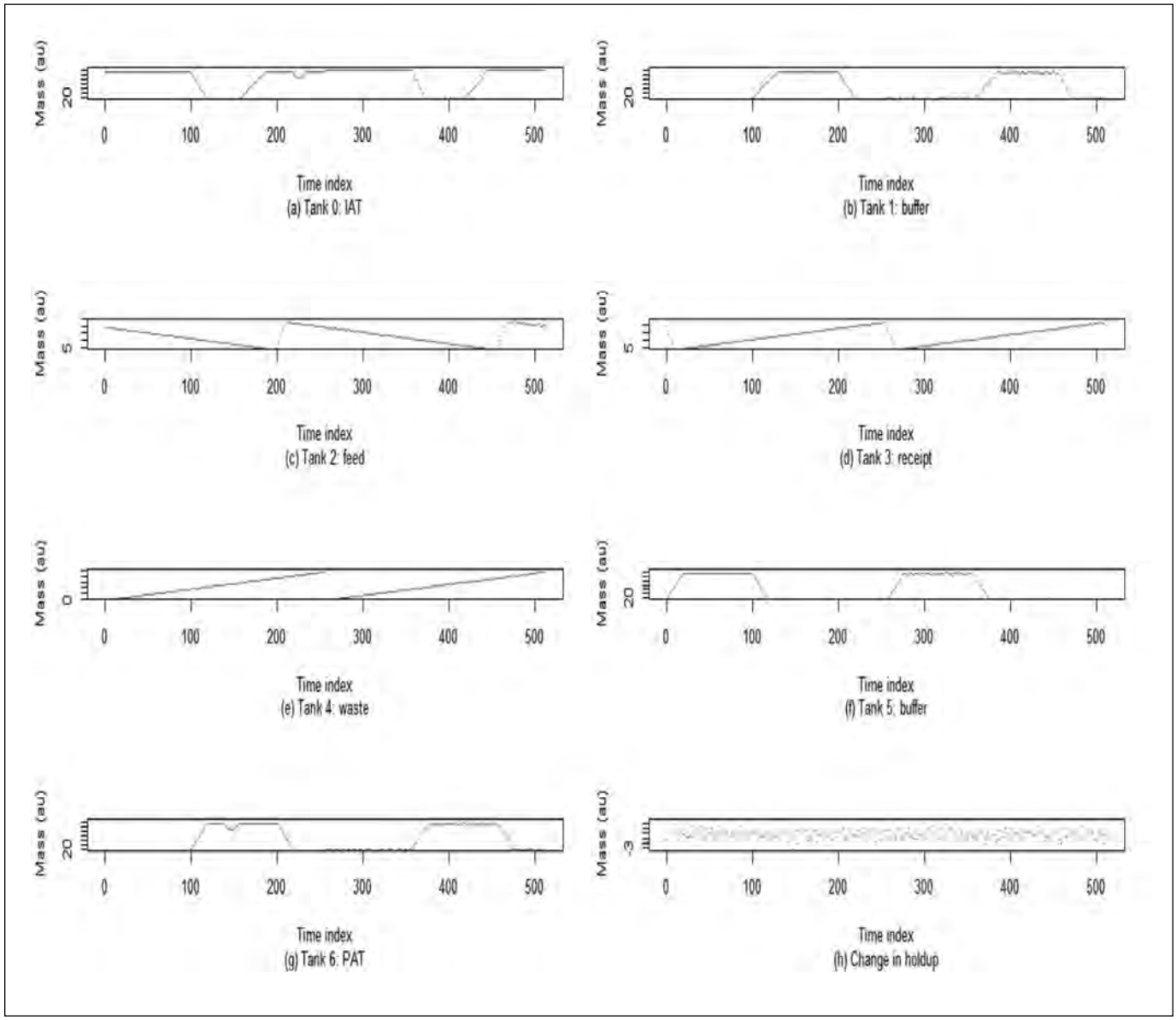

Finally, suppose in-tank *V* and *M* bulk measurements could be replaced with in-tank V and Pu mass measurements using an in-line Pu concentration measurement. Recall that Avenhaus and Jaech[21] showed that more frequent balance closure in NMA does not increase loss DP for widespread (protracted) diversion over time. In fact, less frequent balance closure has higher DP if the loss vector describing the loss at each balance period is proportional to the sum of the rows of the MB covariance matrix Σ (which has Σ_{MB} along the diagonal and covariances between MBs at different balance periods on the off-diagonal). A similar conclusion holds for widespread diversion over time and space (multiple tanks in our context). Therefore, unless novel concepts such as "observing no solutions flowing" where they should not and/or effective model-based book values are invoked, even in this simple two-tank material balance area (MBA), the IAEA protracted loss DP goal cannot be met.

Three-tank Problem with Waste Generation

Extend the previous example by adding a separations area between tank 1 and 2 that is not instrumented but that generates waste. This mimics the monitoring of feed and receipt tanks surrounding a separations area plus a waste tank. Realistically, the shipments from the feed tank will differ from the receipts in the receipt tank more than in the previous example because of process

Figure 2. Residuals or *scores* from NMA and PM for 7 tanks (tanks 0 to 6)

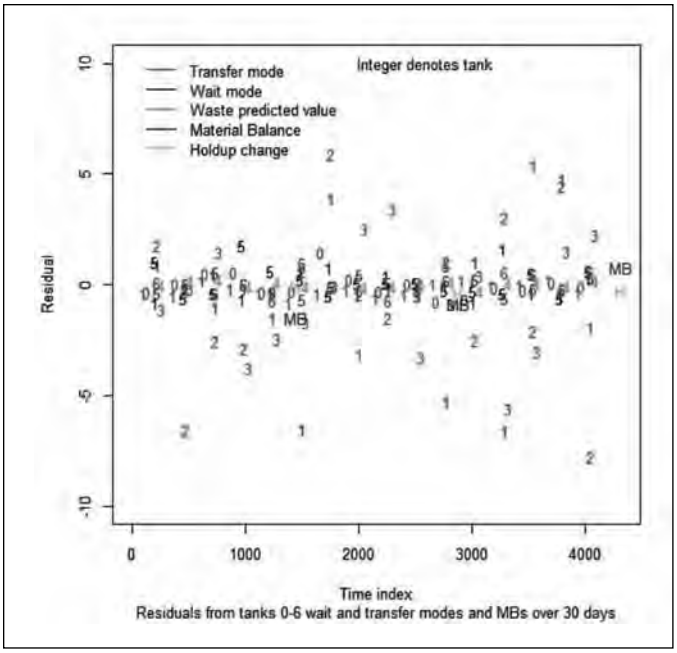

variation in the separations area, so this three-tank system is more difficult to safeguard. The waste is declared to be 0.1 percent and so 99.9 percent of Pu from tank 1 should arrive as output from tank 3. The throughput is 50 kg of Pu per day, 160 operating days per year, which is 8,000 kg of Pu per year with 8 kg in the waste. At 0.3 percent measurement error, this implies σ_{MB} = 24 kg per year, or 0.15 kg per day.

Assume the waste is measured with 10 percent total measurement error standard deviation, and 10 percent of 0.1 percent of 8,000 is 0.8 kg per year, which is acceptably low, so 10 percent measurement error on waste is acceptable. However, diversion could still occur to the waste either by:

(a) changing operations to achieve richer-than-nominal Pu concentration, or
(b) nominally, 8 kg of Pu is in waste, so this could be diverted from waste storage.

The stored waste must be under safeguards due to the Pu quantity; however, this is outside our present scope. Our scope is to develop a good system for predicting H_0 or H_A as applied to the 3-tank system. If 100 percent of the input to tank 1 exited as either waste or product from tank 3, then H_0 is true. In reality, a possible change in the in-process inventory in the separations area must also be considered, plus there should be at least a "catch-all" for "everything else" to include all other possible diversion paths.

If undeclared operations sent 20 kg of Pu per year to the waste, then an explanation would be required because the measurements would lie within approximately 20 +- 2 times 10 percent of 20, or 16 to 24 kg, a range which significantly exceeds the nominal 0.8 kg. More realistically, there will be several feasible diversion routes but the concept is the same as above provided we monitor each possible path.

Seven-tank MBA

Assume a seven-tank MBA example that extends the previous three-tank example by adding buffer tanks in addition to the feed and receipt tanks surrounding a separations area.[6] One tank is a monitored waste tank. This seven-tank MBA includes batch and continuous mode tanks, a separations area between Tanks 2 (Feed) and 3 (Receipt), and the notion of predicted or *book* values for the waste stream exiting the separations area and for holdup in the separations area. Figure 1 plots example simulated data for each tank (numbered 0 to 6) and for the holdup.

To combine PM and NMA on equal statistical footing, both systems report residuals (*scores*) as they arrive. For typical SM, such scores arise by event marking that locates the end of each tank-to-tank transfer. Scores include the *M* and *V* changes during non-transfer modes within each tank and during transfer modes between tanks. Other scores arise in extended SM applied to waste and holdup. Pu mass measurements in waste streams are a component of the MB, and these same waste measurements can be compared to the model-based book value, resulting in two correlated scores, one score being the MB and another score being the comparison between book and measured waste stream Pu mass. Holdup in the separations area is estimated using extended SM as described in Yamaya et al.[8]

As an example of "period-driven" monitoring, Page's cusum can be applied to each of nineteen separate but nonindependent scores from NMA and SM over thirty days spanning three ten-day NMA balance periods. The nineteen scores include three MBs, ten wait and transfer mode scores in typical SM, and in extended SM, three waste measurements compared to the waste book value, and three holdup estimates based on SM data compared to the corresponding holdup measurement. Figure 2 plots example simulated scores over thirty days. Figure 3 is six example pair-wise plots for six of the 171 pairs of nineteen scores. Notice that some pairs of scores are correlated (not independent), such as the input accountability tank (IAT) transfers and MB_1. So, PM data and NMA data are not independent in general. For example, the same dip tubes that measure volume in SM data for each tank are used for the volume measurement for NMA.

Regarding holdup estimation, efforts are underway to resurrect and improve pulsed column models[8] but for our purposes here using simulated data in residuals[34] with random and systematic measurement errors[19] (but no process variation), the pulsed column model is assumed to provide a "book value" for the effluent to the waste stream having a total relative error standard deviation of 10 percent. We have quoted "book value" here because NMA sometimes uses the term book inventory to mean $T_{in}+I_{begin}-T_{out}$, which is compared to physical inventory. The book value therefore comes from a model either in the PM context with waste streams or in the NMA context with MB

Figure 3. Example of relation between some pairs of scores

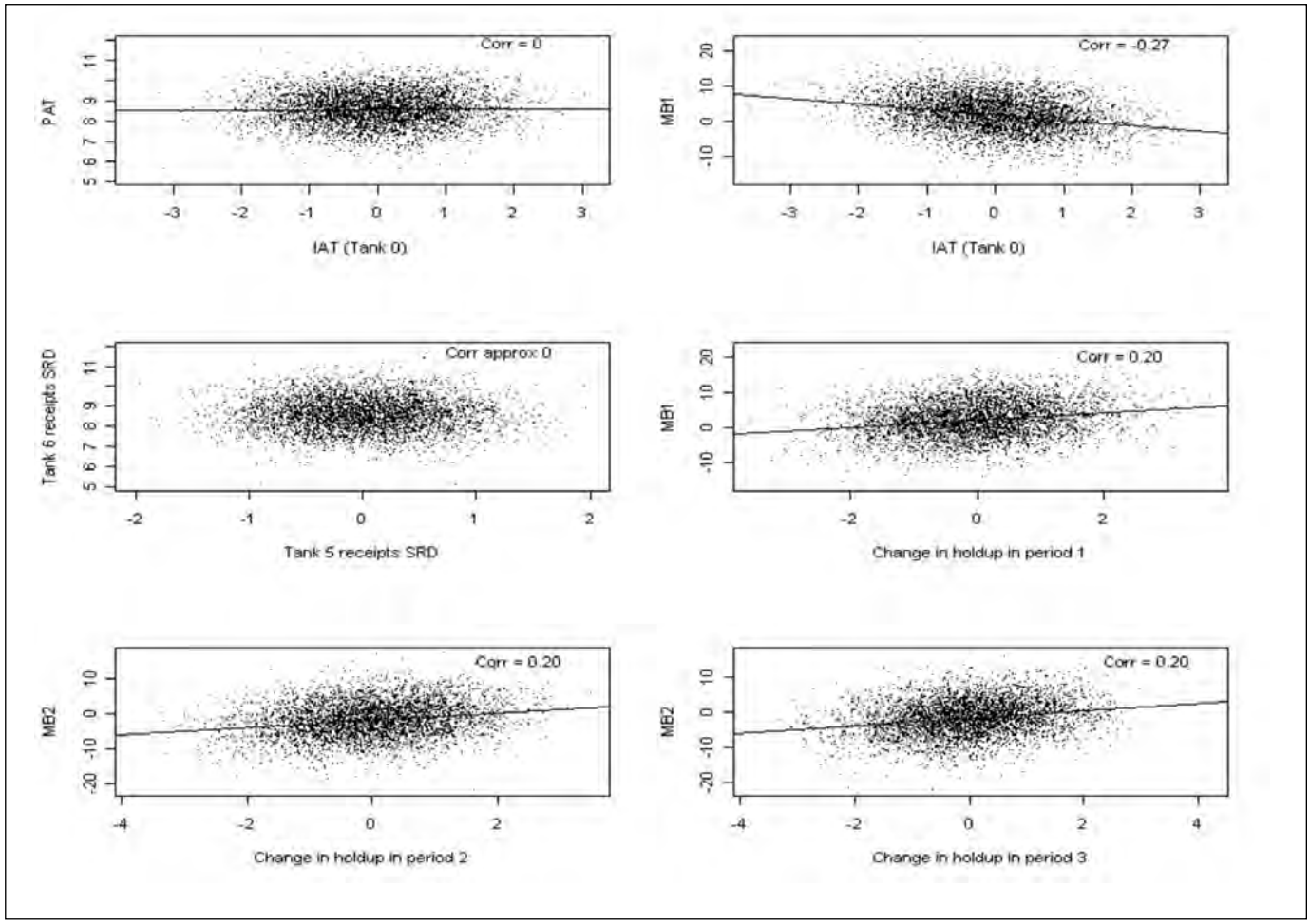

accounting. Also, the term "process variation" is a generic term that captures sources of variation other than pure measurement error effects, such as inconsistent operation of the pulsed columns (i.e., the solvent extractors). For illustration, tank measurements are modelled using random and systematic error relative standard deviations of 0.3 percent.

Combining NMA and SM scores such as those shown in Figure 2 into an overall system having small false alarm probability is ongoing work. Suppose there is a loss from the product accountability tank (PAT) during the first five days of balance period 2 (days 11-15). Figure 4 illustrates the true PAT volumes (random and systematic measurement errors are superimposed on these true volumes) over each of 30 one-day cycles. Subplot (a) has no loss; subplot (b) has a moderate loss totalling 8 kg, and subplot (c) has a large loss totalling 30 kg.

One loss detection option is to run nineteen separate Page's cusums. Figure 5 illustrates one realization of running nineteen separate Page's cusums. Of course running nineteen cusums on nonindependent scores requires careful selection of each of the control parameters k and alarm thresholds h, where $S_t=\max(0,S_{t-1}+R_t-k)$ with R_t being the scaled (to unit variance) residual for one of the nineteen residuals. Alternatively, Crosier's multivariate cusum could be used, but it would have to be adapted to work with cusums that are calculated at different times because the respective scores such as the tank 1 wait mode scores arrive at different time intervals.

A second loss detection option considered here uses a distance-based pattern recognition method applied to the nineteen sequential test statistics. Figure 6 qualitatively illustrates one such option using principal coordinates[35] to display scores from the nineteen separate sequential tests. Burr and Hamada[36] show that the combined NMA and SM data using the Mahalanobis distance (*MD)* from the zero-mean (zero loss) case as the alarm criterion (a relatively simple pattern recognition option) has moderate DP for a moderate loss and large DP for a large loss. The *MD* is defined[35] as $MD^2=(x-\mu)^t\hat{\Sigma}^{-1}(x-\mu)$ where x is the vector of scores over the thirty days, μ is the mean of x in the training data, and $\hat{\Sigma}^{-1}$ is the estimated covariance of the score vector x. To detect a

Figure 4. Example diversion: loss over five consecutive batches in PAT at days 10 to 15. Top: zero loss; Middle: moderate loss; Bottom: large loss.

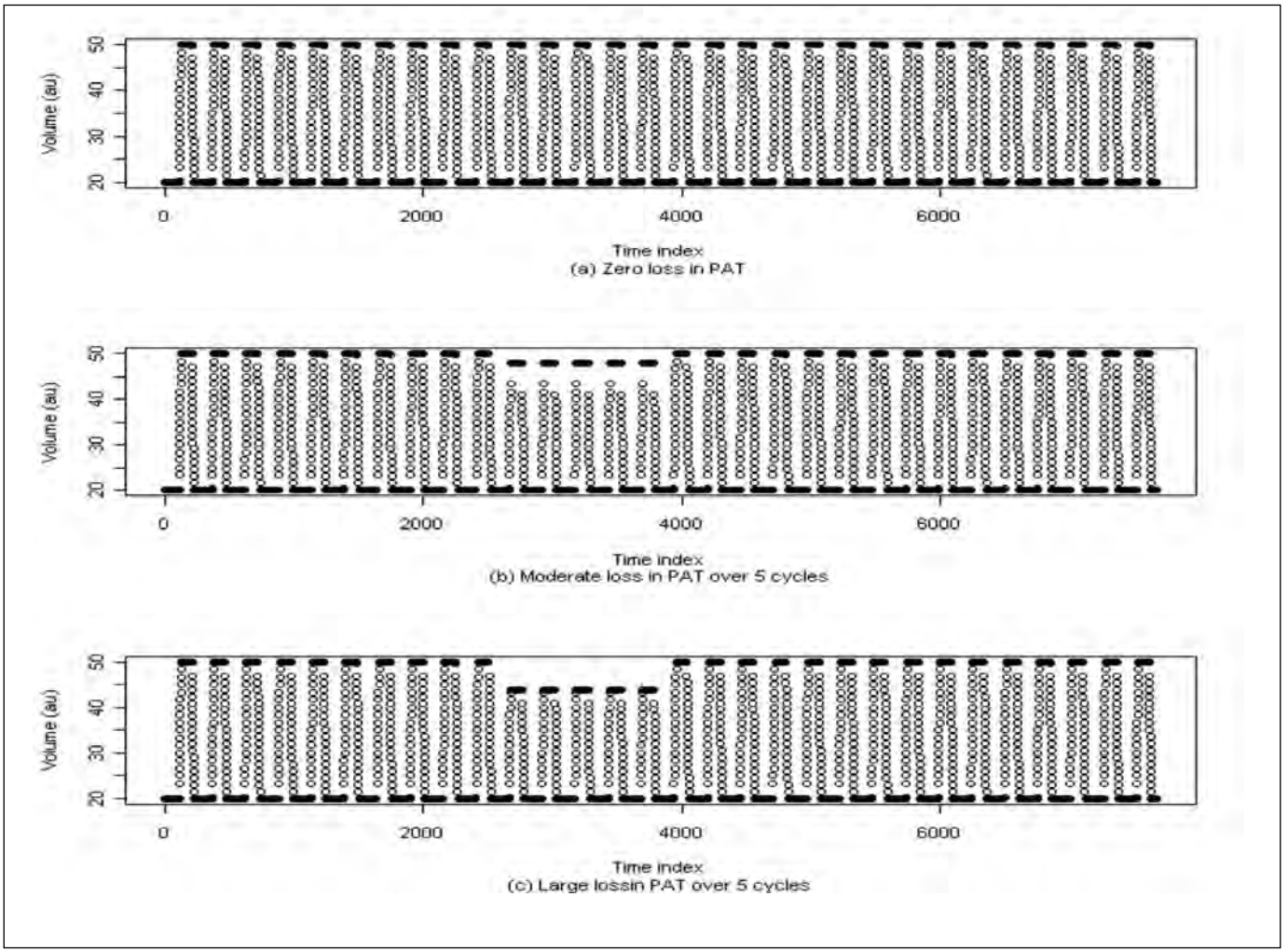

loss, the *MD* can be computed using all nineteen scores, or lower-dimensional principal coordinates.

Because Page's sequential test checks for temporal trends over the thirty days, Figure 5 obviously includes a check for time trends. Figure 6 is intended to evaluate how detectable a sustained (over five tank cycles) moderate or large loss is using the *MD*-based pattern recognition option that does include time trend checking because the *MD* is based on Page's cusums. Figure 7 gives an example comparison of DPs of the first option (nineteen cusums) and the second option (MD) for the thirty-day example with a wide range of false alarm probabilities. The DPs in Figure 7 were estimated using 1000 simulated realizations of the thirty-day period. In this example, option 2 (MD) has higher DPs for low false alarm probabilities. Both options have high DPs for high false alarm probabilities.

Options involving sequential statistical testing applied to NRTA (NMA with frequent balance closure) were first investigated for safeguards in the 1970s and 1980s. Speed and Culpin[2] and Goldman et al.[3] summarize early work on sequential testing in NRTA by several safeguards organizations[5] around the world, including the IAEA. Although various sequential statistical tests such as Page's test are appropriate for frequent MBs in NMA (such as closing balances every ten days), Avenhaus and Jaech[23] showed that more frequent balance closure in NMA does not increase loss DP for widespread (*protracted*) diversion over time. In fact, less frequent balance closure has higher DP if the loss vector describing the loss at each balance period is proportional to the sum of the rows of the MB covariance matrix Σ_{MB}. A similar conclusion holds for widespread diversion over time and space (multiple tanks in our context).

The PM and NMA scores are a multivariate time series. If the multivariate scores are assumed Gaussian, then a similar calculation to that in Avenhaus and Jaech[21] show that less frequent monitoring has higher DP for some loss scenarios that are protracted over time and spread over multiple tanks. Therefore, PM combined with NMA is not a panacea. However,

Figure 5. Page's cusum applied to five of the nineteen scores for the case of moderate loss (subplot b of Figure 4). The alarm threshold is scaled to 1.0 units, shown in the dotted line. The alarming cusum for the transfer modes are for the tank 7 transfers shortly after the loss began, so Page's cusum is behaving appropriately. Similarly, the alarming cusum for the three MBs is behaving appropriately.

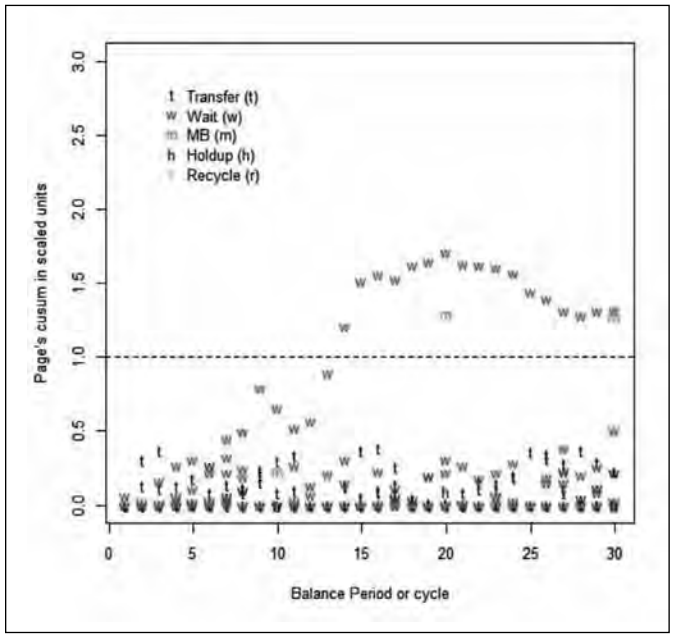

Figure 6. Qualitative assessment of the ability to detect moderate or large loss using scores as in Figure 2 from NMA and PM data. Two principal coordinates (similar to principal components) are used to show distances between nineteen-component realizations. Because Page's sequential test checks for temporal trends over the thirty days, Figure 3 is not intended as a check for trends, but is intended only to evaluate how detectable a moderate or a large loss is with one particular pattern recognition option.

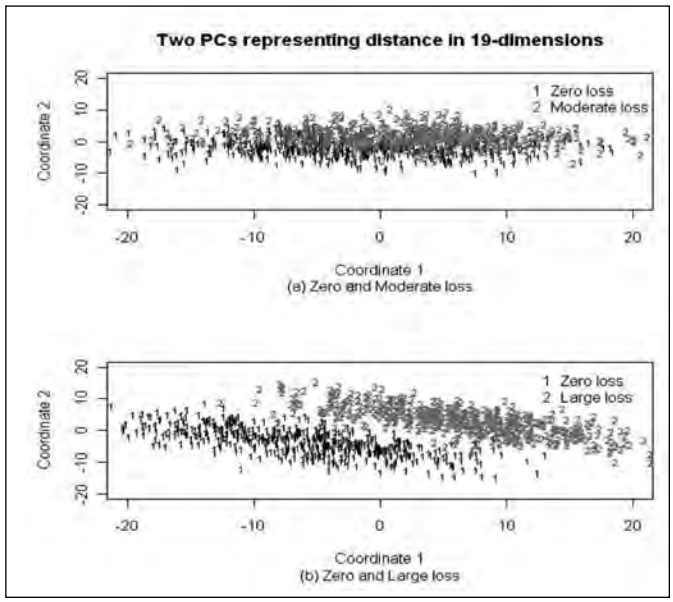

frequent multivariate scores (whether approximately Gaussian or not) as we have assumed are available from PM data will have much higher DP against most loss scenarios, particularly abrupt loss. Analogously, frequent balance closures in NMA performs better in an overall sense than infrequent scores from NMA alone, simply because frequent balance closures leads to much higher DP for abrupt diversion, and only slightly lower DP for protracted diversion.[5] And, alarm rules involving pattern recognition can be made to have almost the same DP against protracted loss as for example an annual NMA-based balance closure. To summarize, it is anticipated that while not a panacea, frequent multivariate scores from NMA and PM will perform better in an overall sense than infrequent scores from NMA alone or from PM and NMA.

Statistical Challenges

Statistical challenges in existing safeguards approaches have been described elsewhere.[2,3,37] The proposed safeguards approach involves combining NMA with PM using some type of residual monitoring, and estimating the overall system DP[6,38] for various scenarios without formal ties to Bayesian decision theory. Statistical challenges in the proposed integrated safeguards approach include: estimating the degree of dependence among subsystems such as PM and NMA (Figure 4), developing custom pattern recognition methods that help determine good system alarm rules (first alarmer subset, democratic, etc.), using models to insert the effects of facility misuse into real or realistic simulated background data,[39] assessing the impact of model uncertainty in the use of model-based book values, improving measurement error models and understanding in solution monitoring data,[40] and developing an authentication strategy for the IAEA that will probably rely on the concept of type 1 and type 2 tanks, where type 1 tanks are equipped with independent IAEA measurement systems.[41]

Summary

We emphasized that safeguards challenges have been further complicated by the broadened scope to monitor for undeclared facilities and for undeclared activity at declared facilities and by the modest budget. We advocate expert elicitation to identify diversion options and to design an overall system that combines NMA with PM (and possibly C/S) to have high detection probability for specified diversions. The approach is to monitor for undeclared activity and evaluate the probability of system alarm, where the system includes both PM and NMA. Three examples were given and additional examples are in Burr et al.[6.] A key new feature in PM is the notion of a model-based book value and resulting scores or residuals that can be monitored on equal footing with residuals (material balances) from NMA.

Figure 7. Comparison of the DPs for option 1 (nineteen cusums) and for option 2 (MD) over the thirty days

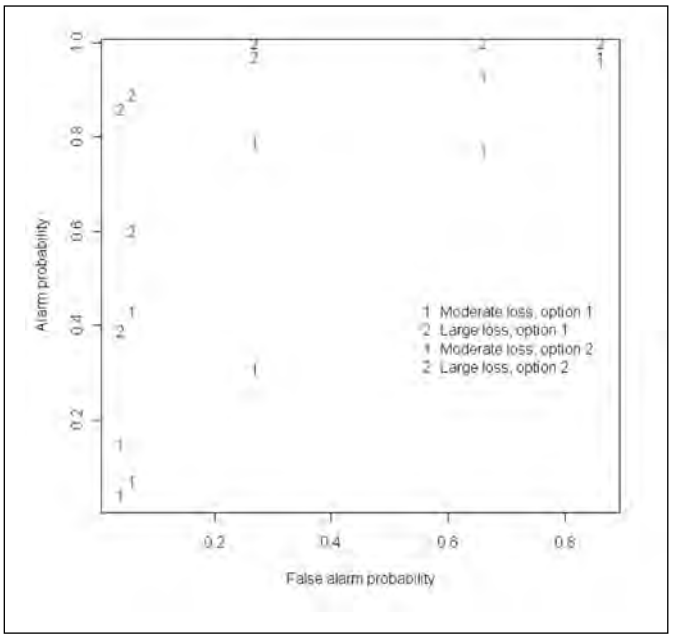

References

1. Cooley, J. 2004. Progress Toward More Effective and Efficient Safeguards: An IAEA status report, *Journal of Nuclear Materials Management,* 32(4), 6-11.
2. Speed, T., and A. Culpin. 1986. The Role of Statistics in Nuclear Materials Accounting, *Journal of the Royal Statistical Society A*, 149(4), 281-313.
3. Goldman, A., R. Picard, and J. Shipley. 1982. Statistical Methods for Nuclear Materials Safeguards: An Overview, *Technometrics*, 24(4), 267–281.
4. Canty, M., G. Spannagel, F. Voss, F., and A. Berliner. 1982. Computer Simulation of the Process MBA for a 1000t Reprocessing Facility, *International Symposium on Recent Advances in Nuclear Materials Safeguards*, Vienna.
5. Jones, B. 1988. Near-Real-Time Materials Accountancy using SITMUF and a Joint Page's Test: Comparison with MUF and CUMUF Tests, *ESARDA Bulletin* 15, 20.
6. Burr T., A. Bakel, S. Bryan, K. Budlong-Sylvester, J. Damico, S. Demuth, M. Ehinger, H. Garcia, J. Howell, S. Johnson, J. Krebs, K. Myers, C. Orton, and M. Thomas. 2012. Roles for Process Monitoring in Nuclear Safeguards at Aqueous Reprocessing Plants," to appear *Journal of Nuclear Materials Management.*
7. Ehinger, M. 1981. Near Real-Time Accounting in a Reprocessing Facility Using In-process Inventory Estimation, *ESARDA Bulletin* 8, 53.
8. Yamaya K., S. Nobuharu, T. Iseki, A. Kawai, and T. Iwamoto. 2009. Plutonium Inventory Estimation of Extraction Cycles at Rokkasho Reprocessing Plant, *Proceedings of the Institute of Nuclear Materials Management 50th Annual Meeting.*
9. Johnson, S., B. Chesnay, C. Pearsall, S. Takeda, K. Fujumaki, and T. Iwamoto. 2004. Meeting the Safeguards Challenges of a Commercial Reprocessing Plant, *Proceedings of the 7th International Conference on Facility Operations-Safeguards Interface.*
10. Johnson, S., R. Abedin-Zadeh, C. Pearsall, K. Hiruta, C. Creusot, M. Ehinger, E. Kuhn, B. Chesnay, N. Robson, H. Higuchi, S. Takeda, K. Fujimaki, H. Ai, U. Uehara, H. Amano, and K. Hoshi. 2004. Development of the Safeguards Approach for the Rokkasho Reprocessing Plant, *Proceedings of the 7th International Conference on Facilities Operations-Safeguards Interface, American Nuclear Society.*
11. Shipley, J. 1978. Decision Analysis for Dynamic Accounting of Nuclear Safeguards, *Proceedings of the Nuclear Safeguards Analysis Non-Destructive and Analytical Chemical Techniques American Chemical Society.*
12. Jaech, J, and D. Sellinschegg. 1986. Comments on, The Role of Statistics in Nuclear Materials Accounting: Issues and Problems, *Journal of the Royal Statistical Society A* 149 (4), 281-313.
13. Johnston, R. 2005. Assessing the Vulnerability of Tamper-indicating Seals, *Port Technology International* 25, 155-156.
14. Bleck, M., C. Cameron, and A. Camp. 1981. The Potential Role of Containment/Surveillance in Integrated Safeguards Systems for Reprocessing Plants, *Proceedings of the Third Annual Symposium on Safeguards and Nuclear Materials Management, Karlsruhe, ESARDA Bulletin* 12, pp., 375-379.
15. Burr, T., A. Coulter, J. Howell, and L. Wangen. 2003. Solution Monitoring: Quantitative and Qualitative Benefits to Safeguards, *Journal of Nuclear Science and Technology* 40(4), 256-263.
16. Burr T., M. Suzuki, J. Howell, and M. Hamada. 2012. Loss Detection Results on Simulated Tank Data Modified by Realistic Effects, *Journal of Nuclear Science and Technology.*
17. Lyman, E. 2001. Can Proliferation Risks of Nuclear Power Be Made Acceptable? *Nuclear Cities Initiative (NCI) 20th Conference*, Washington DC, www.nci.org/conf/lyman.
18. Burr, T., and G. Hemphill. 2006. Multi-component Radiation Measurement Error Models, *Applied Radiation and Isotopes* 64(3), 379-385.
19. 2002. International Target Values for Uncertainty Components in Fissile Isotope and Element Accountancy for the Effective Safeguarding of Nuclear Materials, *Journal of Nuclear Materials Management* 30(2).

20. Ehinger, M., B. Chesnay, C. Creusot, J. Damico, S. Johnson, J. Wuester, S. Masuda, and M. Kajii, M. 2004. Solution Monitoring Applications for the Rokkasho Reprocessing Plant, *Proceedings of the 7th International Conference on Facilities Operations-Safeguards Interface, American Nuclear Society*.
21. Burr, T., J. Jones, and L. Wangen. 1995. Multivariate Diagnostics and Anomaly Detection for Nuclear Safeguards, *Proceedings of the Institute of Nuclear Materials Management 35th Annual Meeting*.
22. Howell, J, and S. Scothern. 2000. An Explicit Model-based Diagnostic Approach in a Plutonium Nitrate Storage Facility, *Control Engineering Practice* 8, 645-656.
23. Avenhaus, R., and J. Jaech. 1981. On Subdividing Material Balances in Time and/or Space, *Journal of Nuclear Materials Management* 10(3), 24-33.
24. Burr, T., and D. Weier. 2009. Hypothesis Testing: Frequentist versus Bayesian with Examples from Nuclear Safeguards, *Journal of Nuclear Materials Management* 37(2).
25. Avenhaus, R., and Canty, M. 1999. Avoiding Useless Quantification: Impressions from the 21st ESARDA Symposium, *ESARDA Bulletin* 30, 21-22.
26. Hakkila, E. A. et al. 1977. Coordinated Safeguards for materials management in a fuel reprocessing plant, Los Alamos National Laboratory Unrestricted Release Report, LAUR-6881,
27. Howell, J, and S. Scothern. 2000. An Explicit Model-based Diagnostic Approach in a Plutonium Nitrate Storage Facility, *Control Engineering Practice* 8, 645-656.
28. Scothern, S., and J. Howell. 1997. A Physical-model-based Diagnostic Aid for Safeguarding Nuclear Material in a Liquor Storage Facility, *Journal of Nuclear Materials Management* 25(4), 20-29.
29. Stanbro, W., and K. Sylvester. 2000. The Role of Expert Judgment in Safeguards, *Journal of Nuclear Materials Management* 28(4), 17-20.
30. Bevan, G., J. Howell, T. L. Burr, and R. Binner. 2009. Solution Monitoring Evaluation System Reasoning Processes, *Proceedings of the Institute of Nuclear Materials Management 50th Annual Meeting*.
31. Burr, T., M. Krick, and A. Mielke. 2004. Statistical Evaluation of Two Triggering Systems: An Application of Conditional Variance, *Nuclear Instruments and Methods in Physics Research A* 524, 314-323.
32. Suzuki, M., M. Hori, S. Nagaoka, and T. Kimura. 2009. A Study on Loss Detection Algorithms Using Tank Monitoring Data, *Journal of Nuclear Science and Technology* 46(2), 184-192.
33. Burr, T., M. Suzuki, J. Howell, M. Hamada, and C. Longo. 2011. Signal Estimation and Change Detection in Tank Data for Nuclear Safeguards, *Nuclear Instruments and Methods in Physics Research A* 640 200–221.
34. R Development Core Team. 2004. R: A Language and Environment for Statistical Computing. R Foundation for Statistical Computing, www.r-project.org.
35. Hastie, T., T. Tibshirini, and J. Friedman. 2001. *The Elements of Statistical Learning,* Springer, New York, USA.
36. Burr, T., and H. Hamada. 2011. Development of Pattern Recognition Options for Combining Multiple Safeguards Subsystems, Los Alamos National Laboratory Report LAUR11-03925.
37. Burr, T. 2008. Statistical Methods in Nuclear Nonproliferation Activities at Declared Facilities, in *Nuclear Safeguards, Security, and Nonproliferation*, Elsevier, Oxford, UK, 2008.
38. Garcia, H., T. Burr, G. Coles, G., T. Edmunds, A. Garrett, M. Gorensek, L. Hamm, J. Krebs, R. Kress, V. Lambertia, D. Schoenwald, C. Tzanos, and R. Ward. 2011. Integration of Facility Modeling Capabilities for Nuclear Nonproliferation Analysis, *Progress in Nuclear Energy*, 1-16, 2011.
39. Burr T., M. Suzuki, J. Howell, and M. Hamada. 2012. Loss Detection Results on Simulated Tank Data Modified by Realistic Effects," to appear, *Journal of Nuclear Science and Technology*.
40. Binner, R., J. Howell, G. Janssens-Maenhout, and W. Sellinschegg. 2008. Practical Issues Relating to Tank Volume Determination, *Industrial Engineering and Chemistry Research* 47(5), 1533-1546.
41. Burr, T., J. Howell, M. Ehinger, and G. Pomeroy. 2008. Reducing Inspector Uncertainty via Solution Monitoring, *Proceedings of the Institute of Nuclear Materials Management 49th Annual Meeting*.

Game Theoretical Perspectives for Diversion Path Analysis

R. Avenhaus, M. J. Canty, and Th. Krieger
Universität der Bundeswehr München, Neubiberg, Germany and Forschungszentrum Jülich, Jülich, Germany

Abstract

Diversion path analysis in the context of nuclear material safeguards is the identification and evaluation of all paths along which nuclear material can be diverted from the peaceful nuclear fuel cycle for military purposes or purposes unknown. Obviously such an analysis must be strategic in nature, giving particular attention to those diversion paths that are most promising from the diverter's point of view. This implies, in turn, the use of game theoretical concepts, a fact that has been long recognized but that has enjoyed renewed interest in recent years by more and more analysts. This paper presents a general framework for game theoretical approaches to diversion path analysis. Starting with the elementary case of only two paths and very simple payoffs to the inspectorate and the state, it is shown how the problem can be formulated and solved in terms of game theory. Then the technically more difficult generalization to an arbitrary number of diversion paths is described. The inclusion of additional complicating aspects in the analysis, such as false alarm and detection probabilities, conversion times and inspection effort is examined and partial solutions are presented, in particular the conditions under which the State is deterred from illegal behavior. A discussion of the usefulness of this kind of analysis concludes the paper.

Introduction

Diversion path analysis in the context of nuclear material safeguards is the identification and evaluation of all paths along which nuclear material can be diverted from the peaceful nuclear fuel cycle for military purposes or for purposes unknown. It is immediately apparent that such an analysis must be strategic in nature, giving particular attention to those diversion paths that are most promising from the diverter's point of view. This implies, in turn, the use of game theoretical concepts, a fact that has been long recognized by a few, but that has enjoyed increased interest in recent years by more and more analysts.

Diversion path analysis has in fact been performed in various ways for over a decade, see, e.g., References 1, 2, 3 and 4 but the underlying mathematical structure has been studied for a much longer time as a strategic sampling problem. See, e.g., Reference 5 where inspection regimes were analyzed in terms of the varying attractivity of posited illegal activities at different locations, only a subset of which could be inspected in a given reference time. This analysis was referred to as "global sampling" and from a mathematical point of view, diversion path analysis and global sampling schemes are essentially the same.

Quite a number of global sampling models have been developed under different safeguards contexts. It turns out, however, that most of them can be reduced to two basic models if one includes the problem of inspection resource distribution over several states.[5] Since multiple state problems do not properly fall into the category of a diversion path model, we do not consider them here explicitly, but mention them in our concluding remarks. It is the purpose of this contribution to develop the basic model for diversion path analysis and to show how some of its generalizations can be obtained by simply re-interpreting the parameters involved. It will also be shown how other generalizations, which also can be deduced from the basic model, require some additional modification.

By generalization, we mean in the present context beginning from a simple model that covers only a few features of an inspection problem and then proceeding to add more features, like errors of the first and second kind, timeliness, etc. This contrasts with a mathematician's conventional idea of generalization: a simple model, which implicitly contains all relevant features in the appropriately defined model parameters, is the most general one.

The global sampling approach to nuclear safeguards problems was long preceded by more technical analyses involving variable and attributes sampling, and for a good reason. In global sampling, gains and losses (in game-theoretical terminology, utilities) need to be directly taken into account, whereas this is not necessary (at least not explicitly) in conventional sampling. To illustrate, here is a simple global sampling example:[6] In a public transportation system there are only random controls. If the passenger buys a ticket, she has to pay the amount d, if she does not, she will be controlled probability p and required to pay the accompanying fine b. Thus, her expected costs are p in case of legal behavior, and $0\ (1 - p) + bp = bp$ in case of illegal behavior. Acting purely rationally, she will behave illegally if bp is smaller than, d, i.e., if $p < d/b$.

In nuclear material safeguards, the situation is not so straightforward. Until now, diplomats and administrators have been reluctant to estimate gains and losses for different locations and states in the case of undetected and detected illegal activities. Furthermore, in the original verification document[7] all states were considered as equal, and the verification effort in different states had to be apportioned according to the size of their peaceful nuclear fuel cycles. In other words, verification effort had to be based on purely technical considerations. It turned

out that this led to a distribution of the verification capacity of the IAEA (finances and manpower) over different states that simply contradicted common sense.[8] In the Additional Protocol a different view was expressed without, however, explicit mention of states' utilities. As one of the fathers of safeguards systems analysis commented,[9] "They are looking for a technical solution to a political problem." Thus far, no serious attempts have been made by the IAEA to introduce utilities, but there are signs of a rising interest in the kind of studies presented here.

The purely technical models mentioned above were based on probabilities of false alarm and non-detection (errors of the first and second kind, respectively) as well as on expected detection times, and quantitative values were postulated. But a quick look at the passenger problem described above shows that even in the simplest cases utilities are lurking around the corner. One may require, e.g., a control probability $p=0.05$. This is however equivalent to postulating a ratio d/b. The real problem arises, however, when different locations or States are considered. Then utilities and technical parameters mix so thoroughly that it is no longer sufficient or even possible simply to postulate numerical values for technical parameters.

A word on methodology: the basic model as well as its generalizations can be represented as non-cooperative two-person games in normal form. The solution of these games is provided by the Nash equilibrium concept.[10] A Nash equilibrium strategy of a non-cooperative game is defined by the property that any unilateral deviation from it does not improve the deviator's payoff. A weakness of this solution concept is that, although at least one Nash equilibrium exists under very general assumptions, it need not necessarily be unique. The Nash equilibria in our models are or seem to be unique so that we need not deal with the difficulties of equilibrium selection, but we will come back to this issue.

This paper is organized as follows: the basic model is presented. Generalizations are introduced, and it is shown which of these are already covered by the basic model if its parameters are interpreted appropriately, and which ones are real extensions. In the concluding remarks (Section 4) further generalizations as well as the distribution of a given verification effort on several states are discussed and some thoughts about the usefulness of this kind of modeling are offered.

The results obtained are presented in form of Lemmata and a Theorem. Standard techniques for their proofs have been applied, but they will not be given here since most of them have been published already. In fact, similar to solving differential equations, it is much easier to prove that guessed equilibrium strategies satisfy the Nash conditions than to find them.

Basic Model for One State

Assume that a single state considers K diversion paths for the acquisition of nuclear material. These diversion paths may be placed in one or several locations. Since the Global Sampling work mentioned before uses the general term locations, we simply use it here, e.g., in the following we consider a single State with K locations in which an illegal activity may take place. By assumption the activity can occur, if at all, in one location only. The inspectorate likewise will by assumption inspect exactly one location and will detect any violation with certainty, should one take place.

This conflict situation will be modeled as a two-person non-cooperative game between two players, an inspectorate and a state. The inspectorate has K so-called pure strategies at its disposal, namely to control one of the K locations. The state has K strategic alternatives: behave illegally at one of the $K+1$ locations or legal behavior. The payoffs to (Inspectorate, State) are given for all possible outcomes as follows:

$$(-a_i, -b_i)$$

for illegal activity and inspection in location i,

$$(-c_i, +d_i)$$

for illegal activity in location i and inspection in location $j \neq i$, $i = 1, \ldots, K$, and

$$(0,0) \qquad (1)$$

for the state's legal behavior, where the payoff parameters satisfy the following conditions

$$0 < a_i < c_i, \; 0 < b_i, \; 0 < d_i \quad \text{for} \quad i = 1, \ldots, K \; . \qquad (2)$$

These conditions reflect the subjective preferences of both players: $a_i > 0$ means that the Inspectorate's highest priority is deterrence of an illegal activity. The worst outcome for the Inspectorate is non-detection, so that $a_i < c_i$. Roughly speaking, b_i reflects the state's perceptions of the consequences (sanctions) of detection and d_i is its incentive to behave illegally nevertheless. Note that, in the case of illegal activity in location i and inspection in location $j \neq i$ the payoff to the Inspectorate is $-c_j$, because we ignore real inspection costs in location j but consider instead a political loss arising from not detecting the illegal activity in location i.

To illustrate we consider first the simplest non-trivial case of two locations, i.e., $K = 2$. The normal form of the corresponding game (referred to as a bimatrix game) is given in Figure 2.1. In this Figure we have replaced the quantities a_i and b_i by

$$A_i = b_i + d_i, \; B_i = c_i - a_i > 0 \quad \text{for} \quad i = 1,2, \qquad (3)$$

for reasons which will become apparent later.

Figure 2.1. Normal form of the bimatrix game for locations as defined above. $\{(P_1,P_2): P_1 \geq 0, P_2 \geq 0, P_1+P_2 = 1\}$ and $\{(P_1,P_2,P_3): P_1 \geq 0, P_2 \geq 0, P_3 \geq 0, P_1+P_2+P_3 = 1\}$ are the sets of mixed strategies of the Inspectorate and the state.

		q_1	q_2	q_3
	State / Insp	1	2	legal
p_1	1	$d_1 - A_1$ $-c_1 + B_1$	d_2 $-c_2$	0 0
p_2	2	d_1 $-c_1$	$d_2 - A_2$ $-c_2 + B_2$	0 0

We seek the Nash equilibria[10] of the game, i.e., those pairs of strategies having the aforementioned property that unilateral deviation does not improve the deviator's payoff. In order to do that we have to introduce so-called mixed strategies, i.e., for the game in Figure 2.1, probabilities p_i with which location i is inspected, i = 1, 2, q_i, for starting the illegal activity in location i, i = 1,2, and q_3 for legal behavior. For short we write

$$\boldsymbol{p} = (p_1, p_2) \quad \text{with} \quad p_1 \geq 0, p_2 \geq 0, p_1+p_2 = 1,$$

$$\boldsymbol{q} = (q_1, q_2, q_3) \quad \text{with} \quad q_1 \geq 0, q_2 \geq 0, q_3 \geq 0, q_1+q_2+q_3 = 1.$$

Let $I_1(p,q)$ and $I_2(p,q)$ be the expected payoffs to Inspectorate and the State, respectively. Then the equilibrium strategies p^* and q^* are defined by

$$I_1^* = I_1(\boldsymbol{p}^*, \boldsymbol{q}^*) \geq I_1(\boldsymbol{p}, \boldsymbol{q}^*) \text{ for all } \boldsymbol{p},$$

$$I_2^* = I_2(\boldsymbol{p}^*, \boldsymbol{q}^*) \geq I_2(\boldsymbol{p}^*, \boldsymbol{q}) \text{ for all } \boldsymbol{q}.$$

Explicitly, for the game given in Figure 2.1 they are given in our first lemma for all model parameters satisfying (2); we do, however, not consider equalities between them here and in the subsequent cases, since these parameters cannot in any case be estimated precisely.

Lemma 2.1

Given the non-cooperative two-person 2x3 bimatrix game that is represented graphically in Figure 2.1.

- Under the assumption

$$\frac{d_1}{A_1} + \frac{d_2}{A_2} > 1$$

the unique equilibrium strategies are

$$p_i^* = \frac{d_i - I_2^*}{A_i}, \qquad q_i^* = \frac{c^* + I_1^*}{B_i}, \qquad i = 1,2, \tag{4}$$

with payoffs given by

$$\sum_{i=1}^{2} \frac{d_i - I_2^*}{A_i} = 1, \qquad \sum_{i=1}^{2} \frac{c^* + I_1^*}{B_i} = 1, \qquad \sum_{i=1}^{2} \frac{c^* - c_i}{B_i} = 0$$

where the inspectorate's equilibrium payoff is bounded as follows

$$0 < I_2^* < min\,(d_1, d_2)\,.$$

- Under the assumption

$$\frac{d_1}{A_1} + \frac{d_2}{A_2} < 1 \tag{5}$$

the equilibrium strategy of the Inspectorate is not unique and that of the State is legal behavior,

$$\frac{d_1}{A_1} \leq p_1^* \leq 1 - \frac{d_2}{A_2}, \qquad p_2^* = 1 - p_1^*,$$

$$q_1^* = q_2^* = 0, \qquad q_3^* = 1, \tag{6}$$

but the equilibrium payoffs to both players are unique and equal zero.

End of Lemma

Under the first assumption in the statement of the lemma, both locations are inspected with positive probabilities since the illegal activity is also carried out with positive probabilities in both locations and vice versa. This will be different in the case of more than two locations. Although it is easy to give explicit expressions for p_i^*, q_i^*, I_1^* and I_2^*, we have chosen the forms given above as they look very similar to the generalized cases to be discussed below.

Second, the inspectorate's equilibrium strategy for the equilibrium in which the State behaves legally is not unique, but the equilibrium payoffs are unique. This is a well-known property of inspection games. M. Kilgour[11] coined the term *cone of deterrence* for this behavior. Furthermore it can be shown that the equilibrium strategy p_i^* in the illegal case (4) also fulfills (6). Thus the Inspectorate is on the safe side if it uses Equation 4. Finally, a necessary condition for Equation 5 to hold is $d_i < A_i$ or $0 < b_i$, i=1,2, which are true by assumption. We will return to this point later.

In order to arrive at a Theorem on equilibrium strategies and payoffs for the general case of K locations, we consider next the case of three locations $K = 3$, since – according to our experience with related problems – it already exhibits many properties of the general case and still can be solved with simple means.

Figure 2.2. Normal form of the 3x4 bimatrix game for *K = 3* locations

		q_1	q_2	q_3	q_4
	State / Insp	1	2	3	legal
p_1	1	$d_1 - A_1$ $-c_1 + B_1$	d_2 $-c_2$	d_3 $-c_3$	0 0
p_2	2	d_1 $-c_1$	$d_2 - A_2$ $-c_2 + B_2$	d_3 $-c_3$	0 0
p_3	3	d_1 $-c_1$	d_2 $-c_2$	$d_3 - A_3$ $-c_3 + B_3$	0 0

The normal form of this game is given in Figure 2.2.

The Nash equilibria of this game are given in our second lemma.

Lemma 2.2

Given the non-cooperative two-person 3x4 bimatrix game which is represented graphically in Figure 2.2, let us assume without loss of generality

$$d_1 > d_2 > d_3 \ . \qquad (7)$$

Under the assumption

$$\frac{d_1 - d_3}{A_1} + \frac{d_2 - d_3}{A_2} > 1$$

the unique equilibrium strategies are

$$p_i^* = \frac{d_i - I_2^*}{A_i}, \qquad i = 1,2, \quad p_3^* = 0,$$

$$q_i^* = \frac{c^* + I_1^*}{B_i}, \qquad i = 1,2, \quad q_3^* = q_4^* = 0$$

with payoffs given by

$$\sum_{i=1}^{2} \frac{d_i - I_2^*}{A_i} = 1, \qquad \sum_{i=1}^{2} \frac{c^* + I_1^*}{B_i} = 1, \qquad \sum_{i=1}^{2} \frac{c^* - c_i}{B_i} = 0 ,$$

where the Inspectorate's equilibrium payoff is bounded as follows

$$d_3 < I_2^* < d_2 \ .$$

- Under the assumption

$$\frac{d_1 - d_3}{A_1} + \frac{d_2 - d_3}{A_2} < 1 \quad \text{and} \quad \frac{d_1}{A_1} + \frac{d_2}{A_2} + \frac{d_3}{A_3} > 1$$

the unique equilibrium strategies are

$$p_i^* = \frac{d_i - I_2^*}{A_i}, i = 1,2,3,$$

Figure 2.3. Parameter regions for the Nash equilibria according to Lemma 2.2

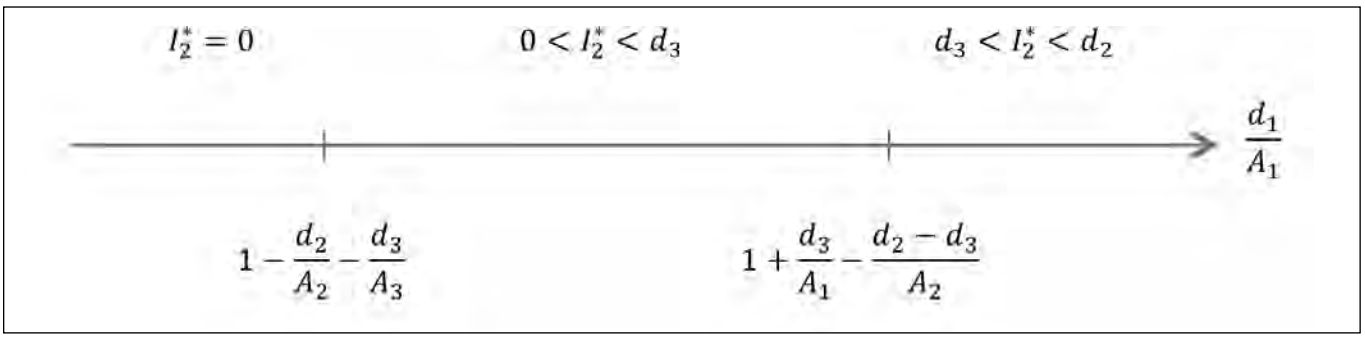

$$q_i^* = \frac{c^* + l_1^*}{B_i}, i = 1,2,3, \qquad q_4^* = 0$$

with payoffs given by

$$\sum_{i=1}^{3} \frac{d_i - l_2^*}{A_i} = 1, \qquad \sum_{i=1}^{3} \frac{c^* + l_1^*}{B_i} = 1, \qquad \sum_{i=1}^{3} \frac{c^* - c_i}{B_i} = 0,$$

where the Inspectorate's equilibrium payoff is bounded as follows

$$0 < l_2^* < d_3 ,$$

- Under the assumption

$$\frac{d_1}{A_1} + \frac{d_2}{A_2} + \frac{d_3}{A_3} < 1$$

the equilibrium strategy of the Inspectorate is not unique and that of the State is legal behavior,

$$p_i^* \geq \frac{d_i}{A_i}, \qquad i = 1,2,3, \qquad \sum_{i=1}^{3} p_i^* = 1,$$

$$q_i^* = 0, \qquad i = 1,2,3, \quad q_4^* = 1,$$

but the equilibrium payoffs to both players are unique and equal zero.

End of Lemma

Again, let us put these results into perspective with two remarks. First, in contrast to the results of Lemma 2.1, not necessarily in all locations inspections resp. illegal activities are performed. Note also that the ordering (7) was not required for $K = 2$ locations.

Second, in order to illustrate the structure of the solutions in the space of the payoff parameters graphically we write the conditions for the three Nash equilibria as follows:

$$\frac{d_1}{A_1} < 1 - \frac{d_2}{A_2} - \frac{d_3}{A_3}$$

$$1 - \frac{d_2}{A_2} - \frac{d_3}{A_3} < \frac{d_1}{A_1} < 1 + \frac{d_3}{A_1} - \frac{d_2 - d_3}{A_2}$$

$$\frac{d_1}{A_1} > 1 + \frac{d_3}{A_1} - \frac{d_2 - d_3}{A_2}.$$

In this way it can be seen that the whole parameter space for the game has been covered, see Figure 2.3.

The results obtained so far, lead us to a conjecture on the structure of equilibria in the general case of K locations, the Theorem of course contains the cases of two (see Lemma 2.1) and three locations (see Lemma 2.2.).

Theorem 2.1 (See Reference 5)

Given the non-cooperative two-person K x $(K+1)$ game the normal form of which is for $K = 2$ given by Figure 2.1 and for $K = 3$ given by Figure 2.2. Let us assume without loss of generality

$$d_1 > d_2 > d_3 > \cdots > d_K > d_{K+1} = 0.$$

Let $k, 1 \leq k \leq K+1$ be so chosen that

$$\sum_{i=1}^{k-1} \frac{d_i - d_k}{A_i} < 1, \qquad \sum_{i=1}^{k} \frac{d_i - d_{k+1}}{A_i} > 1, \qquad (8)$$

where the first inequality has to be ignored for $k = 1$ and the second for $k = K+1$.

- For $1 \leq k \leq K$ equilibrium strategies are

$$p_i^* = \frac{d_i - I_2^*}{A_i}, i = 1, \ldots, k, \qquad p_{k+1}^* = \cdots = p_K^* = 0$$

$$q_i^* = \frac{c^* + I_1^*}{B_i}, i = 1, \ldots, k, \qquad q_{k+1}^* = \cdots = q_K^* = q_{K+1}^* = 0$$

with payoffs given by

$$\sum_{i=1}^{k} \frac{d_i - I_2^*}{A_i} = 1, \qquad \sum_{i=1}^{k} \frac{c^* + I_1^*}{B_i} = 1, \qquad \sum_{i=1}^{k} \frac{c^* - c_i}{B_i} = 0,$$

where the Inspectorate's equilibrium payoff is bounded as follows

$$d_{k+1} < I_2^* < d_k .$$

- For $k = K+1$ the equilibrium strategy of the inspectorate is not unique and that of the state is legal behavior,

$$p_i^* \geq \frac{d_i}{A_i}, \quad i = 1, \ldots, K,$$

$$\sum_{i=1}^{k} p_i^* = 1, \quad q_i^* = 0, \quad i = 1, \ldots, K, \qquad q_{K+1}^* = 1,$$

but the equilibrium payoffs to both players are unique and equal zero.

End of Theorem

As before, let us comment these results with some remarks: First, the theorem is formulated in a way which is more general than necessary here. The second condition of (8) leads for $k = 1$ to

$$\frac{d_1 - d_2}{A_1} > 1,$$

which does not hold, since $0 < d_1 < A_1$; it is, however, relevant for cases discussed subsequently, see, e.g., Lemma 3.1. Consequently we have here $k \geq 2$, i.e., in the general case of K locations at least two locations are inspected with positive probability.

Second, in line with the results of Lemma 2.2, not necessarily in all locations inspections resp. illegal activities are performed. Note again that in all locations in which the illegal activity is carried out with positive probability, also the inspection is performed with positive probability and vice versa.

Third, it can be proven that the conditions Equation 8 on the parameters d_i and A_i, $i = 1,\ldots,K$, completely exhaust the parameter space, as it was already shown graphically in Figure 2.3 for the case $K = 3$.

Fourth, so far we did not prove that for $K > 2$ the Nash equilibria are unique as regard to the players expected payoff's. For $K = 2$ it was proven and for $K = 3$ it was shown for many examples. Furthermore, in a related model it was proven for any K, see [13].

Fifth, for $k = K + 1$, the first condition of Equation 8 is the condition for legal behavior of the state

$$\sum_{i=1}^{K} \frac{d_i}{A_i} < 1,$$

which we should keep in mind, since it returns in this or modified form in all generalizations of our basic model which will be discussed now.

Generalizations

Four generalizations are considered here: first, Attribute Sampling Procedures in which error second kind (non-detection) probabilities have to be taken into account. Second, Variable Sampling Procedures, where error of the second kind and error of the first kind (false alarm) probabilities cannot be avoided. Third, the concept of Critical or Conversion Time,[1] i.e., the idea that an illegal activity requires some time to be completed, is built into the models. And finally, more than one inspection is permitted.

Whereas in the first and third case the basic model of the second section can be used, one only has to reinterpret the model parameters, the second and fourth case require some extensions of the basic model.

Errors of the Second Kind

Assume that, whenever both state and inspectorate choose the same location for illegal activity and inspection, the former will be detected with probability $1 - \beta_i$, i.e., not detected with probability β_i, $i = 1, \ldots, K$.

We are dealing here with what is referred to in statistics as *attribute sampling* which arises, for example, when some fraction of container seals is checked and it can be decided with certainty whether or not a checked seal has been broken.

Using the payoffs (1), the expected payoffs to the (inspectorate, state) are given for all possible outcomes as follows:

$$(-a_i(1-\beta_i) - c_i\beta_i, \; -b_i(1-\beta_i) + d_i\beta_i)$$

for illegal activity and inspection in location i,

$$(-c_i, +d_i)$$

for illegal activity in location i and inspection in location $j \neq i$, $i = 1,\ldots, K$, and

$$(0,0)$$

for the state's legal behavior. Let us now define

$$A_i = (b_i + d_i)(1 - \beta_i),\ B_i = (c_i - a_i)(1 - \beta_i) > 0 \qquad (9)$$

for $i = 1, \ldots, K$.

Then the expected payoffs to (inspectorate, state) are

$$(-c_i + B_i,\ d_i + A_i)$$

for illegal activity and inspection in location,

$$(-c_i, + d_i)$$

for illegal activity in location i and inspection in location $j \neq i$, $i = 1,\ldots, K$, and

$$(0,0)$$

for the state's legal behavior.

This shows that we have the same payoff structure as given in Figures 2.1 and 2.2 for $k = 2$ and $k = 3$, if we replace (3) by (9). However there is an important difference: Whereas (3) implies $A_i < d_i$ for $i = 1, \ldots, K$, this need not be so for (9). This means that we have to consider the following two possibilities

$$d_1 - A_1 > d_2 \quad \text{or}$$

$$d_1 - A_1 < d_2$$

Accordingly, instead of Lemma 2.1 we now have:

Lemma 3.1

Given the non-cooperative two-person 2x3 bimatrix game which is represented graphically in Figure 2.1, where A_i and B_i, $i = 1,2$, are given by (9). Assume without loss of generality $d_1 > d_2$.

- Under the assumption

$$\frac{d_1}{A_1} > 1 + \frac{d_2}{A_1}$$

both players concentrate on the first location and the unique equilibrium strategies and payoffs are

$$p_1^* = q_1^* = 1 \quad \text{with} \quad I_1^* = -c_1 + B_1 \quad \text{and} \quad I_2^* = d_1 - A_1$$

where the Inspectorate's equilibrium payoff is bounded as follows

$$d_2 < I_2^* < d_1 .$$

- Under the assumption

$$1 - \frac{d_2}{A_1} < \frac{d_1}{A_1} < 1 + \frac{d_2}{A_1}$$

the unique equilibrium strategies of both players are mixed,

$$p_i^* = \frac{d_i - I_2^*}{A_i}, \qquad q_i^* = \frac{c^* + I_1^*}{B_i}, \qquad i = 1,2,$$

and the equilibrium payoffs to both players are given by

$$\sum_{i=1}^{2} \frac{d_i - I_2^*}{A_i} = 1, \qquad \sum_{i=1}^{2} \frac{c^* + I_1^*}{B_i} = 1, \qquad \sum_{i=1}^{2} \frac{c^* - c_i}{B_i} = 0 ,$$

where the Inspectorate's equilibrium payoff is bounded as follows

$$0 < I_2^* < d_2 .$$

- Under the assumption

$$\frac{d_1}{A_1} < 1 - \frac{d_2}{A_2} \qquad (10)$$

the equilibrium strategy of the Inspectorate is not unique and that of the state is legal behavior,

$$\frac{d_1}{A_1} \leq p_1^* \leq 1 - \frac{d_2}{A_2}, \qquad p_2^* = 1 - p_1^* ,$$

$$q_1^* = q_2^* = 0 , \qquad q_3^* = 1 ,$$

and the payoffs to both players are unique and equal zero.

End of Lemma

Once again, a few remarks: First, comparing this Lemma with Lemma 2.1 we see that assumption $d_1 > d_2$ was not needed for Lemma 2.1. Furthermore we see that this case is a special case of Theorem 2.1 if we replace A_i and B_i by (9) and where now the case $k = 1$ is relevant (see the first remark after the Theorem).

Second, necessary conditions for legal behavior, i.e., for Equation 10, are

$$\frac{d_i}{A_i} < 1 \qquad \text{for} \qquad i = 1,2,$$

(they are trivial for the basic model). This is equivalent to

$$-b_i(1 - \beta_i) + d_i \beta_i < 0 \ \text{ for } \ i = 1,2 ,$$

which means that legal behavior has to be guaranteed for each location.

Figure 3.1. Normal form of the 2x3 bimatrix game for $K = 2$ locations with errors first and second kind

		q_1	q_2	q_3
	State / Insp	1	2	legal
p_1	1	$d_1 - A_1$ $-c_1 + B_1$	$-f_1\,\alpha_1 + d_2$ $-e_1\,\alpha_1 - c_2$	$-f_1\,\alpha_1$ $-e_1\,\alpha_1$
p_2	2	$-f_2\,\alpha_2 + d_1$ $-e_2\,\alpha_2 - c_1$	$d_2 - A_2$ $-c_2 + B_2$	$-f_2\,\alpha_2$ $-e_2\,\alpha_2$

Third, condition 10 for legal behavior is with Equation 9 explicitly given by

$$\frac{1}{1+b_1/d_1}\,\frac{1}{1-\beta_1}+\frac{1}{1+b_2/d_2}\,\frac{1}{1-\beta_2}<0\,;$$

and expresses a mix between technical ($1-\beta_1$ and $1-\beta_2$) and political (b_1/d_1 and b_2/d_2) parameters, a mix which can no longer be resolved as in the one-location case mentioned in the introduction.

Nash equilibria for the general case $K = 2,3,...$ are now given precisely by Theorem 2.1 if we replace A_i *and* B_i, $i = 1, ..., K$, by (9).

3.2 Errors of the First and Second Kind

Assume again that, whenever both state and inspectorate choose the same location *i* for illegal activity and inspection, the former will be detected with probability $1-\beta_i$, i.e., not detected with probability β_i, $i = 1,..., K$. Assume further that for an inspected location at which an illegal activity has not taken place an error of the first kind, i.e., a false alarm, will be committed with probability α_i, not committed with probability $1-\alpha_i$, and that the associated costs are e_i and f_i to inspectorate and state, respectively. They are assumed to satisfy the following conditions

$$0 < e_i < a_i,\ 0 < f_i < b_i,\ 0 < d_i \quad \text{for} \quad i = 1, ..., K\,, \tag{11}$$

We consider here what in statistics is referred to as *variables sampling* which arises when quantitative measurements of material have to be performed and results are interpreted with the help of appropriate *test procedures* by means of which it is decided whether or not an illegal activity has taken place.

The expected payoffs to (inspectorate, state) now are given for all possible outcomes as follows:

$$(-a_i\,(1-\beta_i) - c_i\,\beta_i - b_i\,(1-\beta_i) + d_i\,\beta_i)$$

for illegal activity and inspection in location *i*,

$$(-c_j - e_i\,\alpha_i, + d_j - f_i\,\alpha_i)$$

for illegal activity in location *j* and inspection in location $i \neq j$, *and*

$$(-e_i\,\alpha_i, -f_i\,\alpha_i)$$

for the state's legal behavior and inspection in location.

Note that in the case of illegal activity in location j and inspection in location $i \neq j$, the payoff to the Inspectorate is $-c_j - e_i\,\alpha_i$, because besides the political loss arising from not detecting the illegal activity in location *j* the false alarm costs in location *i* have to be taken into account. The same holds for the state's payoff.

With the definitions Equation 9 these expected payoffs can be written as

$$(-c_i + B_i,\ d_i + A_i)$$

for illegal activity and inspection in location *i*,

$$(-c_j - e_i\,\alpha_i, + d_j - f_i\,\alpha_i)$$

for illegal activity in location *j* and inspection in location $i \neq j$, *and*

$$(-e_i\,\alpha_i, -f_i\,\alpha_i)$$

for the state's legal behavior and inspection in location $i, i = 1, \ldots, K$.

In Figure 3.1 the normal of the 2x3 bimatrix game is represented graphically.

The structure of the game is clearly more complicated than that of Figure 2.1. In presenting the Nash equilibria in the following lemma it will be assumed that

$$A_i - f_i \alpha_i > 0 \quad \text{for} \quad i = 1,2, \tag{12}$$

a condition which is always fulfilled for so-called *unbiased test procedures,* i.e., for $\alpha_i + \beta_i < 1$ and for (11).

Lemma 3.2 (See Reference 12)

Given the non-cooperative two-person 2x3 bimatrix game that is represented graphically in Figure 3.1, and assume (12) and, as before, without loss of generality $d_1 > d_2$.

- Under the assumption

$$1 + \frac{d_2}{A_1 - f_1 \alpha_1} < \frac{d_1}{A_1 - f_1 \alpha_1}$$

the Nash equilibrium is unique: both players concentrate on the first location

$$p_1^* = 1, \quad p_2^* = 0, \quad q_1^* = 1, \quad q_2^* = q_3^* = 0$$

$$I_1^* = -c_1 + B_1, \quad I_2^* = d_1 - A_1.$$

- Under the assumption

$$1 - \frac{d_2}{A_2 - f_2 \alpha_2} < \frac{d_1}{A_1 - f_1 \alpha_1} < 1 + \frac{d_2}{A_1 - f_1 \alpha_1}$$

the Nash equilibrium is also unique: the state behaves illegally with positive probabilities in both locations,

$$p_1^* = \frac{d_1 - d_2 + A_2 - f_2 \alpha_2}{A_1 - f_1 \alpha_1 + A_2 - f_2 \alpha_2}, \quad p_2^* = 1 - p_1^*,$$

$$q_1^* = \frac{B_2 + e_2 \alpha_2}{B_1 + e_1 \alpha_1 + B_2 + e_2 \alpha_2}, \quad q_2^* = 1 - q_1^*, \quad q_3^* = 0$$

and the payoffs are

$$I_1^* = \frac{-c_1(B_1 + e_2 \alpha_2) - c_2(B_2 + e_1 \alpha_1) + B_1 B_2 - e_1 \alpha_1 e_2 \alpha_2}{B_1 + e_1 \alpha_1 + B_2 + e_2 \alpha_2}$$

$$I_2^* = \frac{d_1(A_2 - f_1 \alpha_1) + d_2(A_1 - f_2 \alpha_2) - A_1 A_2 + f_1 \alpha_1 f_2 \alpha_2}{A_1 - f_1 \alpha_1 + A_2 - f_2 \alpha_2}.$$

- Under the assumption

$$\frac{d_1}{A_1 - f_1 \alpha_1} < 1 - \frac{d_2}{A_2 - f_2 \alpha_2}$$

three cases have to be considered:

- $e_1 \alpha_1 < e_2 \alpha_2$:

The Nash equilibrium is unique; legal and illegal behavior of the state are mixed:

$$p_1^* = 1 - \frac{d_2}{A_2 - f_2 \alpha_2}, \quad p_2^* = 1 - p_1^*,$$

$$q_1^* = 0, \quad q_2^* = \frac{e_2 \alpha_2 - e_1 \alpha_1}{B_2 + e_2 \alpha_2}, \quad q_3^* = 1 - q_2^*$$

with payoffs given by

$$I_1^* = -c_2 \frac{e_2 \alpha_2 - e_1 \alpha_1}{B_2 + e_2 \alpha_2} - e_1 \alpha_1$$

$$I_2^* = -f_1 \alpha_1 \left(1 - \frac{d_2}{A_2 - f_2 \alpha_2}\right) - f_2 \alpha_2 \left(\frac{d_2}{A_2 - f_2 \alpha_2}\right).$$

- $e_1 \alpha_1 > e_2 \alpha_2$:

The Nash equilibrium corresponds to the one given above:

$$p_1^* = 1 - \frac{d_1}{A_1 - f_1 \alpha_1}, \quad p_2^* = 1 - p_1^*,$$

$$q_1^* = \frac{e_1 \alpha_1 - e_2 \alpha_2}{B_2 + e_2 \alpha_2}, \quad q_2^* = 0, \quad q_3^* = 1 - q_1^*$$

with payoffs given by

$$I_1^* = -c_1 \frac{e_1 \alpha_1 - e_2 \alpha_2}{B_1 + e_1 \alpha_1} - e_2 \alpha_2$$

$$I_2^* = -f_1 \alpha_1 \left(1 - \frac{d_1}{A_1 - f_1 \alpha_1}\right) - f_2 \alpha_2 \left(\frac{d_1}{A_1 - f_1 \alpha_1}\right).$$

- $e_1 \alpha_1 = e_2 \alpha_2 = e \alpha$:

The Nash equilibrium of the Inspectorate is not unique, and the state behaves legally,

$$\frac{d_1}{A_1 - f_1 \alpha_1} \le p_1^* \le 1 - \frac{d_2}{A_2 - f_2 \alpha_2}, \quad p_2^* = 1 - p_1^*,$$

$$q_1^* = q_2^* = 0, \quad q_3^* = 1$$

with payoffs given by

$$I_1^* = -e \alpha, \quad I_2^* = -f_1 \alpha_1 p_1^* - f_2 \alpha_2 p_2^*.$$

End of Lemma

Figure 3.2. Normal form of the bimatrix game for locations with critical time

State / Insp	1	2	legal
1	$d_1 - \frac{b_1 + d_1}{l_1}$ $-c_1 + \frac{c_1 - a_1}{l_1}$	d_2 $-c_2$	0 0
2	d_1 $-c_1$	$d_2 - \frac{b_2 + d_2}{l_2}$ $-c_2 + \frac{c_2 - a_2}{l_2}$	0 0

Again, let us comment these results with two remarks: First, apart from the fact that these results are more complicated than what we have seen till now, there is a new feature: For $e_1\alpha_1 < e_2\alpha_2$ and $e_1\alpha_1 > e_2\alpha_2$ the state randomizes between legal and illegal behavior even though its expected payoff is the same as that obtained by behaving legally with probability one. This somewhat surprising result is also characteristic of some other inspection games.[6]

Second, for $e_1\alpha_1 = e_2\alpha_2$ – which we included only for methodological reasons, contrary to our general assumption given before Lemma 2.1 – the equilibrium strategy of the state is legal behavior and that of the inspectorate is not unique, as mentioned. But now, contrary to previous cases, the equilibrium payoff to the state is no longer unique.

For the general case Nash equilibria have not been determined and it will be very difficult, if not impossible, to present them in closed form. This pessimism is supported by the fact that even for the equilibrium payoffs for the illegal cases cannot be presented in the simple implicit forms we have seen earlier.

In the special case that all expected false alarm costs of the Inspectorate and also those of the state are the same,

$$f_i\alpha_i = f\alpha,\ e_i\alpha_i = e\alpha \quad for \quad i = 1 \ldots, K,$$

however, all Nash equilibria can be determined for $K > 2$ since we arrive again at the previous form by adding $e\alpha$ and $f\alpha$ to the Inspectorate and state payoffs, respectively, and replace B_i by $B_i + e\alpha$ and A_i by $A_i - f\alpha$ by . In particular, the condition for legal behavior is given by

$$\sum_{i=1}^{K} \frac{d_i}{A_i - f\alpha} \leq 1,$$

and the equilibrium payoffs to inspectorate and state are $-e\alpha$ and $-f\alpha$.

3.3 Critical Times

We consider next two locations and a reference time interval, such as a calendar year, in which a state commits at most one illegal activity. Assume that there time intervals exist location-specific critical within which detection of the activity at the respective location must take place if it is to be of use to the Inspectorate. One thinks here of conversion times, for example, the time required to convert diverted nuclear material to a clandestine weapon. Suppose that the reference time at locations 1 and 2 can be split evenly into $l_1 > 1$ and $l_2 > 1$ critical time intervals, where both l_1 and l_2 are integers, and precisely one inspection is carried out at one location during the reference time.

We describe the situation again as a non-cooperative two-person game with the players inspectorate and state. If the state decides to act illegally in one of the two locations, then it will do so at the start of each of the critical time intervals with probability $1/l_i$, = 1,2, for each location. This is because such a strategy renders the Inspectorate indifferent as to choice of inspection time and hence will be part of any Nash equilibrium. The inspectorate has two pure strategic alternatives: to inspect location 1 or 2, the state has three pure strategies: to act illegally in location 1 or 2 or to behave legally.

The payoffs to (inspectorate, state) are given for all possible outcomes as follows, note the difference to (1):

$(-a_i, -b_i)$

for timely detection of the illegal activity in location i

Figure 3.3. Normal form of the 4x4 bimatrix game for K = 2 locations L1, L2 and L3 and either one or three inspections

		q_1	q_2	q_3	q_4
	State / Insp	1	2	3	legal
p_1	$n=1$ L1	$d_1 - A_1$ / $-c_1 + B_1$	d_2 / $-c_2$	d_3 / $-c_3$	0 / 0
p_2	$n=1$ L2	d_1 / $-c_1$	$d_2 - A_2$ / $-c_2 + B_2$	d_3 / $-c_3$	0 / 0
p_3	$n=1$ L3	d_1 / $-c_1$	d_2 / $-c_2$	$d_3 - A_3$ / $-c_3 + B_3$	0 / 0
p_4	$n=3$ L1L2L3	$d_1 - A_1$ / $-c_1 + B_1$	$d_2 - A_2$ / $-c_2 + B_2$	$d_3 - A_3$ / $-c_3 + B_3$	0 / 0

$(-c_i, +d_i)$

for no timely detection of the illegal activity in location *i,* and

$(0,0)$

for the state's legal behavior;

where the payoff parameters satisfy the following conditions

$$0 < a_i < c_i, 0 < b_i, 0 < d_i \quad \text{for} \quad i = 1,2,$$

In Figure 3.2 the game is represented in normal form.
As an example, the payoff to the inspectorate in the upper left box is determined as follows:

$$-c_1\left(1-\frac{1}{l_1}\right)-a_1\frac{1}{l_1}=-c_1+\frac{c_1-a_1}{l_1}.$$

If we compare Figure 3.2 with Figure 2.1, then we see that we have the same game if we define for $i = 1,2$,

$$A_i=\frac{b_i+d_i}{l_i},\ B_i=\frac{c_i-a_i}{l_i}>0.$$

This in fact also holds if we consider K ≥ 2 locations so that Theorem 2.1 applies here as well if we define A_i and B_i appropriately.

Moreover, we can take errors of the second kind into account. Then the payoff given above is

$$-c_1\left(1-\frac{1-\beta_1}{l_1}\right)-a_1\frac{1-\beta_1}{l_1}=-c_1+\frac{(c_1-a_1)(1-\beta_1)}{l_1}$$

and so on, that is, if we define for $i = 1,2$

$$A_i=d_i-\frac{(b_i+d_i)(1-\beta_1)}{l_i},\ B_i=-c_i+\frac{(c_i-a_i)(1-\beta_1)}{l_i}$$

then we have the same game as before. This applies also to $K \geq 2$ locations, so that Theorem 2.1 holds yet again.

3.4 More Inspections

Assume now that there are $K \geq 2$ locations at which, other than in the second section, $n > 1$ inspections are planned. We consider two possibilities: either n is fixed and a natural number, or n represents an *expected* number of inspections and may be a real number in general. We will assume throughout that any given location will be inspected at most once.

Beginning with the natural number case, if there are K locations and $n \leq K$ inspections, there are $\binom{K}{n}$ inspection possibilities and, as before pure strategies for the state, thus leading to a $\binom{K}{n}$ x $(K + 1)$bimatrix game. We can, however, proceed differently and in such a way that the case of a given expected number of inspections (now called z) is also covered. We mix the cases of one inspection (K possibilities) and K inspections (1

possibility) such that the expected number of inspections is z. In this way we obtain a $(K + 1)$ x $(K + 1)$ bimatrix game with an additional boundary condition of the inspectorate's mixed strategy.

These two ways (in fact there are more) of treating one and the same inspection problem exist due to the special structure of the payoffs. We will illustrate this for the case of $K = 3$ locations.

The normal form of a game for three locations with either one or three inspections is represented in Figure 3.3.

The expected payoffs to both Inspectorate and State are

$$I_1(\boldsymbol{p},\boldsymbol{q}) = \sum_{i=1}^{3} q_i \left[-c_i + (p_i + p_4)\, B_i \right]$$

$$I_2(\boldsymbol{p},\boldsymbol{q}) = \sum_{i=1}^{3} q_i \left[d_i - (p_i + p_4)\, A_i \right]. \qquad (13)$$

Let us now introduce the probability $\tilde{p}_i$, $i = 1,2,3$, that the i – th location is inspected. We have

$$\tilde{p}_i = p_i + p_4, \qquad i = 1,2,3, \qquad (14)$$

thus, the expected payoffs (13) can be written as

$$I_1(\tilde{\boldsymbol{p}},\boldsymbol{q}) = \sum_{i=1}^{3} q_i \left[-c_i + \tilde{p}_i\, B_i \right]$$

$$I_2(\tilde{\boldsymbol{p}},\boldsymbol{q}) = \sum_{i=1}^{3} q_i \left[d_i - \tilde{p}_i\, A_i \right]. \qquad (15)$$

Herein lies the secret of the above mentioned different ways to treat the inspection problem with more than one inspection: With the help of the $\tilde{p}_i$, $i = 1, \ldots, K$ the payoffs of all cases can be represented in a form like (15).

The $\tilde{p}_i$, $i = 1, \ldots,4$, are normalized according to

$$\sum_{i=1}^{4} p_i = 1,$$

and the expected number of inspections is:

$$1 \sum_{i=1}^{3} p_i + 3\, p_4 = z, \qquad (16)$$

With Equation 16 we get, however, for the $\tilde{p}_i$, $i = 1,2,3$, given by Equation 14

$$\sum_{i=1}^{3} \tilde{p}_i = z. \qquad (17)$$

Thus, we have arrived at a game which is very similar to that given in Figure 2.2 – the expected payoffs have not been given there – if we replace the p_i by the $\tilde{p}_i$ and change their normalization according to Equation 17. The Nash equilibria of this game are given in the following Lemma.

Lemma 3.3

Given the non-cooperative two-person game with the mixed strategy set

$$\left\{ (\tilde{p}_1, \tilde{p}_2, \tilde{p}_3) \in [0,1]^3 \;:\; \sum_{i=1}^{3} \tilde{p}_i = z, \qquad 1 < z < 3 \right\}$$

of the inspectorate and

$$\left\{ (q_1, q_2, q_3, q_4) \in [0,1]^4 \;:\; \sum_{i=1}^{4} q_i = 1 \right\}$$

of the state and the expected payoffs given by (15). Assume, as before, without loss of generality $d_1 > d_2 > d_3$.

- Assume

$$\sum_{i=1}^{3} \frac{d_i}{A_i} > z. \qquad (18)$$

- For $1 < z < 2$ and

$$\frac{d_1 - d_3}{A_1} + \frac{d_2 - d_3}{A_2} > z \qquad (19)$$

the unique equilibrium strategies are

$$\tilde{p}_i^* = \frac{d_i - I_2^*}{A_i}, i = 1,2, \qquad \tilde{p}_3^* = 0, \quad q_i^* = \frac{c^* + I_1^*}{B_i}, i = 1,2, \qquad (20)$$

$$q_3^* = q_4^* = 0$$

with payoffs given by:

$$\sum_{i=1}^{2} \frac{d_i - I_2^*}{A_i} = z, \qquad \sum_{i=1}^{2} \frac{c^* + I_1^*}{B_i} = 1, \qquad \sum_{i=1}^{2} \frac{c^* - c_i}{B_i} = 0,$$

where the inspectorate's equilibrium payoff is bounded as follows

$$d_3 < I_2^* < d_2$$

whereas for

$$\frac{d_1 - d_3}{A_1} + \frac{d_2 - d_3}{A_2} < z$$

the unique equilibrium strategies are

$$\tilde{p}_i^* = \frac{d_i - I_2^*}{A_i}, i = 1,2,3, \quad q_i^* = \frac{c^* + I_1^*}{B_i}, i = 1,2,3, \qquad q_4^* = 0 \qquad (21)$$

with payoffs given by

$$\sum_{i=1}^{3} \frac{d_i - I_2^*}{A_i} = z, \qquad \sum_{i=1}^{3} \frac{c^* + I_1^*}{B_i} = 1, \qquad \sum_{i=1}^{3} \frac{c^* - c_i}{B_i} = 0,$$

where the inspectorate's equilibrium payoff is bounded as follows

$$0 < I_2^* < d_3 .$$

- For $2 < z < 3$ we have again the equilibrium strategies and payoffs as given by (21) – no analogue to (19) and (20).
- Assume

$$\sum_{i=1}^{3} \frac{d_i}{A_i} < z$$

the equilibrium strategy of the inspectorate is not unique and that of the state is legal behavior

$$\tilde{p}_i^* \geq \frac{d_i}{A_i}, i = 1,2,3, \qquad \sum_{i=1}^{3} \tilde{p}_i^* = z,$$

$$q_i^* = 0, \qquad i = 1,2,3, \quad q_4^* = 1$$

and the payoffs to both players are unique and equal zero.

End of Lemma

In this Lemma we mix $n = 1$ and $n = 3$ inspections in order to arrive at a given inspection effort z with $1 < z < 3$. We mentioned before that there are other ways. In fact we also could have achieved z with $1 < z < 2$ by mixing $n = 1$ and $n = 2$, and z with $2 < z < 3$ by mixing $n = 2$ and $n = 3$. The only difference consists in the relation between the p_i and the $\tilde{p}_i$, as we will show now: In the case treated here quite generally we have with (14) and (17) the unique relation between p_i and the $\tilde{p}_i$:

$$p_i = \tilde{p}_i - \frac{z-1}{2}, \qquad i = 1,2,3, \qquad p_4 = \frac{z-1}{2}. \qquad (22)$$

If we mix $n = 2$ and $n = 3$ in order to achieve some z with $2 < z < 3$ we have to introduce new probabilities

$$p_1 = prob(L1, L2), \; p_2 = prob(L1, L3),$$

$$p_3 = prob(L2, L3), p_4 = prob(L1, L2, L3)$$

which leads to

$$\tilde{p}_1 = p_1 + p_2 + p_4, \qquad \tilde{p}_2 = p_1 + p_3 + p_4,$$

$$\tilde{p}_3 = p_2 + p_3 + p_4 \qquad (23)$$

or conversely again to a unique relation between p_i and the $\tilde{p}_i$:

$$p_1 = 1 - \tilde{p}_3, \qquad p_2 = 1 - \tilde{p}_2,$$

$$p_3 = 1 - \tilde{p}_1, \qquad p_4 = z - 2. \qquad (24)$$

Of course, we have $(z - 1)/2 > z - 2$, since in the first case more weight has to be put on $n = 3$ inspections than in the second case.

So far, the relation between the p_i and the $\tilde{p}_i$ was deceptively simple namely unique. Consider now the case of achieving z with $1 < z < 2$ by mixing n=1 and $n = 2$. Now the new probabilities are

$$p_1 = prob(L1), \; p_2 = prob(L2), \; p_3 = prob(L3)$$

$$p_4 = prob(L1, L2), p_5 = prob(L1, L3), p_6 = prob(L2, L3)$$

which leads to

$$\tilde{p}_1 = p_1 + p_4 + p_5, \qquad \tilde{p}_2 = p_2 + p_4 + p_6,$$
$$\tilde{p}_3 = p_3 + p_5 + p_6.$$

These equations cannot be uniquely solved for $P_1, \ldots, P_6$. Therefore, we have in this case infinitely many Nash equilibria in the original game which, however, lead to the same equilibrium payoff, so that no equilibrium selection is necessary.

Let us continue with a problem of practice. In reality it is not the same to postulate an expected number of inspections or a deterministic one. In the latter case, one would have to resort to the $\binom{K}{n}$ x $(K+1)$ bimatrix game mentioned at the beginning of this section. Again, the only difference is a different relation between the p_I and the $\tilde{p}_i$ as defined before: For $K = 3$ and $n = 2$ we have in the deterministic case

$$p_1 = prob(L1, L2), \; p_2 = prob(L1, L3), \; p_3 = prob(L2, L3)$$

and furthermore

$$\tilde{p}_1 = p_1 + p_2, \qquad \tilde{p}_2 = p_1 + p_3, \qquad \tilde{p}_3 = p_2 + p_3$$

which leads to the unique solutions

$$p_1 = 1 - \tilde{p}_3, \qquad p_2 = 1 - \tilde{p}_2, \qquad p_3 = 1 - \tilde{p}_1,$$

other than (14) and (22), and also other than (23) and (24).

Finally, the mixing of $n = 1$ and $n = 3$ in order to achieve some expected number z, $1 < z < 3$, can easily be generalized to $K > 3$ locations and $1 < z < K$. We get for the probabilities

$$p_i = prob(Li), \qquad i = 1, \ldots, K, \qquad p_{K+1} = prob(L1, \ldots, LK)$$

the conditions representing the normalization and the expected number of inspections,

$$\sum_{i=1}^{K} p_i + p_{K+1} = 1, \qquad 1 \sum_{i=1}^{K} p_i + K\, p_{K+1} = z$$

which leads to

$$\sum_{i=1}^{K} p_i = \frac{K - z}{K - 1}, \qquad p_{K+1} = \frac{z - 1}{K - 1}$$

and the probabilities $\tilde{p}_i$, $i = 1,\ldots,K$, for inspecting the i-th location

$$\tilde{p}_i = p_i + p_{K+1}, \qquad i = 1, \ldots, K.$$

In turn the $\tilde{p}_i$, $i = 1,\ldots,K+1$, are again uniquely determined by

$$p_i = \tilde{p}_i - \frac{z-1}{K-1}, \qquad i = 1, \ldots, K, \qquad p_{K+1} = \frac{z-1}{K-1}.$$

The expected payoffs have the same simple structure as before, but a general theorem, corresponding to Theorem 2.1, is still missing. Even though it does not seem to be unfeasible, it will, depending on the values z, look rather intricate in any case.
The condition for legal behavior is for any deterministic or expected number z, as can be shown immediately

$$\sum_{i=1}^{K} \frac{d_i}{A_i} < z \qquad (25)$$

for $1 < z < K$ *and* $K = 2, 3, \ldots$ Of course, this condition can be easily generalized, if also error first and second kind probabilities, and also critical times have to be taken into account.

Concluding Remarks

Among the generalizations considered here, only two, namely those which take into account errors of the second kind and critical times, can directly be reduced to the basic model by reinterpreting the model parameters A_i and B_i, $i = 1,\ldots, K$. errors of the second kind can be included with a slight variation of the basic model, provided that all expected false alarm costs are the same, both for inspectorate and state. It is no real surprise that for the more general cases (arbitrary false alarm costs and more than one inspection) no general Theorem akin to Theorem 2.1 exists, although for the latter case one may be feasible. It should be emphasized that in the Theorem and all Lemmata (except for two special cases in Lemma 3.2), conditions for legal behavior of the state have been formulated.

More generalizations are possible, of course. We just mention one which may be relevant for real applications: The inspection costs (in terms of finances or manpower) may be location dependent. One might then fix the total inspection costs, thus adding another parameter to the problem. First attempts at dealing with boundary conditions on inspection costs have been made in Reference 13. Still further generalizations make sense only if some concrete application justifies them.

Returning to the second class of models mentioned in the introduction, in which the inspectorate distributes its effort over more than one state, consider K states with one location. From a modeling point of view, the situation is different in so far as one is now dealing with $(K + 1)$ -person games and any subset of states may act illegally, see References 13 and 14. There are nevertheless striking similarities, for example the conditions for legal behavior of all States have the same structure as in the models considered here. From a diversion path analysis point of view, nevertheless, such models would only become interesting, if each state had more than one location, i.e., diversion path.

What is the value of the modeling effort presented here and in related papers? Beyond the application mentioned below it is the *quantification of safeguards effectiveness and efficiency* in the framework considered here. A verification system is effective if it deters a state from illegal behavior in the sense of a treaty, i.e., if the state's equilibrium strategy in the conflict between the Inspectorate and the state is legal behavior. Our last formula (25) and the corresponding earlier ones are necessary conditions for such an equilibrium to exist. Furthermore, safeguards is efficient, if the inspection effort is the smallest one fulfilling Equation 25.

Finally, a word on applications. If one compares for instance the enormous technical detail presented in [3] and [4] with our mathematical formalism then it is hard to imagine how the latter can be usefully applied to the former. On the other hand, experts discussing and evaluating diversion paths are aware of the infinite recursions that arise: "if the inspector knows which path is preferred by the state, the state will be aware of that, a fact of which the inspector is also aware, which in turn ...". Game theory, with its solution concept of Nash equilibrium, provides at least a conceptual resolution of such conundrums. But we are also convinced that our models can provide more practical contributions to real-world inspection problems than merely conceptual ones. This will require that both theorists and practitioners approach each other, the former with a willingness to construct very specific models for concrete cases, the latter willing to try to condense and abstract their technical goals in such a way as to be expressible by a relatively small number of model parameters.

References

1. IAEA. 2002. Safeguards Glossary, 2001 Edition, *International Nuclear Verification Series No. 3*, IAEA, Vienna.
2. IAEA. 2010. Research and Development Programme for Nuclear Verification 2012-2011, p. 4, Vienna.
3. Vincze, A. 2011. Directed Graph Methodology for Acquisition Path Analysis: A Possible Tool to Support the State Level Approach, Seventh INMM/ESARDA Joint Workshop, Future Directions for Nuclear Safeguards and Verification, Aix-en-Provence, France.
4. Zentner, M., and R. Bari. 2011. Comparison and Use of INPRO and GIF Proliferation Resistance Methodologies in Safeguards by Design, Pacific Northwest Laboratory, Richland, Washington USA.
5. Avenhaus, R., and M. J. Canty. 1996. Paperback edition 2006. *Compliance Quantified – An Introduction to Data Verification.* Cambridge University Press, Cambridge, UK.
6. Avenhaus, R. 1997. Entscheidungstheoretische Analyse der Fahrgastkontrolle*, Der Nahverkehr* 9, 27-30.

7. IAEA. 1971. The Structure and Content of Agreements between the Agency and States required in Connection with the Treaty on the Non-Proliferation of Nuclear Weapons, INFCIRC/153 (Corrected), Vienna.
8. IAEA. 1997. Model Protocol Additional to the Agreement(s) Between the State(s) and the International Atomic Energy Agency for the Application of Safeguards, INFCIRC/540 (Corrected), Vienna.
9. Bennet, C. A. Personal communication.
10. Nash, J. 1951. Non-cooperative Games, *Annals of Mathematics* 54, 286-95.
11. Kilgour, D. M. 1992. Site Selection for On-Site Inspection in Arms Control, *Arms Control* 13 No. 3, 439-62.
12. Avenhaus, R., and M. J. Canty. 1995. Das Lineare Komplementaritätsproblem und seine Anwendung auf die Lösung von Bimatrix-Inspektionsspielen, Jül-3055, Forschungszentrum Jülich, Germany.
13. Deutsch, Y., B. Golany, and U. G. Rothblum. In print. Determining all Nash Equilibria in a (bi-linear) Inspection Game. *European Journal of Operational Research.*
14. Avenhaus, R., and M. J. Canty. 2005. Playing for Time: A Sequential Inspection Game, *European Journal of Operational Research* 167 No. 2, 475-92.

Submit your articles to the peer-reviewed *Journal of Nuclear Materials Management.*

Put your work before your peers
Network with others
Make yourself more competitive

To submit your paper:

1. ***Read the Author Submission Guidelines below.***
2. ***Email your paper in a Word document to JNMM Managing Editor Patricia Sullivan at psullivan@inmm.org.***
3. ***Respond promptly to review comments.***
4. ***Remember: JNMM is published four times a year in English. All graphs and images are published in black-and-white. References should follow Chicago Manual of Style guidelines.***

Questions?
Contact JNMM Managing Editor Patricia Sullivan at psullivan@inmm.org.

For 40 years the quarterly JNMM has been the premier international journal for the nuclear materials management profession. JNMM readers are the leaders in the field. They work in government, industry and academia around the world.

REACH THIS IMPORTANT AUDIENCE.

Author Submission Guidelines

The *Journal of Nuclear Materials Management* is the official journal of the Institute of Nuclear Materials Management. It is a peer-reviewed, multidisciplinary journal that publishes articles on new developments, innovations, and trends in safeguards and management of nuclear materials. Specific areas of interest include facility operations, international safeguards, materials control and accountability, nonproliferation and arms control, packaging, transportation and disposition, and physical protection. *JNMM* also publishes book reviews, letters to the editor, and editorials.

Submission of Manuscripts: *JNMM* reviews papers for publication with the understanding that the work was not previously published and is not being reviewed for publication elsewhere. Papers may be of any length. All papers must include an abstract.

The *Journal of Nuclear Materials* Management is an English-language publication. We encourage all authors to have their papers reviewed by editors or professional translators for proper English usage prior to submission.

Papers should be submitted as Word or ASCII text files only. Graphic elements must be sent in TIFF, JPEG or GIF formats as separate electronic files and must be readable in black and white.

Submissions may be made via e-mail to Managing Editor Patricia Sullivan at psullivan@inmm.org. Submissions may also be made via by regular mail. Include one hardcopy and a CD with all files. These submissions should be directed to:

Patricia Sullivan
Managing Editor
Journal of Nuclear Materials Management
111 Deer Lake Road, Suite 100
Deerfield, IL 60015 USA

Papers are acknowledged upon receipt and are submitted promptly for review and evaluation. Generally, the author(s) is notified within ninety days of submission of the original paper whether the paper is accepted, rejected, or subject to revision.

Format: All papers must include:

- Author(s)' complete name, telephone number and e-mail address
- Name and address of the organization where the work was performed
- Abstract
- Camera-ready tables, figures, and photographs in TIFF, JPEG, or GIF formats. Black and white only.
- Numbered references in the following format:
  1. Jones, F.T. and L. K. Chang. 1980. Article Title. *Journal* 47(No. 2): 112–118. 2. Jones, F.T. 1976. *Title of Book*, New York: McMillan Publishing.
- Author(s) biography

JNMM is published in black and white. **Authors wishing to include color graphics must pay color charges of $700 per page.**

Peer Review: Each paper is reviewed by at least one associate editor and by two or more reviewers. Papers are evaluated according to their relevance and significance to nuclear materials safeguards, degree to which they advance knowledge, quality of presentation, soundness of methodology, and appropriateness of conclusions.

Author Review: Accepted manuscripts become the permanent property of INMM and may not be published elsewhere without permission from the managing editor. Authors are responsible for all statements made in their work.

Reprints: Reprints may be ordered at the request and expense of the author. Contact Patricia Sullivan at psullivan@inmm.org or +1-847-480-9573 to request a reprint.

Book Review

By Mark L. Maiello, Ph.D.
Associate Book Review Editor

Twilight of the Bombs
2010, 458 pages, soft cover
Richard Rhodes
Vintage Books, Random House Inc.,
New York
ISBN 978-0-307-38741-7

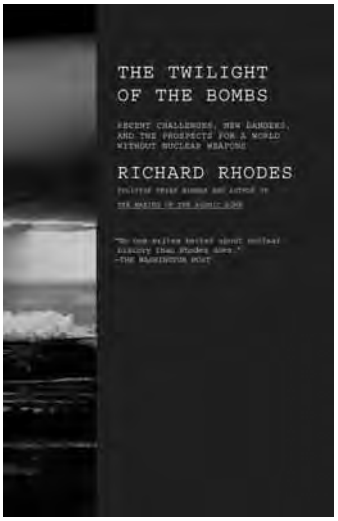

Richard Rhodes presents his recent history of nuclear nonproliferation efforts in this culmination of three previous historical treatments of nuclear weapons. They explained in turn the development of the atomic bomb, the hydrogen bomb, and the post-war arms race between the United States and the USSR. One hopes that the current title is as accurate as it is hopeful.

Rhodes describes a series of nuclear weapons related events all with potentially devastating consequences roughly within the period of 1985 to the present. These are primarily but not exclusively the stories of the nonproliferation efforts in response to the consolidation of nuclear weapons in Russia after the breakup of the USSR, and the clandestine nuclear weapons programs of Iraq, South Africa, and North Korea. Since this is a recent history, the reader benefits immensely from the records Rhodes was able to access and the interviews he was able to conduct with those that were intimately involved in the efforts to analyze these events or to negotiate with the governments involved. The recollections, writings, and actions of such important personalities as Richard Gallucci, Hans Blix, Mikhail Gorbachev, Jimmy Carter, Sam Nunn, U.S. diplomat Thomas Graham, Jr., Australian diplomat Richard Butler, and many others add very special perspectives that immediately elevate the book above a mere historical narrative.

This work is also valuable for its vivid description of the political, military, and proliferation environment of the period covered. It is a richly detailed narrative that provides deep insight into this complex period of huge political change. The background information is essential to understanding the motives behind the nuclear weapons developments of the era and the efforts to forestall them. Some were hair-raising episodes such as the experiences of the UNSCOM inspection teams in Iraq and the 1991 coup that almost ousted Gorbachev from the first and last presidential seat of the Soviet Union. Personal accounts of the inspection field work in Iraq and the clean-up efforts in the former Soviet republics as retold by the author's well-practiced hand keeps the reader involved. For example, initial U.S. contacts with Soviet nuclear weapons personnel in the early 1990s initiated as a response to the impending breakup of the USSR, had a humanizing effect on the American Cold War scientists who finally met their Soviet counterparts. Other examples include the threat-reduction project code-named Sapphire in which 1,278 pounds of highly enriched uranium (HEU) originally intended for a new Soviet class of submarines was removed by American specialists from the Ulba metallurgical plant at the request of the Kazakhstan government in 1994. The material was eventually blended into reactor fuel at Oak Ridge. The story is illustrative of the discovery of material by the Kazakh government after its abandonment by the USSR, the hard work of American laboratory personnel, and the dedication on both sides to carefully and properly remove it. While in Kazakhstan, the Americans arranged aid for a nearby orphanage, supplies for which were flown in during a terrible blizzard by U.S. Air Force personnel assigned to fly out the HEU.

The passages about the August 1991 coup that so deeply affected Gorbachev and terrorized his family are most compelling. During the coup, the status of the USSR's nuclear weaponry was for a time a dicey question—but as U.S. officials learned, the risk of deploying them was minimal due to the Soviet command and control structure. However, lurking not far in the future was the fractionation of the USSR that concerned men like U.S. Senator Sam Nunn who worried about insecure bombs and bomb-making material in Soviet republics that were about to declare their independence. Nunn visited Moscow after the coup to gauge the political climate and meet with Gorbachev. That visit galvanized his efforts to secure their nuclear weapons.

This work is to a degree an historical assessment as well. Rhodes appears to be objective but is not afraid to opine about the George W. Bush administration's inaccurate reasoning to declare hostilities with Iraq a second time or to describe the paranoid mindset in the U.S. government post 9/11 and post-anthrax attacks that gave rise to the "1 percenters" (those that prepare—and spend to excess—for low-probability terrorist events as if they were sure to happen).

Not being a proliferation expert,

Rhodes understandably cannot offer much in the way of a solution to reach zero nuclear weapons. He does explore the idea of zero and in so doing exposes some of the current obstacles such as the continued Cold War thinking of many in the American government and military. Rather than explain a strategy he focuses on societal trends that indicate to him that zero is possible. Mention is made of the worldwide pervasiveness of technology and the effect it apparently has on reducing personal violence (and ultimately the violence of war). This, he extrapolates, will one day result in the possession of nuclear weapons being classified as a crime against humanity.

As the reader might expect, there are few technical aspects in this work for the nonproliferation expert. Its value is in the history. The payoff is learning how recent events have sculpted the present state of affairs regarding nuclear weapons proliferation. Others with aspirations to make policy will find the descriptions of the work Gallucci, Butler, and others have done to complete the challenging inspection or diplomatic missions assigned to them or to complete those that they initiated themselves of great interest.

For the ability to tell us why we are where we are, and to perhaps prove history's claim true that we are bound to repeat mistakes should we ignore the past, this is recommended reading.

Associate Book Review Editor Mark L. Maiello, PhD, is a health physicist with an interest in radiological and nuclear security. He is a contributing editor for Health Physics News. *Maiello recently co-edited and published a book with Dr. Mark Hoover of NIOSH titled,* Radioactive Air Sampling Methods *(CRC Press).*

Taking the Long View in a Time of Great Uncertainty

Sustaining the Institute

By Jack Jekowski
Industry News Editor and Chair of the Strategic Planning Committee

In previous Taking the Long View columns, we have explored the critical external uncertainties ("externalities" in the vernacular of the original INMM Strategic Planning Working Group) of today's world that impact the INMM. These externalities have been encapsulated in ten questions that were posed to stimulate strategic discussions among leadership and members of the Institute (see the spring 2012 *Taking the Long View* column for the latest version of this list). In the spring column, we looked back over the past decade ("A Decade of Tumult") to capture the historic context of events that have shaped the environment we live in today, as well as taking a look forward at the uncertainties of the next decade to anticipate those possible strategic events that could impact the Institute. In that column we also identified "research areas" for the coming decade based upon the questions that have been created. Research provides a method to "connect the dots" of current events and drive strategic discussions to better understand what impact these externalities might have on the INMM and the path to the future. Such research areas form the basis for analysis in scenario planning, as the likelihood of future consequences can be surmised from sequences of current events. All of this work provides the underpinning for strategic discussions that our membership and leadership should be engaged in to ensure the relevancy and vibrancy of the Institute.

2012 – Already a Remarkable Year

We live in extraordinary times, where events on a global scale seem to be occurring on such a regular basis that one has difficulty skipping only a day or two of news without losing the trail created by these events. Such has been the case for the first quarter of 2012, where many events have been strategically linked to the future of the INMM. As this column goes to press, we are seeing the U.S. fiscal crisis impacting reductions at the U.S. national laboratories – with 557 employees at Los Alamos National Laboratory taking a voluntary reduction in force. The Obama administration continues down its path toward reduced reliance on the nuclear stockpile for its national security strategy, including proposed delays for large dollar weapons delivery systems such as SSBN(X) Ohio Class ballistic-missile submarines and preliminary discussions on tactical weapons reductions with Russia with hints that tradeoffs may be made on missile defense to secure such agreements. Criticism of the U.S. nuclear security enterprise continues to increase with the release of new reports by the National Academies and GAO, as the impending budget battles in FY13 loom ominously, potentially further complicated by a traumatic sequestration event on the heels of the U.S. presidential election this fall. These battles have already have taken their toll on the planning for the CMRR facility in Los Alamos, which is now at risk of a five year delay.

On the other side of the world environment, the North Korean's long-range missile launch has failed, and there is a concern that to save face their new leader, Kim Jong-un, will now proceed with the testing of a third nuclear weapon. The international impasse over the Iranian nuclear program worsens, as concerns continue that secret underground facilities may be enriching weapons grade materials, and there are open discussions almost daily of military intervention. The presidential election in Russia has resulted in Vladimir Putin being reinstated, and in a policy paper titled "Being Strong" he discusses the importance of revitalizing Russia's nuclear deterrent to their future security posture, a seemingly opposite position to that being taken by the current U.S. administration. All of this comes amid the second Nuclear Security Summit held in Seoul where the commitments of the 2010 Summit were reconfirmed, but no real breakthroughs were announced, and the goal of securing the world's most dangerous nuclear materials seems to be more distant than the 2013 time frame set in Prague on April 5, 2009.

Sustaining the Institute – The Strategic Connection to World Events

As a nongovernmental organization (NGO), the INNM is mission-focused on sustaining international expertise in all aspects of nuclear materials management, independent of political influences and external agendas, as well as promoting research and establishing standards. The Institute should be a comfortable hearth around which the world's nuclear expertise can gather to share technical knowledge in a non-threatening environment. The need for this has been reinforced by the events that we have examined in our externalities analysis, but how do we ensure the continued viability of the INMM particularly with respect to the subject matter expertise that has to be sustained in future generations? Since the success of the Institute is directly related to its membership, we must ensure that the people part of INMM is sustained and robust.

This leads us to three issues that have arisen recently in strategic conversations with Institute leadership and membership that give us pause to step back and look at with respect to the sustainability of the INMM mission and its continuing role to positively impact events in a dramatically changing world:

1. Global economic and fiscal crisis. Driven by an historic downturn in the economy worldwide, most nations, including the U.S., are under severe fiscal stress. This stress rolls down to individual companies and organizations which are likewise facing reduc-

tions in funding. Two easy targets for cost reductions in most organizations are travel and training costs (including participation in workshops and conferences). This could result in a challenge to the Institute to ensure the continuing engagement of its membership at annual meetings and workshops. INMM needs to be prepared for a "long drought" in attendance based on the current fiscal environment. Ideas for addressing this might include greater use of technology to bring content to our membership (e.g., using WebEx for plenary sessions) and perhaps reducing the cost of attendance for presenters, students, and others who actively participate in the organization.

2. Loss of Critical Expertise. As we look around the plenary session at the annual meeting we can see the graying of our membership. As our membership reaches retirement age, or otherwise leave the Institute, we need to aggressively seek new members, mentor and engage them in Institute activities, and change the way we do things to keep them engaged. We also need to look at how we can keep our senior members and fellows actively engaged, particularly after retirement. Ideas for addressing the issue with our aging members might include reducing the cost of attendance at the annual meeting and workshops, particularly for those who wish to stay active and serve as mentors.
3. Engaging the Next Generation. In the past ten years the Institute has come a long way in developing student participation. We now have ten student chapters. This year we have forty-seven student papers submitted for our annual meeting in Orlando, down from last year's record seventy-one papers, but significant nonetheless, compared to the handful of papers that we saw for many years in the first decade of the new millennium. This dramatic growth in our student member participation is a direct result of a strategic vision of the Institute's leadership in the late 1990s, including the INMM President at the time, and now Fellows Committee chair Obie Amacker, who challenged the participants at the first meeting of the Southwest Chapter in 1998 to help the Institute engage the next generation of nuclear stewards. The late J. D. Williams also picked up that challenge, along with former INMM President John Matter, to encourage the Institute to support the formation of student chapters, and participation in the annual meeting by student presenters. Our annual Student Paper Awards are named after J. D. in honor of his role in this endeavor, and today, in addition to the ten student chapters around the country, we are in discussions about the formation of the first foreign student chapter. Mark Leek of PNNL was our first Student Activities Committee chair, being replaced this past year by Steve Ward of the U.S. Nuclear Regulatory Commission. John Matter continues to offer his support, despite his retirement from Sandia, as chair of the INMM Chapters, and in particular, is active in working with the student chapters.

Today we have eighty-five student members, compared to twenty-one in 2005. But we have not yet reached the goal line—some of our student chapters struggle to sustain themselves, but we are beginning to better understand the critical components of a successful student chapter, not the least of which is a committed and enthusiastic faculty advisor, and how to make chapters sustainable with the ever-changing cycle of students that move through the chapter. Steve Ward is proposing to make some changes in how we support and mentor our student attendees this year at the annual meeting, but we will have to continually adjust our strategies to ensure that we engage the younger generation. This includes reaching out to them through social media, and including them as full participants in the decisions of the Institute.

We encourage *JNMM* readers to actively participate in these strategic discussions, and to provide your thoughts and ideas to the Institute's leadership. With your feedback we hope to explore these and other issues in future columns, addressing the critical uncertainties that lie ahead for the world and the possible paths to the future based on those uncertainties.

Jack Jekowski can be contacted at jpjekowski@aol.com.

End Notes

1. "*…It is possible that our deterrence goals can be achieved with a smaller nuclear force, which would reduce the number of nuclear weapons in our inventory as well as their role in U.S. national security strategy.," Sustaining U.S. Global Leadership: Priorities for 21st Century Defense, January 2012, p. 5,* http://www.defense.gov/news/Defense_Strategic_Guidance.pdf
2. See http://www.nap.edu/catalog.php?record_id=13367, *Managing for High-Quality Science and Engineering at the NNSA National Security Laboratories;* and http://www.nap.edu/catalog.php?record_id=12849, The Comprehensive Nuclear Test Ban Treaty
3. See GAO-12-473T, *Observations on NNSA's Management and Oversight of the Nuclear Security Enterprise,* http://www.gao.gov/products/GAO-12-473T
4. http://premier.gov.ru/eng/events/news/18185/
5. See Steve Ward's *Communicator* article, http://www.inmm.org/Student_Activities/2944.htm.

Calendar

September 23–28, 2012
The 9th International Conference on Facility Operations-Safeguards Interface
Hilton Savannah Desoto
Savannah, Georgia USA
Sponsors: American Nuclear Society and the Institute of Nuclear Materials Management
Web site: http://icfo-9.org/

October 23–25, 2012
Strategies to Validate Safeguards & Security System Performance Workshop
Rothchild's Conference Center
Knoxville, Tennessee USA
Sponsor: INMM Central Chapter
Contact:
Shannon Morgan at
morganss@ornl.gov
Web Site: www.inmm.org/events/

January 15–16, 2013
INMM 28th Annual Spent Fuel Seminar
Crystal Gateway Marriott
Arlington, Virginia USA
Sponsor: INMM Packaging, Transportation and Disposition Technical Division
Web Site: www.inmm.org/events/

July 14–18, 2013
54rd INMM Annual Meeting
JW Marriott Desert Springs
Palm Desert, California USA
Sponsor: Institute of Nuclear Materials Management
Contact: INMM
+1-847-480-9573
Fax: +1-847-480-9282
E-mail: inmm@inmm.org
Web site: www.inmm.org

August 18–23, 2013
PATRAM 2013
Hilton San Francisco Union Square
San Francisco, California USA
Hosted by the U.S. Department of Energy, the U.S. Nuclear Regulatory Commission, and the U.S. Department of Transportation in cooperation with INMM
Web site: http://www.patram.org

INMM Membership Application

MEMBERSHIP

All information should be printed or typewritten.

Name _____ Date _____

Employer _____ Title _____

Address

Address _____

City _____ State/Province _____ Country _____ Zip _____

Telephone _____ Fax_____ E-mail _____

If you would like your INMM mail sent to an alternative address, please indicate preferred mailing address:

Address _____

City _____ State/Province _____ Country _____ Zip _____

Occupation

❑ Commercial Utility ❑ Government Contractor ❑ Nuclear Material Processing
❑ Equipment Manufacturer ❑ Government or International Agency ❑ Research or Consulting
❑ Other (describe): _____

Field(s)/Subject(s) of expertise _____

Total number of years work experience in nuclear materials management field(s) _____

Education (If you are applying for a student membership, indicate the year that you anticipate receiving your degree)

College/University Major/Degree Year Degree Obtained/Expected

1. _____

2. _____

3. _____

If you are applying for a student membership, provide contact information for a faculty advisor to verify your full-time status:

Name _____ Telephone _____ E-mail _____

Membership Type Desired

❑ Student $20
❑ Regular $50

Sustaining:
❑ 0 – 19 employees $250
❑ 20 – 49 employees $500
❑ 50 or more employees $750

From the categories listed below, please indicate your top 3 areas of interest within INMM (1 being the greatest interest):

___ Facility Operations
___ International Safeguards
___ Materials Control and Accountability
___ Nonproliferation & Arms Control
___ Packaging, Transportation and Disposition
___ Nuclear Security and Physical Protection

Membership in other scientific and technical societies (Attach additional sheet if necessary)

Society Names and Membership Grades _____

Signature _____
PAID BY: ❑ Check ❑ MasterCard ❑ VISA ❑ American Express ❑ Diners Club

Card No. _____ Exp. Date _____

Complete the application (keep a copy for your records) and mail or fax it with membership dues to:

INSTITUTE OF NUCLEAR MATERIALS MANAGEMENT
111 Deer Lake Road, Suite 100 • Deerfield, Illinois 60015 USA
+1-847-480-9573, Fax: +1-847-480-9282
E-mail: inmm@inmm.org • Website: www.inmm.org

INMM
INSTITUTE OF NUCLEAR MATERIALS MANAGEMENT

Decommissioning?

The new AURAS-3000 Box Counter from ORTEC will make short work of those bulky free release construction waste containers!

www.ortec-online.com/solutions/waste-assay.aspx

- Free Release Assay of large waste containers up to 3 m^3: B25 ISO Box, smaller boxes with demonstrated regulatory compliance.[1]
- Container Weights up to 6000 kg, with on-line weighing to 3000 kg and 1 kg resolution.
- Full Quantitative Assay of all detectable gamma emitters, with non-gamma emitter estimates by correlated scaling factors.
- FAST: High sensitivity, large area integrated HPGe detectors (85 mm diameter) achieve rapid release levels.
- Individual and averaged activity AND MDA reporting.
- Highly automated.
- Extensive Safety Protection.
- Tested to EMC, Electrical and Safety standards.

[1]http://www.ortec-online.com/download.asbx?AttributeFileId=0b1f5761-c46b-4901-91ac-e0b810655b6a

801 South Illinois Ave., Oak Ridge, TN 37831-0895 U.S.A. • (865) 482-4411 • Fax (865) 483-0396 • ortec.info@ametek.com
For International Office Locations, Visit Our Website
www.ortec-online.com

ORTEC®

AMETEK
ADVANCED MEASUREMENT TECHNOLOGY